EXPERIMENTAL INVESTIGATION ON THE DURABILITY OF FIBRE REINFORCED CEMENTITIOUS MATERIALS FOR STRENGTHENING OF MASONRY

Dissertation

submitted to and approved by the

Department of Architecture, Civil Engineering and Environmental Sciences

University of Braunschweig – Institute of Technology

and the

Department of Civil and Environmental Engineering

University of Florence

in candidacy for the degree of a

Doktor-Ingenieur (Dr.-Ing.) /

Dottore di Ricerca in Processes, Materials and Constructions in Civil and Environmental Engineering and for the Protection of the Historic-Monumental Heritage

by

Daniela Sinicropi

born July 8th, 1980

Hartford (CT), USA

Submitted on	16/03/2015
Oral Examination on	12/05/2015
Professorial advisors	Prof. Harald Budelmann
	Prof. Michele Paradiso

2015

Acknowledgements

In these acknowledgments I have many debts of gratitude to express. First, my appreciation and thanks to my Italian advisor, Professor Michele Paradiso, for encouraging my research and allowing me the freedom of completing a dissertation on a subject of particular interest to me. Next, a distinct expression of gratitude to my German advisor, Professor Dr. Harald Budelmann, whose advice on my research during my sojourns in Braunschweig proved invaluable. I would especially like to thank Professor Antonio Borri, who provided the ongoing help and supervision without which this dissertation would not have been possible. And deep thanks go to Professor Dr. Marco Corradi who so generously shared his time and advice during the last period of this work.

Professor Dr. Marco Tanganelli and Dr. Valerio Alecci enabled me to overcome technical obstacles in difficult moments and furnished precious suggestions; my thanks to them for their valuable help.

Special thanks also go to Dr. Stefano Galassi, for his continuous availability and counsel, and to Dr. Gianfranco Stipo for his technical support and friendship.

In these acknowledgements, a place must be reserved for Ruredil and FibreNet, for having provided the materials that made the experimental campaigns possible, and also for Mr. Paolo Arcangioli for his unfailing problem-solving ability during my many hours in the Laboratory of the Department of Architecture of the University of Florence.

I would also like to thank my fellow PhD students for being great company and thoughtful listeners throughout this extraordinary experience. In particular Maria Pianigiani, who shared not only laughter, trips and exhilarating ideas, but also tears and fears. Tommaso Massai, for his patience and support. Valentina Chiarello, for believing in me from the very beginning and not letting me get overly discouraged. These friendships have been part of the many gifts of this exceptional period. My thanks also go to Giulia Misseri, who shared not only an office at the University of Florence, but also time and advice. I would like to thank my friends who were not part of the PhD programme, but who bolstered me throughout these years. Elisa Bechelli, Elisa Galli, Irene Morfini, Nadia

Migliorato and Riccardo Monducci. Thank you for being there both in good times and bad.
I would also like to express my gratitude to the Italian Ministero dell'Istruzione, dell'Università e della Ricerca, for the Fellowship awarded me which made these three years of research feasible.

A special thanks to my family - to my mother, to my father, and to Davide - for your support, patience and sacrifices which sustained me and motivated me to strive towards my goal. I cannot adequately describe how important you have been throughout this process.

ABSTRACT

This dissertation is the product of a research project which focused on the behaviour of Fibre Reinforced Cementitious Matrix (FRCM) for the reinforcement of masonry structures in service conditions and its latest applications. The research was conducted both experimentally and analytically, first considering the results from a preliminary state of the art investigation and then providing an original contribution regarding the durability and new applications of FRCM.

Based on the literature and existing regulations on fibre reinforcements for masonry structures and their durability in service conditions, it appears clear that although in the past two decades much work has been done on this subject, still very little is known. Specific conversion factors are provided in a Bulletin on Technical Recommendations for Constructions composed by the Italian National Research Council pertaining to service conditions and Fibre Reinforced Polymers (FRP). Although there are currently no specific guidelines regarding the environmental effects on FRCM, these are to be carefully considered and evaluated before designing these systems. The first step towards a better understanding of the physical behaviour of such systems is through experimentation, but experimental investigations on FRCM systems when subjected to environmental conditions are virtually non-existent. Hence the original contributions of this work, as resulting from four experimental campaigns. The methodology of the procedure for durability testing on FRCM analysed in the present dissertation was derived from the literature review of the testing performed on FRP systems. The first two campaigns are directed toward investigating the behaviour of fibres combined with cementitious matrices after they have been subjected to artificial ageing. In the first campaign freeze/thaw cycles are carried out whereas in the second campaign specimens are subjected to wet/dry cycles in sodium chloride solutions. The third and the fourth campaigns regard durability testing on masonry reinforced FRCM subjected to wet/dry cycles, specifically on small pilasters reinforced through glass and steel fibres, and masonry panels reinforced with a new FRCM technique known as Reticolatus.

The conclusions drawn about FRCM reinforcing systems for masonry in this dissertation are able to answer questions about these reinforcements that are important in the renovation and restoration of historical structures, such as how long the reinforcement will be able to function effectively and how much time passes between onset of the degradation of the system and the need for replacement.

In the Appendix, a preliminary non-linear procedure has been proposed for the numerical analysis of masonry panels with the reticolatus technique, procedure which implements the non-linearity of the material in an iterative numerical technique correcting the elastic-linear solution after having evaluated it, step by step, pursuing the final goal of respecting congruence. Every mortar joint is represented in discrete form as a curtain of trusses positioned perpendicularly to the interface of the block and one truss placed in a tangential direction. The trusses perpendicular to the interface of the blocks are able to transmit only compressive strength and therefore the deformations are comparable to elastic cushions interposed between the masonry blocks. The reinforcement is constituted by a mesh made by a steel wire of limited section (ca 1 mm) in such a way that it can pass through the scraped mortar joints and the clutch in the steel bars inserted in the panel. Since the section of the wire is limited it can sustain only tensile strength, and therefore the reinforcement is modelled as a sequence of trusses connected to each other and fixed at the ends on the nodes. FEM modelling was used and an iterative calculus process was proposed for the numerical analysis of this specific type of FRCM. Three model panels were calculated with the proposed iteration model, with random positioning of the reinforcement wire, in order to check the method of the analysis. All model panels were subjected to a diagonal compression impressed only on the upper right corner and then tested. The second step of the numerical analysis was to recalculate the panels using the modified strength values found from the experimental campaigns described above.

Experimental Investigation on the Durability of Fibre Reinforced Cementitious Materials for Strengthening of Masonry

PART I: Prolegomena to the Critical Enquiry

Chapter I: Masonry....3

1. General Overview: properties and characteristics....5
2. Structural Reinforcement: brief historical excursus....7
3. Structural Reinforcement: recent methods....10
    a. Various techniques....10
    b. Fibre Reinforced Cementitious Matrix (FRCM)....13
        • Experimental Research: State of Knowledge....14
        • Codes for Design Calculation....18
    c. Reticolatus....21
        • State of Knowledge: synopsis....21
        • Experimental Testing....24
        • Existing Design Calculations applied to Reticolatus....32
        • Reflections on compatibility and reversibility....36

Chapter II: Durability of Reinforcements....39

1. State of Knowledge....41
    a. Codes and Regulations....42
    b. Durability of Fibres and Resins....45
    c. Durability of FRP reinforced Concrete....51
    d. Durability of FRP reinforced Masonry....58

PART II: New Work

Chapter III: Experimental Campaigns....67

1. Freeze/Thaw durability on reinforced mortar specimens....71
    • Experimental Programme and Materials....72

- Test Set-up and Instrumentation....76
- Results....77
- Conclusions....82

2. Wet/Dry durability on reinforced mortar specimens....83
   - Experimental Programme and Materials....83
   - Test Set-up and Instrumentation....86
   - Preliminary Considerations and Results....86
   - Conclusions....96
3. Wet/Dry durability on brick masonry reinforced pilasters....97
   - Experimental Programme and Materials....98
   - Test Set-up and Instrumentation....101
   - Results....103
   - Conclusions....130
4. Wet/Dry durability on brick masonry panels reinforced through the Reticolatus method....131
   - Experimental Programme and Materials....131
   - Test Set-up and Instrumentation....134
   - Results....136
   - Conclusions....143

Chapter IV: Conclusions....145

Appendix I: Preliminary Proposal for Numerical Analysis Applied to Reticolatus....151

1. A proposed technique....153
2. The FEM Model....157
3. Case Study: Reticolatus Reinforced Panels illustrated in Chapter III.4....162
4. Case Study: Reticolatus Reinforced Panels tested at a Laboratory in Udine, Italy by Prof. A. Borri's research team....167

Bibliography....171

PART I: Prolegomena to the Critical Enquiry

Chapter I. Masonry

1. General Overview: properties and characteristics

The objectives of the present work concern the durability of fibre reinforcements applied to masonry structures through cementitious matrices. As will be treated more in depth in the second section of the present Chapter, the main benefits of FRCM applied to masonry structures lays in their compatibility with masonry itself, as it allows permeability, and in its reversibility when compared to FRP reinforcements. Nevertheless, as background material to enhance the present discussion, a general overview of the main properties of masonry as a building material are described in the following paragraphs.

Masonry has been used as a building material for centuries. One need only consider the Coliseum in Rome or the villas in Pompeii, just to mention the most obvious architectural monuments in Italy, but the examples are countless worldwide. In these historical constructions, masonry does not present itself as a standardized material. In fact, there are many types of masonry which may be found, depending on the location and age of buildings. It is generally constituted of blocks, which may be of natural stone, clay bricks or compressed earth, with or without a layer of mortar interposed, and variations depend on geographic location and age of construction. Masonry is therefore a heterogeneous material, and as documentations as early as Vitruvius' *De Architectura* (ed. 2011) show, both virtues and issues were well known. Vitruvius in fact speaks of a solid part of masonry, which corresponds to what has been defined as the central core of inertia, and of the importance of the blocks in masonry constructions being compact. The Romans in fact believed that the more compact clay bricks were stronger, and brought more stability to the building, and thus they substituted early on the larger natural stones with bricks in larger and more important buildings. Bricks were not only more compact and therefore considered more stable, thanks to the techniques used in their manufacturing, but they were also easier to fabricate than to extract large stones from quarries, and to transport, and finally to lay into place along regular beds lined with mortar. The fact that it was used so commonly as a building material allowed for early on observations of the problems it presented. It was apparent that for high elevations a larger base was necessary in order for the forces to proceed vertically from the highest point of the building down to the ground level. The importance of corners and connections was also noted, as was the danger of humidity in direct contact with the masonry structure constituted of clay bricks, or stone, and the mortar they were bound with, which absorbed humidity causing degradation to the

structure. Many different patterns of assemblage were known to the Romans, but in order to keep this section concise and focused we will briefly mention here only the most relevant assembly techniques used in historical masonry constructions in selected geographical areas.

The *opus quadratum* is the first type of organized blocks of tufa stone, found since the IV century B.C. The blocks, of dimensions ranging from 40 to 60 cm in length, were connected through a thin layer of lime or lime based mortar, but this layer was also commonly replaced by wooden or metal connections in the centre of the stones themselves. Later, the *opus incertum*, a technique which used smaller stones bound together by a stronger mortar, achieved a great popularity. This type of masonry was most commonly used for the facing of an inner core of *opus caementicium*, composed of smaller stones (*caementa*) bound together by the resistant mortar used in the facing. This *opus caementicium* was resistant to the point where it could be used as a building material in and of itself, and became widely used given its ability of assuming new shapes and forms (i.e., vaults). Around the I century B.C., the *opus reticolatum* became a common building technique, using regular square shaped tufa blocks placed at a 45° angle, both as a full wall masonry technique or as facing for the *opus caementicium*. This was a transitional period in building knowledge; whereas before builders needed to devote attention in the horizontality applied to the building blocks, now the technique required a simple assembly, since the tufa blocks used were already in a regular square shape. The weaknesses of this system though were well known; as Vitruvius observed in his *De Architectura*, the *opus reticolatum* was particularly prone to cracking in the mortar joints given the oblique positioning of the stones themselves (Baila et al., 2011). This may be one of the reasons for the introduction of the *opus testaceum*, that is the masonry assembly with rectangular blocks placed in horizontal layers and bonded through the use of mortar. Nero was the first Roman emperor to have entire buildings constructed with *opus testaceum* (Mazzanobile, 2005).

It was certainly known to Roman builders that masonry does not cope well with tensile strength while its resistance to compressive strength is considerably higher. This knowledge was further developed and refined throughout the centuries, and today there are methods of analysis available for masonry structures. However, these methods though do not always apply to historical masonry; in fact, since masonry is a heterogeneous material, and therefore the characteristics of both the bricks and the mortar must be considered in any analysis, its properties also depend on the workmanship. This factor presents endless variables, for example when analysing a historical masonry structural element, the bricks do not always belong to the same period if there was a historical

intervention of consolidation, or originate from the same kiln, or the clay may present a different intrinsic constitution. For this reason and for the purpose of the present work, the main structural characteristics will be briefly illustrated as follows, as an in depth analysis of the structural behaviour of masonry would not be relevant to this excercise.

Masonry works best with compressive strength, and is weak when subjected to tensile strength. For safety margins when designing or calculating existing masonry structures, tensile strength is neglected entirely. When subjected to in-plane compressive strength failure is reached for excessive loads causing cracking, in vertical lines parallel to the direction of loading, and subsequently crushing in the masonry element, both in the bricks and in the mortar layers. In masonry structures which present a central core of cemented material unsuccessfully connected to the external façades, elevated compression forces may cause the façades to detach from the inner core, and then collapse due to flexural forces. Shear strength causes collapse through cracks which form within the masonry assembly at about 45°, involving both the mortar joints, in a step-wise fashion, or both mortar joints and brick units. Out-of-plane loading, for example, which occurs during earthquakes or by thrusts transmitted by arches on walls sustaining the imposts, may determine collapse for excessive shear or flexural strength.

Although this short inventory of the main issues inherent in masonry structures is far from exhaustive, it has attempted to give a clear delineation of the problems which the historical techniques of consolidation were facing, and which are further illustrated in the following section.

2. Structural reinforcement: brief historical excursus

In the V century, after the earthquake of 443 which shook Rome, emperor Theodoric was more preoccupied with conserving and repairing buildings which had suffered structural damage rather than demolishing them (Mazzanobile, 2005). In this specific case, his desire remained a good intention, as it did not prevent many of the monuments of Rome from being ransacked. But it is a testimony to a general attitude towards architectural heritage which may be confirmed in the numerous examples of consolidation throughout the centuries, starting from periods of Roman history which long preceded Theodoric.

In the Roman era the most common consolidation techniques were of two main typologies. The first typology could be considered a repair or maintenance technique, more than consolidation

or actual structural reinforcement, although the end result was similar. In fact, repointing of masonry layers which had been eroded or washed away, or substitution of degraded masonry parts were, quite common. For example, the aforementioned *opus reticolatum* often presented extensive cracking in the masonry joints, therefore parts often required substitution and were rebuilt with the *opus testaceum* technique. But the substitution of old materials with new was not reserved solely to cases of *opus reticolatum*; this was a technique frequently used when degraded masonry was in need of replacement. Substitution of masonry parts was also often carried out when cracking appeared due to shear or flexural strength; the consolidation techniques listed below were not always used due to their cost, mostly for workmanship, so the cracked or crushed parts were sometimes simply replaced with new masonry.

Along the lines of maintenance and repair, the acknowledgement that masonry was subjected to degradation caused by excessive humidity, in particular at the foot of the building, was taken into careful consideration when building or repairing buildings. Special terracotta tiles were found applied to the walls of the Domus Transitoria in Rome, with small extrusions which permitted a constant ventilation of the vertical structure in order to avoid dangerous concentrations of humidity (Mazzanobile, 2005). Another method of keeping the humidity away from the walls used in the House of the Faun in Pompeii consisted in nailing sheets of lead to the walls designed for frescoes; humidity was the first enemy of the brilliant colours fixed onto plaster.

The second reinforcement typology consisted in those structural interventions mainly aimed at eliminating out-of-plane loads. Tie rods were commonly inserted in arches or vaults which had produced thrust against their sustaining walls. The iron rods were inserted in the masonry vaulted system, preferably at the height of the impost, at about 30° from the last horizontal voussoirs or ashlars, and heated in the central section. The rod was then fixed to the external sides of the walls sustaining the vault or arch through the use of anchor plates. The heat would cause the rod to dilate and once the rod cooled down it would shorten, applying an action opposite to the thrust of the arch to the sustaining walls.

The other technique used to eliminate out-of-plane loads was with masonry buttresses. By building large sections of masonry up against the structures which had presented fracturing due to out of plane loads, the new masonry augmented its width in those specific sections, increasing the central core of inertia, or the solid part, as mentioned by Vitruvius. It was common knowledge that, in order to be effective, it was necessary to repeat the buttresses along the entire length of

the building at distances that did not exceed the height of the wall which was in need of reinforcement (Mazzanobile, 2005). Often the buttresses were constructed at an inclination towards the wall subjected to excessive forces because the largest thrust was believed to be at the foot of the wall itself. The function of the buttress could formally be carried out by many different types of structures, all with the same intent of impressing on the wall a force contrary to the one causing structural deficiency. When there was not sufficient space to build thick buttresses, i.e. in between buildings or in small side streets, relieving arches were employed, using as imposts the wall in need of reinforcement and the wall opposite to it. In some cases the operation was repeated several times along the entire height of the building. Another expedient for eliminating thrusts could be found in additional architectural spaces added to the building itself. Porticoes were built in front of buildings when the façades were giving signs of inclining externally, as in the case of Livia's Villa in Pompeii (Mazzanobile, 2005). An entire neighbourhood was built at the foot of the Palatine hill in Rome with the function of a retaining wall; when the small popular houses were removed in the XIX century, freeing the Domus Tiberiana, cracks appeared clearly along the walls of the Roman villa. In 1870, masonry buttresses needed to be applied as structural reinforcement. Another method of increasing the stability of masonry structures was through filling in openings, such as found in windows or porticoes. Again, the knowledge from the I century B.C. indicated that walls should be built over the abovementioned solid parts of the structure and not over openings; in the case of openings beneath the walls, Vitruvius warned builders that the structures would not last long. Hence the filling in of openings where more solid part was needed for the structure above them.

These methods of structural reinforcements were used throughout the centuries with little variation until more recent times when reinforced concrete came into use. Towards the end of the XIX century, the enthusiasm of the new technology spilled into the disciplines of consolidation and structural reinforcement. By the end of the third decade of the XX century, reinforced concrete had almost completely replaced the traditional reinforcement techniques mentioned above (Serra, 2005). Around the same period, a long lasting debate on correct consolidation methods commenced, beginning with the Charter of Restoration drafted during the International Conference of Athens in 1931, where the use of reinforced concrete for restoration purposes was approved. The first precautions on the excessive use of this "new" construction technique were put forth during the Charter of Restoration compiled during the 2nd International Conference of Architects

in Venice in 1964. By this time, innumerable interventions with reinforced concrete in historical masonry structures had been completed.

The insertion in a liberal fashion of reinforced concrete ring beams, beams, injections of concrete grout and reinforced concrete floor slabs, although structurally valid, was soon to be discovered as an incompatible solution for various reasons, among which the aesthetic presence of such element, although this may be easily hidden. The greater problems with these solutions lie in the way that these rigid structures modify the statics of a building from elastic to hybrid, that is rigid in the reinforced parts and elastic in others (Baila et al., 2011a). The earthquakes which took place in Italy in the last decades have in fact proven the restricted efficacy of these types of reinforcements, as valid as they might seem for a limited amount of time, until compatibility issues emerge, or in the absence of seismic activity.

Therefore, new reinforcement methods were needed, which could take advantage of the technological advances achieved in the past three decades but which at the same time respected the fundamental principles of restoration, namely reversibility, compatibility and minimum intervention.

3. Structural Reinforcement: recent methods

In the first part of this section recent reinforcement methods will be briefly introduced, including the well-known Fibre Reinforced Polymer (FRP) system, the first type of fibre applications to structures which preceded FRCM reinforcement systems by about a decade. This last method, object of the durability study of the present work, will be discussed in the second part of the present section, and a brief inventory of experimental work carried out on FRCM masonry will be summarised.

a. Various Techniques

Grout injections and steel rod reinforced grout injections are still a common practice in structural reinforcements (Baila et al., 2011b). Although these methods consist in the insertion of a rigid system in an elastic structure, they still seem to be the most effective in the cases of masonry facing and cementitious inner cores which have detached. The grout, which can be cementitious, resinous or of inorganic material, acts as an adhesive between the detached layers of masonry

and cementitious materials, which have often become loose in time. The insertion of steel rods in holes prepared in the same way as for simple grout injections increases the resistance of the reinforcement. However, it is neither a reversible nor a minimally invasive technique.

Small tie rods inserted in holes drilled in the thickness of masonry walls work best in cases of several leaf walls, or walls with inner cores of cementitious conglomerate: the principle of the method is the same as the tie rods used historically to eliminate out-of-plane loads, with the exception that they are used to hold together portions of walls which have lost the effectiveness of their connections or never possessed connections at all. At the extremities of the rods, that is on the external sides of the wall they are inserted in, the traditional anchor plates are replaced by nuts. They may be subjected to a certain amount of pretension, resulting immediately effective after application. Although this method may be considered compatible, the drilling of holes in an already weakened masonry is less than minimum intervention.

Reinforced concrete headers may also be used in the case of masonry walls with inner cores of weakened and non-cohesive material; in order to create the headers a portion of the wall must be removed in order to allow for the allocation of the steel reinforcement and the pouring of the concrete mixture (Baila et al., 2011b). This is a highly invasive and irreversible technique, although effective for shear resistance, for which reason it may be considered useful for certain types of minor architecture.

The use of steel welded meshes applied to the entire height of walls can be further enhanced by the insertion of carbon or aramid fibre rods in the walls in need of reinforcement, moulded in such a way that they clasp over the steel mesh. The entire system is structurally effective, but causes a profound alteration the original structure in terms of section, physical properties of the structural element, ductility of the original structure and vulnerability to corrosion. This type of intervention is not applicable in cases of historically relevant architectural buildings.

Steel tie rods are still commonly used in masonry structures and in the case of columns or pilasters the hooping of these elements through metal rods seems to be a valid alternative to grout injections. The hooping may also be used in combination of the grout injections given that there is no real way of ascertaining the level of penetration of the injected material into the vertical masonry elements. In the case of steel hooping used in the absence of grout injections, this reinforcement method is reversible, compatible and considered a minimum intervention. In fact, if future events were to require the removal of the hoops this would be possible without leaving

permanent damage to the structure. In the case of consolidation interventions which used a combination of metal hooping and grout injections, then the technique is as irreversible and invasive as the injections themselves.

From this brief review of more recent reinforcement techniques with respect to those which designed the addition of reinforced concrete structures it is possible to understand the difficulties today's architect or engineer is faced with when structural reinforcement is required in a historical, and even more complex, in a monumental, masonry building. Of course, traditional techniques such as tie rods, buttresses and replacement of cracked or damaged masonry with new or even historical parts which are intact, are always an option for current consolidation techniques. But in some cases the traditional techniques do not bring sufficient stability to the building, or are not as accurate in their results as more recent albeit more invasive techniques.

The issue of guaranteeing structural stability, while not increasing the masses of the structure as buttresses might, and at the same time with easier and swifter application, was considered close to solved when materials borrowed from the aerospace industry were used in civil engineering. In fact, carbon and aramid fibres were in use since the early 70's in aerospace engineering to repair local damages on aircrafts. About two decades later the technique of applying fibres to structures through the application of epoxy resins (Fibre Reinforced Polymers, FRP) was used in civil engineering as well, giving a start to extensive experimental campaigns, analysis and regulations regarding their use. This material is considered to be a composite material, being constituted of two elements, fibres and matrices, frequently resinous, which, when combined, give the desired effect of reinforcement. The fibres are the element which take on the structural function, and the matrix is the medium through which forces are distributed from the original structure to the fibres. The fibres generally consisted in glass, aramid, carbon and basalt, while matrices were mainly epoxy resins. The first applications of FRPs were primarily to reinforced concrete, such as applied to bridges and beams in reinforced concrete buildings. Soon after the first applications on structures came the concern for the durability of FRP reinforced structures, a topic which will be analysed in *Chapter 2: Durability of Fibre Reinforcements*. By the end of the XX century, FRP was being used in the reinforcement of masonry structures as well, both new and historical. The most acknowledged advantages of FRP reinforcements consist in the highly elevated strengths of structures thus reinforced compared to the unreinforced structural elements, their light weight and ease of application.

Again the issue of reinforced structures arose, that is the transformation from sole masonry structures to hybrid ones, where the fibre reinforcement would produce areas of more elevated resistance than the unreinforced elements in the same structure. Textile fibre reinforcements using carbon FRP, or CFRP, and aramid FRP (ARFP) confer additional tensile strength in the structures they are applied to with a negligible addition of dead loads compared to masonry structures with traditional concrete reinforcements. In fact, the extra mass added by reinforced concrete members in existing masonry structures modifies the dynamic response of such reinforced buildings due to the increased seismic forces.

The real problems with FRPs, both on concrete and masonry structures, consisted in the damage caused to the original structure itself after the fibres were called into action by excessive forces. In fact, experimental campaigns revealed how, in many cases, once the forces were no longer sustained by the masonry or concrete structure, crushing commenced, arriving to total damage of the structure if loads continually increased. Another issue of FRP reinforcements consists in the ripping effect which may occur with debonding; if forces are excessively elevated or concentrated in one specific section, the FRP system may detach from the structure. In many cases, the detachment of the FRP strip carries off significant amounts of material of the original structure, given the elevated adhesiveness of resin matrices. This effect is exceptionally damaging, especially to masonry structures. Furthermore, the non-permeability of the resin matrices can lead to dangerous concentrations of humidity in the masonry structure underlying the reinforcements, leading to other types of damage, such as mould (see *Chapter 2: Durability of Fibre Reinforcements*). Nonetheless, FRP have been widely used in reinforced concrete and masonry, both in new and historical and monumental, structures in the past twenty years. However, the disadvantages of FRP reinforcements lead research in the direction of a similar technique that presented a more compatible and reversible solution for historical structures, for which the risk of being more damaged than helped by the reinforcements was a real concern. This solution is in the application of Fibre Reinforced Cementitious Matrices, or FRCM.

b. Fibre Reinforced Cementitious Matrix (FRCM)

With the replacement of resinous matrices with cementitious types of adhesives, the compatibility issue of applying fibres to historical structures was considered resolved. This of course depends

greatly on the type of cementitious matrix used in the composite reinforcement, as some of the more recent inorganic matrices still prove to be capable of ripping and limited permeability. The strength acquired by the structure reinforced through FRCM systems is somewhat less than that given by FRP. At the same time, FRCM does seem to be a more compatible reinforcement, and according to the type of application, failry reversible, a quality completely missing from FRP materials. Following is a brief state-of-the art on the experimentation carried out on the validity of FRCM reinforcements.

Experimental research: state-of-knowledge

As previously stated, FRP systems have many advantages in structural retrofitting of masonry structures. However, preservation requirements have conducted researchers to investigate the effects of FRCM systems as a valid alternative to their resin matrix equivalents.

In Prota et al. (2006), the in-plane behaviour of masonry tuff walls reinforced through a cementitious mortar grid (CMG) was analysed. Fibres were glass-aramid textiles, while the mortar matrix used was a readymade cementitious mortar with the addition of an acrylic fortifier. Different reinforcement layouts were used on the tuff masonry walls, such as one sided reinforcing, one or two-ply strengthening on both sides of specimens, and after an adequate curing time, the specimens were subjected to diagonal compression loading according to specifications contained in ASTM E519-81. Results were then compared to unreinforced specimens. It was concluded that the CMG reinforcement system increased shear strength of reinforced walls noticeably, in particular in the two-ply specimens, while also increasing ductility compared to unreinforced specimens. All specimens maintained structural integrity at failure, the most important safety characteristic for reinforced structures.

The efficacy of Textile Reinforced Mortar (TRM) was experimentally investigated by Papanicolaou et al. (2007) on three different brick apparatuses, simulating brick walls, brick pilasters and brick lintels. The various configurations all presented control specimens, one and two-ply textile reinforced mortar specimens as well as one and two-ply polymeric epoxy matrix reinforced specimens for result comparison. Fibres consisted in high strength carbon roving, the cement mortar matrix had a 10:1 ratio of polymers by weight, and a two part epoxy adhesive was used for the FRP system. Testing was conducted for both compressive and shear strength in the brick wall and pilaster specimens, whereas flexural testing was conducted on lintel simulating specimens. Con-

trol specimens were loaded monotonically, while reinforced specimens were tested cyclically under in-plane loads. Results proved that TRM retrofitting increased the resistance of the specimens effectively compared with unreinforced masonry apparatuses, albeit about 65-70% less than their equivalent FRP configurations. On the other hand, TRM reinforced specimens presented a much more elevated deformability, of high importance when considering the reinforcement of structures subjected to out-of plane loading (i.e. seismic activity).

Papanicolaou et al. (2008) continued the extensive testing in exactly that direction on brick wall specimens subjected to out-of-plane loading. In this case, the brick specimens simulated only pilasters and lintels, and the out-of-plane loads were positioned for failure planes parallel to the bed joints in the first case and perpendicular in the second. As in the previous study for each specimen type both TRM and FRP reinforcements were applied, with one or two plies of fibres of bi-directional carbon roving. As in the previous study, loading was monotonic in the control specimens and cyclic for reinforced specimens. For the specimens simulating masonry piers or pilasters, the TRM reinforcements were particularly effective, more so than the FRP systems by about 22% for one-ply reinforcements, and 17% in the case of two plies. Also, TRM jacketed specimens are less stiff than their FRP counterparts, endowing the system with a higher degree of deformability. In the case of lintel simulating specimens, while TRM is still an effective reinforcement system when compared to the unreinforced control specimens, FRP jacketing presents higher strength (by about 20%) and deformability (about 15% at failure). The authors attributed the difference in the values of TRM versus FRP in the two different specimen types to failure mechanisms which involve tensile fracture of the textile reinforcement in lintel simulating specimens.

Although in this present work attention is mainly directed towards examining the success of FRCM systems applied to masonry, following is a study conducted on FRCM reinforced concrete. In Hashemi et al. (2008) the effectiveness of cement based bonding material for fibres was tested on concrete beams. Four different types of cement mortar matrices were used, consisting in a simple cement mortar without additives and silica fume, latex or micro-cement modified mortar. Results showed how all FRCM systems improved load carrying capacity of concrete beams when compared to unreinforced specimens.

Returning to masonry reinforcement, Augenti et al. (2011) conducted an experimental campaign on a tuff masonry specimen intended to simulate the behaviour of a wall portion with an opening (i.e. a window, door, etc.), and tests were directed towards verifying whether the weak span-

drel obtained improvement from FRCM reinforcement after damage had already occurred in the structure. The specimen used in the present experimentation underwent three different testing phases; a first phase was tested as built, under monotonic vertical and horizontal in-plane loads. A second phase consisted in the cyclic loading of the panel repaired through repointing where cracks had appeared during the first testing phase. The third phase of testing was conducted with a cyclic loading on the specimen with glass fibre and cementitious matrix jacketing applied to both sides of the spandrel and to the joint areas between the spandrel and the piers. Observations after the last phase of testing showed spread cracking in the reinforced area, indicating an even distribution of stresses due to the good anchorage of the mortar matrix to the tuff masonry wall. Results confirmed that the inorganic matrix grid (IMG) not only restored the strength of the masonry wall to the levels it presented as built, but degradation also occurred at more severe displacement values. Given the in-plane nature of the forces applied to the structure, debonding did not take place in this campaign, avoiding therefore damage to the masonry substrate and abrupt collapse mechanisms.

In Parisi et al. (2013), again tuff masonry was reinforced through different glass fibre IMG layouts and tested under diagonal compression as specified in the ASTM E 519-07 document. Three series of reinforced panels were tested and results were compared to as built unreinforced specimens. The three different layouts consisted in double-sided IMG strengthening, single-sided IMG strengthening and single-sided strengthening with steel FRP ties inserted in the masonry and folded over the glass fibres. The observation of the physical models after testing highlighted how no specimen displayed debonding of the reinforcement system, and slight out-of-plane bending occurred only in one sided strengthening systems. This effect was noticeably reduced in the specimens with SRP ties, and disappeared completely in two-sided strengthening systems. The ductility of the masonry walls increased in particular where the SRP ties were present, an important quality needed in seismic resistant structures.

In Balsamo et al. (2013), testing was conducted on reinforced concrete beams, strengthened with both traditional composite systems, i.e. carbon laminate with epoxy resin, and SRCM (steel reinforced cementitious matrix). The specimens were then subjected to four point bending. Results show that both reinforcements increase the flexural load carrying capacity in comparison with the unreinforced specimens, and although the net areas of the steel fibre reinforcement was half that of the carbon laminate, the SRCM reinforced beams displayed a failure load only 20% lower than that of the CFRP reinforced beams.

Differently to what has been reported so far, De Santis et al. (2014) conducted an experimental campaign on the tensile strength of glass-aramid textiles with four different mortar matrices, as opposed to the behaviour of structural elements reinforced with FRCM systems. One natural hydraulic lime mortar was used, and three mortars containing various binders. Results indicated that under tension FRCM systems undergo three phases, un-cracked, crack development and crack widening. The prevalent collapse mechanism consists in the crack development phase, where strong load reductions were reached.

Continuing along in this investigation technique, De Felice et al. (2014) carried out uniaxial tensile FRCM coupon testing and bond tests on brick and stone substrates. Steel, carbon and basalt fibres imbedded in cementitious mortars are used in the coupon testing, and results of this first part of the campaign confirmed the three phases determined in De Santis et al. (2014), that is uncracked, crack development and crack widening, indicating that the contribution of the mortar matrix is prevalent in the first two stages, whereas in the crack widening phase the stiffness and the ultimate tensile strength of the composites are very similar to the values of the fibres alone. Regarding the experimentation on the bond between FRCM systems and the substrate they are applied to, the same types of fibres as in the coupon testing were used. Failure modes were divided into three different typologies, that is, debonding at substrate-matrix, debonding at the fibre- matrix interface and slipping of the fibre from the matrix. The first failure mode was found to be more common in short anchorage lengths of SRG reinforcements, while the second and the third failure modes were more common for long anchorage lengths of carbon and basalt fibres, due to the difficulty of complete penetration between fibres and matrices. In closing, the higher bond performance was found in those reinforcement systems which presented higher mortar strength and stiffer textiles and on substrates which had been suitably prepared, for example through sand-blasting techniques. Unfortunately, it is not always possible to adequately prepare the substrates with such techniques, as they may prove excessively aggressive for historical and monumental masonry.

Through this brief excursus of the experimentation conducted so far on FRCM systems, it is clear that although the elevated values of load carrying capacities of FRP systems are not always levelled by their cementitious matrices equivalents, their application always increases the performance of structures in comparison with their unreinforced state. Furthermore, the possibility of using compatible materials is in compliance with requirements of restoration techniques of historical masonry. Although the degree of reversibility has still to be investigated and determi-

ned, the experimentation analysed up to this point has shown that in the case of debonding the substrate-matrix interface is often not part of the reinforcement system involved. The fact that the masonry surface possibly could remain intact is a factor that should not be underestimated in the case of reinforcements of monuments.

Codes for Design Calculation

One of the major issues architects or engineers must face at the present time is the design of an FRCM reinforced masonry structure, without specific design codes for calculation or guidelines. In fact, the codes and guidelines which are currently used in experimentation and structural reinforcement have been borrowed from those documents concerning FRPs. There is a formulation of a document referring to the use of FRCM's in construction within the Italian National Research Council, but this document has not been approved at the time of this writing. Therefore, at the moment two documents in particular are useful in that they provide a sense of the verifications which need to be completed on a reinforced structure, the CNR-DT 200/2004, and the National Italian Guidelines of 2012 on the "*qualifications and acceptance control of fibre reinforced composite materials for the structural consolidation of existing structures*".

The CNR-DT 200/2004 Bulletin compiled by an Advisory Committee on Technical Recommendations for Constructions, put together by the Italian National Research Council, is a detailed guide for application and use of FRP's on reinforced concrete, pre-compressed concrete, and masonry structures. Its contents vary from the definition of FRP's, to technical calculations one should use during their design and application, to their durability (as more explicitly described in *Chapter II: Durability of Reinforcements*). The first part of the document, in fact, consists in the definitions of FRP materials, and what fibres and matrices are part of this reinforcement composite. Within this part, specifically in section 2.2.3.3, other types of matrices are acknowledged: "*(...) the use of inorganic matrices (cement-based, metallic, ceramic, etc.) for production of fibre-reinforced composites for construction is rapidly growing. Even though they are not discussed in this document, their use is deemed possible when accompanied by suitable technical documentation and experimental validation to prove their effectiveness*". Therefore, in the case of a reinforcement proposal containing FRCM, the project must be equipped with sufficient experimental data to prove the validity of the proposed method.

The second part of the Bulletin is dedicated to the application of FRP systems on reinforced con-

crete and, finally, masonry. The first part of the design considerations are not of particular interest to the present work, given that they are specific to the FRP reinforcement of concrete structures. Consequently the indications contained in section 5 of the Bulletin (Strengthening of Masonry Structures) will be described here. Interestingly, the use of these reinforcements on historical and monumental architectural heritage is acknowledged, but in section 5.1.2 the code recites: "*Strengthening of historical and monumental buildings shall be justified only when inevitable; the adopted strengthening technique shall be in compliance with the theory of restoration*". To this regard, the document refers to section 3.1.3: "*If FRP strengthening concerns structures of historical and monumental interest, a critical evaluation of the strengthening technique is requires with respect to the standards for preservation and restoration, the actual effectiveness of the strengthening technique shall be objectively proven, and the adopted solution shall guarantee compatibility, durability and reversibility.*"

In sum, the experimental campaigns conducted to this point on the reinforcement of historical structures through the use of FRP have objectively proven that the principles of compatibility, durability (see *Chapter 2: Durability of Reinforcements*) and reversibility are not respected. Nonetheless, as better described in the second part of the following section, the calculations referring to FRP use on masonry structures in the CNR-DT 200/2004 have been useful as comparison methods for calculations on FRCM systems. The Bulletin, in fact, gives indications on safety requirements (section 5.4), strengthening of structural members with single or double curvature (section 5.5), confinement of masonry columns (section 5.6), and design for seismic applications (section 5.7).

The objectives of the 2012 guidelines mentioned above consist in the qualification and control of composite FRP materials made of glass, carbon or aramid fibres and polymeric matrices. The document takes into consideration the drafting of guidelines for FRP composites which use fibres such as steel, PBO or natural fibres, but these materials would need to be equipped with technical documentations which prove their compliance to technical construction standards. These guidelines are specifically directed towards FRP qualification, and as described above for the CNR-DT 200/2004 Bulletin, when considering FRCM materials architects and engineers involved in the design of such retrofitted masonry structures may draw on the indications contained here. In this specific context of durability of reinforcement systems, the indications given by the guidelines regarding environmental durability are worth mentioning. The following criteria were meant to

be applied to coupons of FRP, that is, the fibres with their (resin) matrices.

Freeze/thaw cycles are defined in the guidelines as a 20 cycle process. Each cycle is defined by 4h at a -18°C temperature alternated with a 12 h period at +38°C temperature at 100% R.H. At the end of the cycles carried out with these indications, a first visual observation is required in order to evaluate if superficial alterations took place, such as erosions or micro cracking due to the freezing of water particles within the FRP, expanding during the 4 h at -18°C. This observation is particularly important in cementitious matrices due to the role of water during freeze/thaw cycles. As the water in moist cementitious materials freezes, it expands about 9% its original volume, producing pressure in the pores. If the pressure developed exceeds the tensile strength of the cementitious matrix, the cavity will dilate and rupture. The accumulative effect of successive freeze-thaw cycles can eventually cause esuperficial alterations such as cracking, scaling, and crumbling of the concrete, effects notable during visual observation. Once thermal cycling is complete, specimens are then subjected to tensile stress in the direction of the fibres. The process is considered to have a positive outcome if the tensile values of the aged specimens do not decrease more than 15% when compared to un-aged specimens during testing.

For ageing which involves humid, saline or alkaline environments, the specimens should be exposed through immersion of 1000 hours. For resistance to humidity the prepared environment is to be at a temperature of 38°C and 100% R.H. For resistance to saline environments, immersion should be at a temperature of 23 ± 1°C, whereas alkaline environments require immersion in a solution with a pH level of 9.5 or more at 23 ± 2°C. Again, visual observation should be carried out for the assessment of degradation such as erosion, micro cracking or peeling. As for freeze/thaw cycles, aged specimens should conserve at least 85% of their resistance values compared to un-aged ones.

The guidelines also specify important mechanical properties FRPs should have both when pre-impregnated, that is, when fibres are already inserted in their matrices in the form of laminates, and when prepared in situ. The description of how these properties can be tested in laboratories following certain standards, and which documents suppliers should provide the composite materials with at the distribution phase is also reported, along with acceptance controls to be conducted in building sites and how to determine equivalence with imported products.

Although the Bulletin and the guidelines described here are not specific to FRCM reinforcement systems, they do provide, in parallel, useful indications for professional figures in the case of

structural retrofitting with fibres in cementitious matrices. There is a certain confidence that the experimental testing which is currently being conducted on FRCM reinforcements will constitute a bibliography for the draft of standards specific to these newer materials.

In the present research, together with the durability study of FRCM systems applied with a traditional method, that is, through cementitious matrices applied to the surface of the structure and reinforcement textiles applied to the cementitious matrix, the application of which is then repeated, a recent development of FRCM is analysed. In the following section this method, called reticolatus by its inventors, is described and analysed, in *Chapter III: Experimental Campaigns*, panels reinforced through this method are tested for wet/dry durability and in *Chapter IV: Numerical Analysis applied to Reticolatus*, a numerical method is tested on models of panels with this type of reinforcement.

c. The Reticolatus Method

State of Knowledge: synopsis

The reinforcement we intend to analyse in the present dissertation is a typology conceived by the research group at the University of Perugia lead by Prof. A. Borri. As is common knowledge with regard to fibre reinforcements, fibres of small dimensions are easily found on the market as mats, or textiles, and in the case of steel fibres, as unidirectional sheets which can vary in length. Unidirectional fibres such as steel fibres are glued on to a net made of polypropane (Fig. 1.3.3), a thermoplastic polymer, reasonably resistant yet flexible material for which it has been chosen as an engineering plastic, or polyester. The steel fibres most commonly found in commerce are produced by Hardwire llcc. and distributed in Italy by Fidia s.r.l., in braided threads composed of a minimum of 3 to 5 single filaments, as may be seen in Fig.s 1.3.1-2. This allows the single fibre

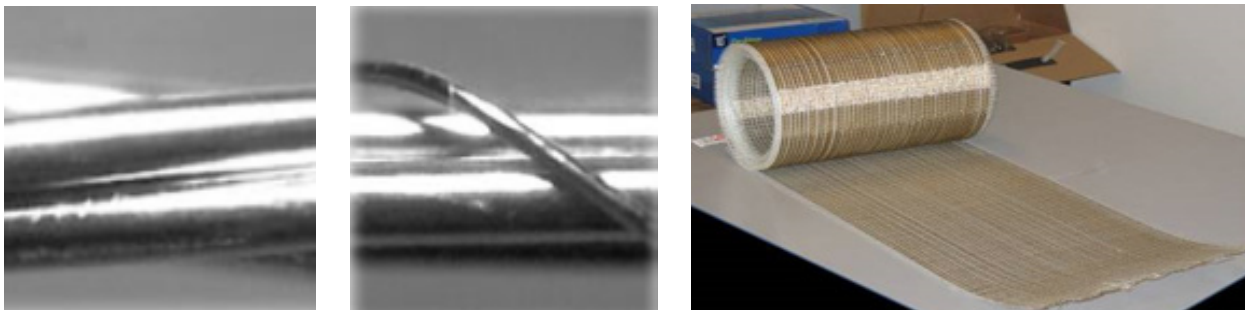

Figures 1.3.1-3. Types of steel fibres distributed by Fidia s.r.l.: 3X2 cord and 3SX cord. A coil of type 3X2 cord.

to be very flexible and adaptable to surfaces of various shapes and form while at the same time maintaining a certain stiffness characteristic of the material.

Recently, other companies such as TECI s.p.a. have produced stainless steel ropes which can be used for reinforcing purposes in historical structures, being composed of wires in variable number and diameter. In the technique proposed by Prof. A. Borri and his research team, the filaments or ropes are used singularly, detached from the polymeric net they may have been originally glued to and are placed in the structure, be it brick or stone masonry, of regular or irregular construction, within the thickness of the mortar layers, a part of which has been previously removed to accommodate the steel wires. Usually the process of mortar removal from structures proves to be considerably easy since historical mortars are often brittle and crumble at touch. These single fibres are then drowned in a new layer of mortar and anchored to the structure in such a way that the created mesh is subjected to a tensile effort. This anchorage, often obtained through rebars or riveted steel bars that occupy the entire width of the structure, has proven not to provide any relevant pretension in the structure itself. If the mesh on one side of the structure is united by anchoring bars to a similar mesh placed on the other side of the structure, the reinforcement then works as a cage. The steel mesh created in this way can also be connected to foundations, if there be the need, and to the ring beam if one is present at the top of the structure being reinforced. The masonry wall reinforced with such a procedure doubles its tensile strength with respect to the original capacity of the structure, without excessively increasing its stiffness. In Fig. 1.3.4, a hypothetical reinforcement through the Reticolatus technique is shown applied to irregular stone masonry. The anchoring bars

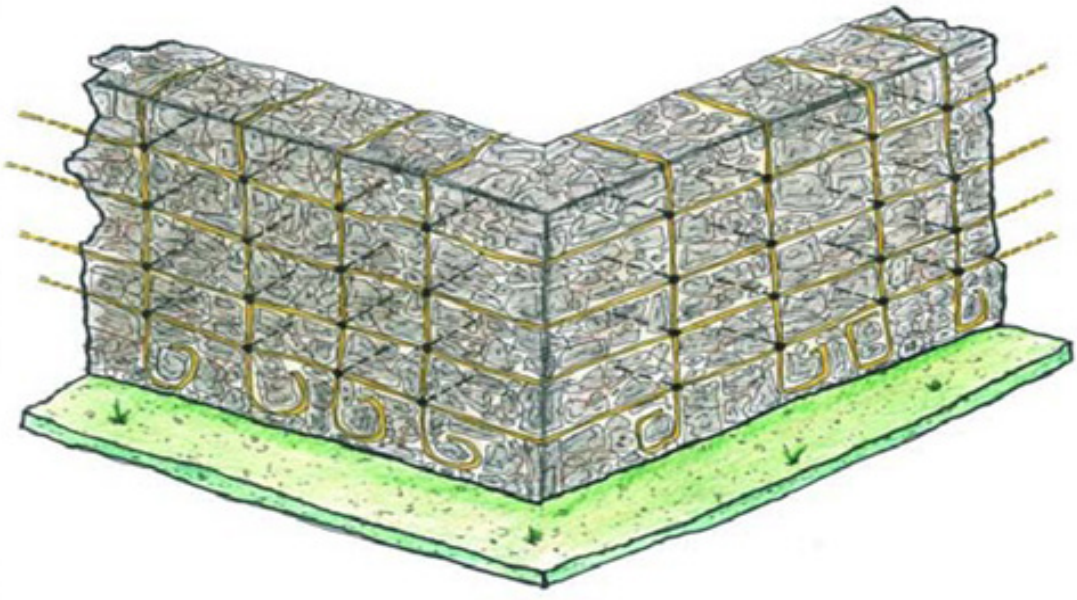

Figure 1.3.4. Reticolatus applied to an irregular stone masonry structure. Image taken from Borri et al. (2010a)

in this case cross the entire width of the stone masonry, which is possible in cases of poor masonries built with a high mortar to stone ratio. This consolidation system may be applied on masonry or stone structures without altering the aesthetic quality since the mesh is placed in the mortar fillers and is also covered with mortar itself. The reinforcement is thus hidden in the structure. This method of reinforcement could therefore prove to be a valid alternative to composite materials in situations in which the reinforcement should not be seen at all, such as in buildings of historical or architectural value. In Europe a large part of the architectural heritage consists of monumental masonry buildings, many of which are in need of maintenance or consolidation to ensure the survival of the historic evidence they represent, and to guarantee safety conditions for those who still use or visit them today (eg. Domus Aurea, Pompei). With today's technologies it is important that consolidation materials rehabilitate a structure at risk without altering its architectural or aesthetic qualities. Equally important is the advancement of knowledge of consolidation materials so that informed choices can be made in their application. Better choices must be made even for those buildings which are not necessarily architectural treasures, but which are part of a complex whole, where if single pieces are lost, the whole is jeopardized. Such is the case of the city of L'Aquila where, following the 2009 earthquake, the buildings of the historical centre were declared unsafe and the inhabitants where forced to evacuate.

The reticolatus technique also enhances connections between horizontal and vertical structures which may have weakened in historical centres or in areas hit by earthquakes. Italian legislation, in the promotion of the new regulations which constitute the NTC 2008 (D.M. LL. PP. 2008), has highlighted how the collapse mechanisms of building portions constitute a critical aspect of historic constructions. For this reason legislation has promoted the evaluation of seismic risk and degree of stability completing the global analysis of buildings with localized analysis to prevent potential collapse mechanisms. These critical areas are usually identified by the absence of connections between the resistant elements of the construction, for example between vertical elements such as walls and horizontal elements, such as floor slabs or foundations. The absence of connections may also be found between multiple panels constituting a single wall built without the use of diatonic elements.

For this technique, as mentioned above, a removal of the most superficial layer of mortar is necessary in order to insert the steel fibre in the layers between the joints. The procedure of removing a superficial layer of mortar in brick masonry and its subsequent replacement with new mortar en-

dowed with enhanced mechanical qualities given by its age and thanks to technological advances, also by its composition, is not new; it was iknown to builders for centuries that mortar if exposed to difficult environmental conditions for long periods of time would eventually loose adhesion and crumble or detach itself from the masonry facing. The loss of portions of mortar was the first step towards losing entire pieces of the masonry structure. Without the "glue" which not only kept the bricks together but consented a correct structural functioning of the masonry typology – that is a dispersion of compressive strength evenly throughout what may have been vertical or vaulted elements in a building – a domino effect of other small detachments could commence. When a building façade was to be restored, in the past as often as in the present, this included what is called a repointing of the mortar between the layers of brick or stone, i.e. replacing the old and brittle mortar to about 6-8cm in depth with a newer and more resistant filling. This method has been proven by experimental testing (Corradi et al., 2008) to be a good reinforcement in and of itself, as a new layer of mortar increases shear strength as a consequence of good adhesion between bricks, allowing for forces to flow through the structure without creating dangerous concentrations of stress in one area rather than another. It is also a valuable alternative to resin injections given the incompatibility of these materials with masonry in time. Repointing works particularly well in multiple leaf masonry, where the outer layers have lost connection with inner leaves. The effectiveness of this repair method is however limited in walls which present elevated thicknesses.

Experimental testing

The first campaigns designed to test the efficacy of the reticolatus technique were carried out mainly after April 2009, soon after of the above mentioned earthquake which severely damaged the historical centre of L'Aquila, in the Abruzzo region of Italy. Here in fact, taking advantage of the program of demolition of dangerous and unsafe buildings laid out by the municipal authorities, it was possible to use real models on which in situ destructive tests could be performed (Borri et al., 2010). These tests were brought out on masonry panels of buildings programmed for demolition, some of which had been reinforced for the occasion with reticolatus. The experimental campaigns were carried out through vertical and diagonal compressive strength tests, with hydraulic jacks, and flexural tests. Subsequent to a first verification of the validity of the method, more campaigns were programmed. Vertical compressive tests (Borri et al., 2009) were performed on portion of 14th century walls in the town of Trevi, near Perugia, in the Umbria Region of Italy.

In this case, the masonry constituting the city walls is a triple-leaf type limestone masonry, made of elements of roughly 18cm of length connected with lime mortar. Many problems can arise when dealing with multiple leaf historical masonry, deriving from poor connection between the leaves, or more often no connection or diatonic elements at all, and the poor quality of the mortar between the vertical layers. Triple leaf masonry can represent in fact an example of masonry walls where the repointing technique could be considered inconsequential.

Five portions of the city walls of Trevi were tested for vertical compression, measuring c.a 50 cm in height each. Hydraulic flat jacks were inserted in slits cut in the masonry previously made to accommodate the jacks, which were operated manually. Mechanical gauges were applied to the portions of masonry to measure the deformations obtained during testing, placed at an original distance of 30 cm from one another. The first portion of masonry was tested without reinforcement, as a control specimen for the original resistance of the masonry. In fact, when testing triple leaf masonry with flat jacks, the inner leaves of the structure are not involved in the effective testing, as the flat jacks themselves reach only a certain predetermined depth in the masonry. The first unreinforced specimen tested serves as a good comparison for the results obtained with reinforced masonry. Of the four remaining portions tested, two were simply repointed with new mortar, of known flexion and compressive strength, and two were reinforced using the reticolatus technique, with a quantity of cord of 12 m/m^2. The results of the stress – strain diagrams were very positive with regard to the reticolatus technique, given that the compressive strength of the reticolatus reinforced wall portion tested amounted to over 110% of the compressive strength of the unreinforced wall portion. As mentioned above, deep repointing is also considered a good reinforcement, and proved here to provide the structure with 40% more compressive strength than the same unreinforced wall portion.

Two interesting facts can be highlighted from this series of testing, and specifically in the failure mode and in the variation of elastic moduli of the structures tested. The failure modes of the non-reinforced and deeply repointed specimens were altogether very similar, displaying a small number of large vertical cracks until failure occurred. The reticolatus reinforced masonry specimens instead show a considerable increase in the number of cracks but with a diminution in their size. This is a factor which repeats itself in the numerical model analysis which has been carried out in the following pages of the present work. The elastic moduli instead appeared to the authors of the experimental campaign to be quite scattered, and this fact was attributed to both the fact

Figures 1.3.5-7. From left to right, masonry form the panels tested in Pale, Foligno and L'Aquila. Image taken from Borri et al. (2010).

that with hydraulic jack testing only the outermost leaf is fully loaded and that the stones in each portion were variable in length as in height, so in some cases there could be a higher/lower stone to mortar ratio, hence modifying the elastic modulus of each specific test not necessarily due to different reinforcement techniques.

The diagonal compression tests were completed according to the ASTM Standard E519-10 (Standard Test Method for Diagonal Tension (Shear) in Masonry Assemblages, American Society for Testing Materials, 2010), in which diagonal compression is used to simulate shear tensions in structures. For a first series (Borri et al., 2010), nine stone masonry panels were set up for on-site testing, extracted from three different buildings in Pale and Foligno (in the Umbria Region of Italy) and L'Aquila in the Abruzzo Region. The buildings belong to different historical periods, but have in common the construction technique of rough cut stone masonry. In Fig.s 1.3.5-7, the three different irregular stone masonry typologies are shown, respectively, from left to right, in Pale, Foligno and L'Aquila. All panels were cut to a size of about 120x120 cm as required by the ASTM Standard E519 10, and were free on all sides with the exception of the side (lower left hand corner) to which they remained attached to the original structure by about 70 cm. The panels in Pale are of the most interest in this case, as there are comparative results for unreinforced, deep repointed and reticolatus reinforced panels. The thickness of these panels varied between 52 and 53 cm, and the double leaf masonry comprehends roughly cut travertine, white limestone and solid bricks, connected by a lime based mortar, but no apparent connection between the two leaves. The structure was in a degraded state, with cracks in the mortar and loose elements. Once the testing was completed, cylindrical samples of the white limestone and travertine stones were taken for compression tests, from which a mean compressive strength greater than 35 MPa was found for all specimens.

The test set-up consisted in metal beams attached to the upper right and lower left corner of the masonry panels, connected by steel bars. A hydraulic jack attached to one of the corners applied stress to the structure through a manually operated pump, loading and unloading the structure with increases of 10 kN until failure occurred. Four displacement transducers measured deformations on both sides of the panels. In the panel reinforced with the reticolatus system, steel fibre was placed on both sides of the panel, and transversal steel bars were used as locking devices for the cords. This prevented the separation of the masonry leaves during testing. The repointing both for the reticolatus reinforced panel and for the deep repointed panel was of the same type as the mortar used in the vertical compression tests. As in these previous tests, both the repointed and the reticolatus panels showed significant improvements in shear strength, with 170% increase for the panels reinforced with steel cords and a 70% increase for the repointed panels. Again, the failure mechanism for unreinforced and repointed panels are similar, as all stones resulted undamaged and the cracks were all contained in the mortar joints, simulating the 45° angle that shear stress crack align to. The failure mechanism for the panel reinforced with the reticolatus technique resulted in a debonding in some areas of the cords from the mortar, in areas where the cord locking device was not present and which involved in diagonal mortar cracks. The shear elastic moduli of these panels showed a less significant increase in the case of the reticolatus reinforcement than in the repointed panels, a fact probably due to the quality of the new mortar, compared to which the original mortar presented a higher stiffness.

A second series of diagonal compression tests (Borri et al., 2013) were completed on three different types of masonry panel in a Laboratory in Udine, in the Friuli Venezia Giulia region of

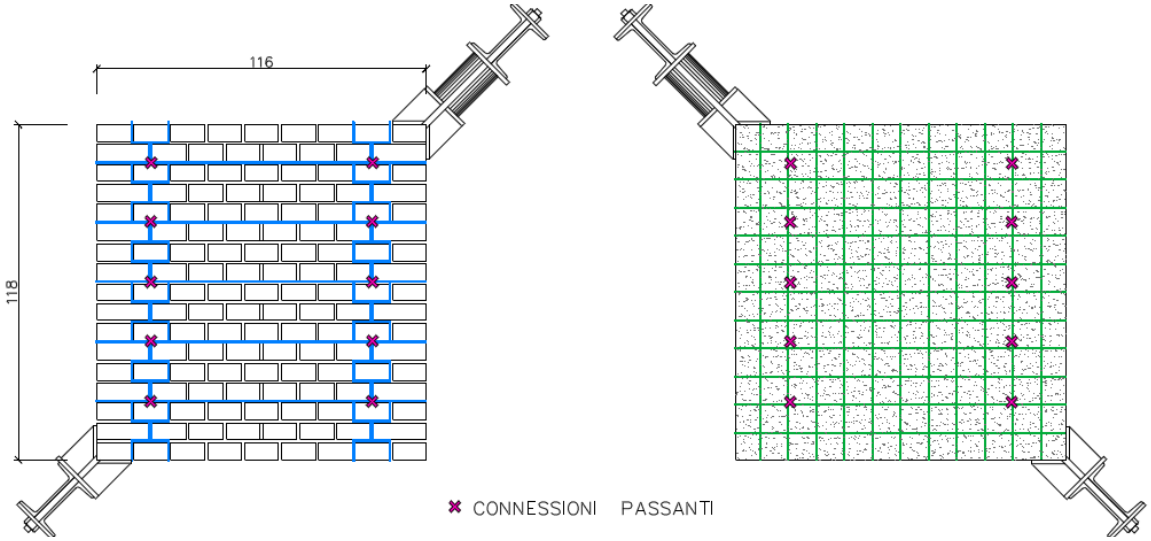

Figure 1.3.8. Reinforcement design of the brick masonry panels; to the right the panels reinforced with both horizontal and vertical steel cords.

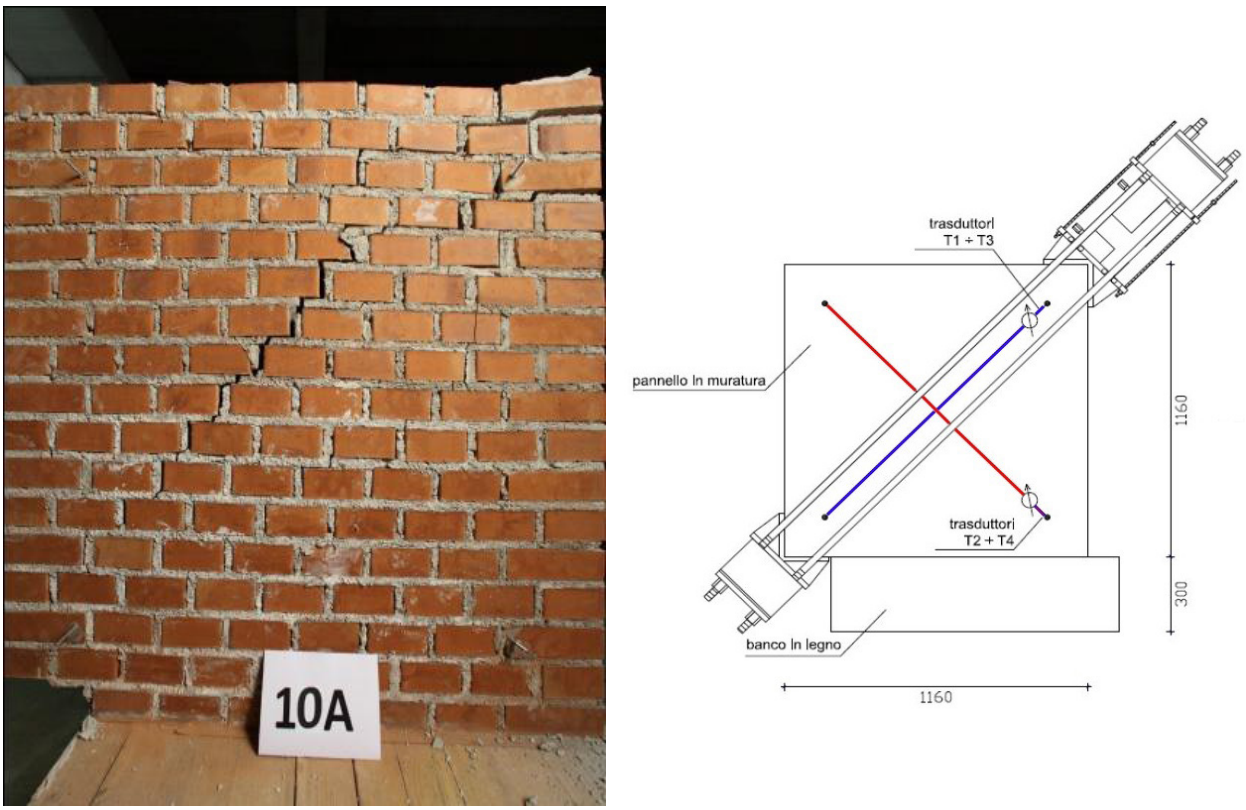

Figures 1.3.9-10. Non reinforced masonry panel and testing device.

Italy. Roughly cut stone, cobblestone and brick masonry were used to build panels aproximately 120x120 cm (±2 cm), reinforced with reticolatus either on one or two sides of the panels, with a variation in the brick masonry panels where the panels were reinforced with reticolatus on one side and GFRP (glass fibre mesh) on the other. The eccentric response was negligible given the comparable stiffness of the glass reinforced plaster and the masonry panels. For the application of the reticolatus technique studied in this work, only the solid brick masonry panels will be illustrated. These panels were built using bricks as diatonic elements, as shown in Fig. 1.3.8. A total of six panels were built and tested: two unreinforced, two reinforced with only horizontally displayed steel cords and two with both horizontal and vertical steel cord disposition, as may be seen in the panel in Fig. 1.3.8. These panels were reinforced on one side as shown with the blue lines through the Reticolatus technique, while on the other side the reinforcement consisted in a glass fibre reinforcement (green mesh). Only one of the unreinforced panels was repaired with the Reticolatus technique after testing.

The panels were built on a wooden platform and after a suitable drying period a part of the platform was removed in order to allow the positioning of the testing device. The testing device is very similar to the ones described above: a hydraulic jack placed on a metal beam in the upper right corner of the panel connected to another beam in the lower left corner of the panel by two

steel bars, as illustrated in Fig. 1.3.10. Four displacement transducers fixed on the two diagonals of the façade of the panel registered movements and deformations. Two additional transducers were placed on the central points and the upper corner diagonal of the unloaded façade in order to check for out of plane loading of the structure. The load was applied in cycles, between 8 and 12 in number, increasing by about 15 to 30 kN with each cycle and at least two post-peak load cycles. The panels reinforced with both vertical and horizontal steel cords presented average values of about 46% increase of the maximum load supported by the unreinforced panels, whereas the increase of maximum load was higher for the panels reinforced with steel cords positioned only horizontally, of an average value of 55%. The tensile strength, calculated as $f_t = \alpha\ (P_{max}/A)$, where A is the horizontal section of the panel and α is considered 0,5, according to RILEM 1994 specifications, was found to increase by respectively 40% and 48%, and shear strength was calculated proportionately as $\tau_0 = f_t/1.5$ (Turnsek – Cacovic). The results regarding the repaired panel should be mentioned in this state-of-the art outline of the Reticolatus technique as it seems to be a common situation when reinforcements are required. The maximum load value, the tensile strength and the shear strength were all above the average results of the unreinforced panels: respectively 11%, 9% and 4%. Comparatively with the sound panels, reinforced before they were subjected to load cycles, these increments in value are noticeable lower, but still represent an increase from the unreinforced results.

Flexural tests have also been performed on reticolatus reinforced panels (Borri et al., 2010). Two panels were built with rubble stone for the exclusive purpose of reinforcing and then testing. The panels were built in a vertical position and subsequently to a due drying period were laid hori-

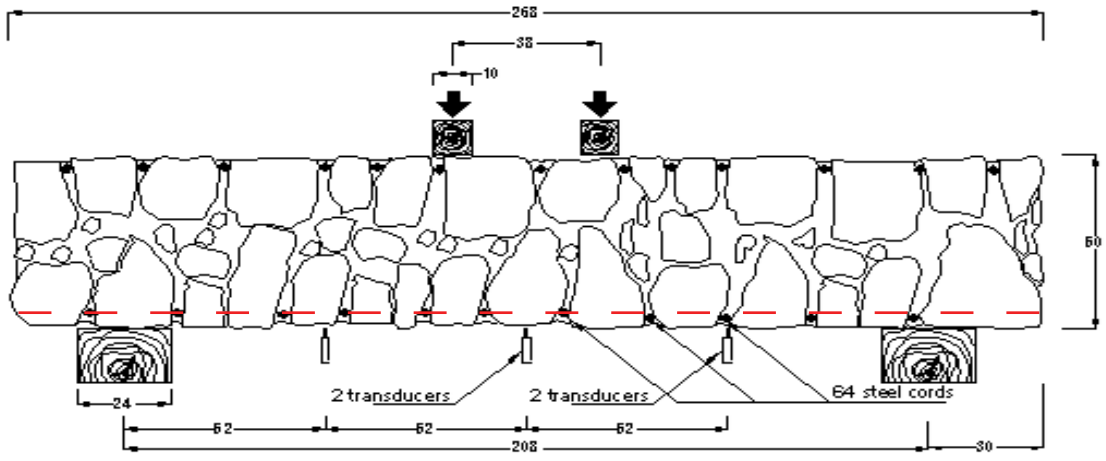

Figure 1.3.11. Set up of Panel 1 for flexural testing. The red line indicates the horizontal steel cords imbedded in the masonry which contrast flexural strength. Image taken from Borri et al. (2010b). Dimensions in cm

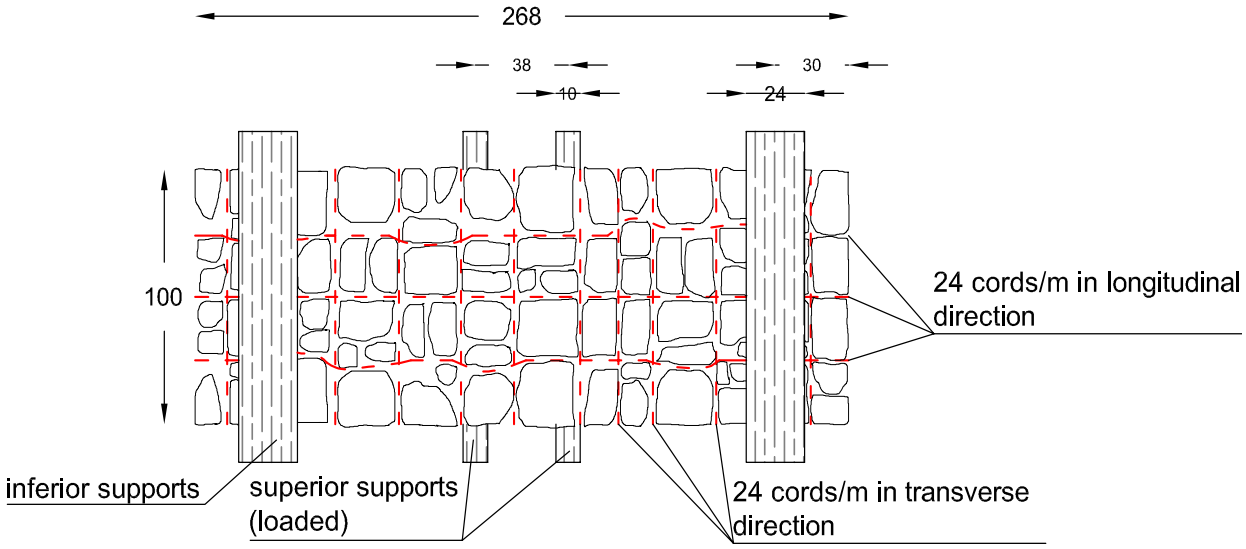

Figure 1.3.12. Set up of Panel 1 for flexural testing, view from below. The red lines indicate the steel cords imbedded in the mortar layers of the masonry. Dimensions in cm.

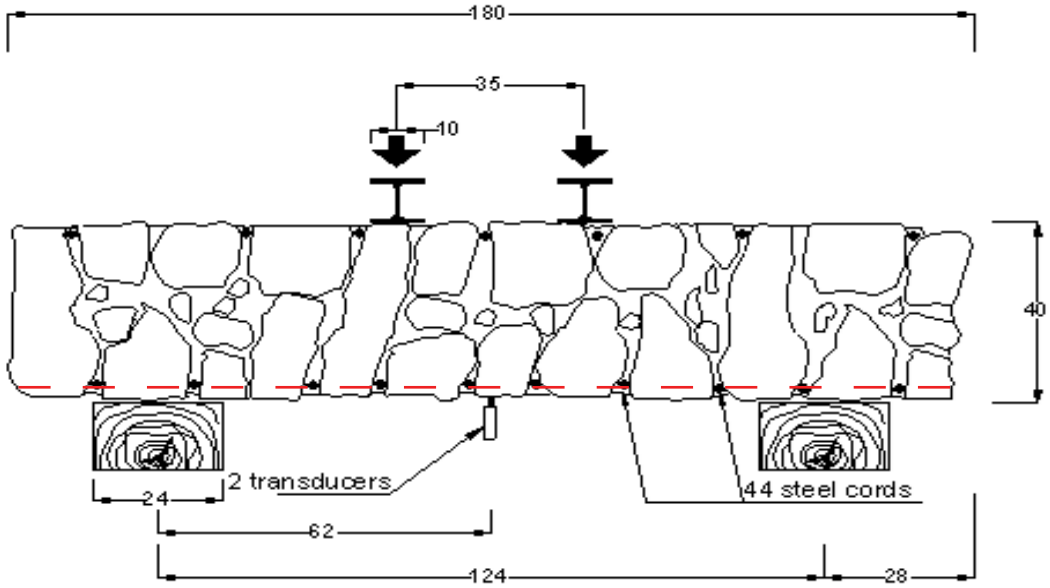

Figure 1.3.13. Set up of Panel 2 for flexural testing. The red line indicates the horizontal steel cords imbedded in the masonry which contrast flexural strength. Image taken from Borri et al. (2010b). Dimensions in cm

zontally on two wooden supports. The difference between the panels lies in the dimensions of the panels themselves and the ratio of steel cords used for reinforcement. Both panels were tested on site.

In the first panel (Fig. 1.3.11), of larger dimensions (50x268x100 cm), the cords placed longitudinally in the compression zone were 12 cords/m, half in number of those fixed to the structure in the area which was to be subjected to tension. Another 24 cords/m were fixed transversally, creating a mesh cage around the panel at a depth of about 3-4 cm in the mortar. The vertical load was placed on a two point loading surface, which, combined with the two points on which the panel had been placed in its horizontal position, created a four point loading arrangement (Fig.s 1.3.11-

12). The two points on which the load was placed were about 38 cm apart, whereas the supports were 208 cm apart. Six displacement transducers were placed along the sides of the panel, three per side, at midpoint, one fourth and three fourths of its length. The panel was loaded with its own weight, as well as vertical loads of 1.5 kN increments at a time. At the third load increment (4.5 kN), first signs of failure appeared through cracking parallel to the supports in the area subjected to tension. The cracks widened until the fourth load step at 6 kN; at this point, blocks of stones fell out of the panel given the detachment of mortar needed to keep them in place and the panel reached failure.

The second panel tested for flexural strength was shorter and wider than the first panel tested, being 40x180x198 cm (Fig. 1.3.13). This panel was reinforced in a very similar was to the first, with 12 cords/m both longitudinally and transversally in the area to be subjected to compressive strain and 24 cords/m in both directions on the opposite side of the panel. Very similarly to the first panel, this second one was also loaded trough a four point system, two points being the supports on which the panel rests, and two being the wooden beams through which the applied load is transmitted to the panel. The load applied to panel n° 2 was increased in step of 1 kN at a time. This panel never reached failure point, even after a load of 20 kN was positioned on the two wooden load bearing beams. The authors of this test (Borri et al., 2009), carried out a preliminary investigation, considering the steel cords placed only parallel to the direction of the flexural stress and the compressive strength of the masonry within normal values of the type used for the panels in question. Through these considerations, failure values of about 1800 kg for panel 1 and 8000 kg for panel 2 were the results. These values, as described above, were not reached, in the first case given the horizontal position of the panel, which facilitated the expulsion of stones in the tensile area, and in the second case given the in situ nature of the experimentation, for which it was necessary to carry out testing through manual loading (cement sacks) and not through machinery.

Tests have been carried out on other structural elements, such as columns. Masonry columns are a common structural element in specific architectural typologies, such as convents, churches, and civic buildings which may be considered in some cases valuable architectural heritage. Experimentation on the wrapping of columns with different fibres such as steel or carbon has already been completed, proving its good worth as a structural solution, but this leaves the masonry columns covered in the resins or mortars used as matrices. Again, reticolatus has proven in laboratory testing to be a good alternative to traditional FRP use.

The technique of steel fibre wrapping of the joints has been proposed in Jurina (2010) and developed further by the authors of the reticolatus technique in the campaign reported here (Borri et al., 2013). In the case of these experimental results, different shapes of masonry columns have been analysed: octagonal, square and rectangular, given the consideration that these sections seem to be the most common typologies of masonry columns, all about 53 cm in height. The reticolatus technique has been modified for these structures to function as follows: the mortar joints are stripped of the old mortar to a variable depth, one steel wire is wrapped around half of the masonry

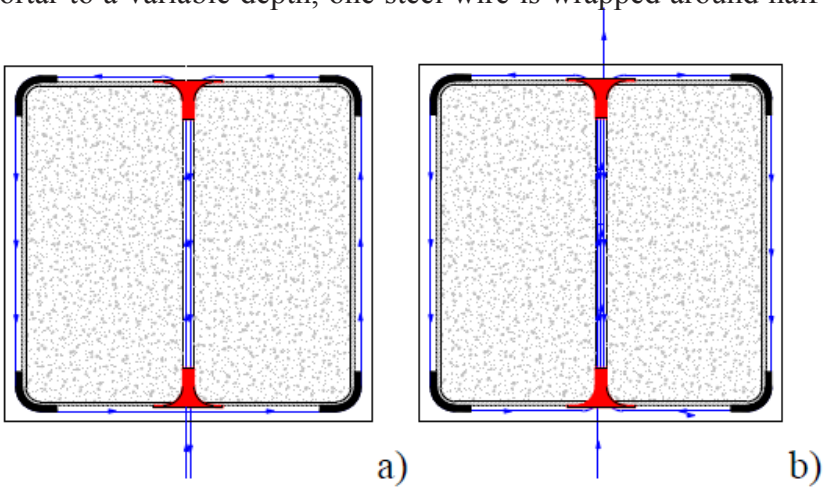

Figure 1.3.14. Two schemes for steel cord wrapping around a square column. Image taken from Borri et al. (2013b).

diameter and then enters through a small hole previously drilled through the width of the column in order to accommodate the cords which pass through the hole. Another steel cord is wrapped around the other half of the column and passed through the same hole (Fig. 1.3.14). Two different procedures were used based on the direction of the second steel cord. In the case of Fig. 1.3.14.a, both cords around the first and the second half of the column are inserted in the hole and wrapped around the column in a counter clock-wise direction. In the case of Fig. 1.3.14b, the cord on the left half of the column is positioned in a counter clock-wise direction while the second cord is placed in clock-wise direction, specular to the first. The number of times a steel cord is made to pass through the central hole in the tests described here is one and two for each column shape. The corners of the column are protected by angle brackets in order not to cause the resection of the cord due to shear forces, and a specially made bracket is inserted in the central hole. The mortar layers are then repointed and the hole through the column injected with new mortar in two specimens out of three for each column type, and with resin for the third specimen of each shape.

The reinforcement in this specific case of structural element was provided with a pretension: a dynamometer impressed on the steel cords wrapped in the mortar joints about 1/10 of their spe-

cific collapse load. The purpose of this pretension was to give the reinforcement an active role in the tensile strength of the structural element. The columns thus reinforced were then subjected to monotonic axial compression with four displacement transducers along its height for measuring deformations. Failure modes of the unreinforced columns exhibit a fragile behaviour: large vertical cracks increasing in number and dimension occur until failure. Reinforced columns of all shapes show a common crisis for deformation of the mortar through vertical cracks which create several sub-columns with limited stability. The containment action given by the reticolatus slows down the process of the formation of cracks and increases the failure resistance of the specimens. The values of maximum resistance to compression in the reinforced columns differ according to number of times the steel cord was wrapped in the mortar joint and whether resin or mortar was used for repointing, but calculating an average with the shape of the column as a common denominator the following increments in resistance were found: 158% for octagonal columns and 75% for square and rectangular columns. As the initial mechanical characteristics of the structural element diminish, a more relevant increase of resistance may be observed, for example in the case of the octagonal columns. With respect to the unreinforced columns, the reinforced ones show more diffused cracking scheme, with fewer lesions. This experimental campaign was addressed also for the reinforcing of octagonal masonry columns in a case study building, namely in the cloister of the convent of S. Girolamo in the town of Spello, in the Umbria region of Italy.

Existing Design Calculation applied to Reticolatus.

An essential part of reinforcement methods and their experimental testing is verifying that they conform to the national or international regulations, or that the calculation method can be adapted to express numerically structures with these new reinforcements. The two codes currently most used and available for calculating the resistance factors designed in reinforcement for masonry are Eurocode 6, part 1-1, and CNR DT 200/2004 and its updated version 200/2012.

In the experimental campaigns examined above, namely in the diagonal compression testing on panels from Pale, a design criteria based on the indications given in the codes were adapted to the specific reticolatus reinforcement used. In the CNR DT 200/2004 regulations, the value of the shear strength in the reinforced panels is considered a sum of the shear resistance offered by the unreinforced masonry and that of the steel cords composing the reticolatus mesh:

$$V_{rd} = V_{rdm} + V_{rdf} \quad (1)$$

$$V_{rdm} = f_{vd} \bullet t \bullet l \quad (2)$$

$$V_{rdf} = 0.9 A_{sw} \bullet f_{yd} \quad (3)$$

where f_{vd} is the design shear strength of masonry, t the thickness of the panel, l the length of the panel, A_{sw} the total area of the horizontal shear reinforcement over the part of the panel being considered including a reduction factor for safety (0.9), and f_{yd} the design strength of the reinforcing steel.

The authors of this experimentation consider the same sum of efforts contributing to the shear strength, but, as is necessary since the regulations consider fibres in the form of sheets and textiles or near surface mounted bars, some modifications have been made:

$$V_{rdm} + V_{rdf} = f_{vd} td + 0.9 d \rho_t f_{yd} t \quad (4)$$

In the equation for the shear resistance, we find the length of the panel substituted by its effective depth, which is the actual thickness of the wall considering only the section of mortar and masonry beyond which the reticolatus is fixed to the section. This is in fact considered in the regulations for masonry walls or beams reinforce with steel. The shear resistance offered by the steel reinforcement (3) is rewritten as

$$V_{rdf} = 0.9 d \rho_t E_{tw} r \left(\frac{\varepsilon_{tw}}{\gamma_{rd}} \right) t \quad (5)$$

where E_{tw} in the Young modulus of the steel cord (reported as 206 GPa), ε_{tw} is the ultimate strain value of the steel cord (reported as 1.8%), γ_{rd} is a partial factor for the resistance model, taking account of uncertainties of the assumed model, considered $\gamma_{rd} = 1$ here, and r is a partial factor depending on the type of application of the fibre reinforcement material and its failure mode (rupture = 1.10/1.25; debonding = 1.20/1.50). Given that in the specific case of reticolatus the reinforcement can still be effective even if debonding occurs, due to the transversal clutch system implemented in the mortar joints, here it is considered $r = 1$.

In the verification of the experimental campaign with the design calculations offered by the abovementioned regulations and considering the variations just detailed, the authors have found the comparison between experimental results and calculations to be valid.

The comparison with regulations was also brought out regarding the experimental campaign on masonry columns. Currently, CNR DT 200/2004 considers confined masonry columns very effective for a tri-axial confinement and for their anti-seismic improvement, and regards the reinforcement as sheets or bars: “Confinement with composites may be performed by using FRP sheets or bars. FRP sheets are applied as external reinforcement along the perimeter of the member to be strengthened in form of continuous or discontinuous wrap. Instead, FRP bars are inserted in spread holes drilled through the member that requires upgrade.” The authors of the campaign on reticolatus reinforced masonry columns (Borri et al. 2013) have found the regulations to be conservative in their results.

The axial capacity N_{rmcd} of an FRP reinforced member is given by the following equation:

$$N_{rmcd} = \left(\frac{1}{\gamma_{rd}}\right) A_m f_{mcd} \tag{6}$$

where γ_{rd} is the partial factor for the resistance model mentioned above, and for confinement γ_{rd} = 1.10, A_m is the cross sectional area of the confined element and f_{mcd} is the design compressive strength of the column. This last element can be written as:

$$f_{mcd} = f_{md} + k' \bullet f_{leff} \tag{7}$$

where f_{md} is the design compressive strength of unreinforced masonry and f_{leff} is the effective confining pressure of the reinforcement. k' is a non-dimensional factor which can be considered as follows:

$$k' = g_m/1000 \tag{8}$$

where g_m is the mass density of the masonry, expressed as kg/m^3. The effective confining pressure f_{leff} is in function of the shape of the cross section of the column and the reinforcement system, and can be put into relation with horizontal and vertical efficiency coefficients:

$$f_{leff} = k_h \bullet k_v \bullet f_l \tag{9}$$

The values of the horizontal efficiency coefficient vary with the shape of the reinforced column, and the authors (Borri et al. 2013) have found the following equations for square, rectangular and polygonal shaped columns:

$$k_h = \begin{cases} 1-\frac{2}{3}\frac{(b-2\cdot r)^2}{A_m} & (10) \\ 1-\frac{(b-2\cdot r)^2+(d-2\cdot r)^2}{3\cdot A_m} & (11) \\ 1-\frac{\pi\cdot b_{ed}}{12\cdot a_{ed}} & (12) \end{cases}$$

where b, r and d are as explicated in Fig. 1.3.15.

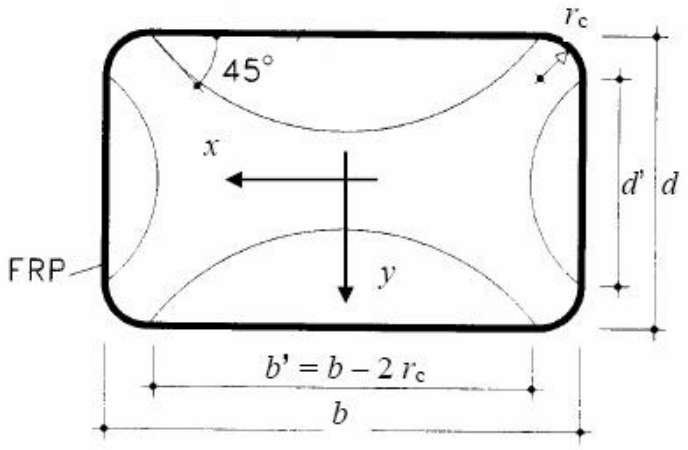

Figure 1.3.15. Scheme for design calculations of confined masonry columns. Image taken from CNR technical Document (2004).

Regarding the vertical efficiency coefficient, for discontinuous vertical reinforcements as the reticolatus method is, the width of the reinforcement b_f and its centre to centre spacing p_f is considered in the following equation, adopted by the authors:

$$k_v = \left(1-\frac{p_f - b_f}{2\cdot \min\{b;d;2\cdot a_{ed}\}}\right)^2 \quad (13)$$

The confining pressure in cases of continuous horizontal wrapping can be defined as a function of

the Young modulus of the reinforcement:

$$f_l = \frac{1}{2}\rho_f \cdot E_f \cdot \varepsilon_{fd,rid} \tag{14}$$

where ρ_f is an a-dimensional parameter indication the geometric ratio in function of the area of the reinforcement.

Comparing the numerical values following the calculations described above with the experimental values of the reticolatus reinforced masonry, in most values the authors have found regulations to be conservative, confirming again that the technique is valid and presents parameters which can be considered satisfying for further studies and on site use.

Reflections on compatibility and reversibility

In the previous parts of the present section on the reticolatus method, the procedure of this specific type of reinforcement has been illustrated. Now, referring to the requirements of the theory of restoration, also mentioned in the CNR-DT 200/2004 Bulletin, the inevitable question arises: is the reticolatus method an effectively compatible ad reversible reinforcement system? A positive answer to this inquiry would certainly solve many of the issues that arise when considering valid options for structural consolidation of the large historic and monumental built heritage of Europe.

The issue of compatibility is of a material nature and the answer lies within the chemical constituents of the structural substrate and the elements used in reticolatus, that is, steel and mortar. It depends on the type of substrate (masonry or stone with or without historical mortar joints) and the type of mortar used for repointing. With an adequate evaluation of these elements prior to the design of the reticolatus reinforcement, the system very well may be compatible, in the sense that its presence does not, with time or environmental conditions, damage the structure or introduce elements, such as epoxy resins, which for example prevent vapour permeability or deformability of the structure.

The reversibility question seems to be intrinsically more complicated. It appears that the concept of reversibility is naturally connected to that of minimum intervention, or of minimum invasiveness of the original structure. The answer to the issue of reversibility could be comprised in the definition itself of historic and monumental architecture. In fact, many authors interested in the issue of consolidation of historic architecture have addressed the question of what type of

constructions are to be considered of historical value. In (Baila et al., 2011a), it is specified that historic constructions are not only buildings of monumental importance, that is, those for which we could consider ourselves as custodians for the future generations. There are also traditional types of constructions which hold importance because they belong to urban fabrics which define historical or rural centres comprised in the UNESCO lists together with monumental architecture. In this specification one could find the difference between invasive (or not) consolidation techniques: when considering a monumental heritage, the invasiveness of an intervention is considered through a sort of magnifying glass, therefore the reticolatus technique, which requires the scraping of mortar joints and drilling of holes for transversal connections, may be considered in fact invasive, and not perfectly reversible. Within this consideration, it must be mentioned that no reinforcement technique presents these pure characteristics. Instead, when analysing what may be defined as "minor" and traditional architecture, then the reticolatus method is of minimum intervention as possible, since it does not vary in any way the aesthetic characteristics, the stiffness or the mass of the original structure.

Therefore, the reticolatus method can be considered a success in structural reinforcements, as it is compatible, and as minimally invasive as recent methods of reinforcements may be.

Chapter II. Durability of Reinforcements

1. State of Knowledge

The previous sections have amply shown the evidence for the numerous advantages deriving from the use of fibres as reinforcements or as a repair method to damaged structure. Recent literature, however, is starting to investigate the durability of FRP reinforcement. In engineering the term durability indicates the length of time an object, or assembly, or in this specific case a reinforcement technique, will provide its intended function. The effectiveness of the system is an important criterion for repair techniques, from the standpoints of safety and costs. From an economical point of view, in fact, it has been considered lately more cost effective to repair and strengthen structures, especially when the historic context is not an issue, rather than demolish and rebuild. This requires precise design calculations which can ensure that the structural functioning of the object of intervention is up to par with safety regulations.

Durability is not a new issue. Historically, certain types of building techniques were conceived to contrast the ageing and wear of structures, such as the use of ceramic tiles in many places in the vicinity of the sea and with the combined presence of wind, two environmental factors which can damage both masonry and wooden structures. Another typical building protection known of since medieval architecture is the large overhang of roof structures (i.e. Florence), built to protect walls from the rain. External plastering over the brick and stone facades, was not only a matter of the elegance and beauty of a palace but principally for the protection of the structural exoskeleton. The same can be said for the typical Florentine/Italian constructive detail of reinforced corners: these were in a certain way the weakest part of the building, where structural interconnections were most important, and at the same time these elements are the most exposed to environmental conditions. Hence the large stone applications, which were then considered a decorative element, or an element through which historical and noble families could show their wealth and status, bringing the fashion of applying the large family coat of arms not only over the central entrance of city palaces, but on the corners as well. Stone applications were also commonly used at the lower floors of buildings as protection from rising dampness. The idea of a concrete cover in and of itself is for the durability of reinforced concrete beams, since the steel used as the reinforcement will lose its resistance through corrosion. These were what may be considered passive techniques to protect buildings form environmental conditions, but active techniques have long been known as well. The technique of repointing for example, which was considered also a strengthening techni-

que, could very well solve problems caused by environmental conditions in non-plastered buildings: rain, wind and thermal cycles will cause the poor quality mortar used in modest architecture to crumble, leaving the masonry structure without the "glue" which guarantees solidity and the flow of forces throughout the building elements. A simple procedure of replacing the missing or deteriorated mortar with new mortar was considered sufficient. This was true also for wooden elements, and when protective coatings became available, the durability of wooden elements, both with regard to environmental conditions and biological attacks, increased significantly.

Today, the increased awareness of two main factors has put the durability of structures in the spotlight of scientific research. The first factor which has gained importance exponentially over the last century is safety. Structures must be safe, and be reasonably reliable through violent episodes such as earthquakes or other natural disasters. And the second factor can be defined as a sense of architectural and cultural responsibility towards historic buildings. This latter sensibility has not always existed; one need only remember the many palaces that have been partially demolished, enlarged, subjected to gross renovations throughout the centuries, without too much attention to the original nuclei of the structure, or the cathedrals, torn down and rebuilt to accommodate a quickly growing religious community.

a. Codes and Regulations

The fibre reinforcements studied in this work are subjected to the same environmental conditions as the structures they reinforce. Stresses and loading are not the only causes for debonding and degradation of the reinforcement. In fact, crisis may also be caused by real-life environmental conditions, or service conditions, such as temperature and moisture cycles. The investigation of the extent of deterioration or loss of effectiveness of fibre reinforcements was originally studied for the sector in which they were first used, that is the aerospace industry. Since the 1990's, it has been a common question in building science as well. Although the literature regarding experimental results for FRP durability has consistently increased in the past 20 years, the generalized perception is that not much is known. Even more relevantly is the fact that there are few documents which indicate the correct design regulations for fibre reinforced structures subjected to environmental conditions, while the experimental studies which have been carried out on the subject are scattered and not easily accessible, as rightly noted by Karbhari in the gap analysis

on durability of FRP reinforced infrastructures (Karbhari et al., 2003). In Karbhari's preliminary study, aimed towards identifying areas of much needed attention, the authors give the following definition for the term durability, which otherwise may be loosely interpreted: "*the durability of a material or structure was defined as its ability to resist cracking, oxidation, chemical degradation, delamination, wear, and/or the effects of foreign object damage for a specified period of time, under the appropriate load conditions under a specified environmental conditions*". The gap analysis investigation collects data on the perceived and actual lack of data in durability in specific environmental conditions, among which moisture, alkaline environment, thermal effects and ultraviolet exposure. In the conclusion of the survey, the recommendations are to collect data, experimentally and numerically, through long term testing, and to develop a standardized protocol for the design of fibre reinforcements in certain environmental conditions. This survey however is limited to civil infrastructures and is concentrated on fibre reinforced concrete structures.

Regarding design regulations of FRP reinforced masonry, one must refer to the CNR-DT 200/2004. In 2004 the Italian National Research Council createdan Advisory Committee on Technical Recommendations for Constructions, with the specific aim of producing guidelines for the use of FRP's on reinforced concrete, precompressed concrete, and masonry structures. The resulting Bulletin gives many specific application criteria for FRP and methods of calculation, as was mentioned in *Chapter 1.b. Fibre Reinforced Cenentitious Matrix (FRCM)* and in *Chapter 1.c. Reticolatus*. There is a brief description, in section 3.2, of the durability requirements that an FRP system is expected to present: "*A strengthening application shall be designed such that deterioration over the design service life of the strengthened structure does not impair its performance below the intended level. Environmental conditions as well as the expected maintenance program need to be carefully addressed. Durability is of fundamental relevance and all the operators involved in the FRP-based strengthening processes shall pursue such requirement.*" Among the factors that the Bulletin recommends be taken into account during the design of an FRP reinforcement, such as loading conditions, quality of workmanship and maintenance programs, there are also the expected environmental conditions. These are considered to necessitate special design and "*shall be identified at the design stage to evaluate their relevance for a durability point of view, assign proper values of the conversion factors, and take the necessary provisions for protection of the adopted FRP system.*" The conversion factors η_a are provided by the Bulletin as specified in Table 2.a.

As can be observed, the environmental conditions which are considered in the conversion factor are divided into internal, external and aggressive. In paragraph 3.5.1 of the Bulletin, the aggressive environment which may cause detrimental effects to the mechanical properties of FRP systems are specified as alkaline environments, moisture, extreme temperatures, thermal cycles, freeze/thaw cycles and ultraviolet radiations. Although this document may be considered a general overview of the environmental conditions which do in fact affect the mechanical properties of FRP systems, as in the case of the abovementioned gap analysis, these are considered solely for fibre reinforced polymers. FRCM systems remain without a clear reference framework for durability issues. The CNR-DT 200/2004 Bulletin attempts to cover this gap by adopting conversion factors, specifying in paragraph 3.2 section 4 that "*When conversion factors for a particular FRP system are not available, any possible reason of degradation of the adopted strengthening configuration shall be accurately estimated. Such estimation can be accomplished through theoretical models, experimental investigations, experience on previous applications, or any combination of the above.*" These conversion factors, intended to represent the performance of FRP reinforcements after

Exposure conditions	Type of fiber/resin	η_a
Internal	Glass/Epoxy	0.75
	Aramid/Epoxy	0.85
	Carbon/Epoxy	0.95
External	Glass/Epoxy	0.65
	Aramid/Epoxy	0.75
	Carbon/Epoxy	0.85
Aggressive environment	Glass/Epoxy	0.50
	Aramid/Epoxy	0.70
	Carbon/Epoxy	0.85

Table 2.a. Environmental conversion factor η_a for different FRP types and exposure conditions according to the CNR-DT 200/2004 Bulletin. Table taken from CNR-DT 200/2004.

exposure to certain environmental conditions, consist in deduction factors or conservative estimates to be used when calculating design strain or ultimate tensile strength of FRP's, based on the typology of fibres and resins employed and the environmental conditions expected. Therefore, although there are currently no specific guidelines relating to the environmental effects on FRCM, these are to be carefully considered and evaluated before designing such reinforcement systems. The first step towards a better understanding of the physical behaviour of such systems is through experimentation.

Following is an excursus of experimental research that has been carried out regarding the durabili-

ty of FRP composite systems until this day. These experimental campaigns were directed towards answering questions of how environmental conditions varied the behaviour and the mechanical properties of the reinforcement itself. For clarity, the state-of-the-art review has been divided into three different groups, according to the object of laboratory testing: durability testing on FRP coupons not considering the interaction of the structure, durability testing on FRP reinforced concrete and durability testing on FRP reinforced masonry.

b. Durability of fibres and resins

The first concerns regarding the long term durability of fibres were directed towards their resistance at service conditions in aircrafts. In fact, the experimental testing carried out by Adamson (1980), on the NASA research team at the time of the publication, considers the response of composite materials towards thermal expansion and swelling due to temperature and moisture variations, which could arguably simulate aircraft service conditions. The main concern in these tests was not the effects of environmental factors on the graphite fibres themselves, as their mechanical properties do not vary significantly, but rather the reactions of the composite fibre-resin matrices. Testing was concentrated on cured epoxy resin, which presents on a molecular level a rigid network structure resistant to molecular rearrangement (Adamson, 1980). The coupons of fibre

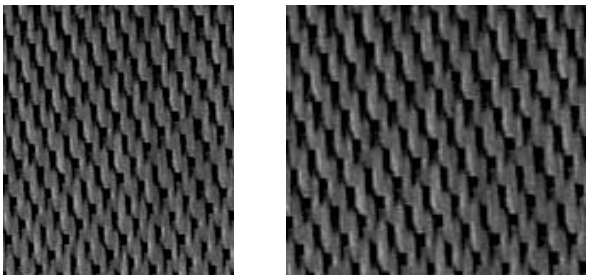

Figures 2.1.1-2. 8HS type weave.

and resin were then moisture saturated and exposed to various temperatures. Results indicate that moisture content triggers an increment in thermal expansion, and an increase in moisture content is observed when a drastic reduction of temperature is imposed on the specimens, a phenomenon which has been termed reverse thermal effect.

An extensive study of the environmental effects on Kevlar reinforced resins was conducted by R.E. Allred (Part I, 1981), divided into two parts, according to the different orientation of fibre layers used for testing. In the first part the fibre layers were made of 12 plies of 8HS (8 harness

Satin type weave) stacked in the same direction, while part II examined the behaviour of 12 8HS plies with 45° angle orientation (quasi-isotropic).

Specimens of Kevlar plies underwent flexural testing before and after extreme temperature exposure and moisture sorption. The temperatures ranged from -55°C to 150°C, temperatures which are not usually seen in structural elements or buildings reinforced with fibres. Not only the time period, but the experimental parameters adopted in these tests confirm that attention was still focused on the long term durability of fibres used in the aircraft industry. The results indicate that hygrothermal degradation can be extensive, in both ply orientation cases. Failure due to maximum load carrying capacity diminishes after exposure to elevated temperatures, but not at a catastrophic level. Moisture content also affected strength noticeably, at temperatures as low as 21°C, as the plasticization of the resin allowed the filaments to buckle more easily under the three point bending test appliance, showing a loss of stiffness up to 40% compared to dry specimens at room temperature. The recommendation which followed the testing on Kevlar fibre-resin composites was that highly stressed designs be limited to temperatures of 120°C if exposed to atmospheric moisture before heating (Allred, 1981, Part I).

The conclusions seen in the experimental studies carried out on these specific typologies of resins are however valid solely for the aerospace industry, and aerospace grade resins are usually not applied in engineering and architecture given their excessive costs. Furthermore, the durability of composite materials exposed to environments such as those of the aerospace, automotive and marine industry are usually not required by structures.

Approximately 15 years after R.E. Allred conducted experiments on Kevlar fibres, the innovation of fibre reinforced structures is well on its way to becoming a common structural practice. Interest in long term durability of CFRP reinforced concrete beams is shown, due to the harsh conditions in which reinforced bridge structures may be subjected to in environments such as those found in North America. Researchers from the National Research Council of Canada (Rahman et al. 1996), studied the effects of ageing on carbon fibre reinforced polymers and glass-carbon fibre reinforced polymers. For these tests fibre grids were used, not fabrics of woven filaments, and therefore both tensile and junction strengths were evaluated before and after exposure to environmental conditions. Specimens were tested both under stressed and unstressed conditions, and the environmental conditions they were subjected to consisted in saline solutions (20% $CaCl_2$), alkaline solutions (1% $Ca(OH)_2$), a mixture of saline and alkaline solutions, UV radiation and wet/dry cycles and

finale freeze/thaw cycles (5°C/-18°C, 5 cycles per day). The periods of time the specimens were subjected to each exposure varied from 120, 240 and 360 days. These exposures were designed to exaggerate the harsh conditions of bridges during Canadian winters. When unstressed specimens were tested for tensile strength, the carbon only fibre specimens showed a constant decrease, albeit small, for all types of exposures. The glass-carbon fibre specimens instead showed a constant increase in tensile strength for all exposures, which the authors attributed to a statistical aberration, given the small percentile average of increase (4.5%), and conclude that the real effect of the exposures on the tensile strength of this fibre type was insignificant. The large loss of strength in both fibre type specimens subjected to all exposures was found in the junctions but only up to 240 days. Once the specimens had been exposed for 360 days, an unexpected gain of junction strength was found in almost all specimens subjected to all types of exposure. However, some scattering of data was encountered, requiring further testing.

The same principles of evaluating long term durability of fibre reinforced infrastructures motivated the experimental research conducted by Gomez et al. (1996), which focused on the problems faced earlier in the aerospace industry on FRP coupons. For this experimental campaign, fibreglass coupons with two different types of resins as matrices were used. Coupons were divided into two groups according to the nature of their edges, namely if they were sealed with an extra coat of epoxy coating or not. All specimens were subjected to a saline solution, while a part of the specimens were also subjected to 50, 100, 150, 200, 250 and 300 freeze/thaw cycles (4.4°C/-17.8°C). The coupons were then tested to flexural failure, and load versus deflection plots demonstrate how the freeze/thaw action provokes a loss in load bearing capacity, a fact which is enhanced in the non-sealed coupons. Although small amounts of moisture were absorbed during freeze/thaw cycles, the loss of flexural strength can be compared to values observed due to higher moisture sorption. The authors have attributed this fact to the expansion of moisture during the freeze phase which caused a loss in strength, rigidity and toughness. Damage to the bond between fibres and matrix also appeared during testing. The coupons not subjected to thermal cycles all showed a loss of Young's modulus of less than 5% compared with the unexposed coupons. Data scattering was observed here as well, in both virgin and exposed specimens, and was attributed to statistical scattering of results.

Micelli et al. (2001) investigated the durability of GFRP and CFRP rods to aggressive environments as potential substitutes for steel in reinforced concrete. Different diameters, fibres (carbon

and glass) and external surface treatment of the rods were combined with different resins and then subjected to thermal cycles and alkali exposure. Two thermal cycles were carried out, a freeze/thaw program (-18°C/+4°C) and a high temperature cycle (16°C/49°C) alternated with relative humidity cycles, both combined with UV radiation exposure. The alkali exposure was carried out at 22°Cor 60°C and for two different exposure periods, 21 or 42 days. The CFRP and GFRP rods were then tested for tensile and shear strength, and both ultimate strength results of the specimens subjected to thermal cycles were insignificant for all types of rods. Regarding the specimens subjected to alkali exposure, there was no substantial decrease in tensile strength for the carbon fibre rods, and the glass fibres lost tensile strength only when the resin barriers failed, namely in the case of the polyester resin. Ultimate shear strength proves how fundamental the role of the resins are in the durability of fibres, since the epoxy coated carbon fibres were more resistant to the alkali exposure, although they showed a decrease in strength due to cracking at the adhesive/fibre interface, compared to the glass fibres with polyester matrix in which shear strength decreased by 91% of its original value.

In Hulatt et al. (2006) the fibres used in the experimental campaign were unidirectional carbon fibres, biaxial glass fibres and stitched biaxial glass fibres positioned at a -/+45° angle, all pre-pregnated fibres with cured resin matrices. The tests conducted on the fibre specimens were aimed at the evaluation of their longitudinal tensile strain after exposure to different temperatures (22°C, 45°C and 60°C), to water and accelerated wet/dry cycles on pre-stressed specimens at 22°C, to salt solutions and accelerated wet/dry cycles on pre-stressed specimens at 22°C and to UV radiation. Test results show a noticeable scattering of data, which the authors attribute to manufacturing defects in the case of the unidirectional carbon fibres and biaxial glass fibres, and to the elevated presence of voids in the -/+45° GFRP, which also has an elevated quantity of resin due to its particular plying. However, when exposed to heat, the longitudinal moduli of the specimens decrease as the temperature increases, that is, as the temperature approaches the curing temperature used for the FRP system. For the other exposures, no significant variation is registered in the longitudinal moduli.

In the campaign carried out by Abanilla et al. (2006), the wet layup process of applying matrices to fibres was used. This kind of technique, as mentioned in a previous chapter, is becoming increasingly common in structural rehabilitation since it presents a significant flexibility in its application to structural elements. The disadvantage of this method of application of fibres consi-

sts mainly in the fact that it is manually applied, and therefore could present irregularities due to workmanship in the thickness of the adhesive, such as air voids which lead to cracking, causing an undesirable inconsistent performance in terms of ultimate loading capacities. The specimens used in this experimental campaign were unidirectional carbon fibres in thicknesses of 2, 6 and 12 layers. The authors specify that this last thickness, while not common in structural rehabilitation could present interesting scientific results in terms of moisture sorption. The samples of composites were exposed to immersion in deionized water at 23°C, 37°C and 60°C, to immersion in salt water at 23°C, to immersion in concrete leachate at 23°C and to freeze/thaw cycles (-10°/23°, 1 cycle per day) for periods lasting up to 100 weeks. Five specimens for each thickness and environmental condition were then tested for tensile strength and flexural strength, and the results were compared to unexposed specimens. The results for the moisture uptake in salt or deionized water presented small variations; the values of moisture sorption for the specimens immersed in the concrete leachate solution were higher, a fact which the authors attributed to the deterioration caused by the alkaline salts in the fibre-matrix interface. This is an important demonstration of how, although the carbon fibres themselves may not be influenced by environmental factors, the bond between the fibres and the matrix is susceptible to weaknesses which effect the entire composite system. The evaluation of the tensile strength results required some considerations to be made on the curing of wet layup systems: in the 100 total weeks of specimen exposure, a slow progression of cure was noticed in the unexposed sample, thus increasing the values of tensile strength and modulus. The results of the exposed specimens were therefore compared to this variation of strength, and in the two-ply specimens all deterioration which could be caused by exposure remained within the range determined by the slow cure effect of the unexposed samples. For 6 layer samples the degradation was more evident, since after a 20 week period all results were below the slow cure range.

The authors indicate that the difference of response between 2-layer specimens and 6-layer specimens could be attributed to a major quantity of resin matrix due to the higher number of fibre-resin interfaces, concluding, reasonably, that the fewer the layers the better the structural response of FRP reinforced elements. Regarding flexural strength, the specimens present overall a greater degradation than noticed in tensile strength loss. The reasons could be again found in the interfaces between fabric and resin. For the specimens subjected to immersion, degradation seems to be reversible, especially for the samples subjected to lower immersion periods. A lowering of the

glass transition temperature was also studied in the process of this campaign.

Another study concentrating on the durability of wet lay-up applied FRP systems, Sciolti et al. (2010), tested unidirectional CFRP fabric and Glass alkali resistant fibres, both with epoxy resin matrices, for tensile strain and elasticity modulus after being subjected to immersion in distilled water at 23°C and to heating under nitrogen atmosphere. Water absorption and thermal characterization were also analysed. This experimental campaign confirms that the deterioration of mechanical properties of the composites due to moisture sorption and thermal effects is mainly caused by the plasticization effects of the resins, whereas the tensile strain of the composite measured in the direction of the fibres is not significantly affected. The testing also revealed that the complete curing time of wet lay-up composites is over 20 weeks, well above that suggested by suppliers, and about the amount of time in which the 6-layer composites started to deteriorate in the previous study.

By the year 2010, experimental research had seemed to prove that it was not the fibres that were responsible for the deterioration of mechanical properties when subjected to environmental effects as much as the resin matrices used in composites, both in wet lay-up and prepreg techniques. In this perspective it is important to know how fibres other than Kevlar, carbon and glass, such as steel, may offer resistance to environmental effects. To this end, Borri et al. (2011) carried out experimental testing of steel fibre specimens after being exposed to both natural and artificial ageing processes. The steel fibres tested consisted in two types differing by their coating - zinc or brass - and by the type of filament, and the matrices used were one of two different types: a cement based mortar or a hydrated lime based mortar. These matrices present a better compatibility when the fibre reinforcing system is used on masonry, as mentioned in previous chapters. A third type of matrix was used, consisting in an inorganic mortar with fibres in its mixture. The aim of the campaign was to evaluate the long term durability of these composite materials when exposed to environmental effects, and the different behaviour between zinc and brass coated steel fibres. Mechanical tests were performed on the specimens in order to evaluate the tensile strength of unexposed and exposed specimens. The fibres used in the following experimental campaign were produced by Hardwire, LLC. Testing was carried out on two different typologies of steel

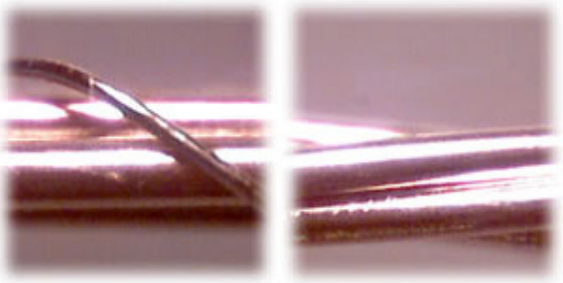

Figure 2.1.3-4. 3SX and 3X2 cords.

fibres. Fibre 3SX (Fig. 2.1.3), the most voluminous type of cord produced by the abovementioned company, is formed by three wires, each 0.48 mm in diameter, externally swathed by one wire of approximately 0.012 mm in diameter. The wires used to produce the 3SX type cord are made of steel with a high content of carbon coated in brass. The 3X2 type cord (Fig. 2.1.4) is constituted of three wires swathed by two wires in a helical manner, all of the same diameter: 0.35 mm in the case of the brass coated steel wires, and 0.37 in the case of the zinc coated wires. A total of 100 specimens were prepared, 64 of which used a 3SX type cord and 36 used a 3X2 type cord, 18 with brass coating and 18 with zinc coating.

Eighteen specimens, 6 of each different typology, remained unexposed, whereas the remaining specimens were exposed to several ageing processes: immersion in a neutral magnesium chloride solution at 100°C and immersion in nitric acid solution at 110°C for 24 hours, artificial ageing in a salt spray fog chamber at 35°C for 1, 2 and 4 weeks, and exposure to natural ageing in different areas, such as near a thermal power station and a cement plant, for 57 and 114 weeks. Mechanical tests carried out on the specimens without matrices subjected to immersion in neutral and acid PH solutions did not show substantial variations of the tensile strength (-6%), whereas larger percentiles of strength loss were found in specimens with hydraulic and inorganic matrices, which the authors of the campaign attribute to the formation of corrosion channels within the matrix. The percentages of deterioration are inferior for the specimens immersed in neutral solutions. The brass coated specimens subjected to ageing in the salt spray fog chamber presented a decrease in mechanical properties in the initial week of treatment, whereas after 2 and 4 weeks the tensile strength improves somewhat. The zinc coated specimens however resist to these environmental effects presenting a less than 5% decrease in mechanical properties throughout the entire period of exposure. Specimens subjected to natural ageing gave the worst results in terms of tensile strength, and comparatively, the specimens with hydraulic mortar matrix behaved worse than specimens with no mortar: 30% and 42% less resistance respectively at only 57 weeks exposure. The differences between the locations of the specimens did not cause a substantial difference in resistance for the specimens without matrix after 57 weeks of exposure, whereas this difference was noticeable in the specimens with hydraulic mortar. After 114 weeks, the specimens near the cement plant behaved considerably better compared with those near the thermal power plant.

c. Durability of FRP reinforced concrete

This section will be devoted to an analysis of the durability of fibre reinforcements when applied to reinforced concrete structural elements. Thus, new phenomena will be observed and compared to the material in the section reviewed above which, as has been noted, concerned solely the FRP system. In the following review, prediction models have been put forward regarding FRP reinforced concrete in service life conditions. Since these prediction models regard a specific type of structural elements (concrete or reinforced concrete) with FRP systems as opposed to FRCM, object of the present dissertation, they will not be examined in depth but rather acknowledged as a fundamental part of the continuing research on FRP systems in service conditions.

The first concerns regarding the durability of FRP on reinforced structural elements were directed towards concrete infrastructures, much like the initial FRP testing on coupons which was carried out simulating conditions such as those found on bridges (Rahman, 1996).

Sen et al. (1993) investigate the durability of pre-tensioned fibreglass and steel specimens in an environment such as that which piles driven into tidal waters are exposed to. The application of FRP examined in this experimental campaign consisted in the insertion of strands, steel or fibreglass, in the section of the concrete beam. Since the glass strands were pre-impregnated with epoxy resin, they may be considered as an internal application of GFRP. Both cracked and un-cracked specimens were subjected to tidal simulation and then tested under a four point loading set-up for ultimate load capacity. Twenty-four sample concrete beams were tested, 12 of which reinforced with steel strands and 12 with fibreglass. Six specimens of each type were pre-cracked on the extrados and intrados at mid-span, and 16 of the total specimens were subjected to tidal wave simulation, an effect achieved by placing the beams in an inclined position in tanks in which the level of a sodium chloride solution varied every 7 days. Un-cracked specimens were removed from the tanks for testing at intervals of 1.5, 6, 12 and 18 months and cracked specimens were tested after 3, 9, 15 and 20 months of exposure. The results of the steel reinforced beams proved that there was no significant loss of load capacity or ductility due to exposure, and 9 out of the 12 beams tested failed through compression mode as anticipated while the remaining three failed in shear mode. The fibreglass specimens reacted with a larger load capacity loss, consistently decreasing with the exposure period, and evidenced a new failure mode termed corrosion mode, where failure occurs immediately after cracking without warning, as if the beams had not been

reinforced, and without evidence of slip, meaning that bond loss was not an issue. The failure of the exposed fibreglass reinforced beams seemed to pass from compression to shear to corrosion, without external visible signs of deterioration. Ultimately, the authors suggested that fibreglass pre-tensioned beams should not be used for piles driven in water.

A larger experimental campaign conducted soon after by Chajes et al. (1994) tested a total of 60 small scale beams, with and without composite reinforcement, obtained through different types of fibres: aramid, glass and graphite with epoxy resin matrices. The beams were exposed to aggressive environmental effects, namely freeze/thaw and wet/dry cycles, while immersed in a calcium chloride solution. The freeze/thaw cycles consisted in placing the beams in airtight containers and immersed in a calcium chloride solution. The beams were then placed in a freezer at -17°C for 16 hours and then at room temperature for 8 hours allowing them to thaw. This procedure was repeated for 50 and 100 times, after which the beams were tested. The wet/dry cycles consisted in 16 hours of immersion in the same calcium chloride solution used for the freeze/thaw cycles, alternated with a dry period of 8 hours. These cycles were also repeated 50 and 100 times before beams were tested. The results of the four point loading tests indicated that the wet/dry environment caused more severe deterioration than the freeze/thaw cycles. The authors of this investigation note how there is a failure mode change in the aramid and graphite reinforced beams, from flexural to shear in some cases, and debonding in others, indicating a loss of bond adherence due to environmental deterioration. Altogether though, the testing demonstrated that an increase of ultimate load capacity was maintained by the exposed reinforced specimens compared to unreinforced and unexposed specimens. The aramid and glass reinforced beams lost in average half their strength after environmental exposure, whereas the graphite reinforced beams maintained up to a 120% increase even after 100 wet/dry cycles, indicating that this type of fibre is the least susceptible of the three to environmental deterioration.

Toutanji et al. (1998) investigate the freeze/thaw and wet/dry durability of fibre wrapped concrete columns, using three different types of fibres, two carbon and one glass, and epoxy resin. 24 specimens were prepared, and divided into three groups of 8 specimens, 6 of which reinforced, and 2 unwrapped. The first group remained unexposed, whereas the second group was subjected to wet/dry cycles and the third to freeze/thaw. The columns were reinforced through the wet lay-up technique, and left to dry at room temperature for 7 days before exposure commenced. The first group was tested 75 days after reinforcement. The second group was exposed to 300 cycles of

immersion in a saltwater environment for 4 hours, and then in 35°C and 90% RH (relative humidity) for 2 hours. The third group was subjected to 300 freeze/thaw cycles, -17.8°C to 4.4°C for 4 hours, while immersed in a saltwater solution.

Testing was performed through uniaxial compression. The unexposed specimens confirmed an increase in compressive strength of about 100% for the glass fibre reinforced specimens, and 200% for the carbon reinforced specimens compared to the compression value of unwrapped columns. In general, the carbon fibre exposed specimens behaved better than the glass fibre ones, where the reduction after wet/dry cycling was up to 10% compared with the insignificant reduction of the carbon fibre reinforced columns. Freeze/thaw exposure determined a decrease in compressive strength in both carbon and glass fibre reinforced specimens, but very little effect on stiffness. The failure of the specimens subjected to this type of exposure was more catastrophic when compared to unexposed and wet/dry. However, regarding the comparison to the first group, the results could depend on the fact that while the unconditioned specimens had 75 day to cure (over 10 weeks), the conditioned specimens were allowed to cure for only 7 days. Testing has since then demonstrated (Sciolti, 2010) that the complete curing time for epoxy resins is significantly higher than producers' recommendations (over 20 weeks).

In Jia et al. (2005), not only was the degradation due to environmental exposure investigated experimentally, but a procedure to quantify the degradation of the FRP/concrete bond given by the exposure was also provided. The experimental procedure was carried out on small scale concrete beams, reinforced with unidirectional glass tow sheets with epoxy resin as a matrix, applied through a wet lay-up technique with three applications of resin. After curing, the beams were pre-cracked by three-point flexural loading. Following this pre-cracking, the beams were subjected to a sustained four-point flexural load and then put into four different environmental conditions: dry freeze at 18°C alternated with a wet thaw period of immersion in water three times a week for 4, 8 and 16 months; room temperature condition (20°-25°C) for 12 and 18 months; outdoor exposure in State College, Pennsylvania (USA) for 15, 18 and 23 months; and elevated temperatures (50°-60°C) for 2, 4 and 6 months' time.

The novelty of this experimental campaign rests in the fact that the beams were subjected to loading during the exposure period to various environmental effects. This simulates a situation very similar to service life conditions, as opposed to laboratory conditions in which small scale structural elements are exposed to different types of conditions but without sustaining their service loads,

as has been the case in the studies reviewed above.

The results show that all beams failed because of debonding of the fibre from the concrete beams due to the pre-cracking: since the beams are pre-cracked, the concrete does not provide resistance, and therefore the FRP system sustains all the strain, which, through continued loading, migrates towards the unloaded ends of the fibre reinforcement until debonding occurs. All beams presented failure through debonding except one specimen in which the fibres ruptured, a fact attributed by the authors to manufacturing defects in the fibres. This specimen in fact was not included in the analysis of the test results. Generally, the beams subjected to outdoor exposure, room temperature and elevated temperature present bending moments slightly higher than unexposed specimens, a fact which could be attributed to the elongated curing time they were allowed (Sciolti, 2010). The freeze/thaw specimens instead present lower ultimate bending moments compared to the specimens subjected to other types of exposure. The procedure proposed in this study initiates by taking into account simplified local shear-slip models (Yuan et al., 2001) used to obtain local bond stress-slip distribution analytically. When experimental data is available, the local bond stress-slip relationship can be back calculated, as Savoia et al. (2003) applied, assuming that the FRP was linear-elastic, that there was no strain at the unloaded end of the FRP strip, and that the strain in the concrete was negligible, as in the present experimental campaign. In applying the experimental data to all four models, the model that was the best fitting in terms of correspondence to real behaviour of strain distribution and presented lowest relative error values was adopted and experimental data was inserted.

Once all data was calculated, the results of this simplified model showed that unconditioned, outdoor and room temperature models presented very similar shear stress values, while the 26 freeze/thaw cycle (4 months) specimen shows an increase in values, which could very well be attributed to additional curing. All data, however, presented a downtrend in local slip values. This method of data analysis could therefore be useful for specific FRP designs.

Al Far et al. (2007) investigated the environmental durability of all the components of an FRP system. Thus tests were conducted on resins and CFRP plates, on CFRP applied externally to steel rebar reinforced concrete (RC) slabs (1600x500x120 mm) with high concentrations of salt, and on concrete specimens (150x150x45 mm), CFRP reinforced. The study was carried out in cooperation with the Building Research Centre in Amman, Jordan, which provided severe environmental conditions regarding corrosion of concrete structures, as the Dead Sea environment is characteri-

zed by elevated temperatures and humidity levels, as well as high levels of chlorides in soil water. As in the study reviewed previously (Jia et al., 2005), the concrete slabs in this experimental campaign were also pre-cracked and subjected to sustained loading while exposed to environmental effects. The environmental conditions chosen for the CFRP plates and three different types of adhesives were moisture, water, salt and alkaline solutions at both 23°C and 50°C temperatures, as well as two different ultraviolet radiation exposures (UV 250 at 23°C and UV 500at 50°C). The results on the CFRP plates showed no substantial degradation to their mechanical properties, but on the contrary an enhancement when the plates were subjected to elevated temperatures. This result can be attributed to the post curing time allowed for the CFRP plates.

Regarding the adhesives, their tensile strength after exposure revealed a general deterioration when exposed to high temperatures, to be expected in resins when temperatures close to the glass transition temperature are reached. Alkaline solutions seemed to be the most detrimental for the adhesives tested, especially if associated with elevated temperatures. The RC slabs were pre-exposed, unreinforced and subjected to long-term loading, to different kinds of environmental conditions for four months, including laboratory conditions, the Dead Sea environment, the Aqaba environment (in Jordan's main sea port on the Red Sea) and the environment found in the capitol city of Amman. After retrofitting the CFRP plates, the initial load was increased by 20% and the slabs were exposed again to their conditioning regime for another year. For all RC slabs, the results proved that retrofitting with CFRP plates increased their initial ultimate loads, but failure occurred for all slabs through debonding. While ripping, i.e. the peeling of a thin layer of concrete, occurred for the specimens subjected to normal conditions, this phenomenon was not present in the slabs subjected to severe environmental conditions. The failure of conditioned specimens took place at about the same ultimate loading, evidently not depending on the type of conditioning. The 66 small scale concrete CFRP reinforced specimens were subjected to the same pre-conditioning and post reinforcement exposure as the RC slabs. These prisms were tested under pure shear, and the chloride ion contents tested. Coherently, results were comparable in values and failure modes to the RC slabs tested.

Once testing was completed, a bond capacity model was elaborated for FRP systems exposed to extreme climates. Neubauer and Rostásy (1997) proposed a general model which highlights the relationship between the maximum load and parameters affecting bond behaviour. A new model was proposed by adding an adhesive parameter obtained by performing a regression analysis for

the test results, the concrete compressive strength, and not its tensile strength, as this is not always available to the designer, and a constant dependent on an environmental factor (developed from the test results regarding salt solutions, humidity paired with high temperatures and Amman, Dead Sea and Aqaba environments). The accuracy of this new model to predict failure modes of CFRP reinforced RC slabs in severe environmental conditions was determined to be an average of 98.6%, considering all encountered environments.

Tuakta et al. (2011) carried out an extensive experimental campaign on concrete specimens reinforced with CFRP plates subjected to constant and cyclic moisture intake at room and elevated temperatures and then tested for peel and shear fracture. Material characterization for both mechanical properties and moisture sorption was also conducted on specimens of plain concrete (cylindrical, 50x100mm), epoxy tensile specimens and concrete/epoxy specimens. The tensile strength and Young's modulus of epoxy specimens subjected to continuous moisture ingress decreased, although the specimens subjected to elevated temperatures presented a slightly better value of tensile strength, probably due to the prolonged curing period. The effect of moisture on the concrete specimens was irrelevant at both room and elevated temperatures, while the Young's modulus was in slight diminution. The specimens tested for peel and shear fracture toughness consisted in concrete blocks reinforced with a CFRP plate and epoxy resin; only the type of testing varied between the specimens. These specimens endured continuous moisture ingress (2, 3, 4, 6, 8 weeks) and cyclic moisture exposure (1, 2, 3, 4, 6, 8 weeks with a maximum of 8 wet/dry cycles). The specimens subjected to continuous moisture ingress were tested wet, while the specimens subjected to cycles were left to dry for four days before testing, the amount of time experimentally found to allow a minimum weight loss. The intent of subjecting the concrete blocks to these two types of exposures was to verify if any irreversible degradation was initiated by the continuous moisture ingress. The results of the continuous moisture exposure for both peel and shear fracture specimens showed detrimental effects on specimens after only 2 weeks exposure, both for room temperature and 50°C. After this initial degradation, the values remained similar without substantial variation (asymptotic value for peel fracture specimens after 4 weeks and after 2 for shear fracture specimens, Tuakta et al., 2011).

The same series of tests was performed on specimens subjected to continuous moisture ingress but allowed to dry before testing. This series of testing was aimed towards determining if any moisture reversal was possible. In fact, the specimens allowed to dry showed bond strength reco-

very when compared to specimens tested wet, but substantial decreases are visible from the fourth week on in specimens subjected to elevated temperatures, a fact which the authors attribute to differences in the coefficients of thermal expansion of epoxy and concrete.

Regarding cyclic moisture exposure, the plain concrete samples showed again no decrease in Young's modulus, indicating that initial mechanical properties can be regained after drying. The epoxy specimens instead were unable to gain their initial properties after drying. Reinforced concrete blocks subjected to peel and shear fracture tests after cyclic moisture exposure show reduction in fracture toughness at every intermediate exposure duration, and with every step of exposure bond strength diminished significantly. This was also expressed by the quantity of concrete debris found on the debonded CFRP plate. On the less conditioned specimens there was more debris, and very little on the specimens subjected to longer exposures. Once the experimental campaign was complete, a prediction model was implemented (Tuakta et al., 2011) using the results acquired during testing for a pre-cracked FRP strengthened RC beam under moisture cycles.

d. Durability of FRP reinforced masonry

This section of the state-of-the-art review on durability represents a specific interest for the present study as it regards the durability of the FRP system applied to masonry.

The first study in this review concerned with the durability of the bond between masonry substrates and FRP systems was carried out by Briccoli Bati et al. (2001) in an experimental campaign focused on assessing variation of shear strength in exposed brick CFRP reinforced specimens. For the testing conducted in this investigation, brick specimens composed of three unaligned bricks bonded with cement mortar where built and left to dry. Six specimens remained non-reinforced and 78 were reinforced with CFRP strips on both sides placed across the entire width of the specimens. The reinforced specimens were subjected to wet/dry and freeze/thaw cycles, in the following exposure programs: two different wet/dry conditioning periods for 6, 12, 24 and 48 cycles each, one consisting in 10 minute immersion in water (tap, at 15°C) and 48 hours drying time, and the second with a 20' immersion period followed by a 24h drying time, and 12, 24, 48 and 96 freeze/thaw cycles of 6h at 50°Cand 6h at -8°C, performed in an environmental chamber. After the exposure was complete the specimens were placed in a testing machine which applied shear strength to the CFRP strip by compressing the staggered middle brick of the three composing the

masonry arrangement.

The results for the specimens subjected to wet/dry cycles highlight that a more severe deterioration is noted for the 20'-24h cycles for intermediate cycles up to 12. From this exposure period onward, the values are constant and similar in 24 and 48 cycles for both conditioning types, as about 18% strength loss was observed compared to unconditioned specimens. The failure mechanism does not vary for exposure type but rather for number of cycles; in fact, specimens subjected to 6 and 12 cycles rupture similarly to unexposed specimens while 24 and 48 wet/dry cycles present a more fragile behaviour and failure through debonding occurs with a lager quantity of material attached to the CFRP strip.

The specimens subjected to freeze/thaw cycles showed very little strength loss up to 24 cycles and insignificant alterations of the interface between masonry and CFRP, but for longer cycles the degradation trend increases, up to a 15% reduction of strength after 48 cycles and 50% after 96 cycles. The failure mechanism is more severe as well, as after 48 cycles the first flaws are noted beneath the primer level, and after 96 cycles there was actual detachment between the reinforcement and the masonry, causing the aforementioned 50% reduction in strength of these specimens. The outcome in masonry reinforced durability that can be extrapolated from this first experimental campaign could be that, as for FRP reinforced concrete (Chajes, 1994), it is not the carbon fibre to deteriorate through environmental exposure but the bond between the reinforcement system and the substrate, a phenomenon which could be dangerous even for as little as 96 cycles.

Enquiries as to the validity of the FRP reinforcement method and masonry when exposed to aggressive environments have been carried out by Binda et al. (2011), and an experimental campaign was set up to investigate the durability of fibre reinforced masonry specimens when subjected to salt crystallization tests. Previous studies conducted by the authors had shown that salt crystallization is frequently the cause of surface damage in masonry, and the tests were aimed at verifying whether the application of FRP in presence of a sodium chloride environment would reduce masonry lifetime. CFRP strips were applied through a wet lay-up configuration onto masonry samples. The masonry specimens were constructed with two methods of assemblage of the bricks with lime mortar, one which presented soldier course, which is with the wider faces of the bricks exposed and the thin sides bonded by mortar, and the second with a running bond, that is with the thin sides exposed and the wider faces bonded with mortar, as in typical masonry walls. The CFRP strips were applied in 4 different configurations for each masonry assemblage, from single strips

across the mortar joint to a complete covering of the sample. The accordingly reinforced masonry specimens were then placed into contact with a sodium sulphate solution and stored sealed along the sides but with the upper reinforced face exposed to the laboratory environment (room temperature and 50% R.H.). This type of exposure will show whether the sodium sulphate migration from the contact face of the specimen inward towards the reinforced face produces damage in the interface between the substrate and the reinforcement.

Cycles lasted 4 weeks, and at the end of each cycle a laser profilometer conducted a reading of the surfaces quantifying the damage. Non-destructive infrared thermographic tests were also performed before exposure of the specimens to sodium sulphate and after 7 cycles, detecting any detachment of the FRP from the substrate. At the end of the 7th cycle, both control and reinforced specimens were covered in salt incrustations, but the reinforced specimens also presented mould due to the presence of FRP which prevented the migration of the salts across the surface of the bricks and mortar. The laser profilometer measured one unreinforced and two configurations of reinforced specimens. The maximum area loss (4%) was experienced by a specimen reinforced with two strips of CFRP after the 7th cycle was complete. The analysis carried out through infrared thermography gave proof of detachments between the reinforcement and the CFRP both around the fibre strip and beneath it. One of the specimens was cut in order to verify these results, and crystallization in the layer immediately below the FRP was evident. This was causing the detachments of the FRP and the formation of mould. The conclusive result was that after 7 cycles of exposure sodium sulphite damages irreversibly the FRP system which is no longer fully functional.

Along this same path of research, Valluzzi et al. (2011) tested humidity and temperature durability through pull-off tests on control specimens and CFRP reinforced masonry assemblages through wet lay-up application. In this experimental campaign directed towards the effect of humidity in the FRP bond to the substrate, both single bricks and brick assemblages were subjected to three different moisture conditions denominated environment (5-6% water content), intermediate (14%) and saturated (24%). Different failure modes were observed according to the area of failure following pull-off tests. The most typical failure mode, “A”, with failure within the masonry substrate shows a good adhesion between FRP and substrate. The failure mode “B”, failure between the reinforcement and the substrate, is caused by a loss in bond strength. Two other failure modes were observed but they were deemed to be a cause of anomalies in the fibres or the resins and

not considered in final results. There was a clear correlation observed in failure mode A and a lower water content in the masonry specimens. As the water content passed from environment to saturated, the failure mode went from within the substrate to in the interface between support and FRP, and bond strength experienced a loss of up to 16.8% in areas with both brick and mortar. Therefore, the full functionality of the reinforcement system is compromised, while maintenance on reinforced structures could prevent this type of problem.

Regarding the thermal cycles, single soft mud brick CFRP reinforced specimens were subjected to 40 freeze/thaw cycles (-10°C – 70°C, 3h per cycle). At the end of the 40 cycles, pull-off testing was not possible given that all specimens presented a deep delamination of the CFRP strip at about 1-2 cm under the fibres. The authors attributed the reason for this failure to the fusion temperature of epoxy resins or the differential deformation of the epoxy which penetrated into the brick. This damage was irreversible, as the unloaded specimens presented failure only through environmental exposure. The bricks used were of a particularly porous type, often found in historical masonry, and when testing was repeated on more compact bricks as found in modern constructions, with low porosity, the unexpected failure did not represent itself. However, these tests draw attention to the fact that an important part of pre-reinforcement analysis must be assigned to discovering the mechanical and physical properties of the masonry in need of reinforcement in order to assess a certain durability of the reinforcement.

Bond durability in CFRP reinforced masonry substrate was investigated by Sciolti et al. (2012) after long term immersion in water. This study was conducted as the continuation of a preliminary study reviewed in the first part of the present state-of-the-art (Sciolti, 2010) on unidirectional carbon and glass fibres with an epoxy matrix. The subsequent investigation carries out a bond analysis between carbon and glass FRP experimentally tested in the previous study and a natural calcareous stone common in a region in the South of Italy. The application of the strips with the wet lay-up technique was carried out on both sides of calcareous blocks measuring 10x10x25 cm, attached by a bonded region of 15 cm followed by an non-bonded region of 5 cm. The FRP system applied to these stones was allowed to cure for over 10 months, as the recommendation of the authors' previous study of a longer curing period suggested, before being subjected to long term immersion periods of 8 and 25 weeks. After environmental exposure was completed, the blocks were tested through a shear test set-up, with steel plates attached to the non-bonded ends of FRP strips. Non reinforced stone specimens were also subjected to 14 and 25 weeks of water im-

mersion and then tested for values of compression and flexural strength. In these tests a possible material anisotropy was considered, therefore testing was conducted both in parallel to the layers of the stone and perpendicular to them, resulting in unsubstantial differences. However, it did become clear in the analysis of the results that both compressive and flexural strengths of the stone were consistently almost halved after aging took place. No significant differences were recorded between the two different exposure periods, but this was to be expected as the stones seemed to gain most of their wet weight in the first 24 hours of immersion.

Regarding the shear tests performed on the composite stone-FRP system, it was possible to make several bond type considerations, based on the experimental data collected by the strain gauges attached in several different sections of the strips. All specimens failed through debonding which caused failure in the substrate, ripping a layer of stone away with the FRP strip as it started to detach. Again, it was observed that there was no substantial difference between the results of the reinforced stones exposed to 8 or 25 weeks conditioning. The greatest differences were found between unaged and aged specimens, as the maximum strength registered decreasing of about 22% in the latter, and the debonding began at lower load values in aged specimens respect to those unexposed. Notwithstanding this consideration, there were no relevant differences in the optimal bond length, which is the minimum bond length able to carry out the maximum anchorage force as defined in the abovementioned CNR-DT 200/2004 Bulletin. In this Bulletin, a method for evaluating the bond strength is suggested, and the authors of the present article have established that if the values of the aged materials are used for calculation, then the relationship is still effective. Once more, this study confirms that an attentive pre-reinforcement analysis on the substrate must be carried out for a correct and long-term effectiveness of the reinforcement system.

The effects of moisture content on masonry reinforced specimens subjected to pull-off tests were studied by Ghiassi et al. (2012). Masonry bricks were reinforced with GFRP applied through a wet lay-up application and immersed in water at a 23°C controlled environment for 4 and 8 weeks duration. Reversibility of moisture effects was also examined in this campaign by removing a group of specimens from immersion and allowing them to dry for one week prior to testing, while the other specimens were tested immediately after conditioning. Strength reduction resulting from the pull-off tests demonstrates a negative effect of moisture on the bond strength, of 15% after 4 weeks exposure and 23% after 8 weeks exposure. The linearly constant reduction noticed here as opposed to the insignificant variation of results in the study reviewed above (Sciolti, 2012) could

be attributed to the different substrates used in the experimental campaigns: calcareous natural stone as opposed to clay brick. The failure mode also varied between unexposed and conditioned specimens as in the first type failure occurred within the substrate, whereas in the second, failure occurred in the primer-brick interface, denoting a weakening in the bond. Although the specimens which were allowed to dry for one week before testing recovered an average 3% of bond strength, their reduction was constantly decreasing as well.

The durability of FRP reinforced masonry bricks when subjected to thermal cycles was investigated in a second study conducted by Ghiassi et al. (2013) in an experimental campaign conducted on single bricks reinforced with sheets of glass fibre applied through the wet lay-up technique and tested to shear strength. The specimens were exposed to two different thermal cycles, one ranging between 10°C and 50°C for 6h periods at a constant relative humidity of 90% while the second exposure consisted in -10°C and +30°C for 6h periods at the same constant relative humidity, for a maximum of 200 cycles each; intermediate testing was performed every 50 cycles. The first environmental condition (10°C/50°C) seemed to have the most detrimental effects on the specimens, as soon after 100 cycles the bond strength had decreased by 17%, reaching 45% after 200 cycles. The second condition (-10°C/+30°C) instead showed very little variation of bond strength between an unconditioned state or no conditioning at all, reaching a maximum decrease of 8%.

In conclusion, this-state-of-the-art review has revealed that experimental investigations on FRCM systems when subjected to environmental conditions are virtually nonexistent. The original contribution of this dissertation will be to bridge the gap in the knowledge concerning FRCM durability, by providing new data as a point of departure, responding to this pressing need. Thus, the experimental campaigns analysed up to this point represent a starting point both for method and comparison of results.

PART II: New Work

Chapter III. Experimental Campaigns.

Given the lack of previous durability testing conducted on FRCM, the typology of environmental exposure necessary to proceed was derived not only from the standards (CNR-DT 200/2004; National Italian Guidelines, 2012; see Chapter I.b: Fibre Reinforced Cementitious Matrix (FRCM)), even though specifically designed for FRP solutions, but also by the previous durability testing references on FRP (Chapter II. Durability of Reinforcements). From the original research carried out in this work it becomes clear that environmental conditions created for the purpose of durability testing of fibre reinforced materials - for FRP reinforcements at any rate - should be directed towards temperature variations, humidity sorption and saline and alkaline exposure. Furthermore, due to the fact that testing is conducted on cementitious matrices, classic testing typology for mortars or cementitious materials was carried out, as freeze/thaw cycling.

With the instruments and devices available at the Laboratory of the Department of Architecture of the University of Florence, durability testing on specimens subjected to exposure to alkaline solution was not possible, therefore testing was focused on freeze/thaw and wet/dry cycles, where the wet environment consisted in saline solutions. Furthermore, the experimental campaigns analysed for the state-of-knowledge show that freeze/thaw and wet/dry cycles seemed to be the most aggressive for the long-term functionality of the reinforcement itself. These two types of artificial ageing were not mixed in the following experimental campaigns; in fact, specimens were either subjected to wet/dry or freeze/thaw cycles, but not cycles that combined effects such as freeze in a sodium chloride solution and thaw in a dry environment. The reason for this separation of ageing techniques is that if there were to be specific degradation effects on the FRCM system due to one specific ageing cycle then the combination with the other type of environmental cycle would have made it impossible to identify the true cause of degradation. This being said, in future testing the combination of the environmental effects may display detrimental ageing effects that can be crucial for correct maintenance programs for fibre reinforced structures.

The difference between FRP and FRCM is that the first type of reinforcement uses a polymeric matrix, while the second kind employs a cementitious matrix. As mentioned above, the motivation for the present research is the lack of experimental data on durability testing on cementitious matrices for FRCM reinforcements. The differences in the two types of matrices are such that the results of testing conducted up to this moment on durability of FRP materials may not be transferable to FRCM (i.e., total loss of effectiveness together with damage to the substrate caused by mould and saline concentrations). Cementitious matrices in fact are porous, which is why they are

compatible with masonry, allowing the structural substrate to “breathe”, that is allowing masonry to absorb humidity from the environment and then excrete it once the environmental conditions change. Humidity and liquids are absorbed by cementitious matrices in greater measure than by resins, which are not porous. Furthermore, evaporation of liquids and humidity completes the inverse passage in cementitious matrices, which does not occur in resins thus causing concentrations of humidity and mould between resins and substrate.

Due to the abovementioned porous characteristic of cementitious matrices, one of the effects expected from the wet/dry cycles is sorption of the saline solution used during the wet cycles. This could cause pulverisation of the mortar, since once the solution is absorbed, the subsequent evaporation during the dry cycle may leave the external layers of the specimen brittle or even detached, ultimately causing loss of section. Although the humidity content in the specimens may not be permanent, saline concentrations could also cause cracking as the saline particles migrate towards the centre of the section. More effects caused in general by humidity sorption and evaporation could be a loss of adherence to the fibres imbedded in the mortar, due to the brittleness caused by the evaporation of the solution. In general, if loss of adherence is presented, this could imply the loss of effectiveness of the FRCM system, similarly to what has been found in FRP reinforced systems when detachments occur in the frp-substrate interface. As mentioned before, (Chapter I.3.b: Fibre Reinforced Cementitious Matrix), the expansion of frozen water particles up to 9% their original liquid volume in cementitious materials causes pressure in the pore walls, possibly leading to cracking, at even low percentages of humidity, as those in the settings of the environmental chamber. It is not expected that there be any permanent damage caused to the structural interface, such as mould.

The results of the tests give a better understanding of what happens to FRCM when exposed to environmental agents. Effects caused by specific conditions could be calculated ahead of time smaking possible the formulation of adequate maintenance programmes for FRCM systems. For example, in the case of pulverisation or loss of section due to frequent rain or humidity sorption, a long term plan of verification of the solidity of the matrix and its potential substitution could be put in place. As has been done for FRP systems, (ChapterII.1.a: Codes and Regulations) conversion factors taking into consideration the environmental conditions of FRCM systems could also be adopted when designing such strengthening methods.

The experimental campaigns illustrated in this Chapter were carried out on different types of

specimens that varied in size and followed the differentiation and testing procedures described in Chapter II. Durability of Reinforcements. Similarly to what was discussed previously, where many authors test the durability of FRP systems with and without their structural support, here both reinforced mortar elements and masonry samples have been subjected to environmental exposure and then tested, given the nature of FRCM reinforcements which are immersed in a cementitious matrix. The first testing was conducted on fibres and matrices, then on small masonry elements and finally on larger masonry portions. More specifically, a large number of smaller and more manageable specimens, consisting in the fibres and matrices alone, were tested; next, a small number of masonry pilasters reinforced with common types of FRCM, such as glass reinforced cement matrix; and, finally, four larger masonry panels reinforced through the reticolatus method illustrated in Chapter 1.c:Reticolatus.

Studies in reinforced masonry have shown how the choice of cementitious matrices is a more compatible solution in fibre reinforcement. The present work should determine whether this fact remains true in service conditions, with experimental campaigns aimed toward the comparison of FRCM and FRP reinforced masonry subjected to moisture and temperature cycles.

1. Freeze/Thaw Durability on Reinforced Mortar Specimens

In this first investigation (Sinicropi et al., 2014), mortar prisms created ad-hoc were tested to flexural strength after having been exposed to freeze/thaw cycles. The mortar prisms were subjected to flexural testing and not pull-off tests since the interest here was primarily the analysis of the structural behaviour of the fibre-matrix composite, namely the flexural behaviour of the reinforced element, when subjected to environmental conditioning. The prisms were made and tested

N° of Specimens	Type of Mortar	Type of Reinforcement	N° of Freeze/Thaw Cycles		
27	Lime	Unreinforced (9)	0 (3)	52 (3)	100 (3)
		Steel (9)	0 (3)	52 (3)	100 (3)
		Glass (9)	0 (3)	52 (3)	100 (3)
27	Cement	Unreinforced (9)	0 (3)	52 (3)	100 (3)
		Steel (9)	0 (3)	52 (3)	100 (3)
		Glass (9)	0 (3)	52 (3)	100 (3)
18	MX	Unreinforced (9)	0 (3)	52 (3)	100 (3)
		PBO (9)	0 (3)	52 (3)	100 (3)

Table 3.a. Test matrix. In parenthesis the number of specimens per type.

with both the dimensions and the test setup determined by the European standardization EN 1015-11 on the determination of flexural and compressive strength of hardened mortar.

Experimental Programme and Materials

The experimental program can best be summed up in Table 3.a. A total of 63 mortar specimens were tested. The specimens were divided into series of three for each typology of mortar, reinforcement and number of cycles in order to obtain results which could reasonably represent average values. Each typology of mortar specimen was prepared with the same batch of mixture in order to avoid differences due to varied conditions during preparation. The mortar typologies prepared consisted in lime mortar, cement mortar and MX, an inorganic mortar provided by Ruredil spa. The lime mortar (water, lime sand) proportions used were 2:1:7.5 in weight, while the cement mortar (water, lime, 42.5 MPa cement, sand) proportions in weight were 2:1:1:8.

Lime mortar was commonly used for masonry buildings in the past, given its readily available ingredients. The type of lime mortar used in the present campaigns was chosen for its similarity to historical mortars. Cement mortar is now used in its place, given the added ingredient of cement which increases the mechanical properties of the mortar. These two mortars have been widely used in historical and non masonry buildings, and have proven their complete compatibility, hence their adoption in the present campaigns as fac-simili of an FRCM reinforcement.

The choice of the third type of mortar used in the following experimental campaigns fell on Ruredil's MX mortar. While the first two mortars, lime and cement, are prepared by hand and therefore the proportions of the ingredients may vary according to necessity (i.e., a humid construction environment) or the hand which combines them, MX presents a mortar ready to mix with water, and therefore with known flexural and compressive behaviour listed in its attached specifications. Furthermore, the system MX-PBO fibre is a readymade FRCM reinforcement, which makes it appealing for its use in building sites where the cost of labour is an ever present issue. Regarding its composition, MX is a stabilised inorganic mortar, thus offering all the advantages of cementitious matrices in fibre reinforcement methods, which employs pozzolanic ash as a hydraulic binder. This specific combination of MX mortar with PBO fibres produced by Ruredil and known as X Mesh Gold™, is protected by patent, and for this reason it is not possible to obtain a more detailed description of the ingredients of the mortar itself.

Once the mortar was prepared, it was poured into steel forms with three separate voids of

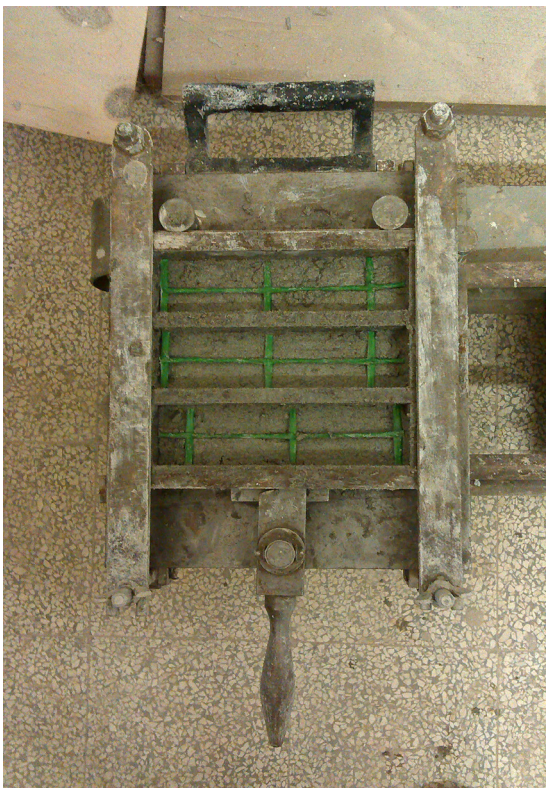

Figures. 3.1.1-2 . Glass reinforcement in cement mortar prisms in preparation in the steel framework used in the moulding of specimens; prisms in the environmental chamber.

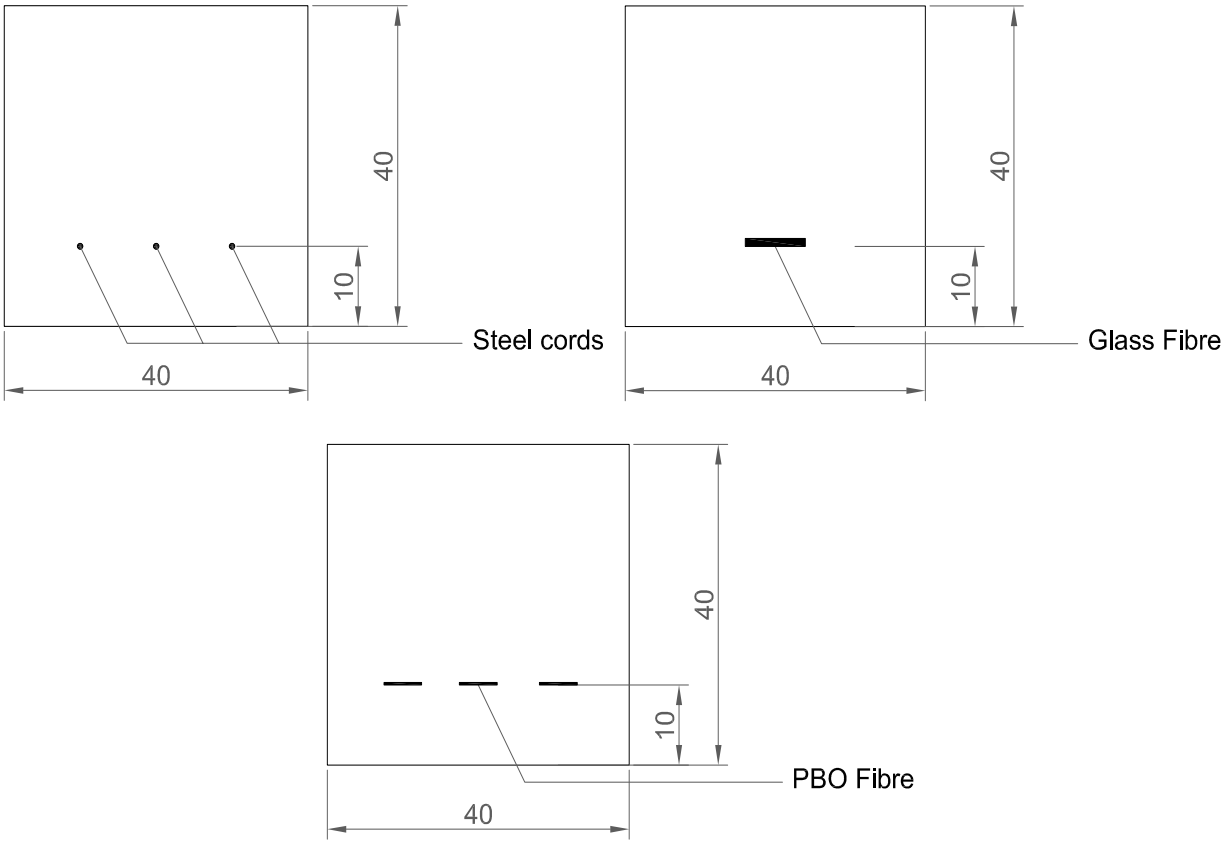

Figures. 3.1.3-5. Position of the fibres in the prisms according to fibre type; dimensions in mm.

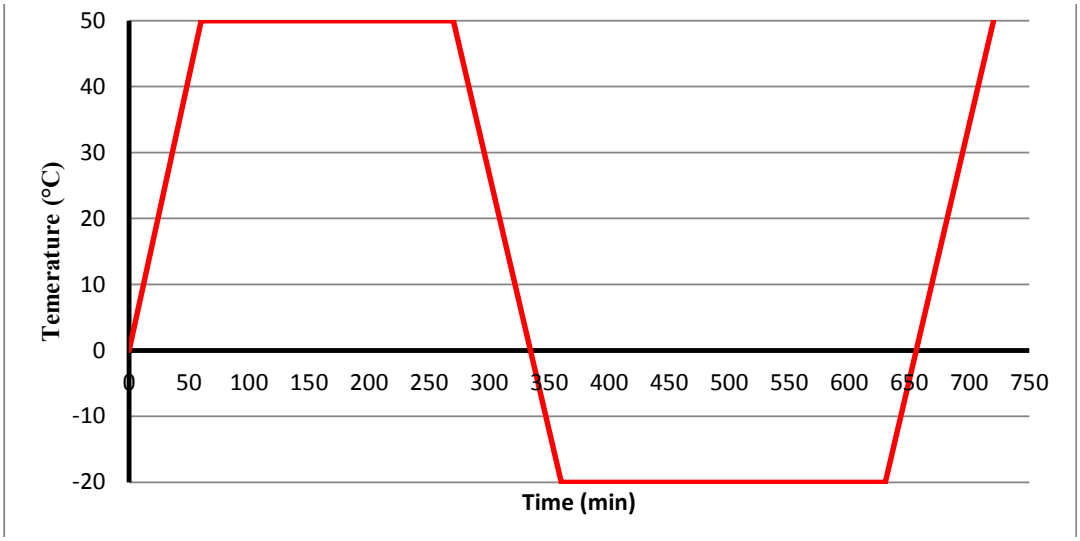

Figure. 3.1.6. Temperature Variation.

4x4x16cm which latched onto a machine that eliminates residual air bubbles or areas of uneven density through beating the wet prisms. In the reinforced prisms the strips of steel, glass or PBO (Poliparaphenylene benzobisoxazole) fibres were positioned at 1cm from the lower section (Fig. 3.1.1), attached to the beating machine in order to render the mortar as compact as possible, hence avoiding slipping of the fibres throughout the section during curing. The specimens were then filled to their final measure and then latched to the machine again. The prisms were then left to cure in a humid free environment for 28 days. The prisms subjected to thermal ageing were placed in an environmental chamber (Fig. 3.1.2), which was programmed to vary its internal temperature from -20°C to 50°C every 6 hours, employing circa 90 mins for the temperature variation, as illustrated in Fig. 3.1.6. One limit of this research consists in the fact that specific relative humidity values were not established for the freeze or thaw settings of the environmental chamber used for this campaign.The chamber was programmed for duration of cycles, and temperature variation. The relative humidity of the chamber, without being specifically set, was therefore an automatic value of 45% circa. As stated in the general introduction to the present Chapter, in the experimental campaigns that constitute the original contribution of this work the effects of freeze/thaw and wet/dry cycles were considered in separate analyses. This approach was used in order to establish damage or the diminution of resistance for separate causes. The limitation of this approach is that the damage due to freeze-wet/thaw-dry does not form a part of the enquiry. Elevated humidity values during freezing of porous materials such as the hand mixed lime and cement mortars used for the experimental campaigns in this work usually cause damage, especially to the external

Steel Cords	Glass Fibre	PBO
Cord Diameter: 0.89 mm	Bar section: 10 mm^2	Fibre Density: 1.56 g/cm^3
Tensile Failure Load: 1540 N	Tensile Failure Load: 3500 N	Tensile Strength: 5.8 GPa
Strain to Failure: 2.1%	Strain to Failure: 1.5%	Strain to Failure: 2.15%

Table 3.b. Mechanical properties of the fibres provided by manufacturers.

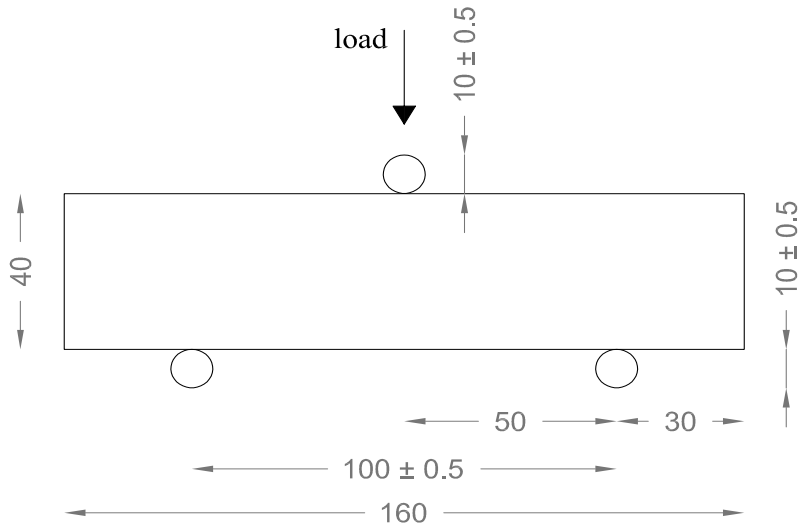

Figure. 3.1.7. Test set-up; dimensions in mm.

Mortar Type	Average Flexural Strength (MPa)	Average Compression Strength (MPa)
Lime	0.17	0.5
Cement	0.42	4
MX	5.83 (3.5)	27.14 (20)

Table 3.c. Average values of flexural and compression strength obtained through testing on mortar specimens.

layers of the specimens. Porous materials present an easy intake of water and humidity, and the damage would consist in scaling of the surface, provoked by the rupture of the pore walls which have been saturated. As freeze/thaw cycles progress, the pressure in the pore walls grows, inducing cracking (Mu et al., 2010). This is what would be expected from porous materials subjected to both temperature and humidity variation. However, in the cases illustrated here, the separate effects of temperature and humidity were investigated.

The steel fibre used in this experimental campaign is the 3x2 Cord provided by Hardwire, llc. It consists in three linear threads wrapped by two threads, all of a 0,35 mm diameter. The glass fibre was FB MESH 66X66T96AR, provided by FibreNet, produced with Textrusion™ technologies, with a 66x66 mm mesh of alkaline resistant glass fibre bars saturated in an epoxy resin. Both the

MX mortar and the PBO fibres were provided by Ruredil. Mechanical properties of the fibres used are shown in Table 3.b.

The mechanical properties of the lime and cement mortar were obtained through testing performed according to the document EN 1015-11: first flexural tests were performed on un reinforced mortar prisms, then compression tests were performed on the two halves of the specimens resulting from the previous flexural tests. The resulting values are shown in Table 3.c. With regard to the MX mortar, the values which were registered in the laboratory on MX mortar specimens are registered in black whereas the values assumed for flexural and compression strength were those provided by Ruredil, in blue in Table 3.c. Experimental values show an increase with respect to the company provided values which were probably calculated using a safety factor.

After the programmed thermal cycles were complete, the prisms were placed onto the test machine for three point bending, set up according to the requirements of the European Standards contained in the document EN 1015-11 and as illustrated in Figure 3.1.7. All tests were performed in the Laboratory of the Department of Architecture of the University of Florence.

Test Set-up and Instrumentation.

The specimens were loaded through a hydraulic actuator with two loading phases: the first phase worked under a displacement control at 2mm/min until reaching a load of 50 N (Soft Start). The second phase can be considered the proper loading phase. This phase, as specified in the EN 1015-11 Standards, should be programmed in such a way that collapse occurs between 30 and 90 seconds. Given the considerable differences of resistance of the three different types of mortar, the speed with which loads were applied was varied ad hoc for each mortar type. Once the load peak diminished by 50%, testing was automatically considered complete and specimens were unloaded. Data was acquired through a National Instrument system in terms of load/displacement diagrams. Maximum load values were then used to calculate flexural strength of unreinforced specimens according to the formula:

$$f_{fl} = 1{,}5\ (\mathrm{F}l)/(bd^2) \qquad (1)$$

where F is maximum load in Newton, l is the distance between the axis of the cylindrical supports, and b and d are respectively the width and the depth of the specimens, equal in this case.

Specimens were given the notation XyZ, where X denominates the type of mortar (L for lime, C for cement and MX), y is the kind of reinforcement (nr for un reinforced, st for steel, gl for glass and PBO) and Z is the number of cycles the specimen is subjected to. For example, specimen 6Lst100 is a steel fibre reinforced lime mortar specimen which has been subjected to 100 freeze/ thaw cycles.

Results

The initial results were quite contradictory since in both lime and cement mortar specimens it seemed as though the artificial ageing process in the environmental chamber inconsistently increased and decreased their flexural values, regardless of the number of cycles they had been subjected to. It was therefore inferred that the extra curing time in the environmental chamber, no matter what the internal temperature, facilitated the specimens to develop higher resistance values. Consequently, testing was repeated on all specimen typologies, with new specimens that were allowed to cure for a minimum of 8 weeks, allowing for the mortar to reach a complete maturing process. After this longer curing period, the specimens were tested either un-aged or put back in the en-

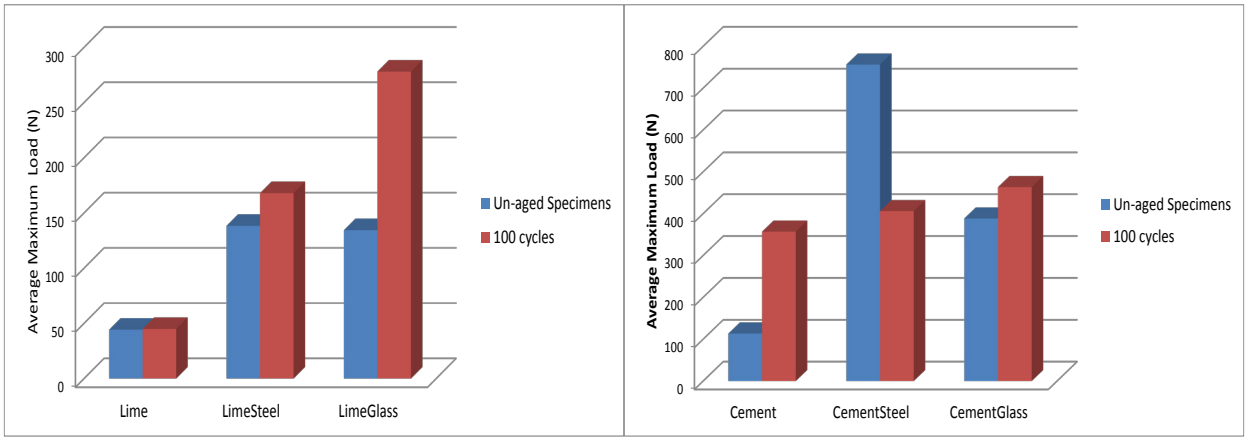

Figures 3.1.8-9. Values for lime and cement mortar specimens when subjected to ageing cycles after a curing period of only 28 days.

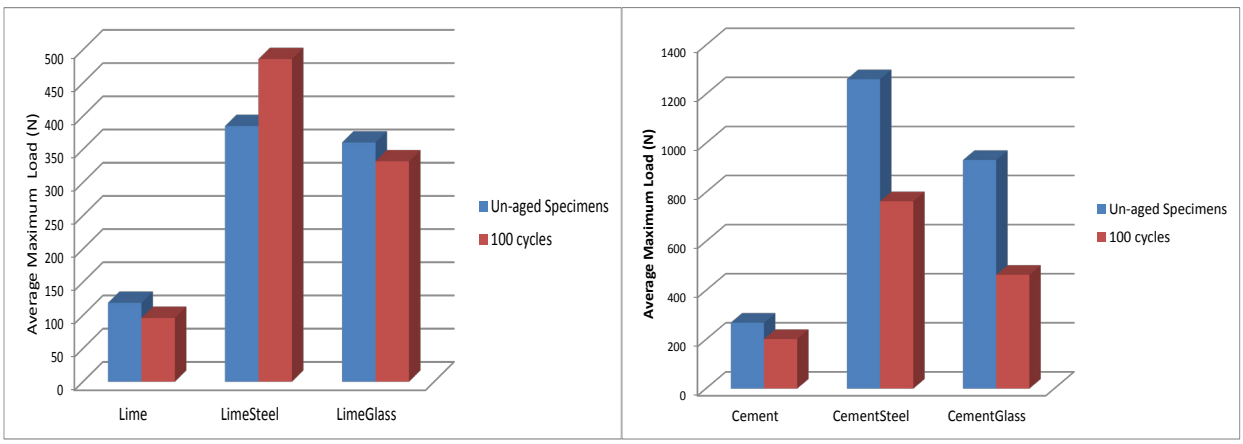

Figures 3.1.10-11. Values for lime and cement mortar specimens when subjected to ageing cycles after a curing period of 8 weeks.

vironmental chamber for freeze/thaw cycling. Although values did not change for the inorganic MX mortar provided by Ruredil, the hand mixed cement and lime mortars showed great benefit from the extra curing time, as shown in the charts below regarding lime mortar specimens where the values of the un-aged specimens almost doubled (Lime Glass and Cement Glass in particular, Figs. 3.1.8-9).

The results illustrated in the following sections are those of the repeated tests on specimens allowed to cure for at least 8 weeks, results which prove to be congruent with a certain expected degradation of the materials after 100 freeze/thaw cycles.

Lime Mortar Specimens

From the photographic survey it appears that failure of reinforced specimens does not occur solely for flexural strength. In Figures 3.1.13 and 3.1.14 the evident fractures are not only vertical, but also at a 45° angle, proving failure to be of a mixed type, of both shear and flexural. The first crack to commence in these specimens is the vertical one, given by excessive flexural strength. The crack then propagates horizontally, causing slipping through bond adherence loss, along the line of the reinforcement, and once it reaches the area of the lower supports shear strength failure prevails, as flexural rupture is prevented by the presence of the fibres. The expected behaviour of the reinforced and aged specimens would be to decrease in a more constant manner: mortar generally presents lower shear resistance that flexural. In fact, the glass reinforced specimens gradually lose resistance as the cycles continue, albeit the largest loss is between 0 and 52 cycles, while there is little variation in the remaining cycles. This may be also said for steel fibre reinforced specimens, while values increase between 0 and 52 cycles. From the observation of the failure mode of the reinforced specimens, it is clear that all specimens present a loss of bond strength to the fibres during collapse.

Lime mortar				
Type of Specimen	Average Flexural Strength (MPa)	Standard Deviation (MPa)	CoV	Flexural Strength Variation (%)
NR	0.17	0.12	0.70	
NR52 F/T	0.21	---	---	-25%
NR100 F/T	0.23	0.06	0.26	35%

Table 3.e. Average values of flexural strength of unreinforced lime mortar specimens subjected to thermal cycles.

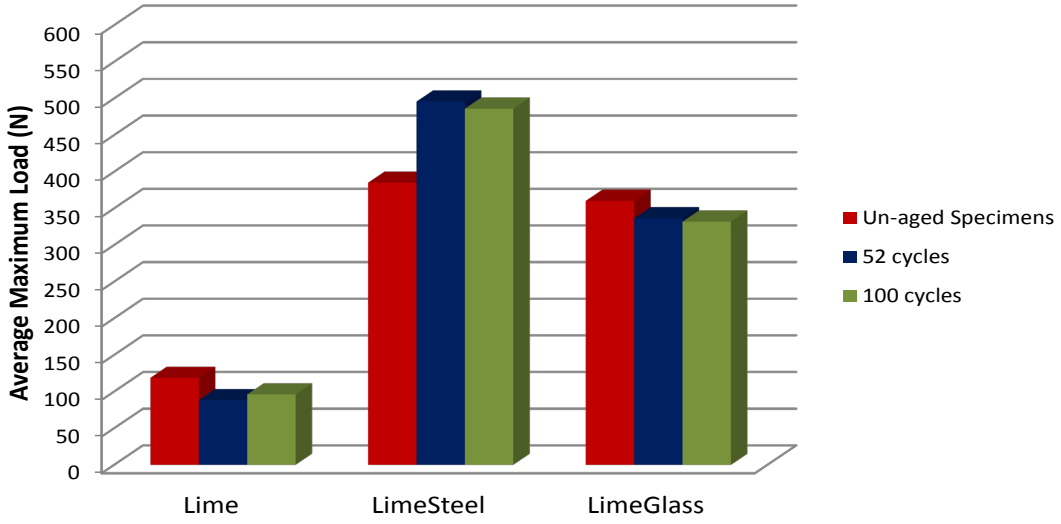

Figure 3.1.12. Average Maximum load of lime mortar specimens, unreinforced, steel reinforced and glass reinforced, subjected to thermal cycles.

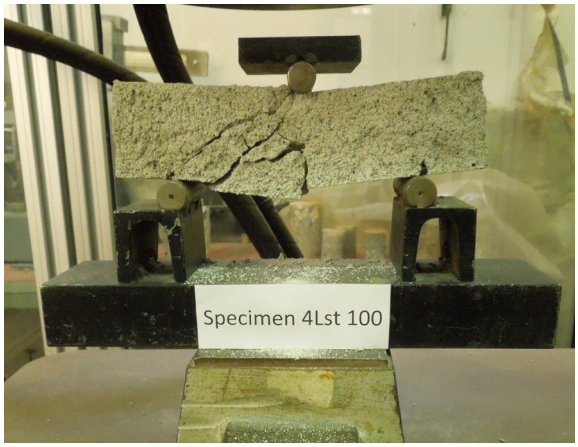

Figures 3.1.13-14. Lime mortar specimens reinforced with steel fibre subjected to 52 and 100 freeze/thaw cycles: mixed failure mechanism.

Cement Mortar Specimens

The testing on cement mortar specimens presents rather different behaviour compared to the previously described lime mortar specimens. There seems to be a recurring recovery of strength in the period between 52 and 100 cycles in the reinforced specimens. The scattering of these results could be due to the aforementioned mixed failure mechanism, present in the cement mortar specimens as well, where the crack propagation goes from flexural to shear following the horizontal line of the reinforcement. In fact, as can be observed in Figure 3.1.15, glass reinforced specimens subjected to 100 freeze/thaw cycles recover about half the strength lost after 52 cycles. Although it is believed that a certain strength loss is in fact given by the ageing process, values which scatter to this extent seem exaggerated. In this case the registered results for specimens subjected to 52 cycles could be misrepresentative of flexural values and more appropriate for shear strength. The glass reinforced specimens present only 3% enhancements of their strength once 100 freeze/thaw

cycles were completed, nonetheless confirming the fact that forced curing increases the flexural strength of reinforced cement mortar. After only 52 thermal cycles however their strength had slightly decreased, but again the mixed failure mode was encountered and loss of strength could partially be attributed to this apparently common occurrence. Bond adherence loss between mortar and reinforcement was observed in every reinforced specimen.

Cement Mortar				
Type of Specimen	Average Flexural Strength (MPa)	Standard Deviation (MPa)	CoV	Flexural Strength Variation (%)
NR	0.63	0.09	0.14	
NR52 F/T	0.68	0.25	0.37	8%
NR100 F/T	0.47	0.03	0.06	-16%

Table 3.f. Average values of flexural strength of unreinforced cement mortar specimens subjected to thermal cycles.

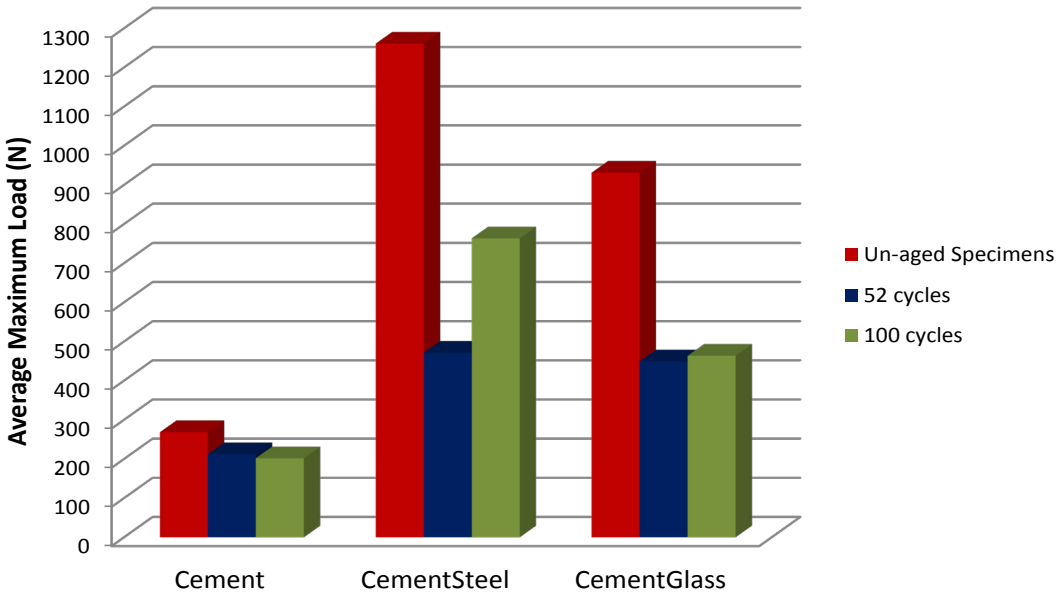

Figure 3.1.15. Average maximum loads for cement mortar specimens, unreinforced, steel reinforced and glass reinforced, subjected to thermal cycles.

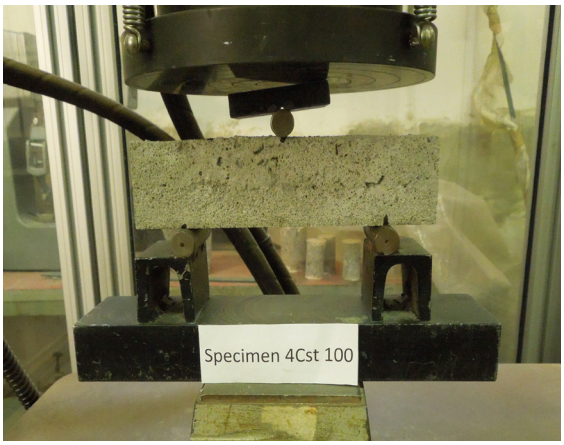

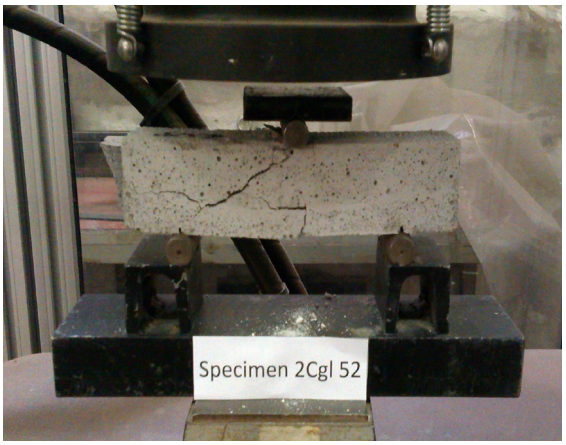

Figures 3.1.16-17. Mixed failure mechanism of steel and glass reinforced cement mortar specimens.

MX Mortar Specimens Reinforced with PBO

This series of testing was significantly different from the first two, both because of the flexural strength demonstrated by the specimens and the failure modes observed. The flexural strength of the MX mortar specimens was considerably higher than that of the lime and cement mortar prisms, as was to be expected given the reinforced nature of the mortar itself and the high mechanical characteristics of the PBO fibres. In this case, ageing seems to steadily increase the flexural strength between 0 and 52 cycles, from an average value of 5.83 MPa of non-aged specimens to 7.64 MPa of the specimens subjected to 52 freeze/thaw cycles (Table 3.g and Figure 3.1.18). In the reinforced specimens a slight decrease in the average maximum load was registered between 52 and 100 cycles, which is more evident in the unreinforced specimens, where in fact a flexural strength decrease of 1% is registered with comparison to the unaged specimens. The observed failure mode was flexural in all specimens, and a yielding in the fibres was observed but not, as in the other mortar specimens, a loss in bond quality (Figs. 3.1.19 and 3.1.20).

MX Mortar				
Type of Specimen	Mean Flexural Strength (MPa)	Standard Deviation (MPa)	CoV	Flexural Strength Variation (%)
NR	5.83	0.84	0.14	
NR52 F/T	7.64	0.56	0.07	31%
NR100 F/T	5.76	0.18	0.03	-1%

Table 3.g. Average values of flexural strength of unreinforced MX mortar specimens subjected to thermal cycles.

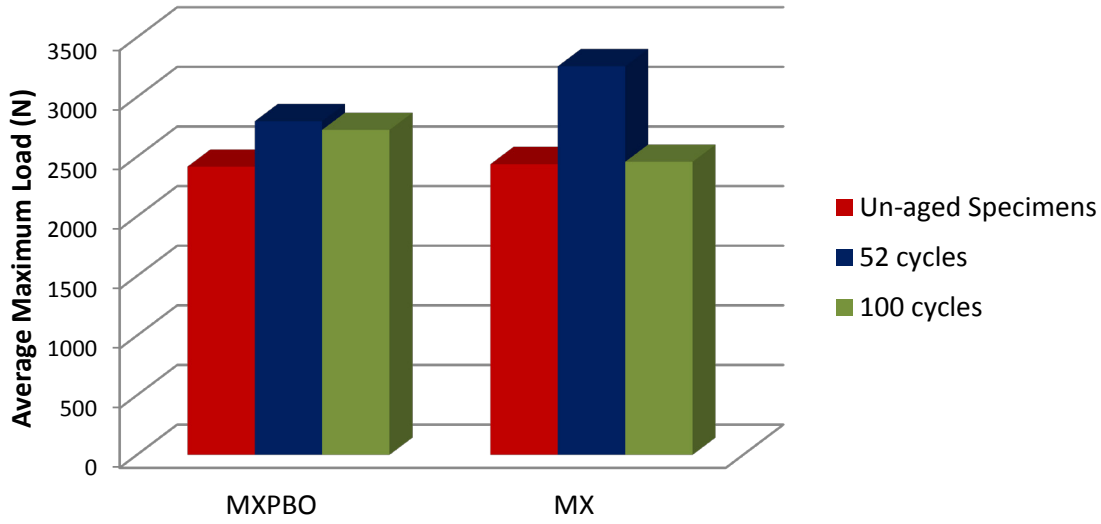

Figure 3.1.18. Average flexural strength of MX mortar specimens reinforced with PBO fibre and subjected to thermal cycles.

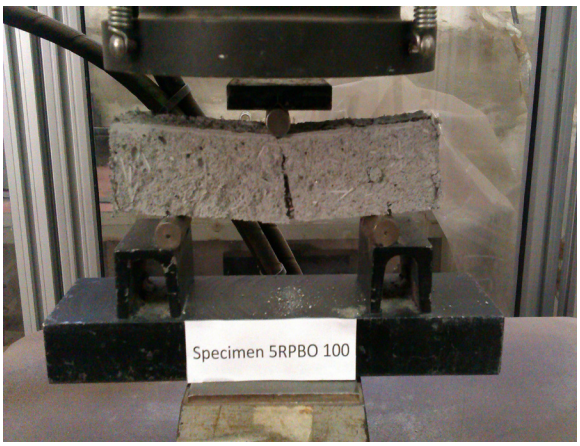

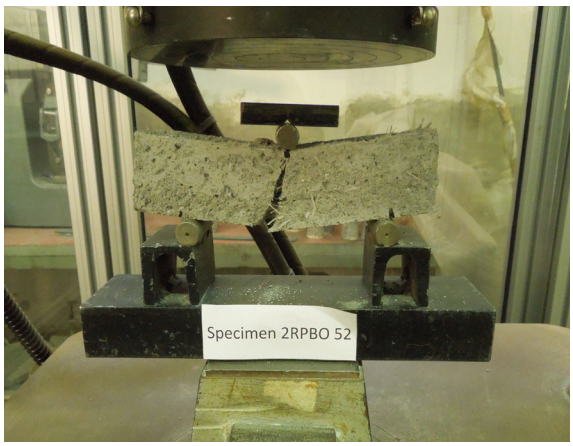

Figures 3.1.19-20. Failure of PBO reinforced MX specimens subjected to 100 and 52 thermal cycles.

Conclusions

From the results of the flexural tests conducted on the 63 mortar specimens subjected to freeze/thaw cycles, the following conclusions can be drawn. Unreinforced lime mortar specimens appear to decrease in flexural strength mainly after going through 52 thermal cycles, while a slight resistance loss is registered between 52 and 100 cycles. Reinforced lime specimens, both aged and unaged, collapse due to a mixed failure mode which could lead to a misrepresentation of test results. Unreinforced cement mortar specimens steadily decrease in flexural strength in the period between 0 and 52 cycles, while there is a recovery of resistance in the remaining cycles. The collapse mechanism is through a mixed failure mode for all reinforced specimens aged and not, which may lead to a misrepresentation of test results. There is always a loss of bond adherence in all reinforced lime and cement specimens. Unreinforced MX mortar specimens present an incongruent peak of resistance after 52 thermal cycles, after which, at 100 cycles, the value of flexural strength returns almost to the value of unaged specimens. MX mortar reinforced with PBO fibres increase their flexural strength after thermal cycles and in every specimen fibre yielding, and not bond loss, is observed.

The results presented in this experimental campaign suggest that Fibre Reinforced Cementitious Matrices are not heavily influenced by thermal cycles.

2. Wet/Dry Durability on Reinforced Mortar Specimens

The second experimental campaign was also carried out on reinforced mortar specimens. The typology of the specimens was identical to those of the first campaign, where lime, cement and MX mortar was used as the matrix component and the fibres consisted in glass and steel for the lime and cement mortar and PBO for MX mortar (fig. 3.1.3-5). The preparation of the specimens was likewise equal to that in campaign number 1.

Experimental Programme and Materials

The experimental program can be best summed up in Table 3.h. Once an adequate number of specimens was defined for each typology of lime, reinforcement and cycle duration, the attention was directed towards the typology of wet and dry cycles to use in the campaign. Specimens were named according to a *nnXyyZZ* lettering system, where *nn* corresponds to the number of the specimen, *X* to the type of mortar (L = lime, C = cement and MX), *yy* to the type of reinforcement (nr = non reinforced, st = steel fibre, gl = glass fibre and PBO) and *ZZ* to the number of wet/dry cycles the specimens has been subjected to. For example, specimen 16Lst100 is a steel fibre lime mortar reinforced specimen which has been subjected to 100 wet dry cycles.

Different variables needed to be determined before the cycles could commence such as the duration of the wet cycle opposed to that of the dry cycle and the type of solution to be used. Through the state-of-the-art research, it appeared that it was most common for wet cycles to last up to 20' for smaller specimens, while the dry period could last up to 24h. Therefore, two types of cycles were tested in order to find the cycle period that would best fit the purpose: an aggressive accelerated ageing process that would allow the specimens to absorb the solution and dry, producing an authentic cyclic action. The first trial was composed of 20' wet cycles and 12h dry cycles at a constant temperature of 40°. During all wet cycles, care was taken that the specimens had at least 25 mm of solution covering the surface of the specimens. This was as specified in ASTM E 2098-00. In the case of this specific standard the specimens consisted in glass fibres, but as has been mentioned above, there are no specific regulations on durability testing of FRCM at this point in time, and therefore many testing procedures have been borrowed from other areas which have their own regulations and standards. The aggressive action of the first trial caused the weight loss of the specimens to be so irrelevant during the dry cycles that it could not have been properly de-

fined as cyclic. Furthermore, after very few cycles of this type, 50% of the lime specimens broke; another indication of the excessive aggressiveness of this cycle. The second type of wet/dry cycles was the one adopted (Fig. 3.2.2): 15' of wet cycle and 24h of dry cycle at a constant temperature of 35°. In this case the specimens were in fact able to lose a more consistent percentage of the

N° of Specimens	Type of Mortar	Type of Reinforcement	N° of Wet/Dry cycles		
36	Lime	Unreinforced (12)	0 (4)	50 (4)	100 (4)
		Steel (12)	0 (4)	50 (4)	100 (4)
		Glass (12)	0 (4)	50 (4)	100 (4)
36	Cement	Unreinforced (12)	0 (4)	50 (4)	100 (4)
		Steel (12)	0 (4)	50 (4)	100 (4)
		Glass (12)	0 (4)	50 (4)	100 (4)
24	Ruredil MX	Unreinforced (12)	0 (4)	50 (4)	100 (4)
		PBO (12)	0 (4)	50 (4)	100 (4)

Table 3.h. Test Matrix for the Wet/Dry durability campaign on reinforced mortar specimens. In parenthesis the number of specimens per type.

Figure 3.2.1. Mortar specimens during the wet portion of durability cycles in plastic basins filled with 5% sodium chloride solution specimens.

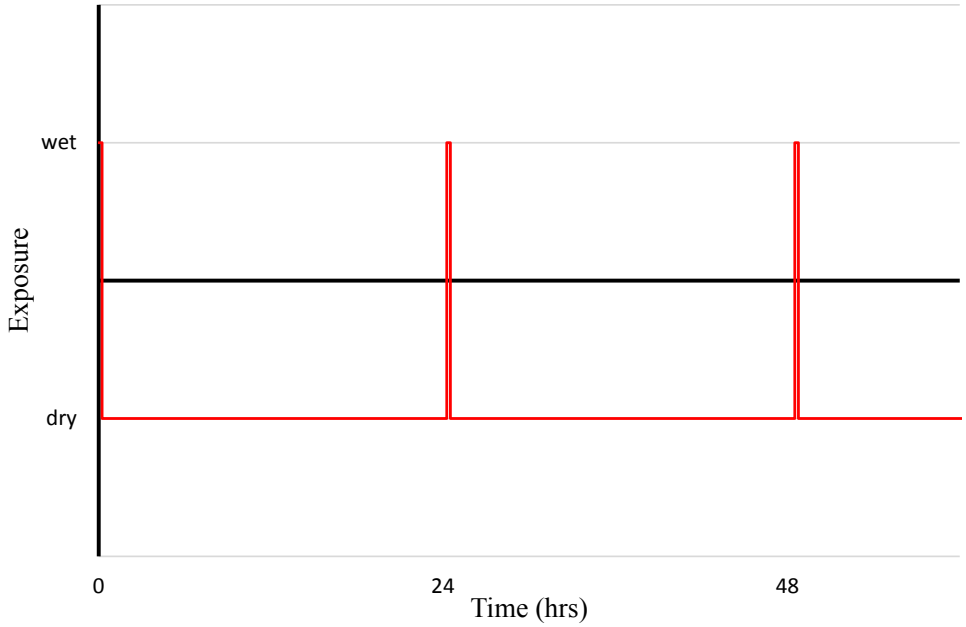

Figure 3.2.2. Wet/Dry variation mortar specimens were subjected to.

weight gained during the wet cycle. The temperature of the dry cycle was decreased so that the difference between the water temperature (20° circa) and the air temperature was not quite 1:2. This was done so that the specimens were subjected solely to a harsh wet cycle and not to a harsh drying period as well, which could have caused a double effect in the results. This was avoided so that the cause of degradation could remain clear.

Regarding the type of solution used for the wet cycle, once again guidance was found in the state-of-the-art research. The type of solution most used consisted of a small percentage of sodium chloride dissolved in water. Other solutions consisted of calcium chloride in distilled water and calcium hydroxide in distilled water. It was decided to use a 5% solution of sodium chloride in tap water, in order to exceed slightly the percentage of sodium chloride contained in the ocean (3.5%, Toutanji et al., 1998).

Another issue on the procedure for the wet/dry cycles arose after the first wet cycle as to whether the water basins containing tap water with a 5% NaCl solution contained in fact the same amount of solution after the cycles as before. The difference would result in the need to constantly change the solution in the water basins. The water was weighed in a 250ml flask (Fig. 3.2.3) before and after the immersion of the mortar specimens, indicating an increase in weight of about 3%, and therefore a difference in the chemical composition of the solution. Hence, the necessity of a fresh solution for every wet cycle.

The objective of the second experimental campaign was not only to verify whether the mechanical properties of fibre reinforced cementitious matrices effectively decrease after cycles of artificial ageing, but if these mechanical properties could in some way be recovered if adequate time was allowed for the specimens to recover. Testing that followed a recovery period was used in Ghiassi et al. (2012) on masonry reinforced through FRP, with scarce results. The intuition that cementitious matrices recover their properties more consistently than polymeric matrices, in which molecular degradation seems to commence after artificial ageing, was the reason for which in this experimental campaign specimens were divided into groups of 4 per mortar type, reinforcement and cycle period, 2 of which were tested at the end of their last wet cycle, still fully saturated with the sodium chloride solution, while the remaining two specimens were allowed a drying period, or recovery period, before testing. The suffix "__REC" in the notation of these specimens is the marker they carry of being tested after a recovery period. There was no time limit given to the recovery period. Specimens were considered to have completed their recovery when their weight

Figure 3.2.3. Flask used for determining weight difference prior to and after wet cycles.

seemed to have reached a plateau: initially (when weighed) the recovery specimens showed a constant decrease in weight, attributable to the constant loss of solution intake during cycles. Although the specimens might not reach their original curing weight before cycles, the weight loss would reach a certain percentage before stopping completely.

Test Set-up and Instrumentation

Both the test set-up and the instrumentation used in this campaign were identical to those described in section 1 of the present Chapter for the first experimental campaign (Fig. 3.1.6). the notation also followed the same principle as the specimens in the previous section.

Preliminary Considerations and Results

Some preliminary considerations of the degradation of the specimens may be made on the basis of the physical observation of specimens during the cycles.

The first consideration is directed towards the loss in specimen section. While the specimens before cycles began were all regularly 4x4x16 cm in size, the cycles produce a large loss in section particularly with regard to the lime specimens. The measured diminution of section varies from a minimum of 5% in the first few cycles, to a maximum of 25% in the lime prisms, where the mortar covering the fibres had almost completely detached (Fig. 3.2.4).

The loss of section in the cement mortar prisms is much less noticeable, varying from a range of 2% to 5%, whereas the section variation in the MX mortar specimens in virtually non-existent.

A second observation of the artificial ageing reveals permanent discoloration of the specimens

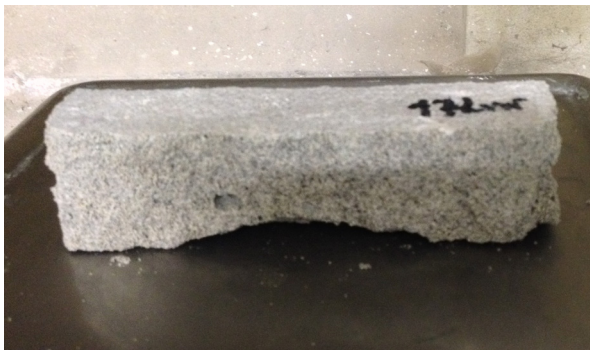

Figure 3.2.4. Evident loss of section after less than 10 cycles in an unreinforced lime specimen.

Figure 3.2.5. Discoloration of lime mortar specimens.In the middle specimen the rust of the steel fibres is evident.

during the progression of the cycles. Figure 3.2.5 demonstrates how the specimens present a light coloration as the curing time is concluded, whereas after cycles their colour reaches darker shades, an apparently non-reversible effect during the dry cycles. This could be due to factors such as the permanent variation of moisture content.

The permanent variation of moisture content of the specimens is shown in graphs in Figures 3.2.6-8. The weight of each specimen was registered before and after every wet cycle. Following are graphs of specimens' weight variation for unreinforced lime, unreinforced cement and unreinforced MX mortar (Figs. 3.2.6-8). Lime and cement mortar have a higher weight variation after the first wet cycle, and this increase remains throughout the cycles. In the case of cement mortar, the weight increase is constant, that is, after an obvious initial weight gain, it seems to settle on an average level of cyclic weight loss and gain. Instead, in the case of lime mortar, the curve that follows the average weight gain/loss is descending, consistent with the physical observation of section loss mentioned above. The conclusions in fact are clear: the sodium chloride solution erodes the surface of the lime mortar specimens with ease, whereas the cement mortar specimens are more resistant. Regarding the inorganic MX mortar, the percentage of initial weight increase is very low, and remains consistent throughout all cycles. Therefore, it may be concluded that the amount of sorption is minimal, and the results of the flexural testing, as well as the lack of section loss, confirm this last observation.

These considerations may not give a complete idea of the variation of mechanical properties during and after artificial ageing via wet/dry cycles, but they do confirm the initial idea of a higher level of degradation than that caused by freeze/thaw cycles.

Testing was carried out on a machine for three point bending as described in the freeze/thaw campaign. Given the great differences in the reactions of the specimens to the wet/dry cycles, the conclusions are again divided by type of mortar.

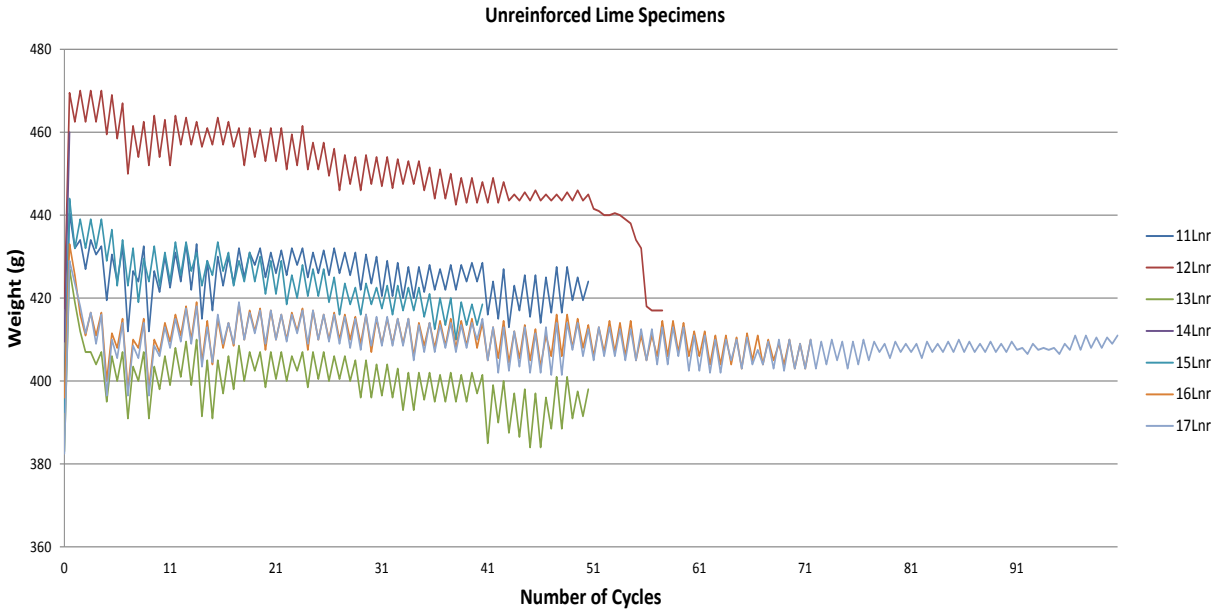

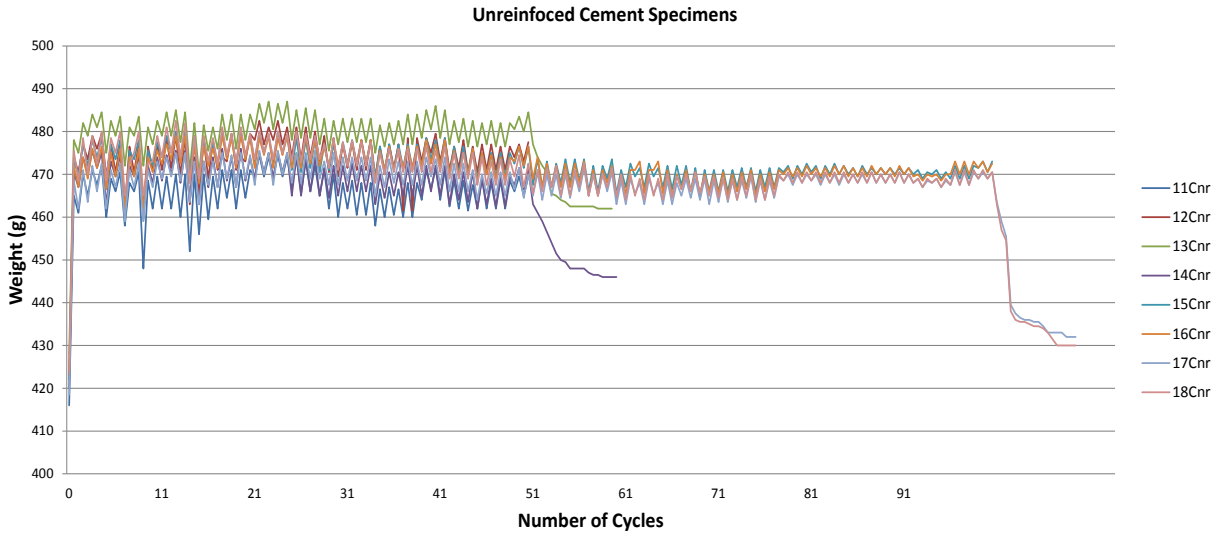

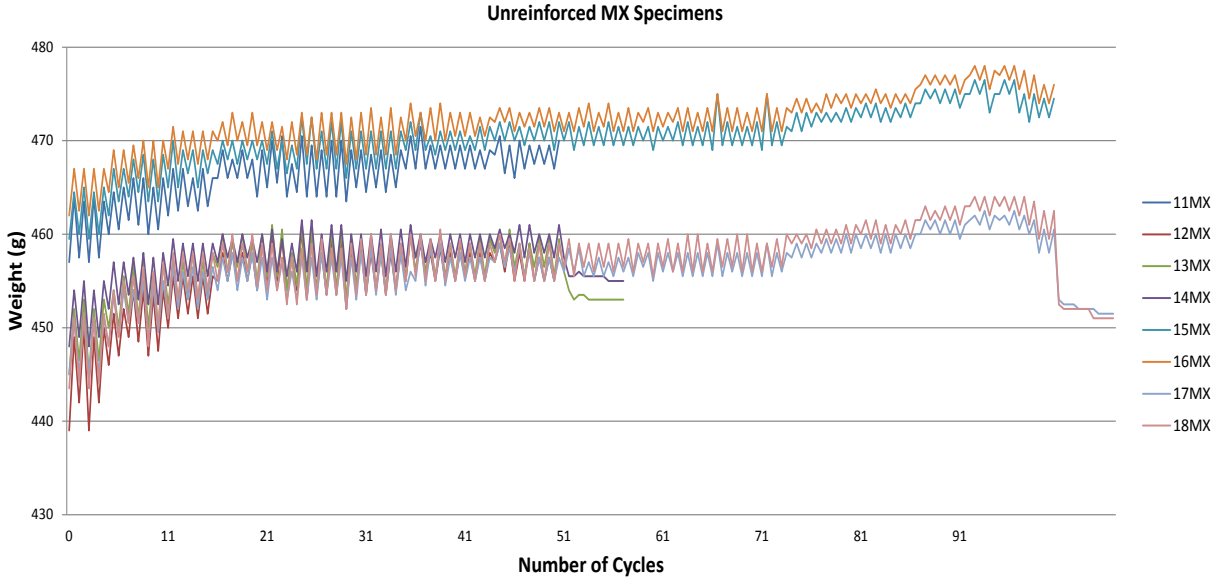

Figures 3.2.6-8. Unreinforced mortar specimens: weight variation.

Lime Mortar Specimens

Lime mortar is particularly delicate, as is clear from the flexural and compression values of unaged specimens provided in the previous section. It was commonly used in historical constructions, without the use of cement, and the sand in its composition was probably river sand, or very fine sand that was available in the area of construction. It does not offer great resistance; this was known to historical notables such as Leon Battista Alberti who, in his *De Re Aedificatoria* (ed. 1991), suggested the addition of ground brick or larger gravel to the mixture of water, lime and sand in order to render it more resistant. In the wet/dry cycles, the delicate nature of this mortar is quite evident, as can be noted by the values in the table and the graphs below. Along with the great loss in section and in weight observed above, the specimens did not always survive the cycles. This in fact was the case for unreinforced specimens 12Lnr50, 14Lnr50_REC, 15Lnr100, and 18Lnr100_REC, and for steel reinforced specimen 12Lst50.

There were also cases in which the specimens survived the cycles but not the soft start phase of the testing machine, such as for 11Lgl50 and 12Lgl50 – which explains the pale blue in the graph, since this value is not taken from the actual loads supported by the specimens but from the loads at which the soft start phase registered rupture. This is in some way an explanation for the peculiar trend in graph ii where the average loads are shown. Notwithstanding this lack of data, some interesting considerations may still be made. In unreinforced and glass reinforced specimens, the recovery period proved that mortar recuperates its original resistance values and even more so when given adequate time to dry.

This was not true for steel reinforced specimens as the rust in the steel fibre, noticeable from as early as the first 10 cycles, had given way to a type of degradation that is not interrupted through drying. The rust was so far advanced in specimens subjected to 100 cycles that, upon rupture, up to 2 cm of loss of the original length of the fibres was recorded (Fig. 3.2.9-10). Considering that the results for the glass reinforced specimens subjected to 50 wet/dry cycles are not reliable, a trend may nevertheless be observed in the results regarding the other specimens: those subjected to 0 cycles, 50 cycles with recovery, 100 cycles and 100 cycles with recovery. In these specimens it seems clear that when tested wet, the specimens lose strength which is regained when dried. If instead one were to consider the results of the glass reinforced specimens subjected to 50 cycles as reliable, then the spontaneous recovery obtained in the specimens subjected to 100 cycles would be consistent with the results found for cement mortar specimens (see section below).

In the weight variation graphs below, showing glass reinforced and steel reinforced specimens, some elements of interest come to light. For both types of specimens, there seems to be a thinning spot in the graph just before a more substantial weight loss in the specimens. This would indicate that the specimens had been fully saturated and in the allocated time for drying were incapable of losing the solution absorbed. This precedes a loss of section, after which the weight gain and loss during and after cycles picks up again. In all cases of reinforced specimens weight at testing was less than the original weight at the end of the curing period.

With respect to the sorption of the sodium chloride solution, in most specimens efflorescence occurs after the 20th cycle. This common effect of sodium chloride is visible mostly around the edges of the specimens as may be noted in Figure 3.2.11. Again, as in the first experimental campaign, reinforced specimens' collapse is due to two main factors: flexural strength and shear strength. This is clear in the photographic and video survey of the specimens during testing, where an initial vertical crack is registered which then gives way to a crack that runs along a 45° angle. In the unreinforced specimens the cracks propagate along the height of the parallelepiped in a vertical manner, given that the collapse is due, in both aged and unaged specimens, solely to flexural strength (Figs. 3.2.11-12). Regarding the behaviour of the fibres in the mortar specimens, as was noticed in the previous freeze/thaw durability campaign, a conspicuous bond quality loss was registered at collapse for both steel and glass reinforced mortar.

Lime mortar				
Type of Specimen	Average Flexural Strength (MPa)	Standard Deviation (MPa)	CoV	Flexural Strength Variation (%)
NR	0.17	0.12	0.70	
NR50 W/D	0.065	0.003	0.05	-32%
NR50 W/D_REC	0.23	---	---	35%
NR100 W/D	---	---	---	---
NR100 W/D_REC	0.014	---	---	-92%

Table 3.l. Values of flexural strength, standard deviation and Coefficient of Variation for unreinforced lime mortar specimens..

Figures 3.2.9-10. Total erosion of steel fibre in specimens 17Lst100_REC and 18Lst100_REC subjected to 100 wet/dry cycles.

Figures 3.2.11-12. Unreinforced specimens with evident efflorescence and flexural collapse and glass reinforced specimen with mixed collapse mechanism.

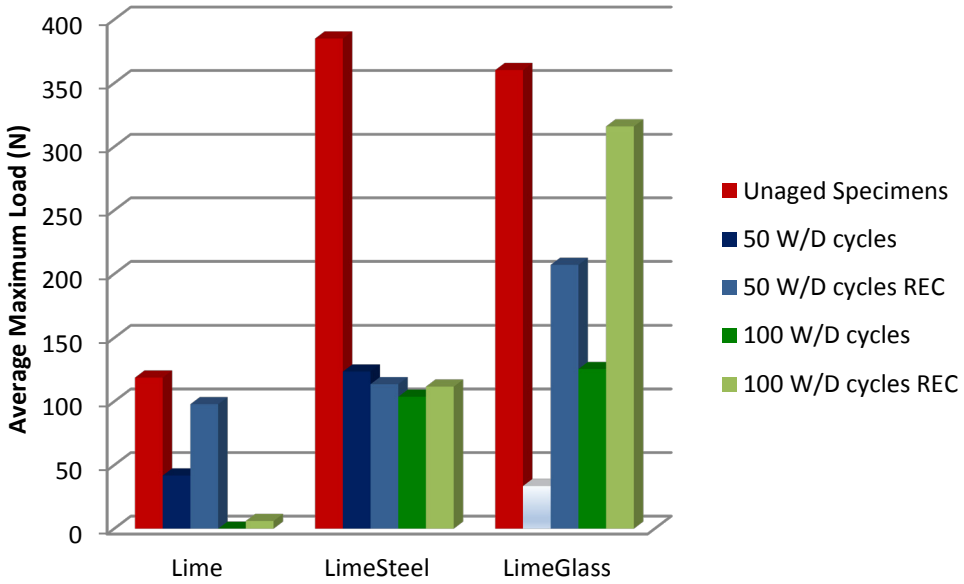

Figure 3.2.13. Average failure loads for lime mortar specimens subjected to none, 50 and 100 wet/dry cycles and relative recovery specimens.

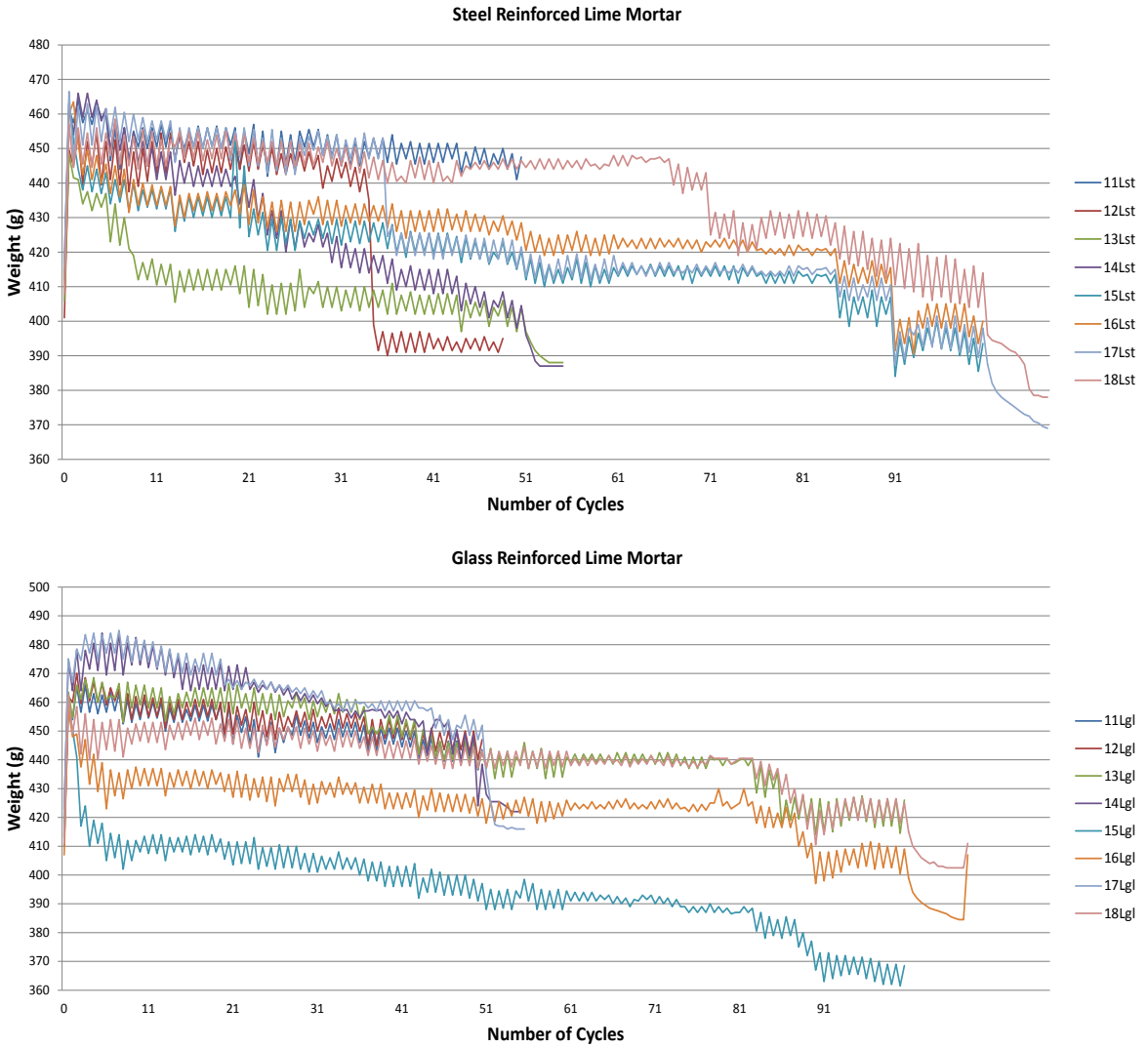

Figures 3.2.14-15. Steel and glass reinforced mortar specimens: weight variation.

Cement Mortar Specimens

Cement mortar is more resistant than the previous lime mortar thanks to the mixture which composes it which contains cement. This gives cement mortar an inherently stronger quality which is observable during cycles and testing, not only through the ultimate load values, but also in the physical phenomena mentioned above such as section variation. Test results in unreinforced specimens for flexural strength are consistent, in that the values progressively decrease during wet/dry cycles, but recover to values greater than original values on unaged specimens. Regarding steel and glass reinforced specimens, it can be observed that maximum loads diminish for 50 wet/dry cycles and then regain strength during the remaining 50 cycles. In fact, the specimens that were allowed a recovery period after 100 cycles returned to their original weight and exceeded the strength of the unaged specimens. In the case of cement mortar, the weight loss due to loss of section is less consistent than for the previously analysed lime mortar specimens; in fact, the en-

velope of the progression of the weight variation graphs is horizontal rather than descending. The loss of section is in most cases insignificant, as mentioned before, and efflorescence is common to most specimens. In the cases of the specimens in the figures below, efflorescence was found to be well embedded inside the section as well as concentrated along the line on which the fibre was placed during the construction of the specimen itself. This leads to the conclusion that the sorption of sodium chloride penetrated to the core of the parallelepiped and gathered around an "obstacle", in this case represented by steel fibres.

The mixed collapse mechanism is verified again in the reinforced cement mortar specimens; the first crack is of flexural type, vertical along the height of the specimen, and then a crack at a 45° angle occurs, causing collapse. Again, as in the lime mortar specimens, there is a loss in bond quality between the mortar and the fibres, and no rupture in the fibres was registered.

Cement Mortar				
Type of Specimen	Average Flexural Strength (MPa)	Standard Deviation (MPa)	CoV	Flexural Strength Variation (%)
NR	0.42	0.06	0.14	
NR50 W/D	0.27	0.05	0.18	-35%
NR50 W/D_REC	0.51	0.03	0.07	-19%
NR100 W/D	0.1	0.008	0.08	-74%
NR100 W/D_REC	0.55	0.01	0.02	-13%

Table 3.m. Values of flexural strength, standard deviation and Coefficient of Variation for unreinforced cement mortar specimens.

Figures 3.2.16-17. Unreinforced specimen with evident efflorescence and flexural collapse and steel reinforced specimen with mixed collapse mechanism.

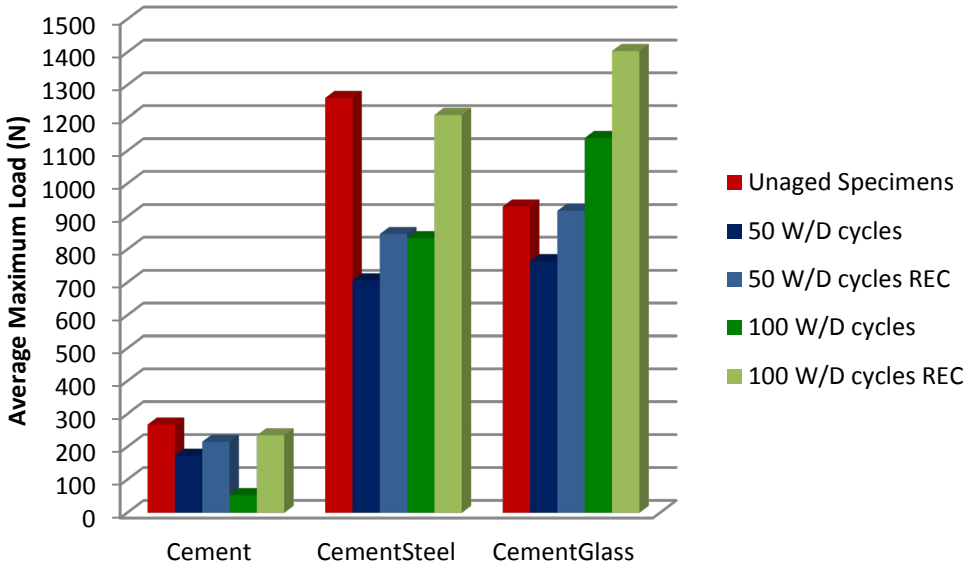

Figure 3.2.18. Average failure loads for cement mortar specimens subjected to none, 50 and 100 wet/dry cycles and relative recovery specimens.

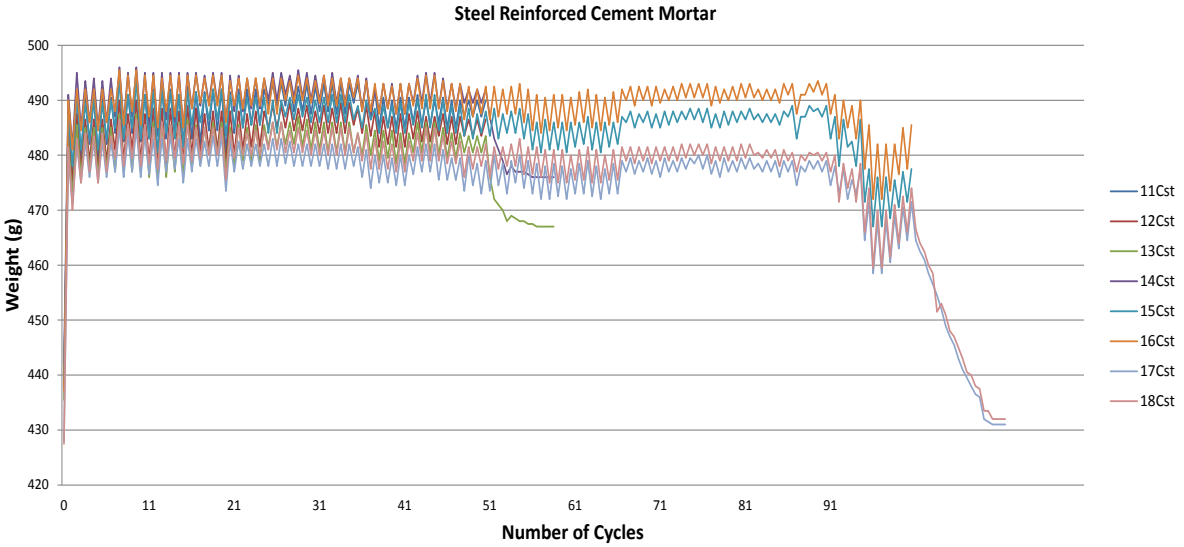

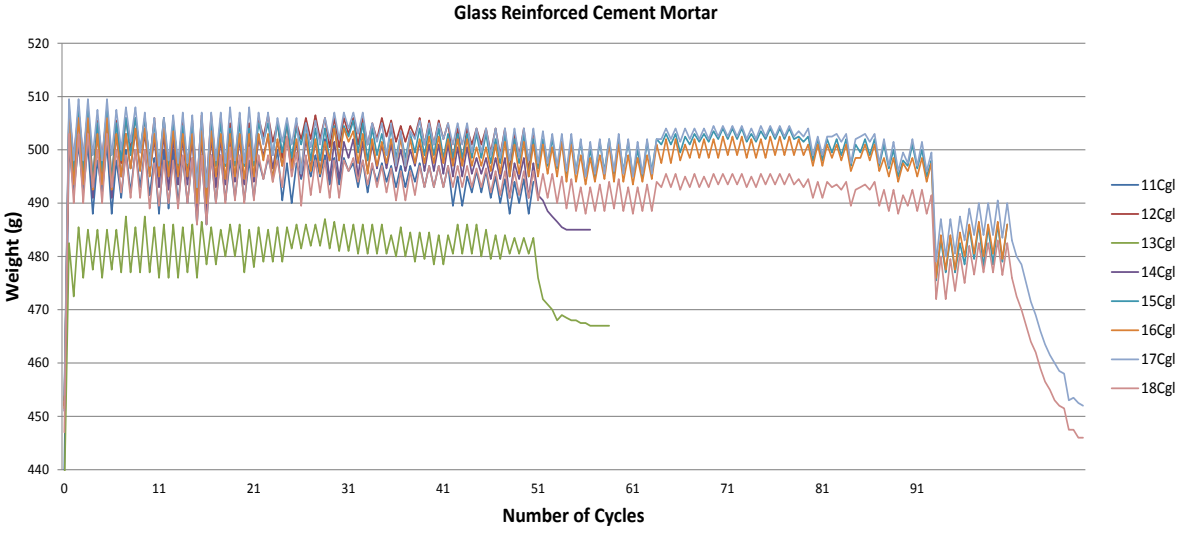

Figures 3.2.19-20. Steel and glass reinforced cement mortar specimens: weight variation.

MX Mortar Specimens

The particular type of inorganic mortar represented by Ruredil's MX mortar when combined with the PBO fibres used in the first experimental campaign described above seems to be quite indifferent to ageing phenomena, and even perhaps to benefit from the cycles it has been subjected to in this and the previous campaigns. In fact, the histogram relative to its average load capacity shows that during cycles the fibre reinforced mortar increases in flexural strength. This is not true for the unreinforced specimens: the mortar in fact, as is described in the table below, gradually loses flexural strength with the progress of the cycles. The specimens allowed to recover after 50 cycles regain strength, above the level of the unaged specimens, as do those allowed recovery after 100 cycles, although not quite to such a high level. However, as can be seen in the weight variation graphs, there is a constant loss for the specimens which are tested wet, notwithstanding the fact that their sodium chloride sorption is limited, and the lack of loss of section. As for collapse mechanisms, similarly to the first experimental campaign illustrated above, both in reinforced and unreinforced specimens the collapse is due solely to flexural strength. The crack propagates vertically starting approximately from the midpoint of the parallelepiped and moving upward towards the point of load pressure (Figs. 3.2.17-18). As in the freeze/thaw durability campaign, bond loss was not observed, while there was fibre yielding.

MX Mortar				
Type of Specimen	Average Flexural Strength (MPa)	Standard Deviation (MPa)	CoV	Flexural Strength Variation (%)
NR	5.83	0.84	0.14	
NR50 W/D	4.85	2.26	0.47	-17%
NR50 W/D_REC	6.76	0.16	0.02	16%
NR100 W/D	1.99	0.11	0.06	-66%
NR100 W/D_REC	4.04	2.35	0.58	-31%

Table 3.n. Values of flexural strength, standard deviation and Coefficient of Variation for unreinforced MX mortar specimens.

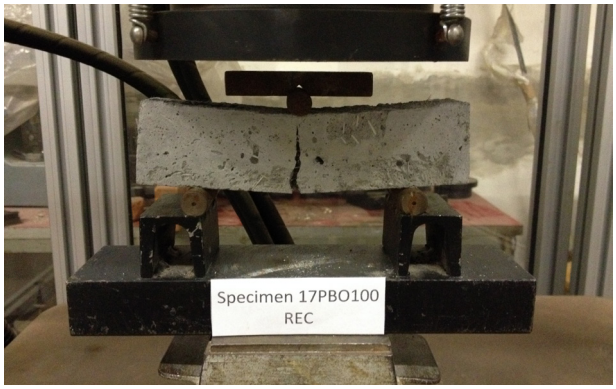

Figures 3.2.21-22. Unreinforced and reinforced specimens with flexural collapse mechanism.

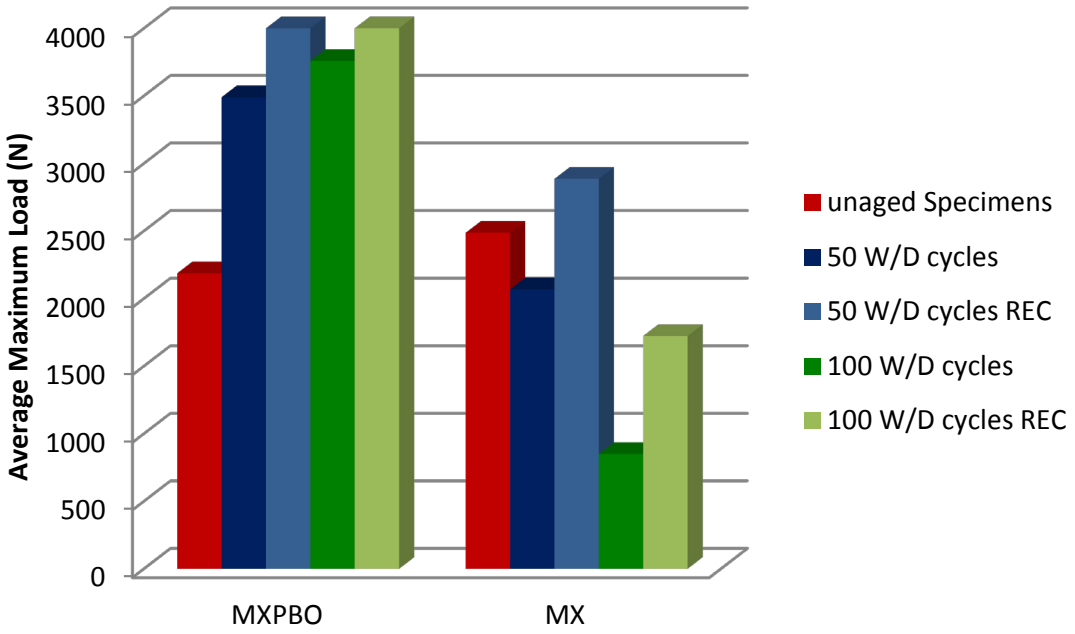

Figure 3.2.23. Average failure loads for MX mortar specimens subjected to none, 50 and 100 wet/dry cycles and relative recovery specimens.

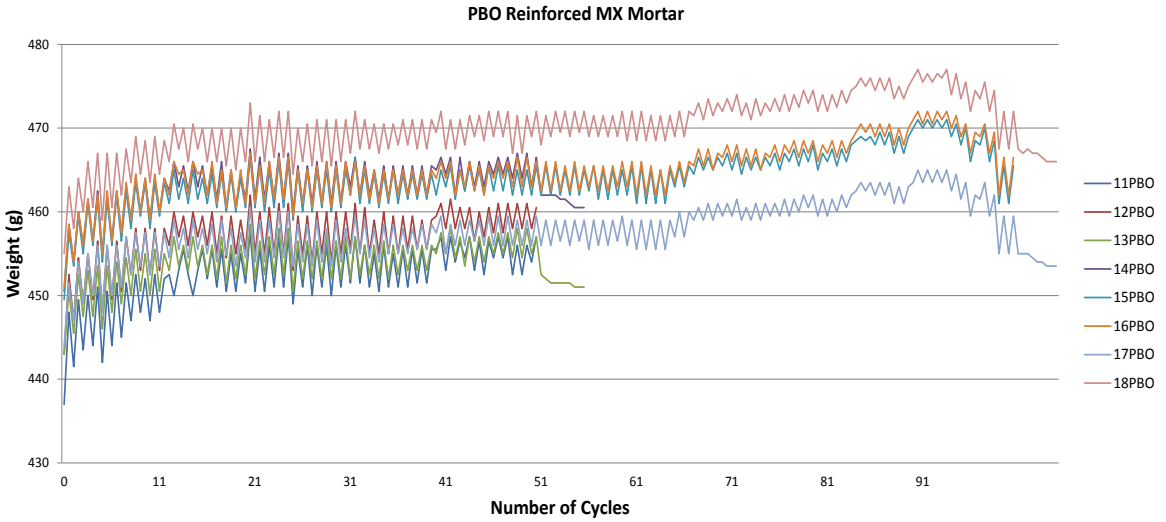

Figures 3.2.24. Weight variation registered in PBO reinforced MX specimens.

Conclusions

Regarding lime mortar specimens, with the exception of those reinforced through steel fibres, the final results show that although the wet specimens decrease their flexural strength consistently, there is a recovery of the strength registered on unaged specimens in those specimens which have been allowed to dry. This phenomenon does not occur in the steel reinforced specimens given the extensive damage to the fibres due to the formation of rust on the fibres themselves, so much so that the original length is diminished. In all reinforced specimens the loss of bond strength is evident during collapse. Cement mortar specimens do show decreased values of resistance when

tested wet, but recovery periods allow the specimens to recuperate resistance: in unreinforced specimens there is not more than a 19% strength loss in recovery specimens after cycles. Again, bond strength loss is evident in all specimens. In both lime mortar and cement mortar reinforced specimens, collapse mechanisms are mixed and failure occurs for both flexural and shear strength. MX mortar, while proving to be more compact, and therefore less penetrable to the sodium chloride solution, is nonetheless affected by the cycles in the unreinforced specimens, with flexural values decreasing constantly when tested wet. It must be noted, however, that only for specimens subjected to 100 cycles and tested wet is the performance less than what is guaranteed by the producer, that is 1.99 < 3.5 MPa, as can be verified in Table 3.c. All other values, though less than the values on unaged specimens registered experimentally for the present work, are above the producer guaranteed value of 3.5 MPa.

There is then significant recovery when specimens are allowed to dry. In the case of the reinforced specimens, as in the first experimental campaign, it seems that the cycles increase the specimens' resistance. In all cases, collapse mechanisms are for flexural strength, and no reinforced specimens present a loss of bond strength.

Considering all results, for all types of mortar, it can be stated that although flexural values may be cut down in wet specimens, in those allowed a recovery period resistance values are often comparable to those for unaged specimens. Therefore it can be said conclusively that wet/dry cycles in 5% sodium chloride solution do not have long lasting effects on FRCM.

3. Wet/Dry Durability on Brick Masonry Reinforced Pilasters

The third experimental campaign focuses on larger specimens. After having tested fibre reinforced mortar specimens and discussed their results, the next step was to verify these results on actual masonry structures. The motivations behind this consequential experimental campaign lie once again in the state-of-the-art research on FRP durability. After an initial period of durability testing solely on the fibres, with and without their polymeric matrix, attention turned to research that would prove if the degradation of the FRP system when applied to structural support would increase damage or simply result in not providing the structural reinforcement it had been designed to give. There were cases in fact in which the degradation which started in the FRP system caused mould or other aggressive attacks to the underlying structural system, provoking more damage

than if the FRP had not been present (Binda et al., 2011). From the data analysed from the first two experimental campaigns, the more aggressive durability testing performed on the reinforced mortar specimens consisted in wet/dry cycles in a 5% sodium chloride solution. Therefore this type of cycle was chosen for the durability on an FRCM reinforced structural element, in the attempt to verify whether the artificial ageing registered in the second experimental campaign described above had the same detrimental effects when the FRCM system was applied to masonry structures.

Experimental Programme and Materials

Small brick pilasters were assembled, subjected to wet/dry durability cycles and tested at the Laboratory of the Department of Architecture at the University of Florence. Each pilaster was composed of five bricks of 20x10x5 cm, bricks smaller than average size (Fig. 3.3.1). It was important for the size of the pilasters to be sufficiently small as to be able to repeat testing and carry out cycles contemporaneously on all specimens. The test matrix below best describes the present campaign (Table 3.o).

N° of Specimens	Type of Cementitious Matrix for Reinforcement	Type of Reinforcement	N° of Wet/ Dry cycles	
8	Lime	Steel (4)	0 (2)	75 (2)
		Glass (4)	0 (2)	75 (2)
8	Cement	Steel (4)	0 (2)	75 (2)
		Glass (4)	0 (2)	75 (2)
2	None	Unreinforced (2)	0 (2)	

Table 3.o. Test matrix for wet/dry durability on brick masonry pilasters. In parenthesis the number of specimens per type.

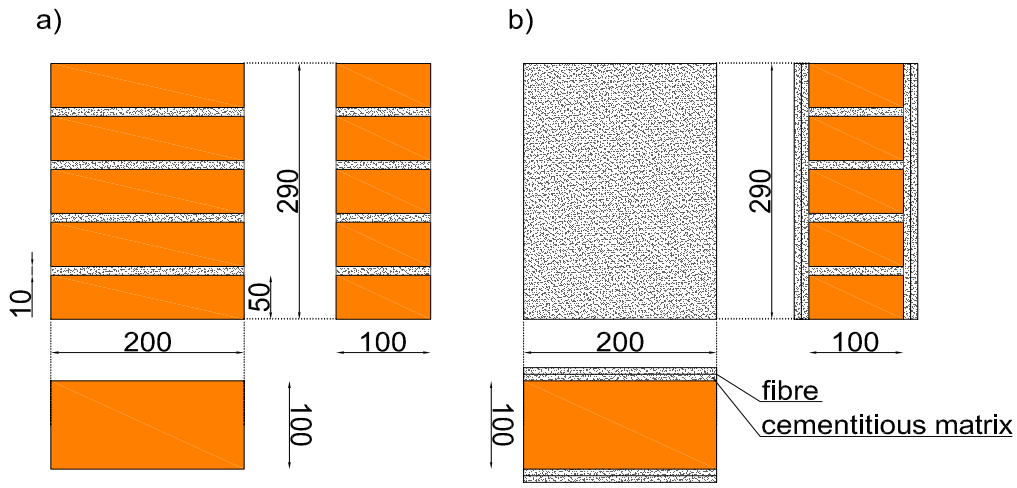

Figure 3.3.1. Graphic scheme with measurements (mm) of the brick masonry pilasters, plan and elevations, a) unreinforced pilaster, b) reinforced pilaster.

Two pilasters of a total of 18 remained unreinforced, as control specimens. All other pilasters, 16 in total, were reinforced though steel or glass fibres placed on the wide faces of the pilasters (20x29 cm) with either lime or cement mortar, in the manner of reinforced plaster.

The steel and glass fibres used in the present campaign were those used and described in campaigns 1 and 2, illustrated in Table 3.b. The lime and cement mortar used as cementitious matrices for the FRCM system were also of the same hand mixed qualities as described in the sections in Table 3.c.

Small cubic specimens of bricks, 4x4x4 cm in size, were tested for compression. Results are shown in Table 3.p. The mortar used in the assembly of the pilasters was a cement mortar, hand mixed (water, lime, cement 32.5 MPa, sand) with proportions in weight 1.5:1:1:6. This mortar was used solely in the building of the pilasters, and not in their reinforcement. Nevertheless, this type of mortar, named hereafter PCement (cement mortar for pilasters) was subjected to freeze/thaw and wet/dry cycles as described for lime, cement and MX mortar in parts 1 and 2 of the present Chapter. The 4x4x16 cm specimens of PCement mortar were prepared in a steel framework and left to dry for 60 days in the same manner as the other mortar specimens described above. Fibres were not used to reinforce the specimens of PCement mortar given that in the present campaign this type of mortar was not used for the reinforcement of the pilasters, but only for the assembly of the bricks. In the following table and graphs, average resistance values, flexural values and

Clay Bricks			
Average Maximum Compression Load (kN)	Average Maximum Compressive Strength (MPa)	Standard Deviation	CoV
14215	47.04	8.57	0.18

Table 3.p. Average Compressive strength, standard deviation and Coefficient of Variation for clay bricks used to build the pilasters.

PCement Mortar				
Type of Specimen	Mean Flexural Strength (MPa)	Standard Deviation (MPa)	CoV	Flexural Strength Variation (%)
NR	0.25	0.04	0.16	
NR52 F/T	1.43	0.32	0.22	572%
NR100 F/T	0.33	0.04	0.11	32%
NR50 W/D	1.18	0.12	0.10	472%
NR50 W/D_REC	1.67	0.08	0.05	668%
NR100 W/D	0.35	0.007	0.02	40%
NR100 W/D_REC	1,34	---	---	536%

Table 3.q. Average Flexural strength, standard deviation and Coefficient of Variation for PCement mortar specimens.

standard deviation for unaged and aged specimens of PCement mortar are shown (Table 3.q, Fig. 3.3.2), as well as weight variation during wet/dry cycles (Fig. 3.3.3).

Once the pilasters were assembled with the cement mortar described above, they were left to cure for 60 days in a humidity free environment at room temperature (circa 19°). Once curing was completed, the pilasters were reinforced, in number and type of reinforcement as described in Table 3.o. A layer of cementitious matrix was applied to the surface of the pilaster, covering the entire façade evenly. The fibre was then applied and pressed to ensure attachment to the applied layer of mortar. A second layer of mortar was applied, thus covering the fibre (Fig. 3.3.4). The reinforced pilasters were left to cure again for another 60 days and in order to ensure complete curing, in order to avoid that this process could occur during the artificial ageing cycles.

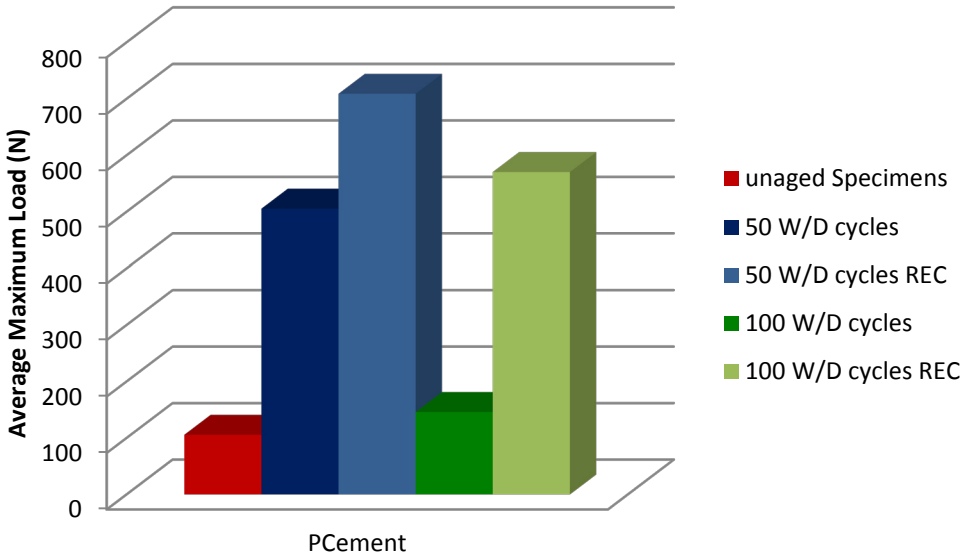

Figure 3.3.2. Average load capacity for PCement mortar specimens subjected to wet/dry cycles.

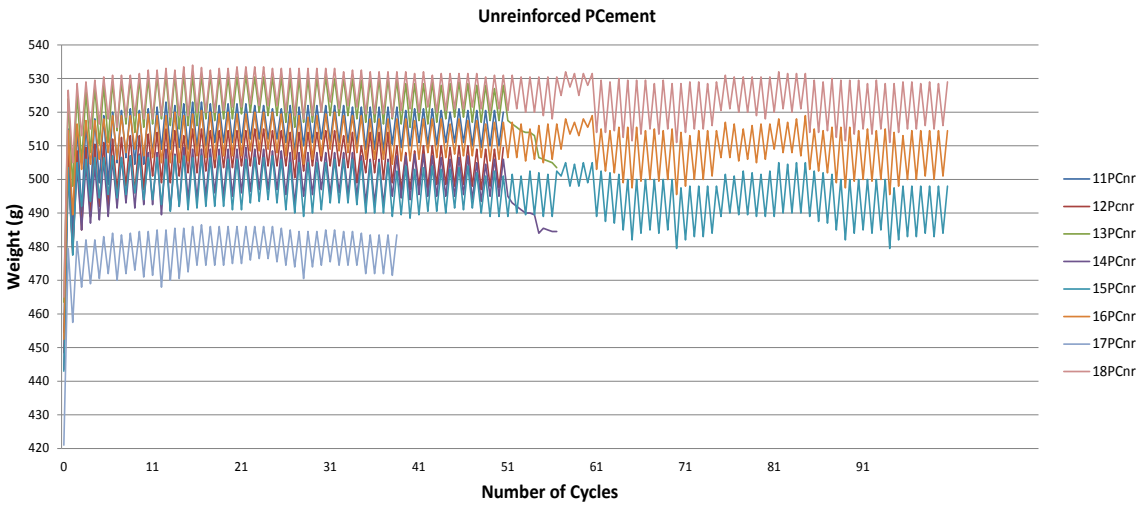

Figure 3.3.3. Weight variation registered for PCement mortar specimens during wet/dry cycles.

Once curing was complete, wet/dry cycles on eight reinforced pilasters commenced. The cycles were similar to the ones performed on the mortar specimens in campaign 2 described above, namely a wet period in a solution of sodium chloride at 5% followed by a dry period in a ventilated oven at 35°C. The period of time the pilasters were left in the solution was of course modified according to the volume of these specimens, noticeably larger than the mortar prisms of the previous experimental campaign. These specimens required a period of time of 45 minutes for complete sorption to occur. This amount of time was determined through weighing the specimens dry, and then at intervals of 5 minutes until weight stabilized indicating sorption was at maximum values (Fig. 3.3.7). The pilasters were immerged in plastic basins with the 5% sodium chloride solution at a level which covered the specimens for at least 2.5 cm (Fig. 3.3.5) and then placed in the oven and left to dry for 24 hours. In this campaign, only one cycle duration of 75 days was chosen for all aged specimens.

Figures 3.3.4-5. Two pilasters, reinforced through glass fibre and cement mortar, and glass and steel fibre reinforced pilasters in a plastic basin filled with the 5% sodium chloride solution. Three pilasters immersed in 5% sodium chloride solution. In the steel reinforced specimens the rust phenomenon is eident after as few as 5 cycles.

Test Set-up and Instrumentation

Testing was carried out through eccentric compression loading. One of the objectives of this campaign was to verify whether the fibres, in an aged condition albeit artificially, could follow the different solicitations they are subjected to when eccentric compression occurs; that is, if the fibres could resist compressive and tensile strength simultaneously. To this end, the central core of inertia was identified in order to ensure that the compressive and tensile forces were actively being applied to the pilasters as is shown in Figure 3.3.6.

Loading was applied through a load cell (TCLP – 10B Tokyo Sokki Kenkyujo Co, Ltd.) with a maximum capacity of 10 kN applying pressure on a steel cylinder positioned at exactly 50 mm to the right of the central axis of the pilaster. The steel cylinder is the exact width of the pilaster,

guaranteeing that the load is applied only on the masonry structure and not on the FRCM on the facades of the pilaster (Fig. 3.3.8). Data was recorded through two mechanical strain gauges (PI-5-100 Tokyo Sokki Kenkyujo Co, Ltd.) on the short sides of the pilasters and two cantilevered displacement transducers (CE-10 Tokyo Sokki Kenkyujo Co, Ltd., Fig. 3.3.9). The two displacement transducers attached to the upper face of the pilasters measured the vertical displacement of the pilaster during loading. The second typology was applied for recording relative movements between the two extremities of the gauges. Shaped as a Greek letter Omega (figure 3.3.10), the ends of these strain gauges are attached to the specimens and their hemispherical central part allows these ends to follow the displacements of the specimen. The data recorded shows whether the extremities of the instrument move closer together or farther apart during testing.

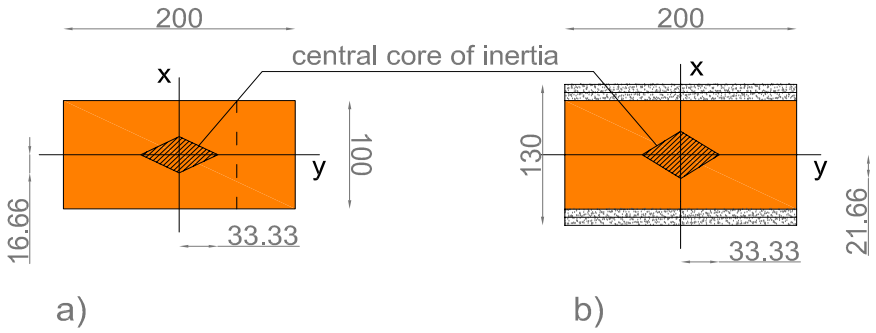

Figure 3.3.6. Graphic scheme of the pilasters (mm), plan and central core of inertia for a) unreinforced specimens and b) reinforced specimens.

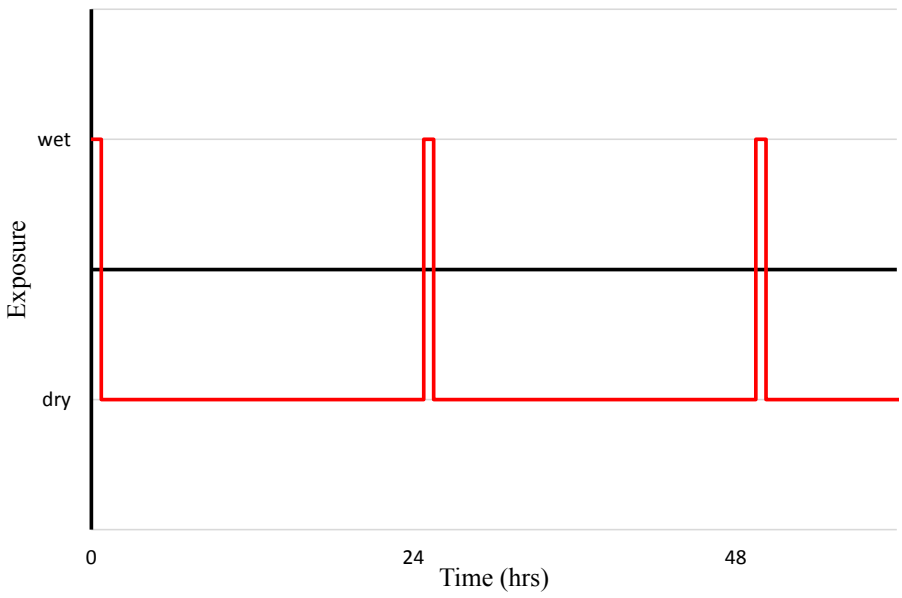

Figure 3.3.7. Wet/dry variation for pilasters.

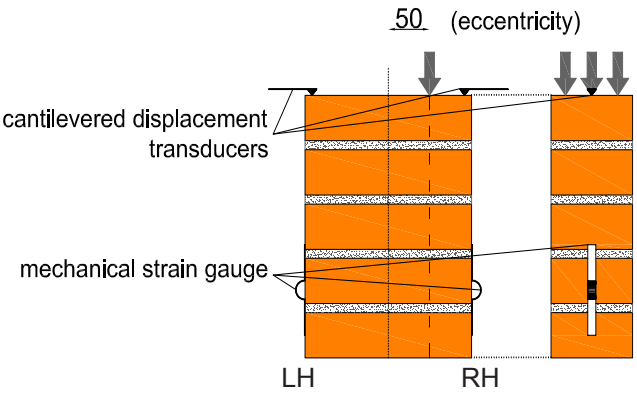

Figures 3.3.8-9. Steel cylinder through which load is applied of the exact width of the masonry and cantilevered displacement transducer. Graphic scheme of the positions of the mechanical strain gauges and transducers during testing (mm), with Left Hand (LH) and Right Hand (RH) sides indicated.

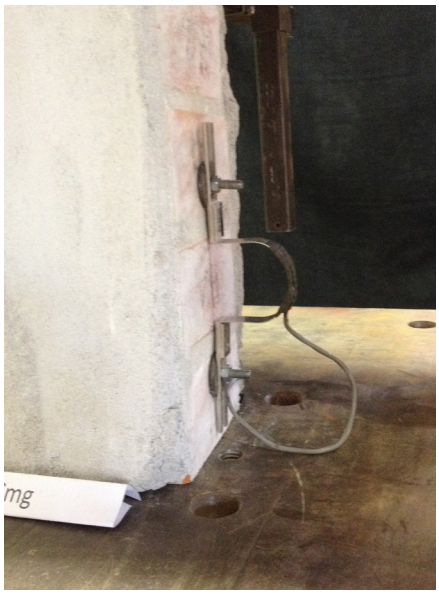

Figure 3.3.10. Mechanical strain gauge.

Results

Some preliminary considerations can be made from the observation of the photographic survey conducted during testing which seem to be relevant to all unaged specimens. Values for both reinforced and unreinforced specimens remain within values that range from 40000 to 50000 N (Fig. 3.3.15). The small variation between reinforced and unreinforced specimens may be due to the fact that the FRCM system is simply applied to the façades of the pilasters without anchoring systems. While the ultimate loads values do not vary greatly, the collapse mechanisms are different. Unreinforced specimens fracture more gradually. Cracks at first appear immediately below the point of load application, given by excessive compression strength at about 30000 N. At this point there is a drop in the load - displacement diagram (Figs. 3.3.16-17). A secondary crack then appears at the bottom of the pilaster opposite the loading point (Fig. 3.3.18a). This mechanism is not visible in the FRCM reinforced pilasters until the fibres detach completely from the side they are attached to, and even when detachment occurs it does not reveal cracks due to tensile strength; the rupture in reinforced specimens is abrupt and due to excessive compressive force as opposed to the gradual collapse verified in unreinforced specimens. In fact, the FRCM system does not prevent the masonry pilaster from cracking due to excessive compression (Fig. 3.3.11). The shorter sides of the pilasters are free from reinforcement. Therefore when cracking or rupture of the bricks occur, there may be a rotation of the elements shortly after the detachment of the fibres commences. This

Figure 3.3.11. Steel-fibre Cement-matrix Specimen 1 after testing; the fibre reinforement has completely detached.

is common in eccentric compression, when the loads are outside the central core of inertia of the pilaster. The fact that the slate of FRCM detaches either completely or only partially makes little difference to the resistance of the pilaster; in fact, once the FRCM begins to detach, it is as if the fibre reinforcement is virtually non-existent. In this regard, there is little variation between glass or steel fibre reinforced matrices, differently from what was observed in the previous two campaigns where the values of the fibre reinforced mortar prisms differed greatly depending mainly on the type of mortar (Figs. 3.3.23-26; 3.3.32-35; 3.3.40-43; 3.3.48-51).

In the graphs shown in the following pages, negative numbers indicate compressive stress while positive numbers indicate tensile stress. The programme which was used to record displacements was developed purposely and specifically for the Laboratory at the Department of Architecture of the University of Florence. This programme was encoded in such a way that when the instruments needed to measure displacements are connected to the computer, settings could be adjusted at will with regard to the sign (+ or -) of the registered movements. This means, for example, that the vertical movements registered by the cantilevered displacement transducers (Fig. 3.3.9) can be set for either negative or positive values for deflections. In this case, deflections registered by the two transducers have been set for positive values. The same can be said for the mechanical strain gauges, where contractions, which correspond to compressions, have been set here to be represented by negative values. Once the graphs were developed, this arbitrariness in assigning the sign of displacements would have given a contrasting report in the outcome of the test, which would have indicated that while the transducers registered positive movements from the upper level of the pilasters, the strain gauges were simultaneously registering negative displacements. Therefore, for clarity, the signs of the transducers have been inverted when positive values indicated negative deflections so that the sign of the displacements of the instruments match.

It is possible that strain gauges and transducers register concurrently opposing displacements (for example, Fig. 3.3.32-33). Due to the position of the instruments, in fact, separated by two bricks

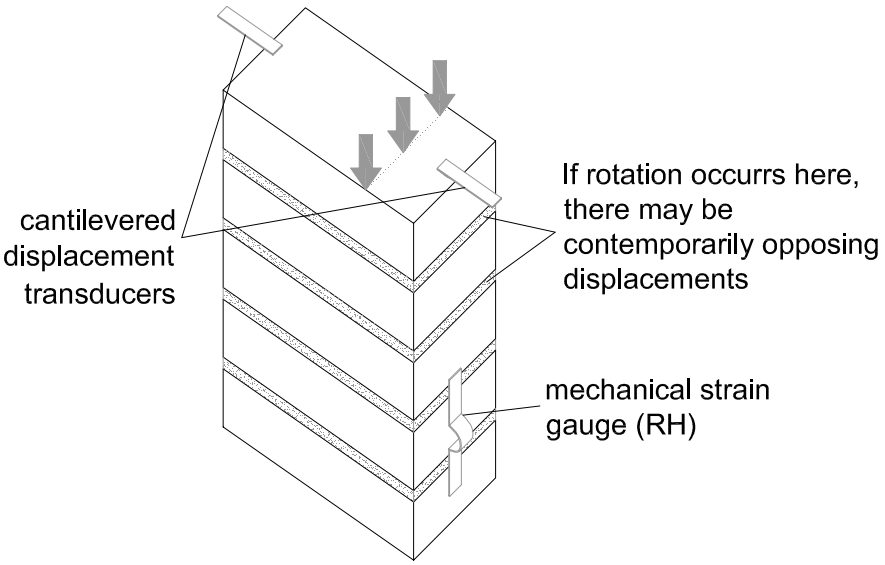

Figure 3.3.12. Axonometry of pilasters with strain gauges and displacement transducers. The mortar layers where possible rotations may lead to discording diagrams are highlighted.

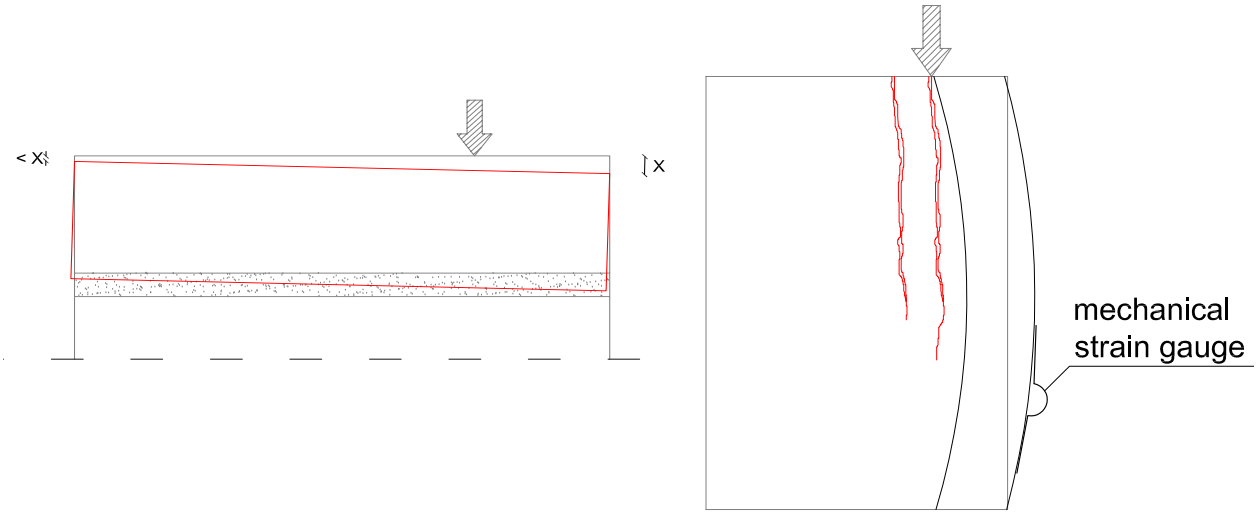

Figures 3.3.13-14. The upper section of the pilaster, showing larger displacements on the right side of the pilasters, and a graphic scheme of elongations that might occur in the right side of specimens.

which may rotate and move in directions other than those of the two bricks the gauges are glued to (Fig. 3.3.12), displacements may have opposing sign when referring to one side of the specimen. However, this is not the case for all the specimens tested, particularly for the unreinforced or unaged ones. In the testing condition of the present campaign, that is eccentric compression, what is certain is that the larger displacement will be registered under the loading point. The displacements on the other side of the pilaster are expected to be smaller, but there may not necessarily be negative values, that is a positive deflection, or even rotations. After collapse, vertical cracks often appear and there may be phenomena of elongation of the right side (Fig.s 3.3.13-14). As

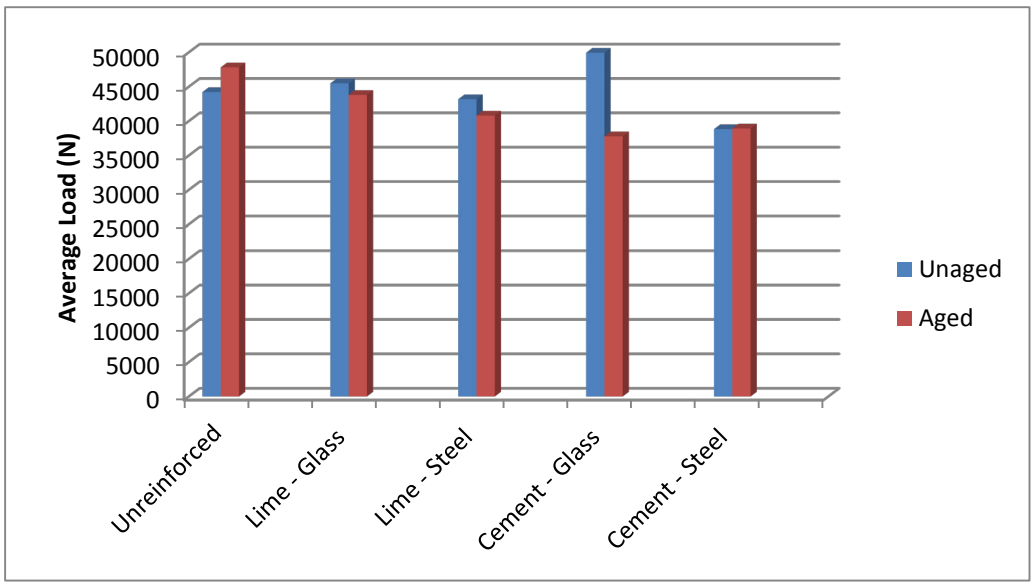

Figure 3.3.15. Average maximum loads for unaged and aged pilasters.

for the differences in behaviour between aged and unaged specimens, none of the values of the aged specimens differed greatly from those of their unaged control specimens, as is clearly shown in figure 3.3.15. The aged specimens were tested after a last 24 h dry cycle, therefore without a proper recovery period in which they were allowed to return to their original weight (c.a 12 kg), in a semi-dry state. Of the eight specimens which were subjected to wet/dry cycles, 2 lost their reinforcement (Specimen 4 Glass fibre - Lime matrix and Specimen 3 Steel fibre Cement matrix) and consequently collapsed before they reached the end of the period of cycles. Therefore, the values in Figure 3.3.15 of the aged specimens Glass fibre - Lime matrix and Steel fibre - Cement matrix are not average values, but values of the only specimens which reached the end of the cycles. One specimen, specifically Specimen 3 Glass fibre - Cement matrix, lost its reinforcement completely but withstood the entire duration of the wet/dry cycles. In this case, the specimen was tested as an unreinforced aged specimen. In comparison to the unreinforced and unaged specimens it increases in resistance when subjected to wet/dry cycles (Fig. 3.3.15), in compliance with the values of the aged cementitious mortar used for the joints (Fig. 3.3.2). Therefore, considering the lack of average values for Glass fibre - Cement matrix aged specimens, it is difficult to determine whether the difference of ultimate load between the aged and unaged specimens shown in Figure 3.3.15 is by chance or due to ageing.

As may be inferred by the following graphs, all of the reinforced pilasters reach their ultimate load abruptly with no substantial differences between aged and unaged specimens. From physical observations of the aged specimens, the most evident effects of the ageing cycles is in the efflo-

renscence of the saline solution on the surface of both the brick structure, visible at the sides of the pilasters, and the cementitious matrix covered faces of the pilasters. The glass fibres did not show any signs of degradation after the artificial ageing cycles were complete, while the steel fibre reinforced specimens began to show rust on the surface of the matrix used to cover them as soon as the 5th cycle. By the end of the 75 wet/dry cycles, the rust was heavily distributed throughout the matrix surface. However, rust was not detected on the surface of the masonry once the reinforcement detached after testing, and no other kinds of spots or smears were detected; the formation of mould which could eventually detach the fibre reinforcements from their structural supports did not appear in the aged specimens.

In the following pages a more detailed description of failure and diagrams is provided.

Unreinforced Pilasters 1 and 2

Unreinforced and unaged pilasters 1 and 2 collapse due to excessive compressive strength at a maximum value of 38716 N and 49742 N, respectively. Collapse is gradual, as cracks appear almost immediately under the point of force application. In the diagram relative to unreinforced pilaster 1 (Figs. 3.3.16-17) there is a drop in the graphs given by the displacements registered by both the strain gauges and the displacement transducers at 25895 N, showing the instant the crack crossed the entire width of the first brick. A secondary crack due to tensile strength appears at the bottom of the pilaster opposite the loading point (Fig. 3.3.18a). In unreinforced pilaster 2 the first crack to form immediately under the loading point goes through the first brick, creating an initial rotation of the right side of the brick and causing the transducer to register positive (upward) vertical movements (Fig. 3.3.21). Once the crack moves towards the mortar layer between the first and the second brick, and eventually reaches the mortar between the second and the third brick, the vertical movements of the right side of the pilaster return to negative values. The strain gauges for both unreinforced and unaged specimens indicate that the sides of the pilasters were subjected to compressive strength on the right side, that is, the side geometrically closer to the point of application of the load, and tensile strength on the left.

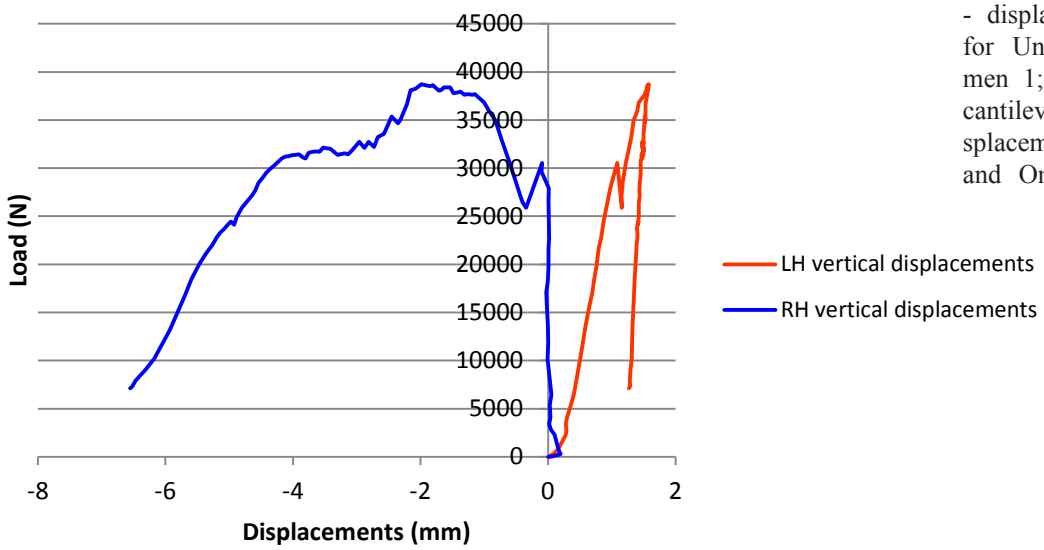

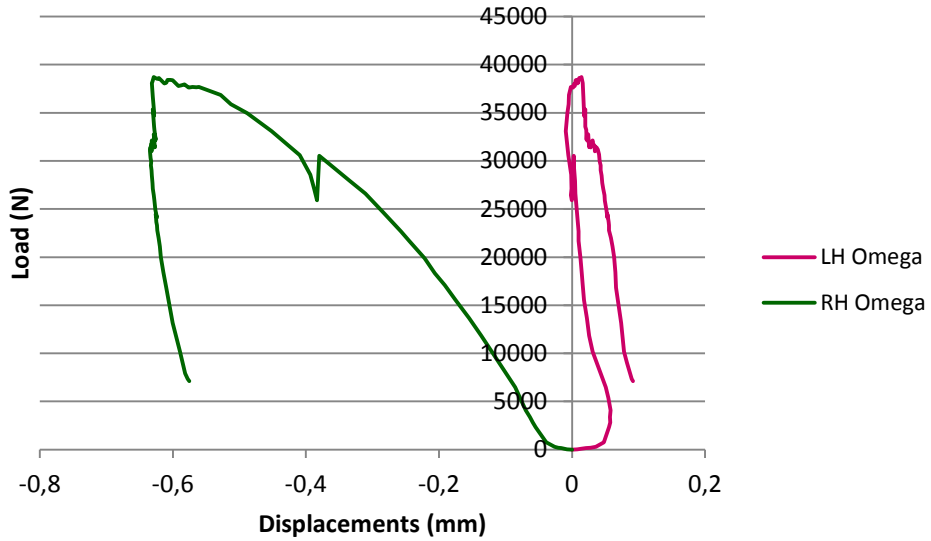

Figures 3.3.16-17. Load - displacement diagrams for Unreinforced Specimen 1; values given by cantilevered vertical displacement transducers and Omega transducers.

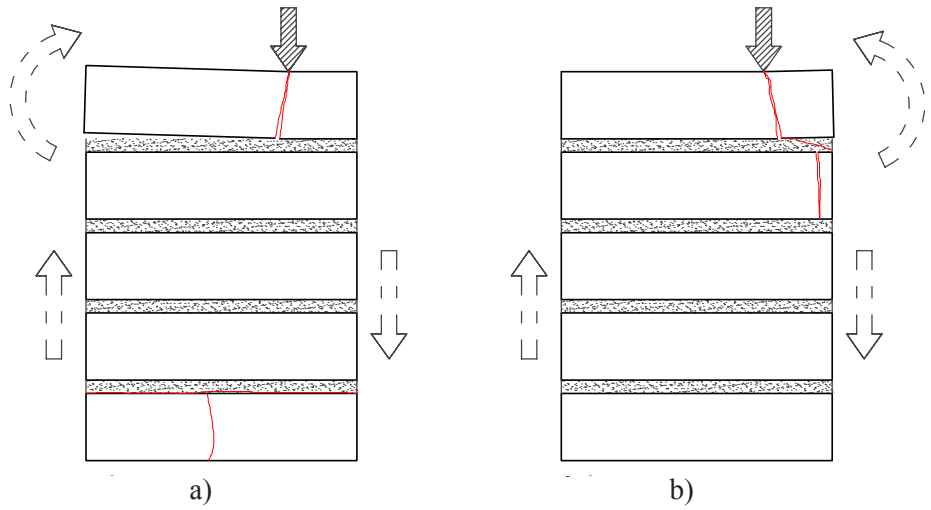

Figure 3.3.18. Graphic description of the cracks that occurred in unreinforced specimens; a) Specimen 1UR and b) Specimen 2UR

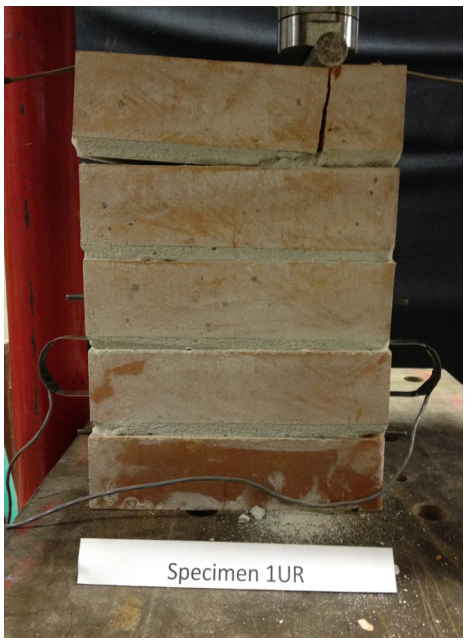

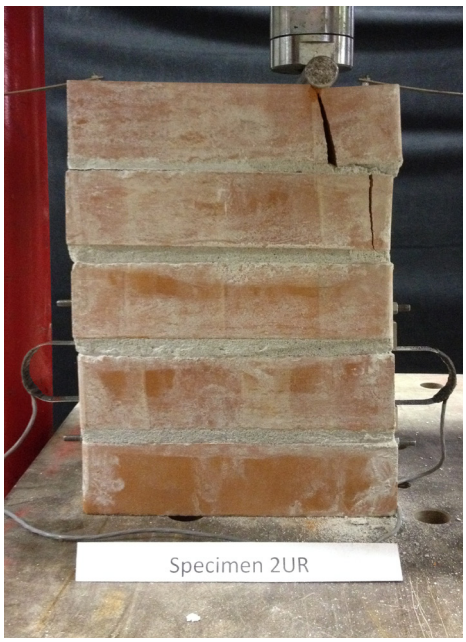

Figures 3.3.19-20. Unreinforced Specimens 1 and 2 after testing.

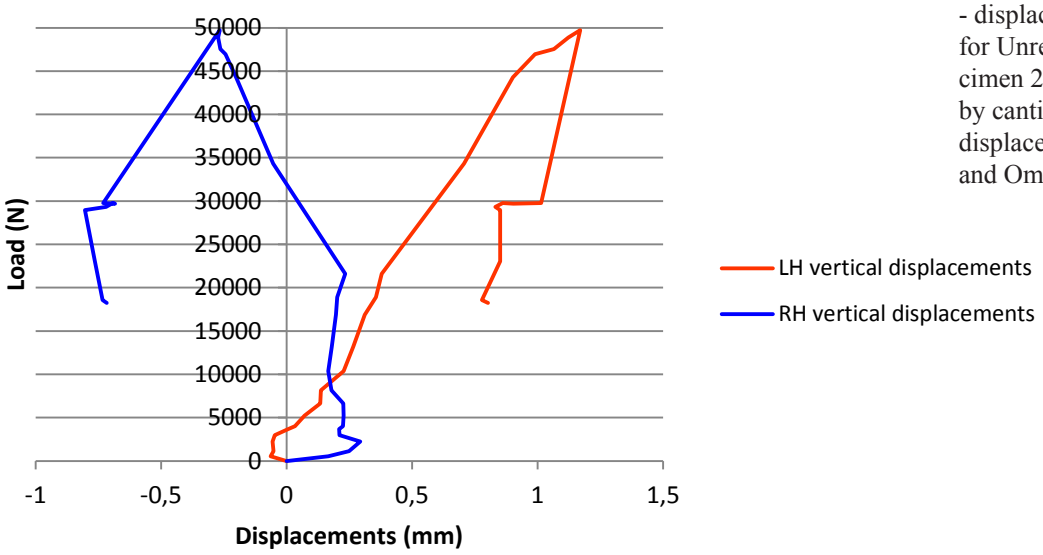

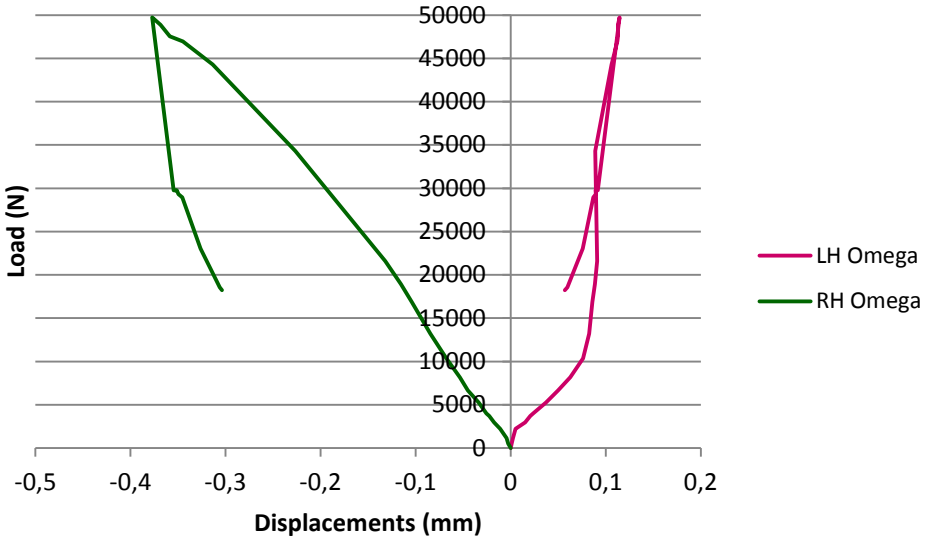

Figures 3.3.21-22. Load - displacement diagrams for Unreinforced Specimen 2; values given by cantilevered vertical displacement transducers and Omega transducers.

Steel fibre - Lime matrix 1 and 2

Unaged Steel fibre - Lime matrix reinforced specimens 1 and 2 collapsed due to compressive strength at 46010 N and 40350 N, respectively. As previously stated, reinforced pilasters tend to collapse more abruptly than the unreinforced pilasters, as resistance diminishes abruptly once the slate of reinforcement detaches, not being attached to the façade of the pilaster by any particular method. In fact, both pilasters form cracks between the slates of steel fibre in the lime matrix almost immediately after testing commences and once the reinforcement is detached from one façade (in both cases the front one, with no damage to the underlying masonry façades) the pilaster is free to crack completely and consequently reach its ultimate load carrying capacity (Figs. 3.3.28-31). Both steel fibre lime matrix reinforced pilasters show one main crack running quasi-vertically from the loading point to the base of the pilasters (Fig. 3.3.27). Smaller cracks appear horizontally, indicating a slight rotation; those on the left side of the pilasters may explain deflection in the left hand displacement transducers, which present both positive and negative values throughout loading (Figs. 3.3.23; 3.3.25).

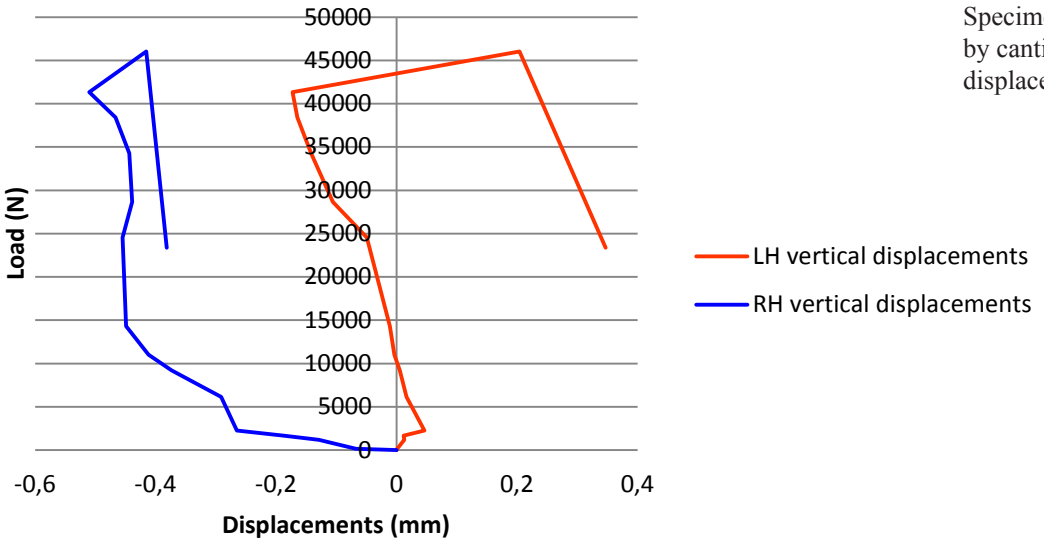

Figure 3.3.23. Load - displacement diagrams for Steel Fibre - Lime Matrix Specimen 1; values given by cantilevered vertical displacement transducers.

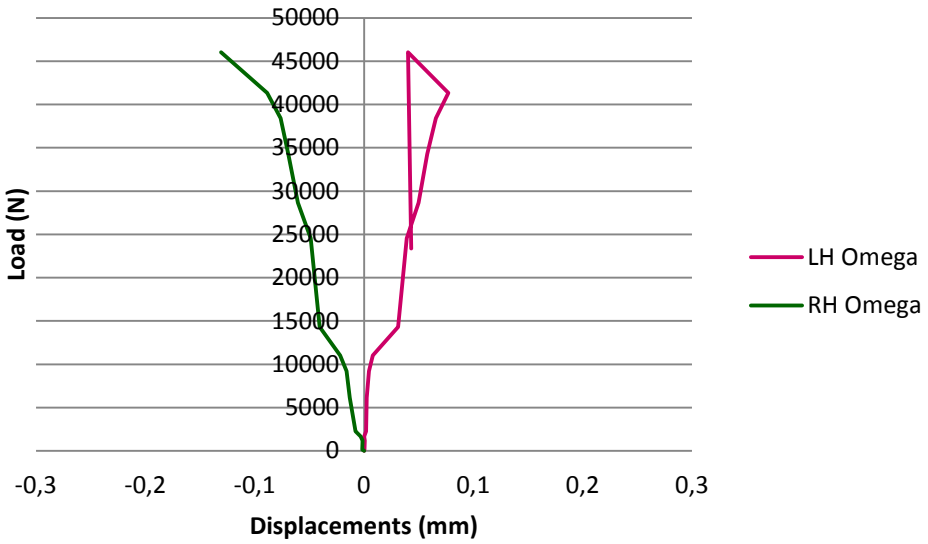

Figure 3.3.24. Load - displacement diagrams for Steel Fibre - Lime Matrix Specimen 1; values given by Omega transducers.

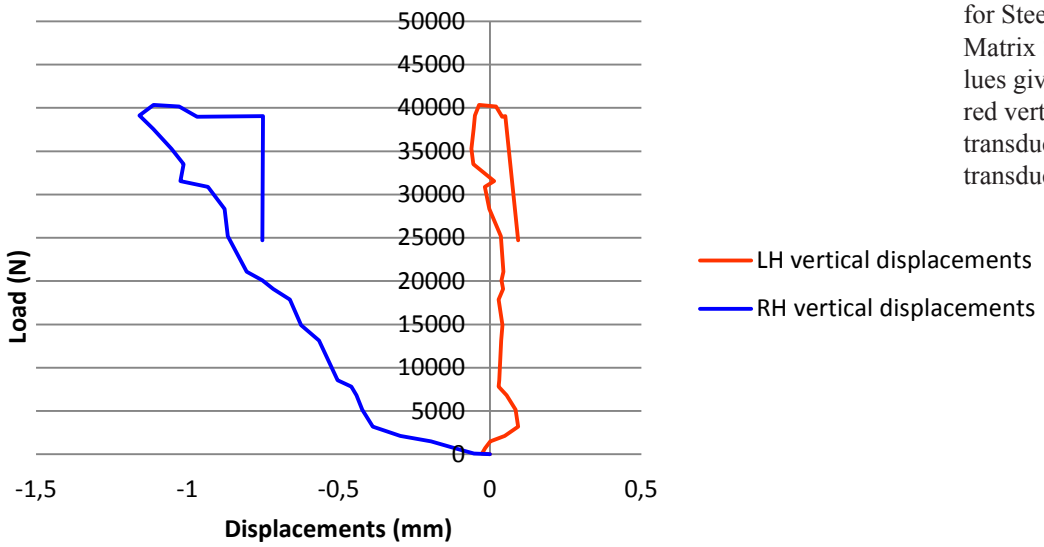

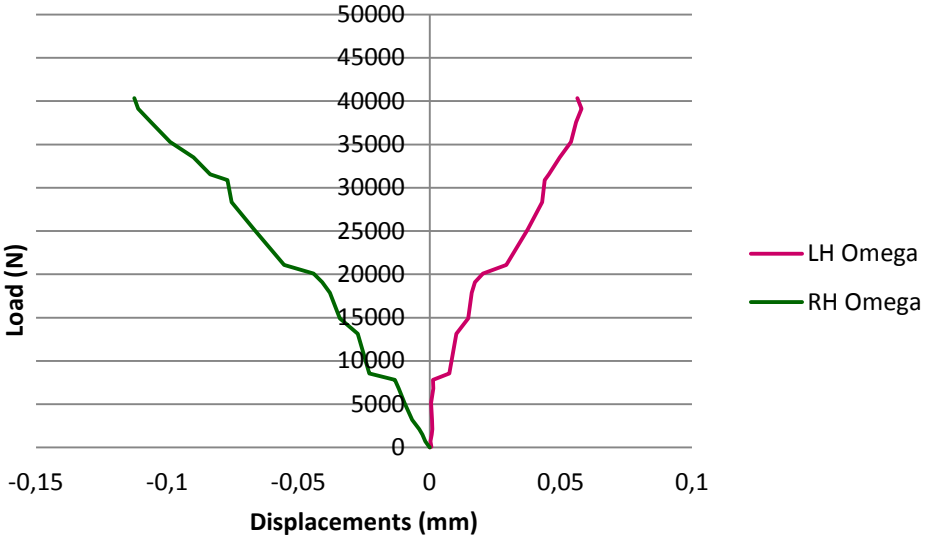

Figures 3.3.25-26. Load - displacement diagrams for Steel Fibre - Lime Matrix Specimen 2; values given by cantilevered vertical displacement transducers and Omega transducers.

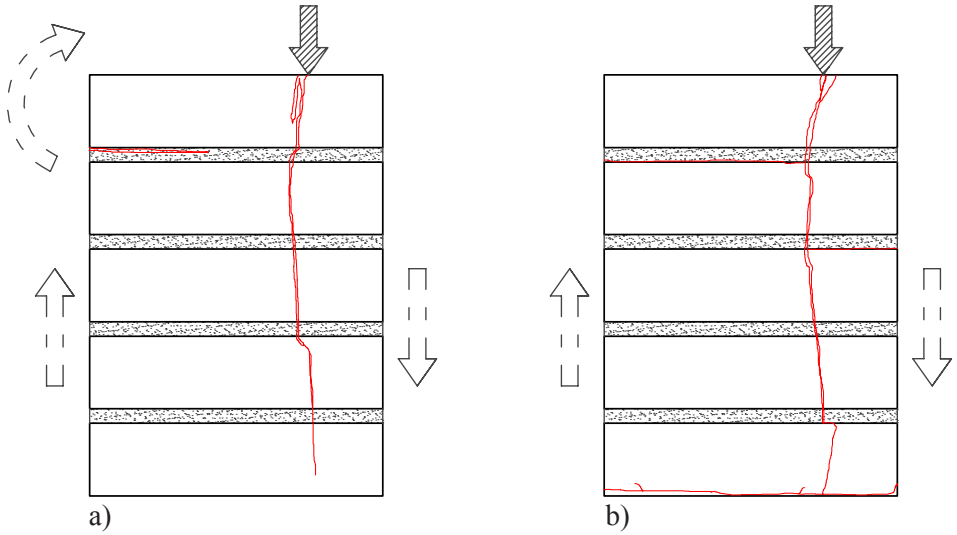

Figure 3.3.27. Graphic description of the cracks that occurred in Steel Fibre - Lime Matrix specimens; a) Specimen 1 and b) Specimen 2.

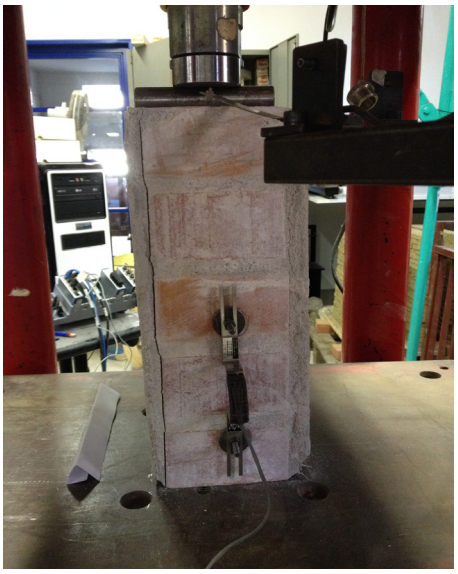

Figures 3.3.28-29. Steel Fibre - Lime Matrix Specimens 1 and 2 prior to fibre detachment.

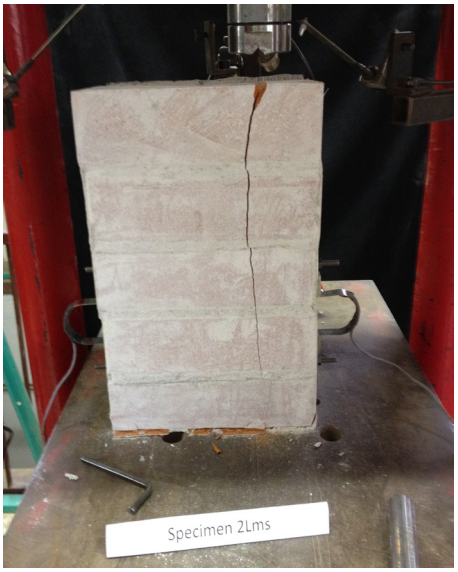

Figures 3.3.30-31. Steel Fibre - Lime Matrix Specimens 1 and 2 after testing.

Glass fibre - Lime matrix 1 and 2

Unaged Glass fibre - Lime matrix reinforced specimens 1 and 2 collapsed due to compressive strength at 47915 N and 43072 N, respectively. In the case of specimen 1, the glass fibre imbedded in the lime matrix detached from the back side, revealing a wide crack initiated under the loading point and running down towards the external angle of the specimen (Fig. 3.3.36). No superficial damage occurred in the masonry beneath the FRCM. In the graphic description of specimen 1 both the front and the back side have been represented, since the crack was visible only from the side on which the slate of reinforcement detached. A noticeable rotation occurred in the slices of bricks created by the crack, indicating in the diagram of the right hand strain gauge attached to the very point of rotation that positive deflections were registered (Fig. 3.3.32-33). On the left side, the strain gauge indicated negative values while the displacements were positive, a difference most likely given by a secondary horizontal crack in the mortar layer between the first and the second brick, causing cracks in the remaining reinforcement slate. In specimen 2, the reinforcement does not detach from either of the masonry façades, but the evidence of cracking under the reinforcement is given by the rotation of the first two bricks on the right side under the loading point (Fig. 3.3.37). The rotation caused the vertical displacements on the right side to be positive, as well as those on the left side. The strain gauges instead register compression on the right side and a slight tensile strain on the left (Fig. 3.3.34-35).

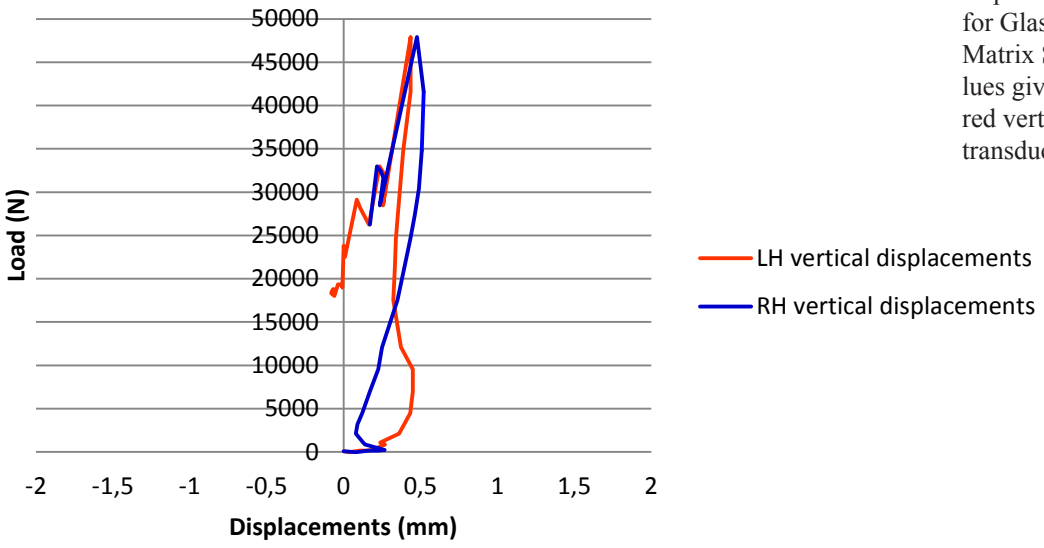

Figure 3.3.32. Load - displacement diagrams for Glass Fibre - Lime Matrix Specimen 1; values given by cantilevered vertical displacement transducers.

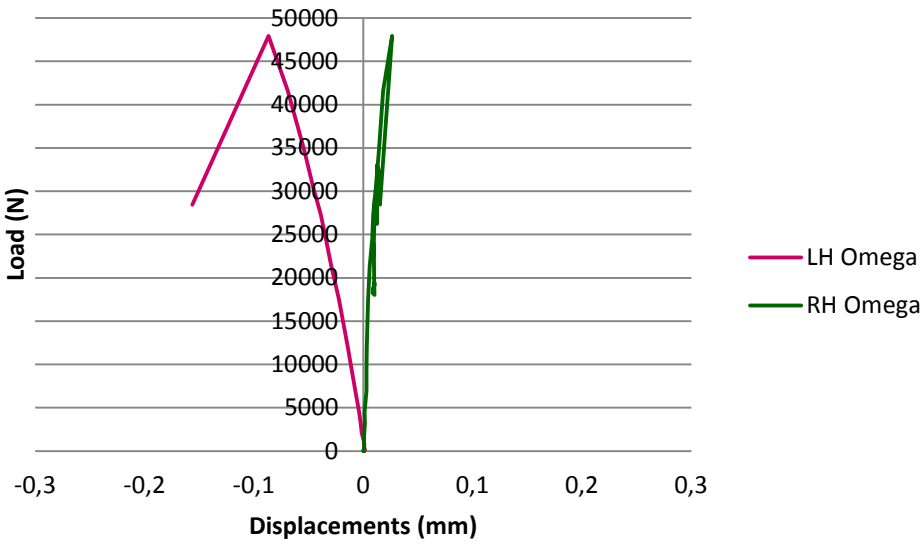

Figure 3.3.33. Load - displacement diagrams for Glass Fibre - Lime Matrix Specimen 1; values given by Omega transducers.

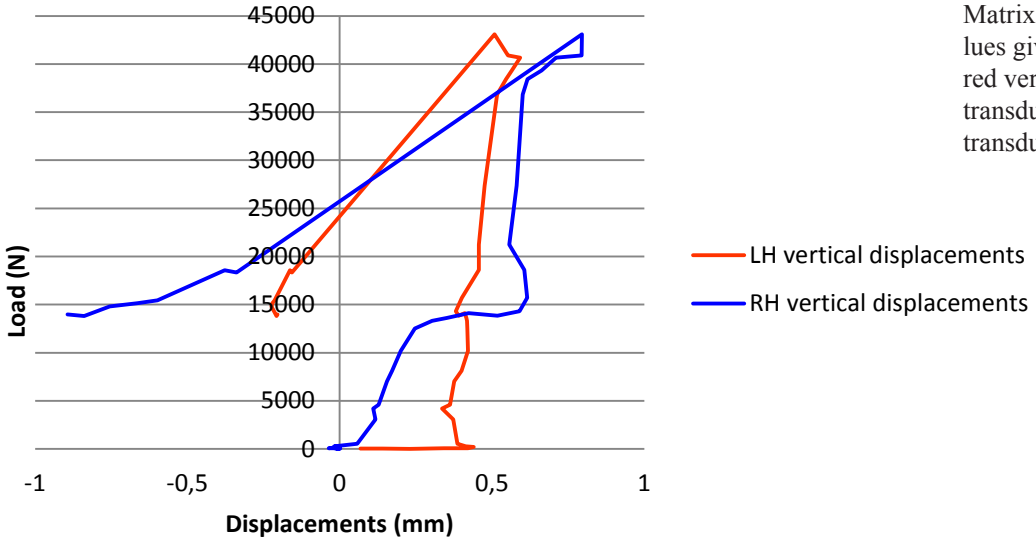

Figures 3.3.34-35. Load - displacement diagrams for Glass Fibre - Lime Matrix Specimen 2; values given by cantilevered vertical displacement transducers and Omega transducers.

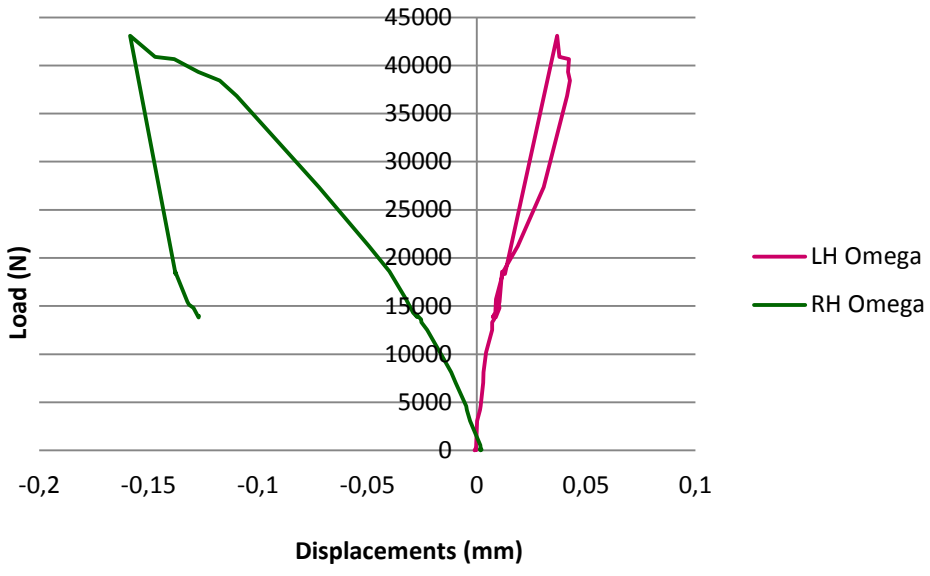

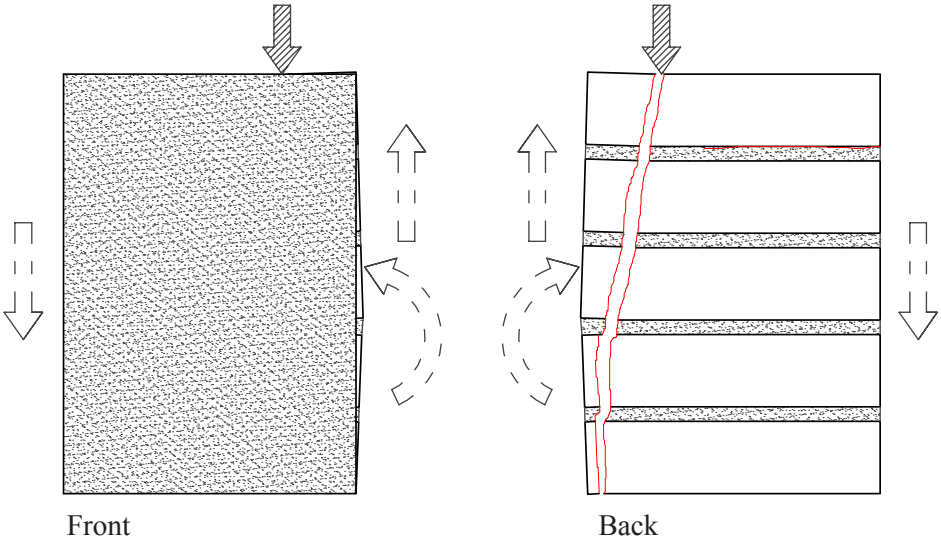

Figure 3.3.36. Graphic description of the cracks that occurred in Glass Fibre - Lime Matrix Specimen 1; front and back.

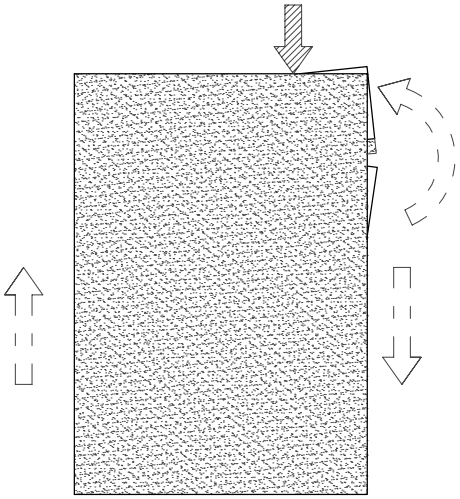

Figure 3.3.37. Graphic description of the cracks that occurred in Glass Fibre - Lime Matrix Specimen 2.

Figures 3.3.38-39. Glass Fibre - Lime Matrix Specimens 1 and 2 after testing.

Steel fibre - Cement matrix 1 and 2

Steel fibre - Cement matrix specimens 1 and 2 collapsed due to compressive force at 40340 N and 37328 N, respectively. Specimen 1 ruptured abruptly, with the full detachment of the fibre slate on its front façade which uncovered a large passing crack running vertically from the loading point to the bottom of the pilaster. The right section of the pilaster, once the crack was complete, slid and rotated as shown in Figure 3.3.44. A secondary crack appeared within the mortar layer between the first and second brick, indicating an initial rotation triggered by the first crack. The diagrams show compression in the right strain gauge, as the rotation pushes that side downward, while the displacement transducer registers positive deflections due to the same rotation (Figs. 3.3.40-41). Both instruments on the left side register tensile strain. Specimen 2 instead does not lose its reinforcement, although large cracks form in the interface between the masonry and the FRCM layer. In the lower left hand corner on the back of the pilaster, under the loading point, the matrix crumbled and detached during testing. The diagrams show compression in the right strain gauge and tensile strain in the left, and a horizontal crack visible on the right side of the pilaster indicates the opening of a rotation in that specific section, confirmed by the positive deflections registered by the right displacement transducer (Fig.3.3.42-43).

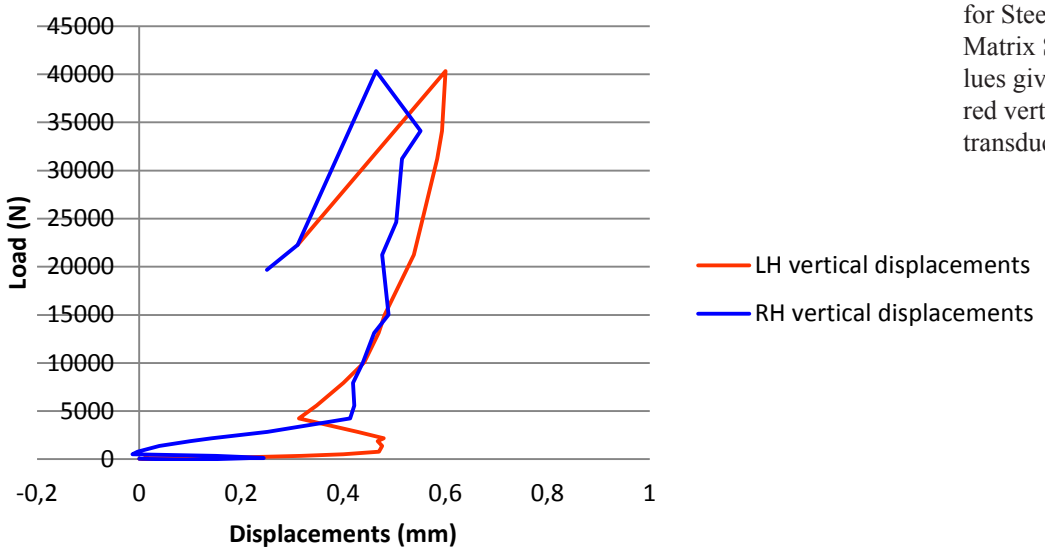

Figure 3.3.40. Load - displacement diagrams for Steel Fibre - Cement Matrix Specimen 1; values given by cantilevered vertical displacement transducers.

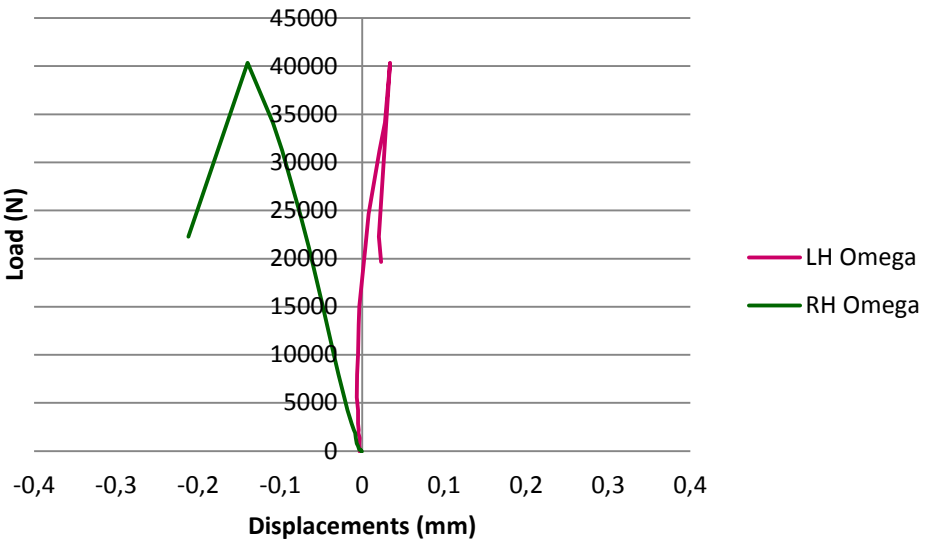

Figure 3.3.41. Load - displacement diagrams for Steel Fibre - Cement Matrix Specimen 1; values given by Omega transducers.

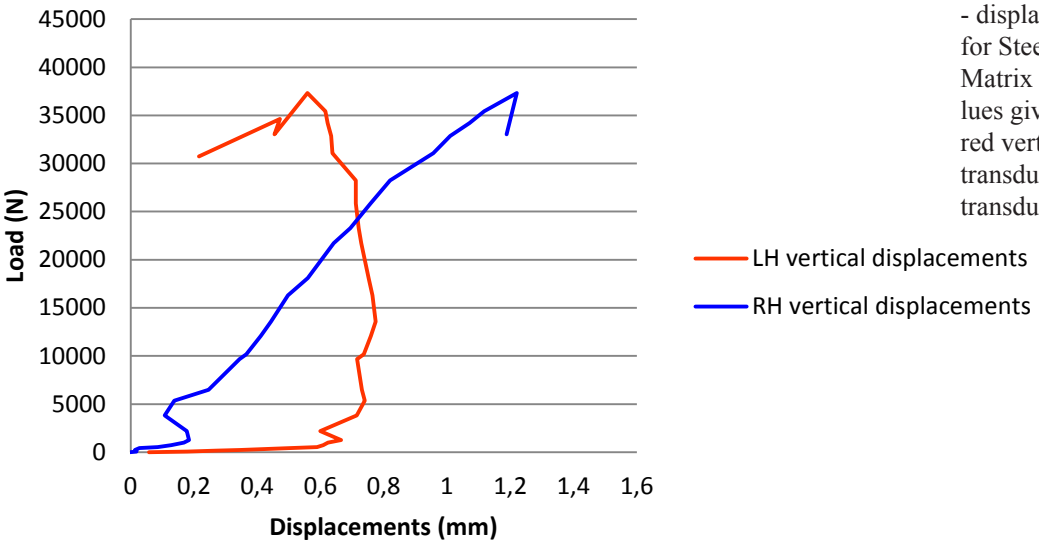

Figures 3.3.42-43. Load - displacement diagrams for Steel Fibre - Cement Matrix Specimen 2; values given by cantilevered vertical displacement transducers and Omega transducers.

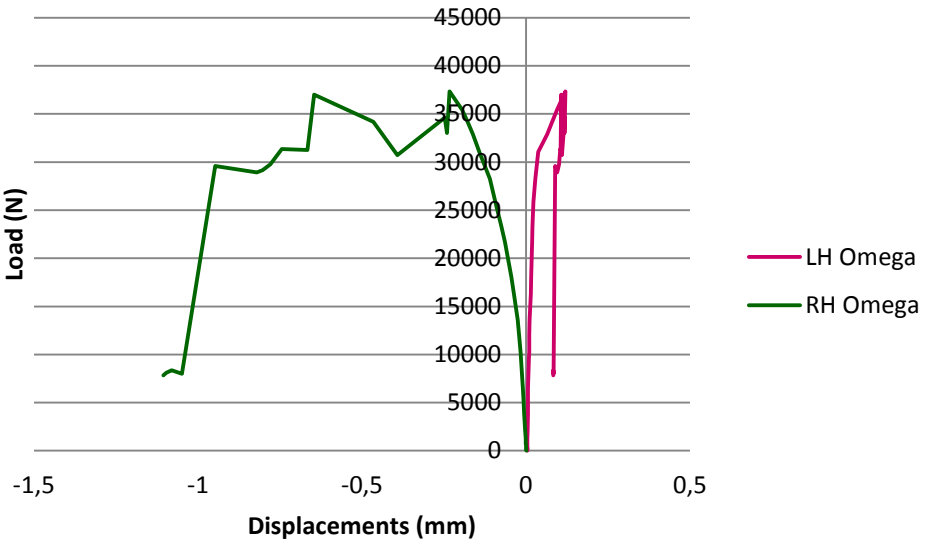

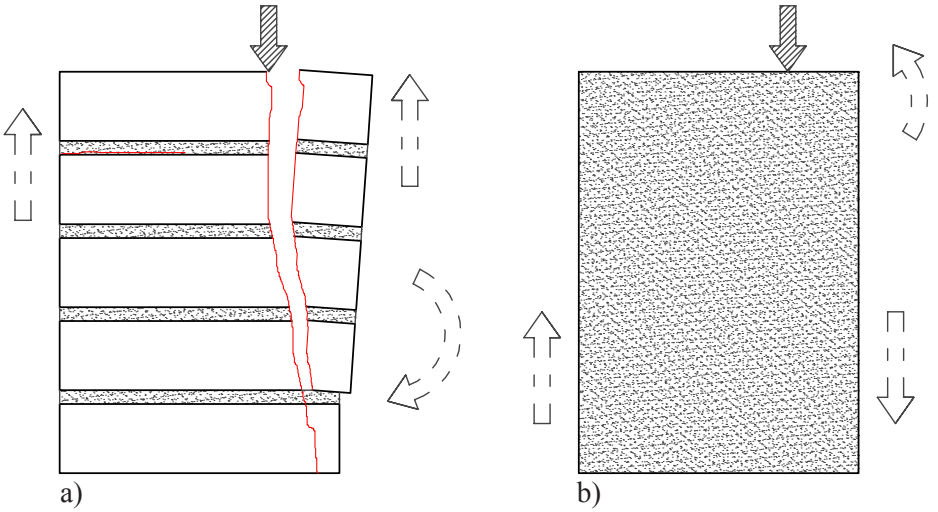

Figure 3.3.44. Graphic description of the cracks that occurred in Steel Fibre - Cement Matrix specimens; a) Specimen 1 and b) Specimen 2.

Figures 3.3.45-47. Steel Fibre - Cement Matrix Specimens 1 and 2 after testing; back side of Specimen 2; crumbling of the matrix on the lower left corner.

Glass fibre - Cement matrix 1 and 2

Glass fibre - Cement matrix specimens 1 and 2 collapsed due to compressive strength at 58594 N and 41294 N, respectively. The FRCM slates did not detach from either specimens during testing, and cracks transferred from the masonry to the reinforcement in specimen 1 (Fig. 3.3.52). In this case, a first crack in the back of the specimen propagates vertically from the top of the pilaster in the area immediately proximate the loading point down towards the bottom. A secondary horizontal crack along the mortar layer appears close to the ultimate load value. Scaling of the matrix is visible in the front of the specimen just before collapse. Diagrams indicate compression throughout the specimen during loading and minimum tensile strain close to ultimate load (Figs. 3.3.48-49). In specimen 2, rotation between the second and third brick begins soon after loading (Fig. 3.3.53), causing the upper right transducer to register positive movements in the diagram while the strain gauge on the same side registers compression (Figs. 3.3.50-51). On the left side of the specimen, slight tensile strain is registered by the strain gauge in the order of one hundredth of a millimetre, while the transducer shows positive deflections.

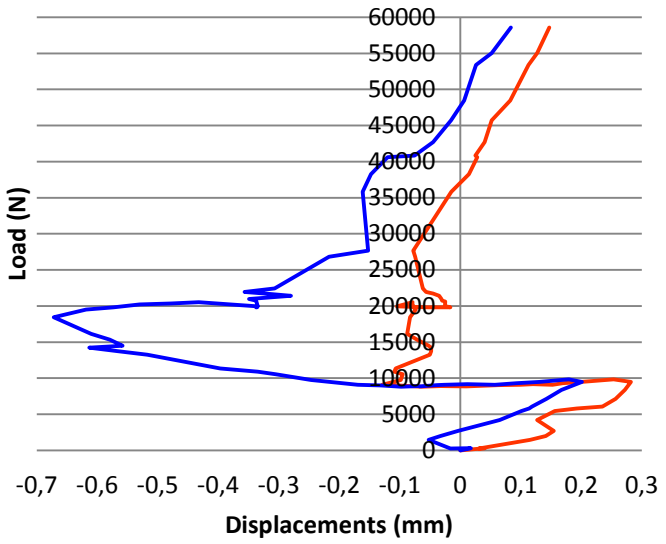

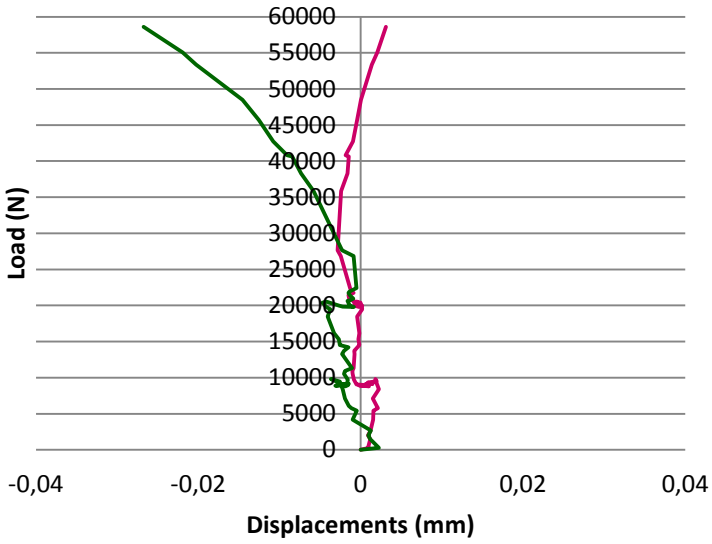

Figures 3.3.48-49. Load - displacement diagrams for Glass Fibre - Cement Matrix Specimen 1; values given by cantilevered vertical displacement transducers and Omega transducers.

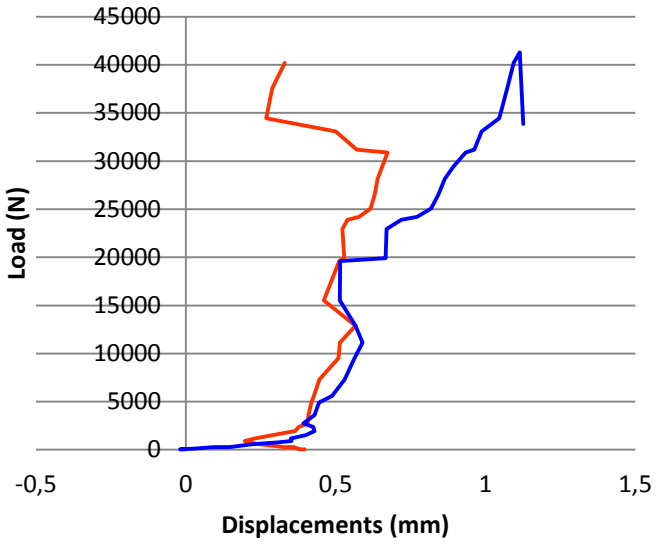

Figures 3.3.50. Load - displacement diagrams for Glass Fibre - Cement Matrix Specimen 2; values given by cantilevered vertical displacement transducers.

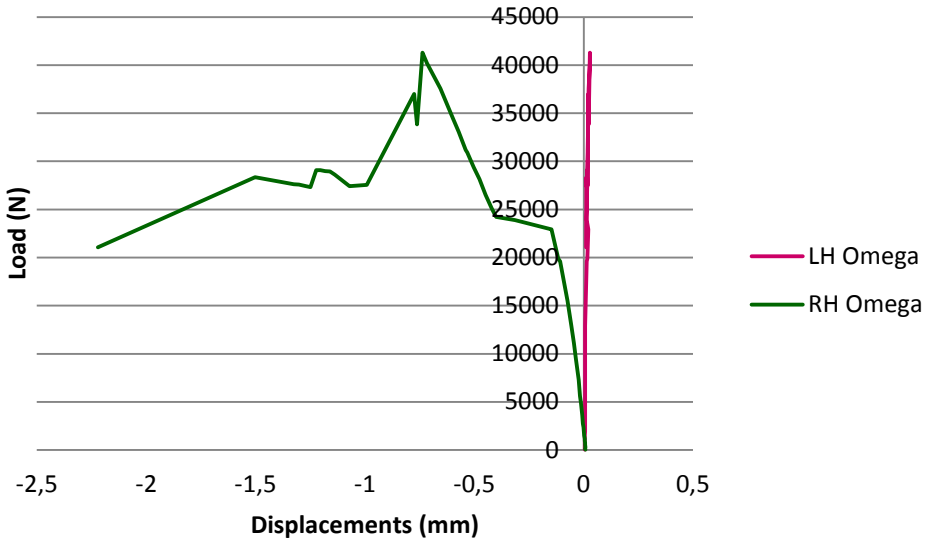

Figures 3.3.51. Load - displacement diagrams for Glass Fibre - Cement Matrix Specimen 2; values given by Omega transducers.

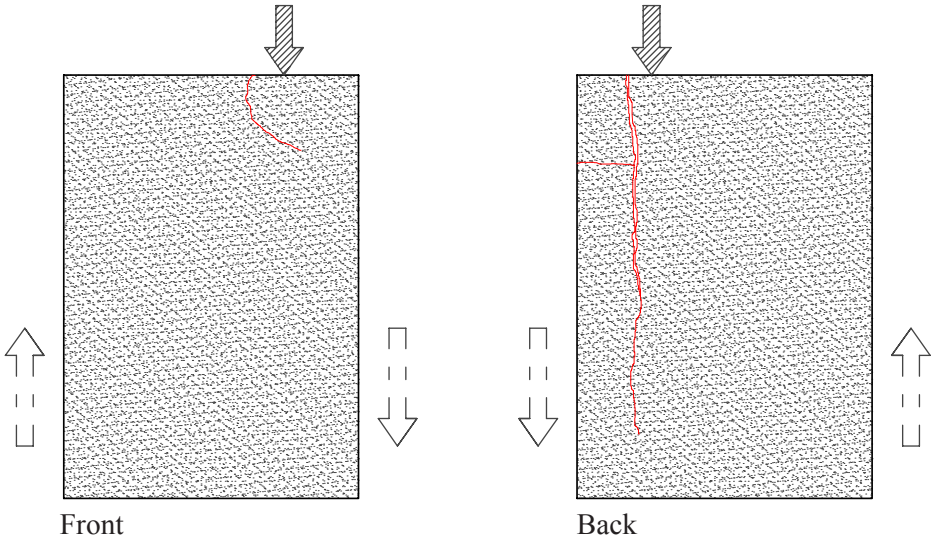

Figure 3.3.52. Graphic description of the cracks that occurred in Glass Fibre - Cement Matrix Specimen 1; front and back.

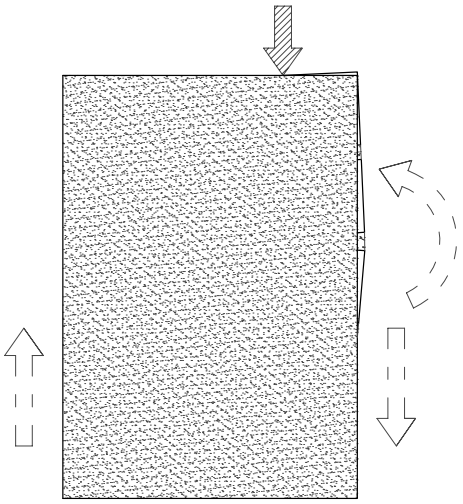

Figure 3.3.53. Graphic description of the cracks that occurred in Glass Fibre - Cement Matrix Specimen 2.

Figures 3.3.54-55. Glass Fibre - Cement Matrix Specimens 1 and 2 after testing.

Aged Unreinforced pilaster

This pilaster, tested as unreinforced and aged, was originally intended to be an aged specimen of the cement matric glass fibre type. After very few cycles, the reinforcement detached from the surface of the pilaster. Notwithstanding, ageing was continued and the specimen was therefore tested as stated. This pilaster collapsed due to compressive strength after extensive cracking at 47816 N. Cracking commenced immediately, and continues according to a slight curve in the direction of the loading point (Fig.3.3.58). As is shown in the diagrams given by the displacement transducers and the strain gauges (Figs. 3.3.56-57), the right side of the pilaster shows compression, while the left side displays tensile strength. The vertical displacement transducer applied to the left side of the pilaster shows negative values for loads decreasing after the ultimate strain, indicating that the left side of the pilaster began deflecting once the small structure was no longer carrying load.

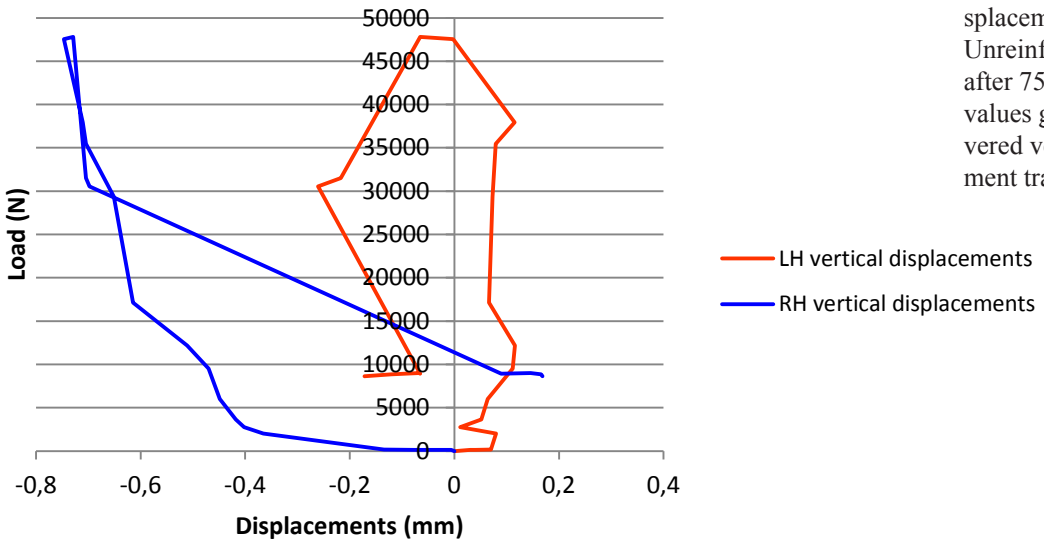

Figures 3.3.56. Load - displacement diagrams for Unreinforced Specimen after 75 wet/dry cycles; values given by cantilevered vertical displacement transducers.

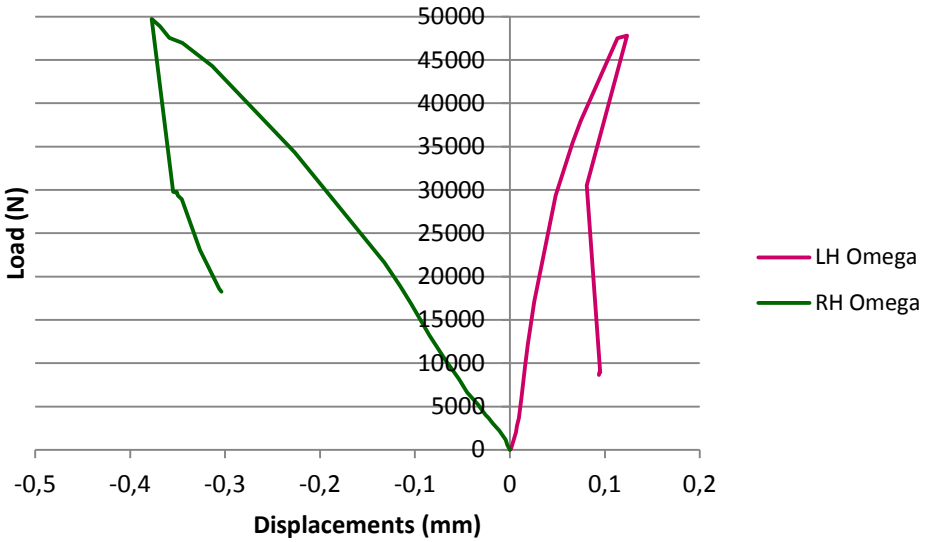

Figures 3.3.57. Load - displacement diagrams for Unreinforced Specimen after 75 wet/dry cycles; values given by Omega transducers.

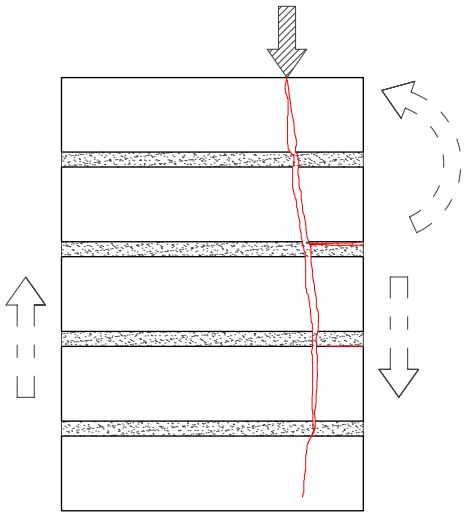

Figure 3.3.58. Graphic description of the cracks that occurred in Unreinforced specimen subjected to 75 wet dry cycles after testing.

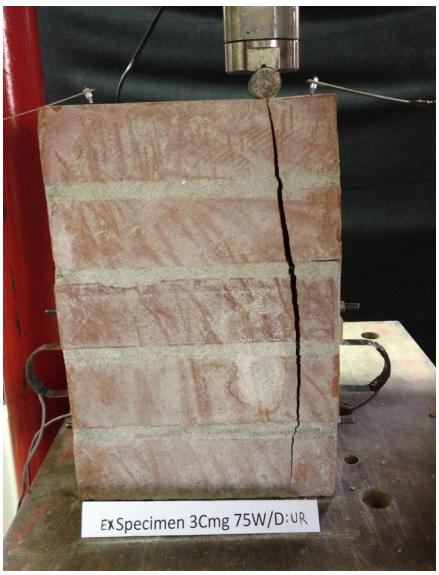

Figures 3.3.59-60. Aged Unreinforced Specimen after testing.

Aged Steel fibre - Lime matrix Specimens 3 and 4

Aged Steel fibre - Lime matrix pilasters 3 and 4 collapsed due to compressive strength at 41562 N and 40041 N respectively. Contrary to what was observed in the unaged equivalents, here the slates of steel fibre imbedded in the lime matrix did not detach from the masonry. Rust and saline efflorescence was present, particularly concentrated around the edges of the pilasters. The cracking occurred in the slates of reinforcement (Fig. 3.3.65), but these were firmly attached to the structure. In the case of specimen 3, the diagrams show that the entire pilaster was subjected to compressive strength, and no tensile stresses were registered, as all displacements were negative (Figs. 3.3.61-62). In the case of specimen 4, although the strain gauges on the left side of the pilaster indicate positive deflections, the displacement transducer on the same side initially show negative values, probably indicating horizontal cracks in the mortar layers (Figs. 3.3.63-64).

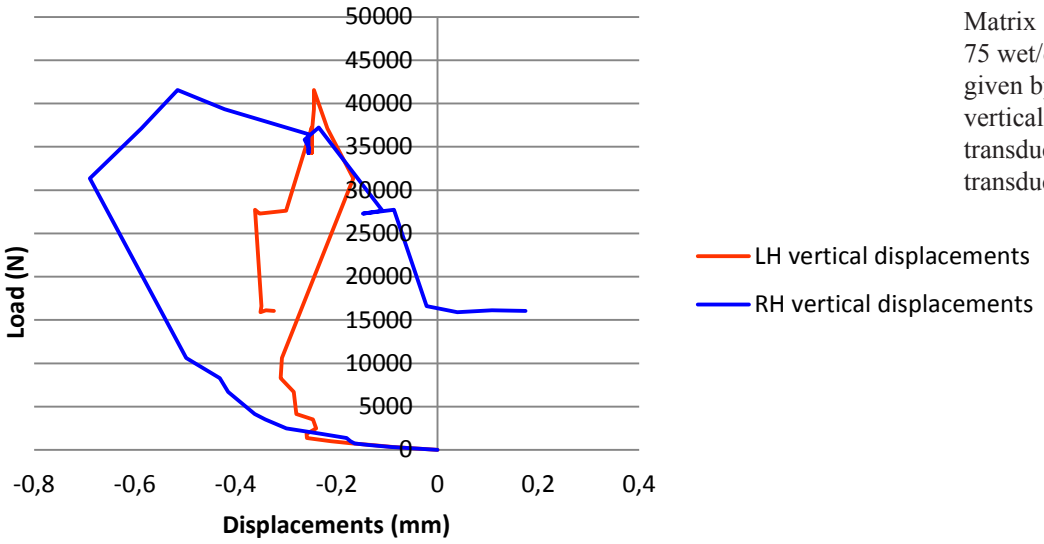

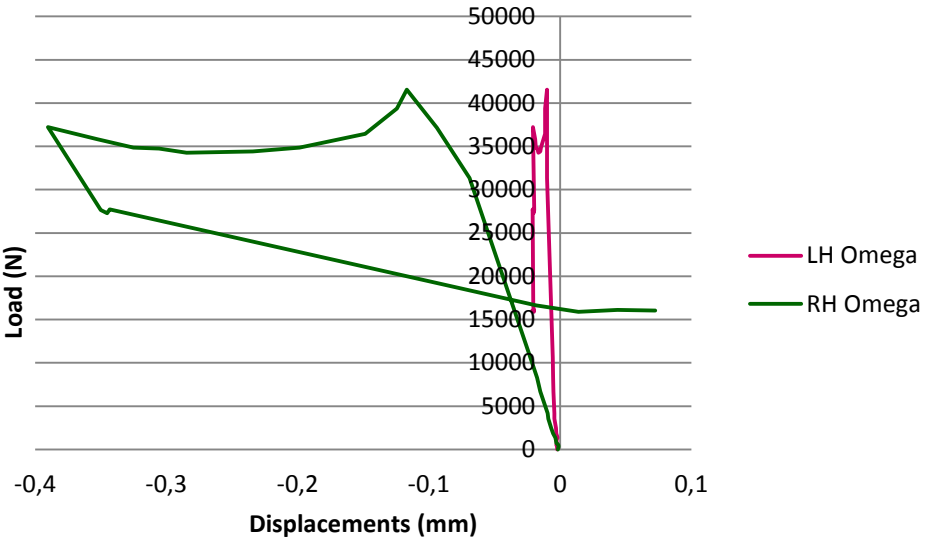

Figures 3.3.61-62. Load - displacement diagrams for Steel Fibre - Lime Matrix Specimen 3 after 75 wet/dry cycles; values given by cantilevered vertical displacement transducers and Omega transducers.

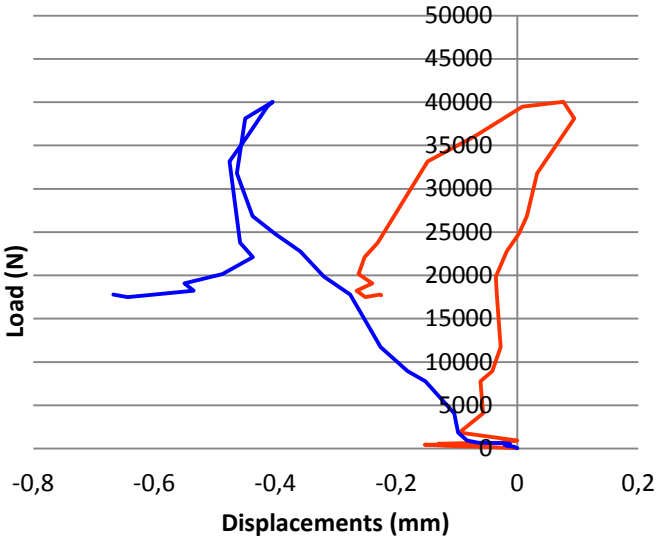

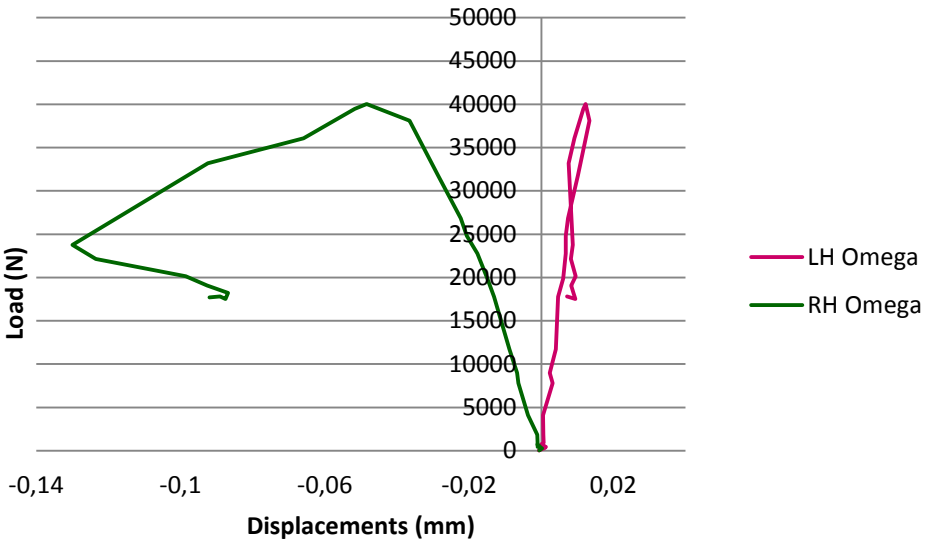

Figures 3.3.63-64. Load - displacement diagrams for Steel Fibre - Lime Matrix Specimen 4 after 75 wet/dry cycles; values given by cantilevered vertical displacment transducers and Omega transducers.

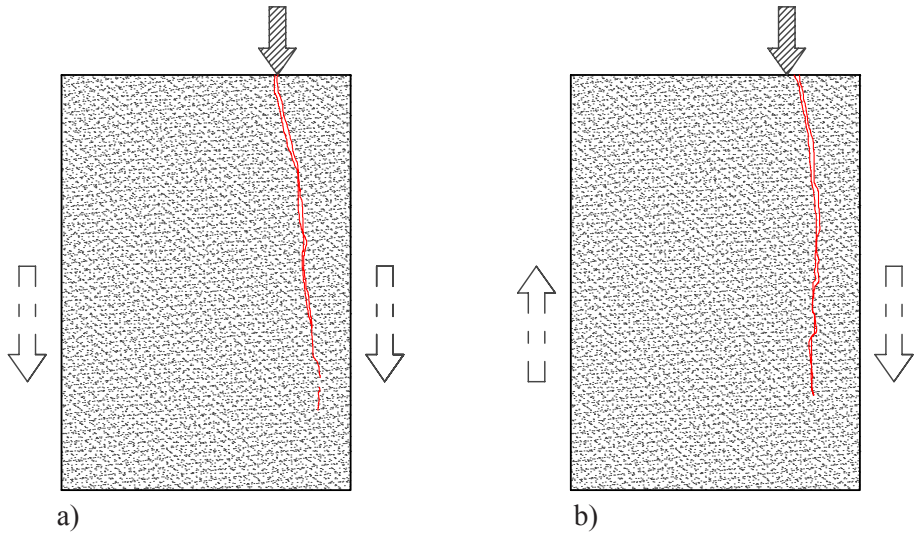

Figure 3.3.65. Graphic description of the cracks that occurred in Steel Fibre - Lime Matrix Specimens subjected to 75 wet dry cycles after testing; a) Specimen 3 and b) Specimen 4.

Figures 3.3.66-67. Aged Steel Fibre - Lime Matrix Specimen 3 before and after testing.

Figures 3.3.68-69. Aged Steel Fibre - Lime Matrix Specimens 3 and 4 after testing.

Glass fibre Lime matrix 3 75 W/D

Aged glass fibre lime matrix specimen 3, the only specimen of this type to have lasted the duration of the 75 wet/dry cycles, collapsed due to compressive force at 43804 N. The reinforcement did not detach from the façades of the specimen (Fig. 3.3.72), and showed cracks only in the upper sides of the reinforcement where it was attached to the masonry. This is an indication of cracks forming in the masonry beneath the reinforcement, as is confirmed by the presence of two hair-line cracks along the horizontal mortar layer between the first and second brick, visible on the short sides of the specimen. The diagrams show positive deflections in both vertical displacement transducers, consistent with the indication observed above of cracks in the mortar layers between the strain gauges and the transducers. Negative compression values are visible in the right hand strain gauge, while the left hand instrument registers values which, albeit negative as well, are in the order of one millionth of a millimetre (Figs. 3.3.70-71), indicating insignificant deflections on that side.

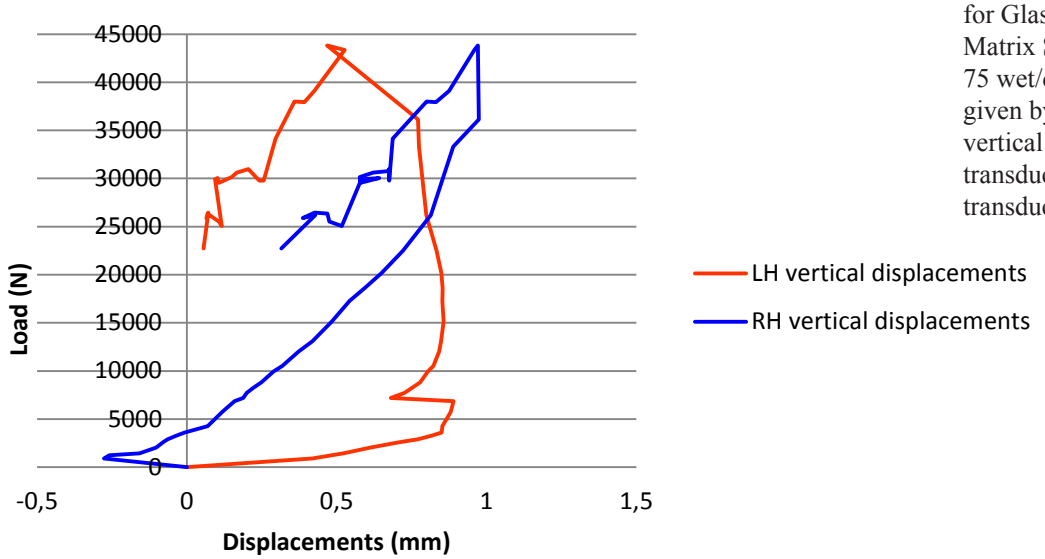

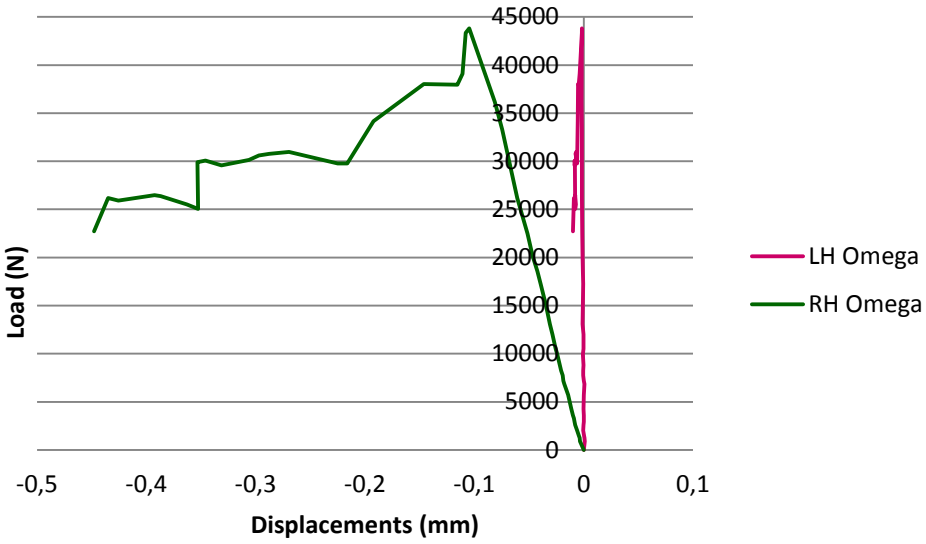

Figures 3.3.70-71. Load - displacement diagrams for Glass Fibre - Lime Matrix Specimen 3 after 75 wet/dry cycles; values given by cantilevered vertical displacement transducers and Omega transducers.

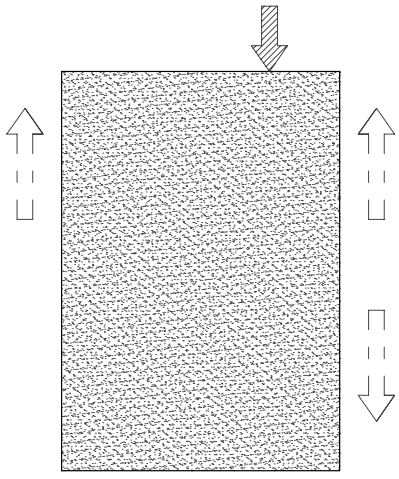

Figure 3.3.72. Graphic description of the cracks that occurred in Glass Fibre - Lime Matrix Specimen 3 subjected to 75 wet dry cycles after testing.

Figures 3.3.73-74. Aged Glass Fibre - Lime Matrix Specimen 3 after testing.

Steel fibre - Cement matrix 4 75 W/D

Aged Steel fibre - Cement matrix specimen 4 was the only specimen with this reinforcement to have lasted the 75 wet/dry cycles, and collapsed due to compressive strain at 38930 N. The FRCM panels presented extensive rusting and saline efflorescence, but remained firmly attached to the masonry interface for the entire duration of the test. A large crack commenced under the loading point and continued opening through the reinforcement, indicating that bonding increased throughout the ageing cycles (Fig. 3.3.77). No other cracks were noticed on the sides of the pilaster, and the diagrams show compressive values registered on the right side of the specimen and tensile strain registered by the left strain gauge (Figs. 3.3.75-76). The left displacement transducer initially presents negative values, which then turn positive as the pilaster reaches its ultimate strength.

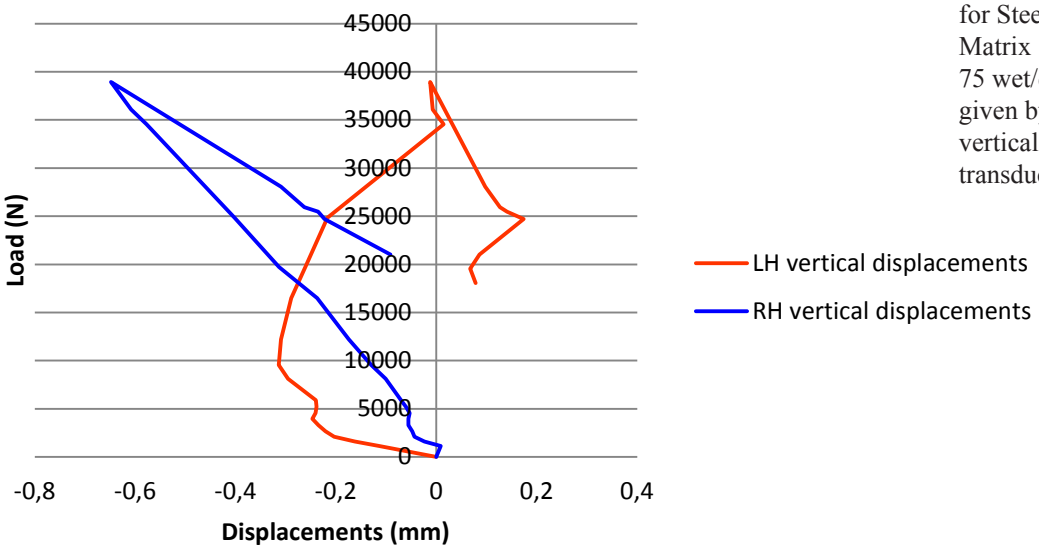

Figure 3.3.75. Load - displacement diagrams for Steel Fibre - Cement Matrix Specimen 4 after 75 wet/dry cycles; values given by cantilevered vertical displacement transducers.

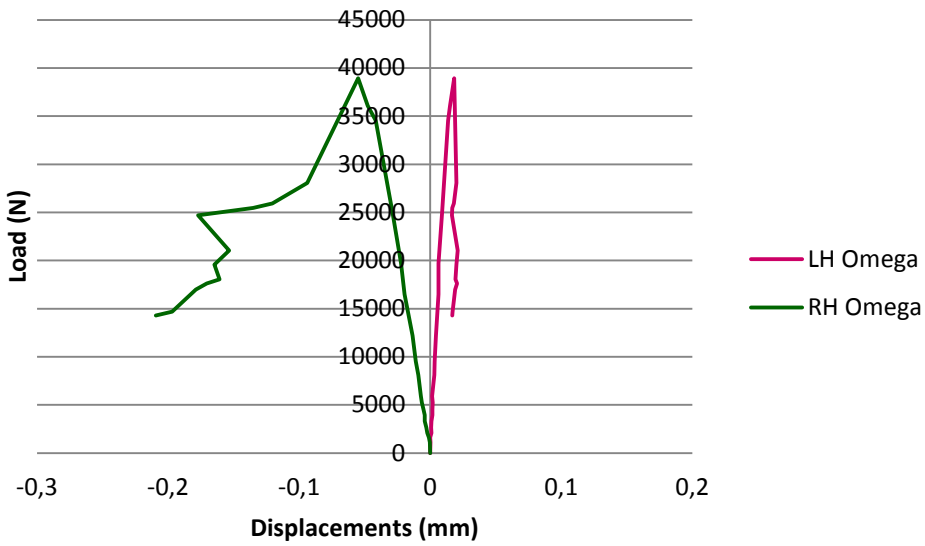

Figure 3.3.76. Load - displacement diagrams for Steel Fibre - Cement Matrix Specimen 4 after 75 wet/dry cycles; values given by Omega transducers.

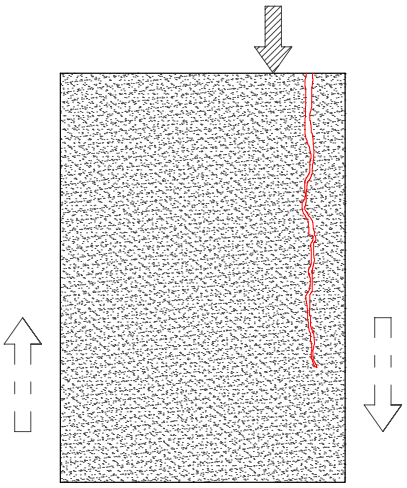

Figure 3.3.77. Graphic description of the cracks that occurred in Steel Fibre - Cement Matrix Specimen 4 subjected to 75 wet dry cycles after testing.

Figures 3.3.78-79. Aged Steel Fibre - Cement Matrix Specimen 3 after testing.

Glass fibre - Cement matrix 4 75 W/D

Aged Glass fibre - Cement matrix specimen 4, the only specimen with this reinforcement to have lasted the 75 wet/dry cycles, collapsed due to compressive strength at 37786 N. The reinforcement slates, presenting saline efflorescence particularly along the exterior, remained attached to the façades of the masonry during testing. If any cracks occurred in the masonry structure, they were not transferred through the FRCM slates (Fig. 3.3.82). The diagrams resulting from the displacement transducers and the strain gauges indicate compressive strain on the right side of the pilaster and tensile strain on the left (Figs. 3.3.80-81).

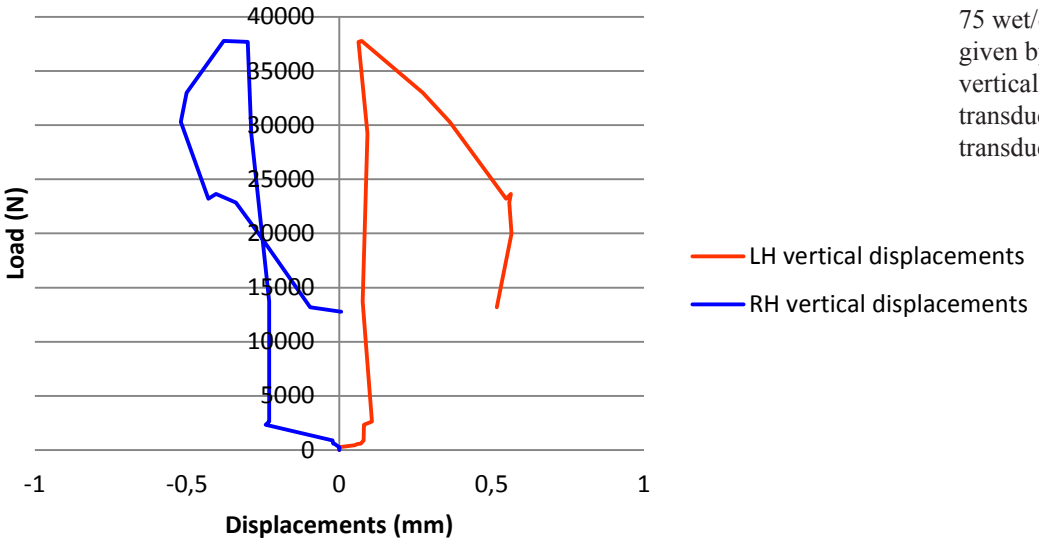

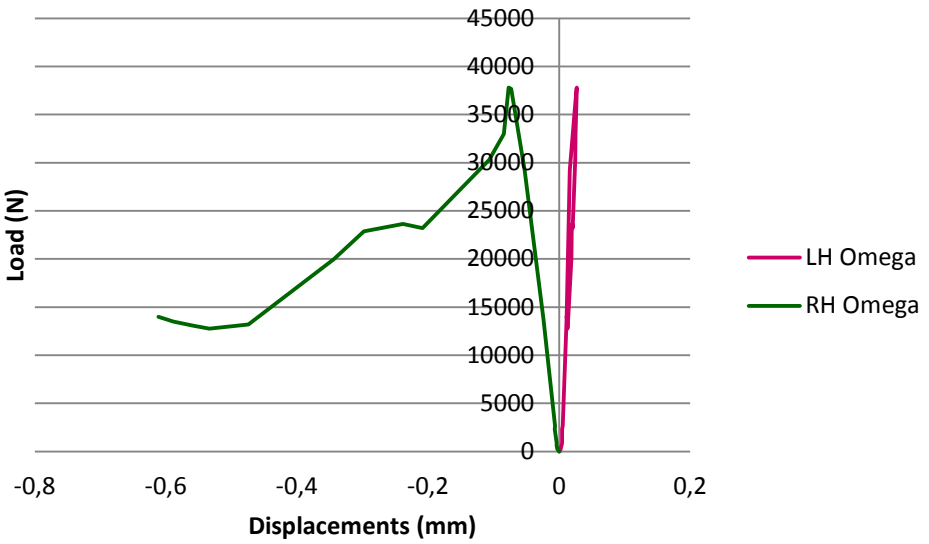

Figures 3.3.80-81. Load - displacement diagrams for Glass Fibre - Cement Matrix Specimen 4 after 75 wet/dry cycles; values given by cantilevered vertical displacement transducers and Omega transducers.

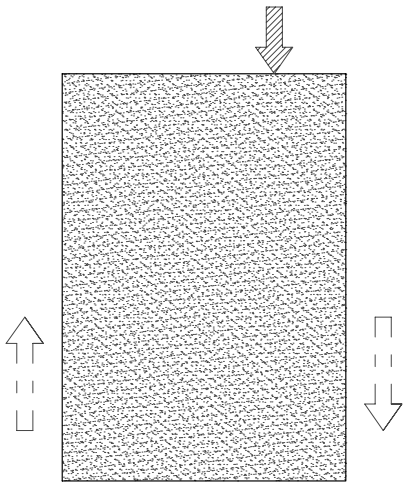

Figures 3.3.82-83. Graphic description of the cracks that occurred in Glass Fibre - Cement Matrix Specimen 4 subjected to 75 wet dry cycles after testing; aged Glass Fibre - Cement Matrix Specimen 4 before testing.

Conclusions

The main inquiry of the present experimental campaign was aimed towards determining whether FRCM reinforced masonry pilasters are severely affected by artificial ageing, achieved in this particular case through wet/dry cycles in a 5% sodium chloride solution. From the analysis of the results it may be conclusively said that the FRCM system does not appear to be affected by the wet/dry cycles. In three cases, reinforced pilasters lost their reinforcement and two of these ruptured during cycles, while in the remaining 5 cases the specimens successfully reached the end of the 75 cycles. While no substantial differences were found between the two types of specimens, probably due to the lack of anchorage of the reinforcement to the masonry substrate, the reinforced ones presented abrupt ruptures, while the unreinforced ones collapsed in a more gradual manner. The degradation caused by the 5% sodium chloride solution appears only in saline efflorescence in all aged specimens, while in the steel fibre reinforced specimens rust was apparent from as soon as the 5th wet cycle. When the FRCM system was removed from the surface of the masonry pilasters after testing, no dangerous mould formations were detected. Regarding the resistance of the FRCM system to the tensile strength to which the pilasters were subjected as a consequence of eccentric compression, cracks caused by tensile stress did not appear in reinforced specimens, leading to the conclusion that the fibres successfully absorbed such stresses.

From the results of testing in the present campaign and the observations conducted throughout the cycles, it can be stated that FRCM reinforced pilasters are not affected by wet/dry cycles as regards the ultimate load carrying capacity. However, the superficial degradation of the specimens, in particular of those reinforced with steel fibre, must be addressed in order to avoid the detachment of the FRCM system as occurred in the three specimens mentioned above.

4. Wet/Dry Durability on Brick Masonry Panels Reinforced through the Reticolatus Method

In the previous campaigns of the present work we saw the experimental analysis of freeze/thaw and wet/dry durability issues on FRCM specimens and small pilasters reinforced through FRCM. Now, the focus turns towards the investigation of the behaviour of brick masonry panels reinforced with the Reticolatus technique (Chapter I.c), subjected to artificial ageing and diagonal testing. Thus, the main goal of this campaign is to verify whether the artificial ageing process hinders in any way the resistance of the panel.

The recovery of the resistance values observed in campaign 2 (where the cement mortar specimens reinforced with steel fibres after being allowed to dry completely showed resistances which exceeded their initial strength) indicates that FRCM reinforcement methods could be functional in service conditions even after exposure to natural elements. Now the question turns towards the durability of actual structural elements which have shown a great increase of resistance when reinforced with the method of Reticolatus (Borri et al., 2010). With regard to resistance, given the positive results of the previous campaigns, where ultimate values of resistance were either not largely affected by the artificial ageing that the specimens were subjected to or the heavily decreased values in resistance were subsequently recovered after a period of time, it is expected that the shear resistance of the masonry panels tested in the following campaign not decrease significantly. As regards material degradation, which would need to be addressed by a proper maintenance program after the reinforcement system is in place, it is expected that there be some loss in section of the newly applied mortar covering the steel cords and probably rusting, as was observed during campaigns 2 and 3. As in the previous campaigns, the preparation and testing of the specimens was conducted at the Laboratory of the Department of Architecture at the University of Florence.

Experimental Programme and Materials

Four brick masonry panels were constructed, with bricks posed as all headers in the masonry fabric, similarly to what had been tested by Borri et al. (2013), but of a much smaller size. In fact, in the experimental campaign carried out in Udine in 2013 the panels were all 120x120 cm in size, whereas in the present testing panels were built to be 51x51 cm in size (Fig. 3.4.1), due to limitations of the containers used for the artificial ageing cycles. The mortar used in the construction of the panels was the same type of cement mortar used in campaigns 1 and 2 for durability testing on

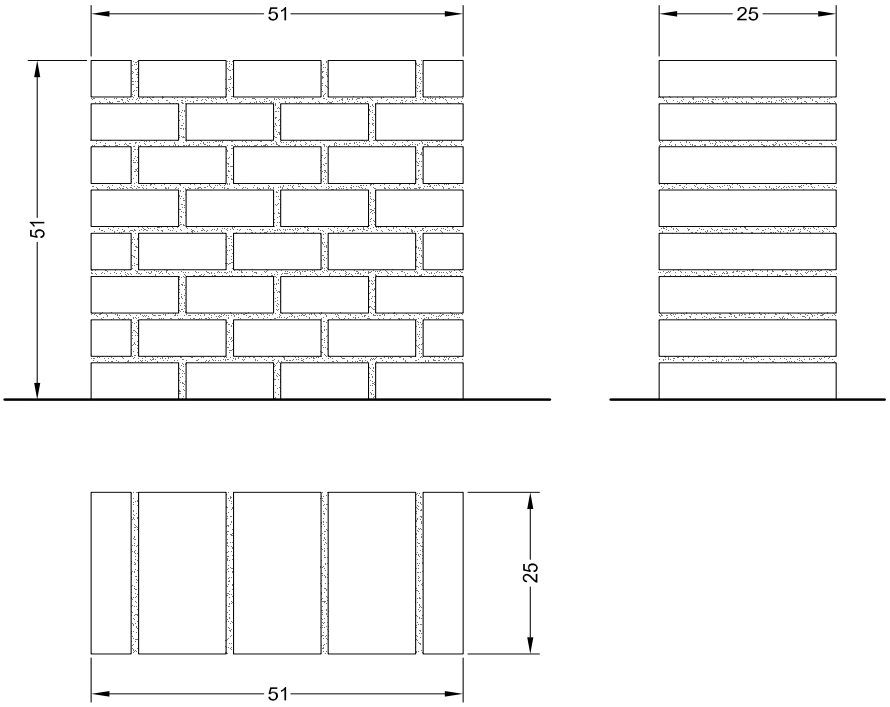

Figure 3.4.1. Orthogonal projection of the brick masonry panels (cm).

reinforced mortar specimens (Table 3.c), and for the reinforcement of the cement matrix pilasters in campaign 3. All panels were reinforced through the Reticolatus method, using the 3x2 steel cords provided by Hardwire, llc., as used in previous campaigns 1, 2 and 3. The design of the reinforcement and its application in the mortar layers of the panels was also based on Borri et al. (2013), as may be seen in Figure 3.4.2. Unreinforced panels were not tested during this campaign as the goal was to verify loss of resistance between aged and unaged panels, if any.

Once the panels had completely cured for a period of over two months, a thickness of about 2 cm of mortar was removed by hand with the use of a chisel. During this process weights were applied to the panels, in order to avoid dangerous vibrations or movements caused by the action of the chisel. The steel cords were then positioned in the mortar layers around single bricks on both façades of the panels, and longitudinal cords were positioned throughout the entire width of the façades in two mortar layers near the top and the bottom of the panels. The steel cords on either side of the panel were connected by threaded steel rods inserted in the thickness of the panels which had been previously drilled to host them. The steel cords were then looped around the end of the steel rods which jutted out from the mortar thickness and small crown shaped elements were screwed onto the rods in order to hold the cords in place. On the side of the panels, the longitudinal cords were well connected to the mortar layer through long screws with large heads, keeping the cords firmly in place. Once this process was complete on both the wider and shorter sides of the panels,

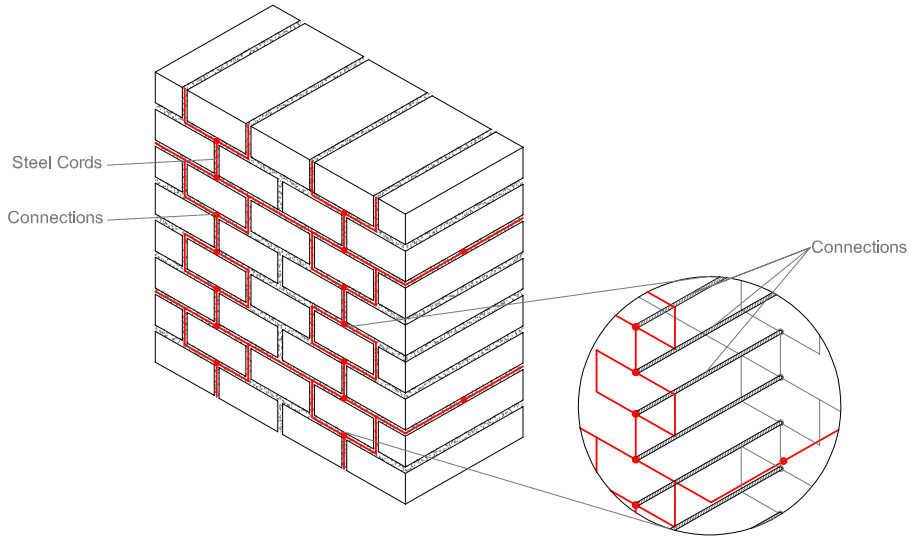

Figure 3.4.2. Scheme of the reticolatus reinforced panels with nodes representing steel threaded rods and crown screws. Detail of connections between the reinforcements on the two faces of the panels.

Average Maximum Flexural Strength (MPa)	Standard Deviation (MPa)	CoV	Average Maximum Compressive Strength (MPa)	Standard Deviation (MPa)	CoV
6.54	0.72	0.11	18.47	2.24	0.12

Table 3.r. Flexural and compression values obtained experimentally from Ruredil, MaltaS mortar specimens.

the mortar layers were carefully repointed. In three cases out of four panels, the mortar used for the deep repointing of the mortar joints was the same as that used for the construction of the panels themselves, that is, the hand mixed cement mortar described above. The fourth panel was repointed with a special inorganic mortar, MaltaS, provided by Ruredil. Flexural and compression values for this mortar type are listed in Table 3.r.

The panel repointed with the special inorganic mortar was not subjected to wet/dry cycles, as is best described in the test matrix in Table 3.s. Two panels were tested unaged, and the remaining two were subjected to wet/dry cycles. Based on a proportion between the weight of the pilasters in experimental campaign n° 3, which were immersed in the sodium chloride solution for 45 minutes, and the weight of the panels, 5 hours of immersion time was estimated necessary for complete sorption of the sodium chloride solution, calibrated at 3% for this campaign. The limitation in the percentage of sodium chloride was determined by the large amount of salt needed to create a 5% solution. The dry period of the cycles was 48 hours long; for this campaign, it was not possible to

N° Panels	Panel type	Reinforcement	N° of wet/dry cycles
1	MALTA S	Reticolatus	0
1	Cement mortar	Reticolatus	0
2	Cement mortar	Reticolatus	50

Table 3.s. Test Matrix.


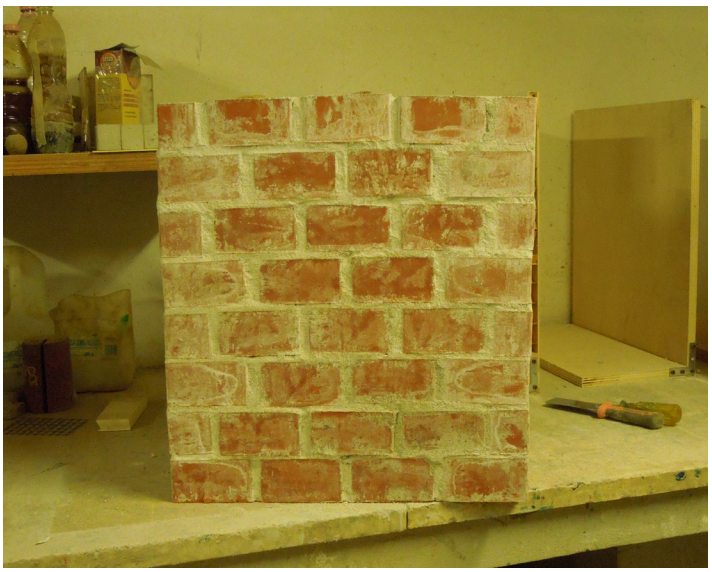

Figures 3.4.3-4. Plastic basin used for wet/dry cycles on the brick masonry panels and a panel before mortar removal.

insert the panels in ovens for drying due to their elevated weight. Instead, the panels were left in the basin used for the wet cycles (Fig. 3.4.3), drained of the sodium chloride solution and air-dried with the aid of a mechanical ventilation system created ad hoc for this campaign. The panels were subjected to a total of 50 wet/dry cycles as described.

Test Set-up and Instrumentation

Once the 50 artificial ageing cycles were complete, specimens were allowed to dry for 48 hours. Testing was carried out according to the ASTM Standard E519-10, in which diagonal compression is used to simulate shear tensions in structures. Diagonal compression is carried out by positioning the panels at a 45° angle under a load cell capable of transmitting compressive strength. Specific metal loading shoes were constructed to hold the panels at a 45° angle as shown in Figures 3.4.5-6.

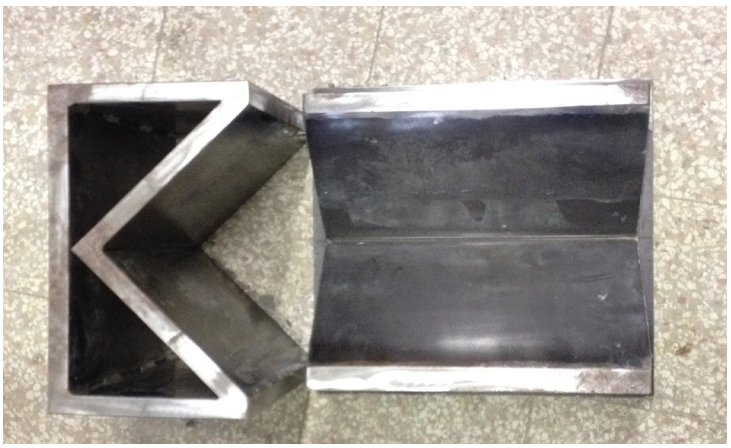

Figure 3.4.5. Loading shoes used for diagonal testing.

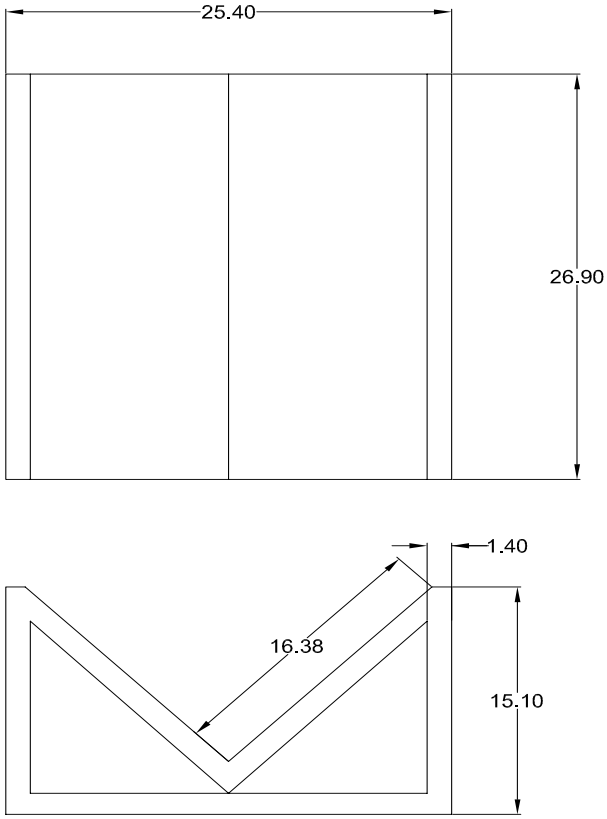

Figure 3.4.6. Graphic scheme of the metallic loading shoe specifically built for this campaign (cm).

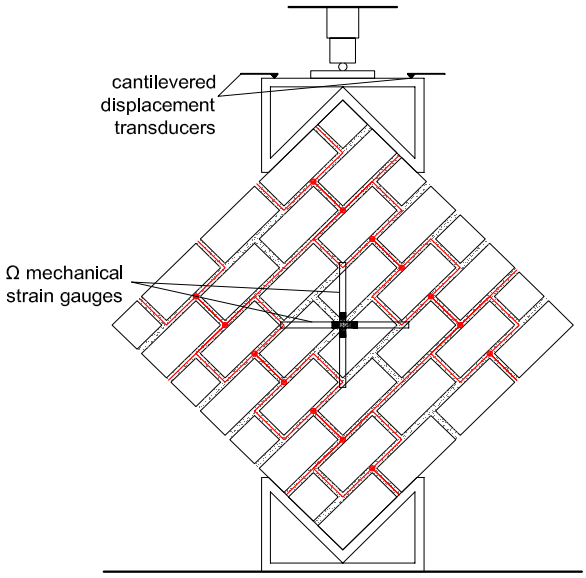

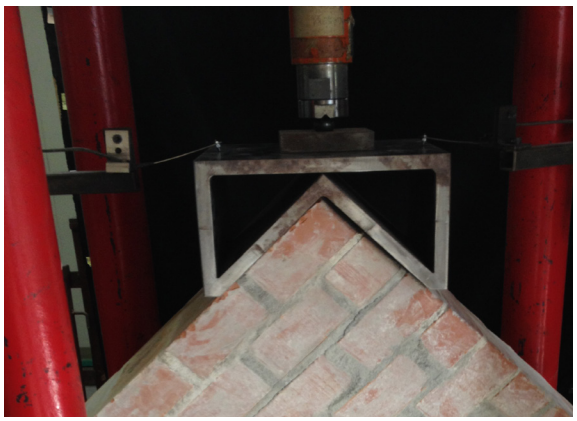

Figures 3.4.7-8. Graphic scheme of the testing apparatus and detail of the load cell applying pressure on metal sphere and plate.

Loading was applied through a load cell (TCLP – 20B Tokyo Sokki Kenkyujo Co, Ltd.) with a maximum capacity of 20 kN applying pressure on a small metal sphere which interlocks in a plate of metal positioned on the top of the second metal shoe (Figs. 3.4.7-8). Two cantilevered displacement transducers (CE-10 Tokyo Sokki Kenkyujo Co, Ltd.) were positioned on the upper side of the top shoe measuring vertical displacements, and four mechanical strain gauges (PI-5-100 Tokyo Sokki Kenkyujo Co, Ltd.), two for each side, were placed in the centre of the panels

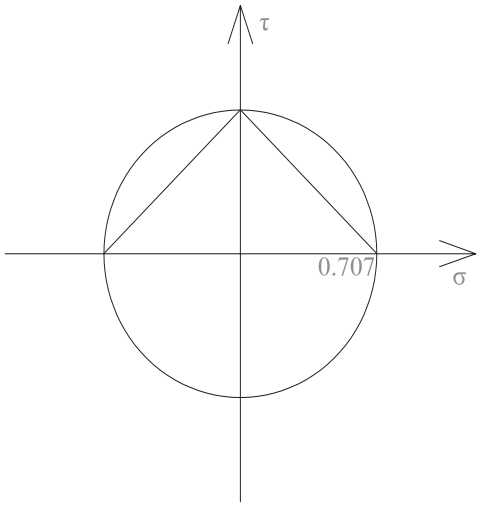

Figure 3.4.9. Mohr's Circle and the representation of a pure shear stress state.

measuring displacements along the diagonals. Testing was conducted via a wheel connected to the load cell turned manually in a clockwise direction, while the strain gauges and transducers were connected to a computer which registered movements in relation to the applied load.

Results

The ASTM Standard E519-10 provides a method for interpretation of the results based on the assumption that the stress state at the centre of the panel is considered pure shear stress and the direction of this tensional state coincides with the diagonals of the panels, as represented by Mohr's Circle in Figure 3.4.9.

The ASTM standard provides the calculation method for specimens' shear stress, S_s, considering net area:

$$S_s = \frac{0.707P}{A_n} \tag{1}$$

Where P is the applied load, in Newton, and A_n is the net area of the specimen:

$$A_n = \left(\frac{w+h}{2}\right)tn \tag{2}$$

where w is the width of the specimen, h the height, and t is the total thickness of the specimen, all in millimetres, n is the percentage of the area which is solid, and, in the case of a square specimen, as is the present case, is considered equal to 1 (Fig. 3.4.10).

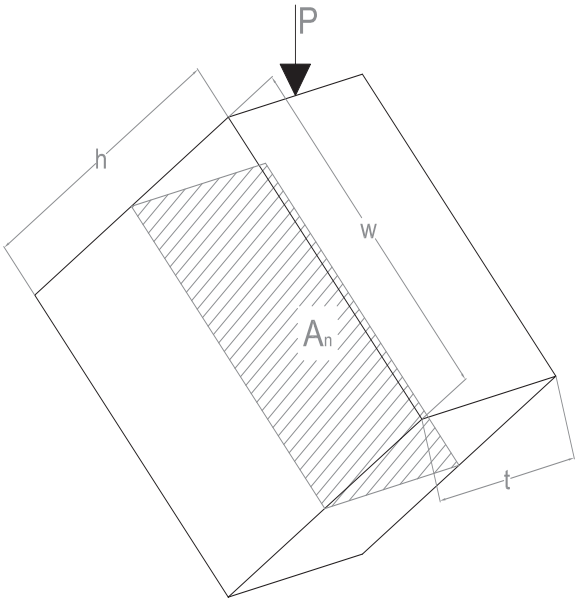

Figure 3.4.10. Net area of the masonry panels with which the shear state is calculated.

The standard also provides calculation methods for shear strain, γ, and consequently the modulus of rigidity G.

$$\gamma = \frac{\Delta V + \Delta H}{g} \tag{3}$$

$$G = \frac{S_s}{\gamma} \tag{4}$$

where ΔV and ΔH are vertical and horizontal shortening and g is the length of the vertical strain gauge (mm), that is, the length of the section where the shortening was measured.

This is not the only method for calculating the shear stress state of specimens tested with diagonal compression (Alecci et al., 2013). A different approach, following RILEM LUMB6 (1994) specifications, considers the stress at the centre of the specimens as not purely shear stress. However, it seems to be the most pertinent to the present case, as the initial assumption is that the material of the specimens is isotropic and homogeneous. Furthermore, calculations carried out by Alecci et al. (2013) following the RILEM LUMB6 methodology seem to be less conservative in comparison to the indications of the ASTM standard. For structural safety reasons, calculating a higher tensional state could be a greater guarantee against collapse. The diagrams in the following sections have therefore been compiled using the calculations provided in the ASTM Standard E519-10.

Unaged panels

The unaged panels consisted of one panel repointed with the abovementioned MaltaS provided by Ruredil, and one panel repointed with hand mixed cement mortar. The mechanical properties of these mortars are described in Tables 3.c and 3.r.

Specimen	Maximum Load (N)	Maximum Shear Stress S_s(MPa)	Maximum Strain γ (%)	Modulus of Rigidity G (MPa)	Collapse Mechanism
MaltaS	237947	1.32	0.0762	17.32	
Cement mortar	122041	0.68	0.0426	15.96	Slipping

Table 3.t. Results of the diagonal compression tests.

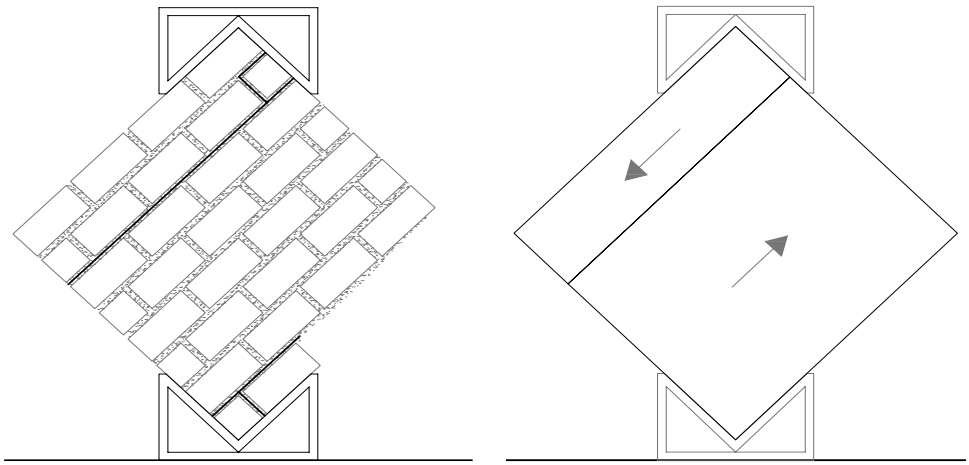

Figures 3.4.11-12. Graphic description of the cracks that occurred in the cement mortar repointed panel and collapse mechanism through slipping.

Figure 3.4.13. Cement mortar repointed panel. Failure after diagonal compression test.

The collapse mechanism of the cement mortar repointed panel, as is shown in Figures 3.4.11-12, occurs by the slipping of the masonry along the mortar joints. The cracks propagate along the longitudinal steel reinforcement imbedded in the mortar. This mechanism suggests that the insertion of the reinforcement by means of the removal of the original mortar actually weakened the panel. The lower right row of bricks collapses at maximum load capacity and there is an additional crack in the area covered by the upper metallic shoe. Failure was sudden, immediately after the upper longitudinal crack appeared the lower row of brick collapsed.

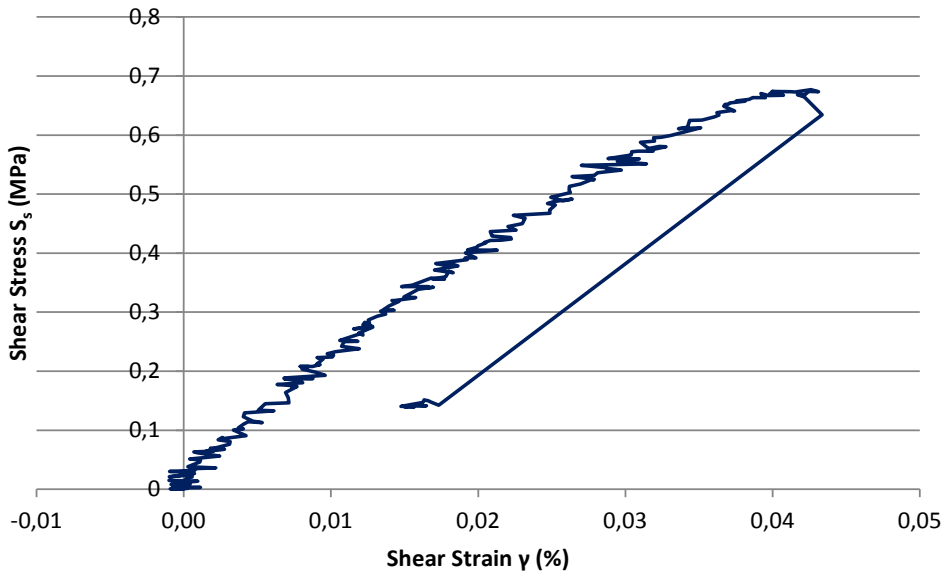

Figure 3.4.14. Shear stress-strain diagram for cement mortar repointed reticolatus.

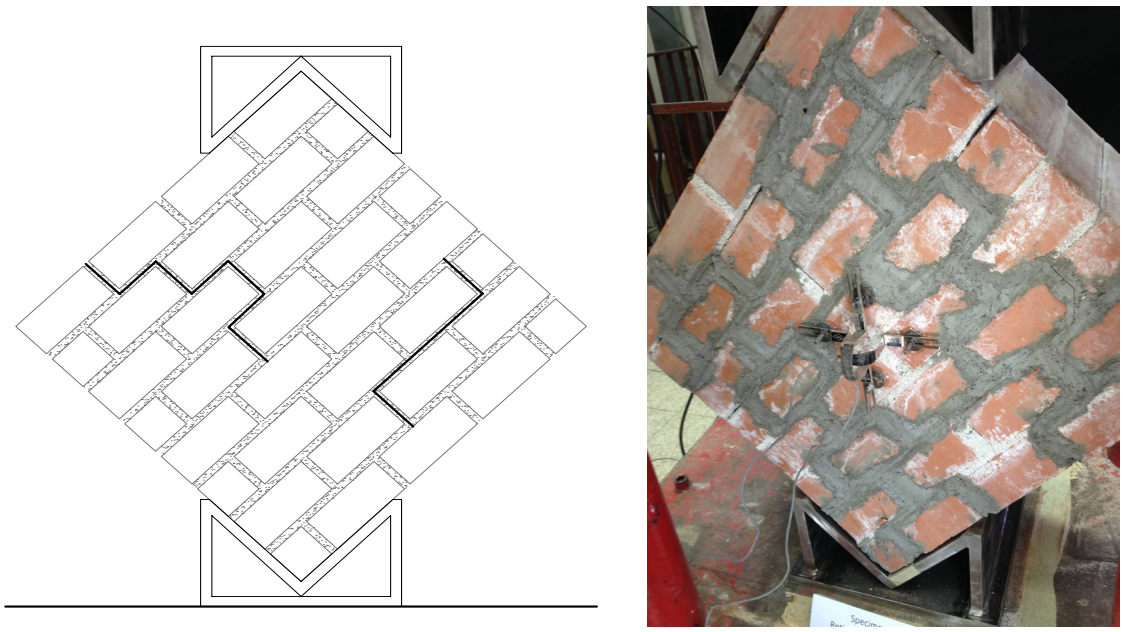

Figures 3.4.15-16. Graphic description of the cracks that occurred in the MaltaS repointed panel and failure after diagonal compression test.

In the MaltaS repointed panel (Figs. 3.4.15-16) failure was again by non-diagonal rupture, but there was no loss of material when the maximum load capacity was reached. Failure occurred gradually, at a much higher load (Table 3.t), a fact which is due to the greater resistance of the mortar used for repointing. The elevated resistance of this mortar, in fact, caused the masonry to behave as two separate pieces reinforced with a resinous type of matrix. Slipping occurs between the two reinforced portions of the panel (Figs. 3.4.15-16), and the section of masonry wedged in between the two portions is subjected to a minimum rotation. Given the stepwise fashion of the collapse, it is difficult to classify the mechanism as purely a slip phenomenon, in contrast to what was shown to be the case in the cement repointed panel.

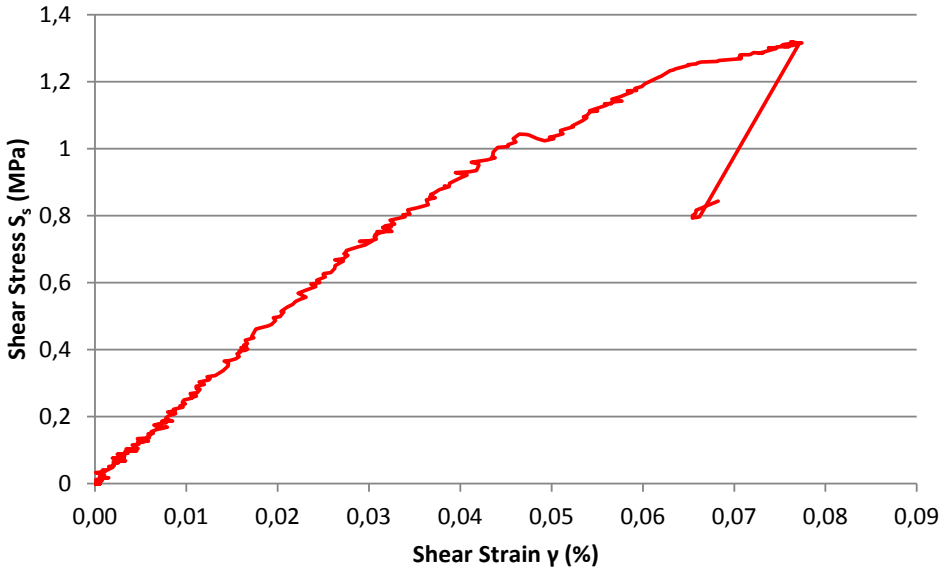

Figure 3.4.17. Shear stress-strain diagram for MaltaS repointed Reticolatus.

Specimen	Maximum Load (N)	Maximum Shear Stress S_s(MPa)	Maximum Strain γ (%)	Modulus of Rigidity G (MPa)	Collapse Mechanism
Aged specimen 1	98757	0.55	0.13	4.23	Slipping
Aged specimen 2	174396	0.97	0.05	19.4	Diagonal cracks

Table 3.u. Results of the diagonal compression tests for aged specimens.

Aged panels

Both aged panels were repointed with the hand mixed cement mortar described in Table 3.c. Once the panels had completed the 50 wet/dry cycles, they were allowed to dry for 24h, after which they were carefully transported under the loading device at a 45° angle as described above. The methodology used for testing was identical to the one used for the unaged panels. Preliminary observations showed slight efflorescence on the surface of the masonry panels and rusting in the crown shaped elements used to block the steel cords around the threaded rods.

The first panel presents a sudden decrease in the shear stress-strain diagram due to the opening of cracks along the horizontal mortar joints (Figs. 3.4.18-19). This specimen reached rupture abruptly, through slipping of two parts of the panel along the horizontal joints which had previously cracked (Figs 3.4.20-21). As in the unaged cement repointed panel, it would appear that the repointed joints, which had previously been subjected to the removal of the original layer of mortar, represent a weakness in reticolatus reinforced panels subjected to diagonal compression. In Table 3.u. the results of the diagonal compression tests on the aged panels are shown, and, with regard to specimen 1, the maximum load reached before failure was over 90000 N, presenting a 19% decrease with respect to the unaged control specimen which also presented a collapse mechanism due to slip.

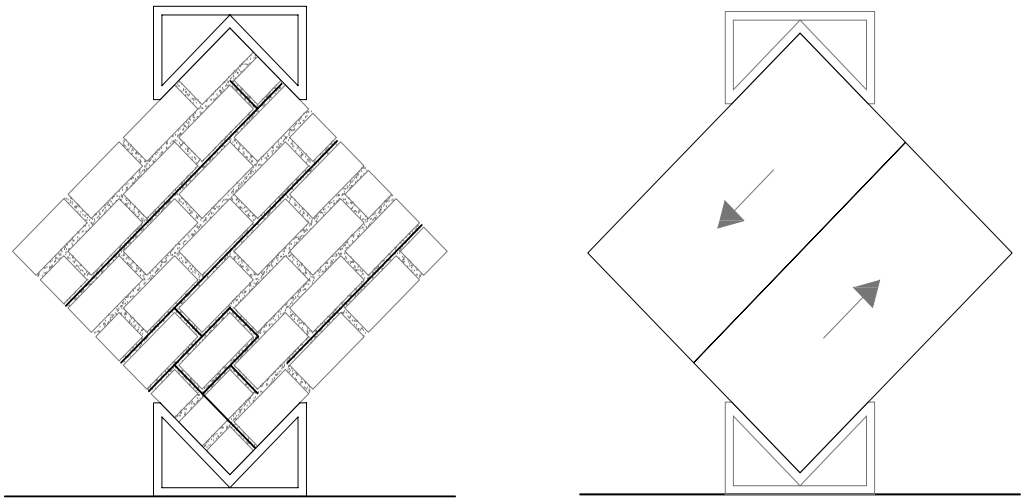

Figures 3.4.18-19. Graphic description of the cracks that occurred in aged specimen 1 instants before failure and collapse mechanism.

Figures 3.4.20-21. Aged specimen 1 after collapse through slipping.

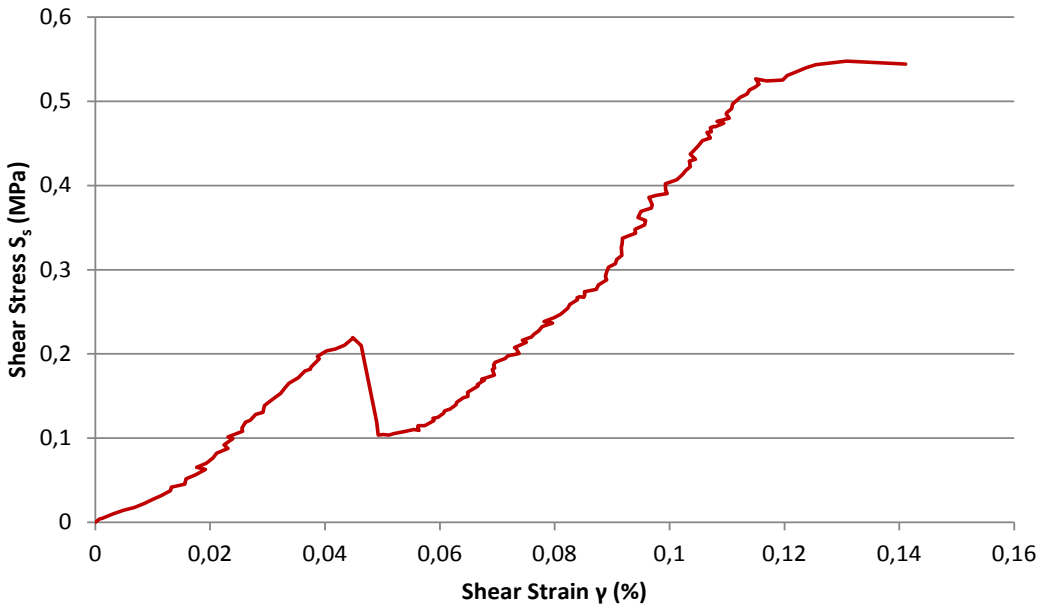

Figure 3.4.22. Shear stress-strain diagram for aged reticolatus reinforced specimen 1.

Aged specimen 2 ruptured more gradually, presenting cracks along the compressed diagonal in a stepwise fashion (Figs. 3.4.23-26). This second panel presents a maximum load of over 170000 N, and a collapse mechanism due to diagonal cracking. In Figure 3.4.27, the stress-strain diagram shows that the panel resists linearly until maximum loading is reached, after which cracking commences and failure occurs. After a strain of 3%, the mechanical strain gauges measuring displacements were removed, thus avoiding damage to these delicate instruments.

In both panels the reticolatus reinforcement remained intact even after specimen 1 collapsed.

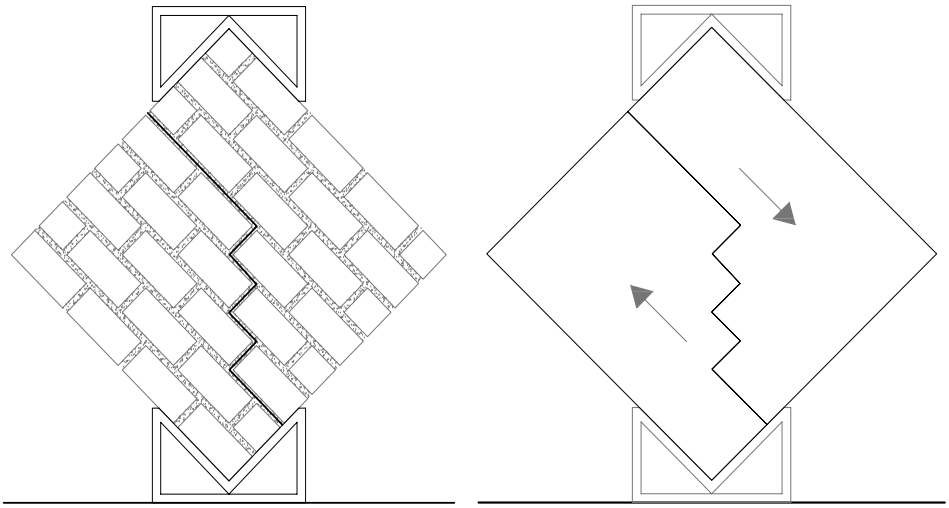

Figures 3.4.23-24. Graphic description of the cracks that occurred in aged specimen 2 at failure and failure.

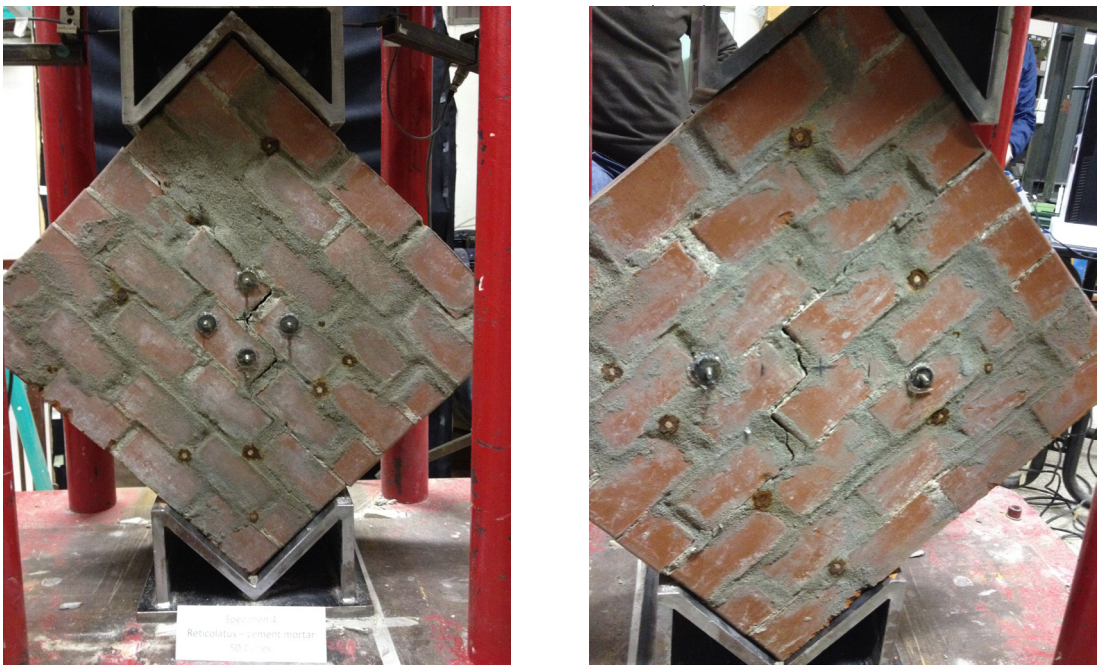

Figures 3.4.25-26. Aged specimen 2 after collapse through diagonal cracking.

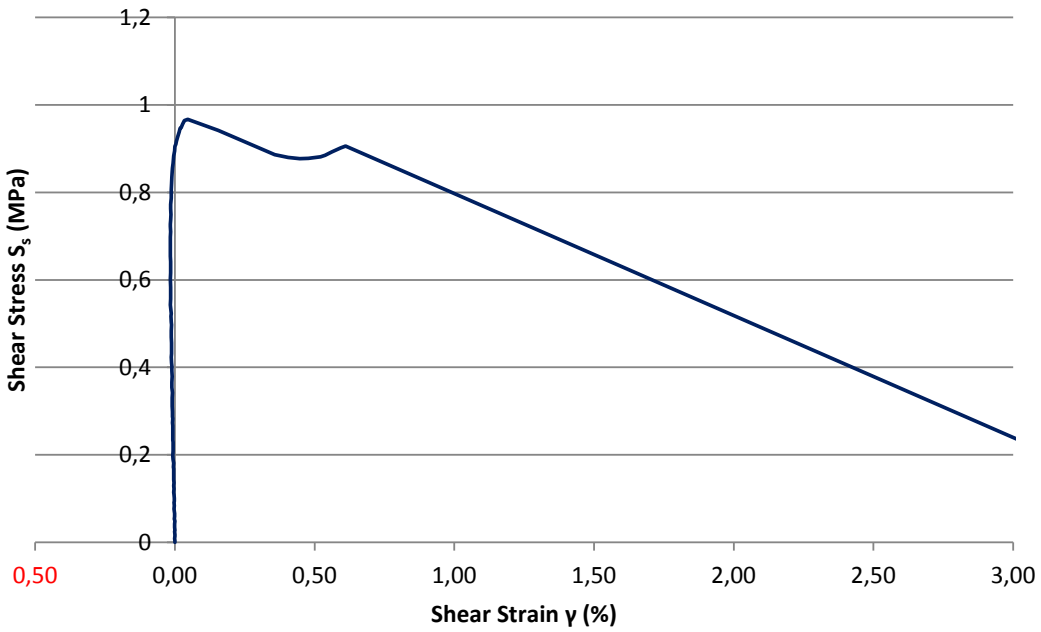

Figure 3.4.27. Shear stress-strain diagram for aged reticolatus reinforced specimen 2.

Conclusions

The elevated scattering of these results confirms the need of a more extensive campaign investigating the durability of reticolatus reinforced masonry. Results are comparable only between the cement mortar repointed panel and aged specimen 1, which both reached failure through a slip mechanism in the mortar joints. The aged masonry panel appears to have a loss of 19% of the ultimate load, but in this specific campaign the results are not averaged with other panels of the same type. The MaltaS repointed panel present results which exceed all the cement reinforced panels, as is to be expected given the values of the mortar itself. However, the excellent load carrying capacity of this mortar constitutes a reason for which it should not be used in the repointing or reticolatus reinforcement of historic masonry. In fact, the behaviour of the panel repointed with MaltaS was that of two rigid blocks, and the mortar is very difficult to remove without damaging the masonry itself.

Future research should include further diagonal compression tests on aged and unaged, unreinforced and reticolatus reinforced, panels in order to gather sufficient data on the durability of this particular reinforcement technique.

Chapter IV. Conclusions

As previously stated in this dissertation, the main objectives of the present work consisted in analysing the behaviour of FRCM systems as both a more compatible and also more effective way of reinforcing historic masonry structures. Compatibility issues arise over time, when the reinforcement has been in place and exposed to the impact of environmental factors. In this perspective, the durability aspect of FRCM reinforcements is an important consideration when designing reinforcements and their maintenance programmes

In a marked difference from the Fibre Reinforced Polymer system, virtually no research has been completed on the question of durability on FRCMs. Hence the original contribution of this work, consisting mainly of four experimental campaigns which analyse the durability of fibres in their cementitious matrices as well as the effects of artificial ageing on FRCMs applied to a masonry substrate.

While state-of the-art research and standards give indications on the procedures to follow when testing the durability of FRPs or FRP reinforced structures, both concrete and masonry, there are no specific indications for FRCM testing. Thus, in the experimental campaigns carried out during the research project, procedures, specimen types and ageing cycles were based on the state-of-the-art research completed on FRP durability.

The first two campaigns were conducted on small, and therefore manageable but most importantly easily repeatable, mortar specimens containing glass, steel or inorganic PBO fibres within their section. The mortar specimens were subjected to freeze/thaw cycles in an environmental chamber, which varied its internal temperature every 6h, from -20° to 50° C. Initially, the traditional curing period of 28 days was followed before testing or ageing cycles commenced. Soon after the first results emerged, it was clear that partial curing had taken place in the environmental chamber itself, producing inconsistent and scattered results. Therefore, tests were repeated on new specimens, assembled in an identical manner to the previous ones, but allowed to cure for a period of 60 days. The results were more congruent in this case, where unaged specimens presented higher resistance values than aged ones. Furthermore, it was noticed that glass and steel reinforced specimens presented a loss of bond adherence, whereas the inorganic mortar specimens presented a yielding of their PBO fibres.

The National Italian Guidelines of 2012, described in *Chapter 1.b. Fibre Reinforced Cementitious Matrix (FRCM). Codes for Design Calculation,* require the FRP specimens to maintain at least

85% of their original strength after thermal cycles, which are defined as a 20 cycle process of 4 h per cycle, at a lower variation of temeratures than those employed here. In the present invesitigation, all the cement mortar specimens, reinforced and unreinforced, displayed resistance losses larger than 15%, as did the unreinforced lime specimens. However, the guidelines did not take into consideration more aggressive environments, which are easily found in Europe, and were better simulated in the campaign descibred above. With these considerations, the differences between aged and unaged specimens were not alarming, contrarily to what is known for FRPs, where the resin matrices are sensitive to temperatures below a certain threshold and higher than the glass transition temperature.

The second campaign on reinforced mortar specimens, prepared in the same manner and with the same fibres and ingredient proportions as in the first campaign, called for wet/dry cycles. The specimens were immersed in a solution of 5% sodium chloride for period of 15 minutes and then allowed to dry in a ventilated oven for 24 h. The time of the wet period was determined through a procedure by which specimens immersed in water were weighed every 60 seconds. Between 12 and 14 minutes the weight of all the specimens ceased to increase in significant percentages, thus indicating saturation, and therefore the duration of the wet cycle was reached. In this campaign, half the aged specimens were allowed a recovery period, in which they were kept in the ventilated oven until their weight reached a plateau.

This drying period allows for the following conclusions: the evident decrease of flexural values as noted in the results of the specimens when tested wet, is completely recovered in most specimens after an adequate drying period, if not altogether surpassed in some.. Therefore, the effects of the immersion in sodium chloride, including bond loss in glass and steel reinforced specimens, are not long lasting on FRCM systems. However, the loss of section noted in the lime mortar specimens, along with the rusting of the steel fibres, require a proper maintenance programme to be in place, which includes the possibility of the replacement of the degraded cementitious matrix, in order to ensure the correct functioning of the reinforcement system.

The third experimental campaign carried out for the present dissertation focusses on the behaviour of FRCM systems subjected to artificial ageing when applied to a masonry substrate. In some cases of FRP durability testing, after artificial environmental exposure, specimens presented mould and dangerous concentrations of saline efflorescence in the interface between reinforcement and substrate. This problem became the incentive for the campaign on masonry pilasters, reinforced

along their façades with glass or lime reinforced lime or cement mortar matrix, and subjected to 75 wet/dry cycles in a 5% sodium chloride solution.

In this case, given the volume of the specimens, the wet cycle lasted 45 minutes while the dry cycle was kept at 24h, as in the previous wet/dry campaign. The reinforcement was simply applied to the pilasters without proper anchoring, since the purpose of the investigation was to verify whether differences existed in the behaviour of aged with respect to unaged specimens, and not the ultimate load carrying capacity of the reinforced pilasters. Differences between reinforced and unreinforced pilasters, in fact, subsist only in the collapse mode: the unreinforced pilasters collapse gradually, with evident tensile stresses in one case, while the reinforced pilasters collapsed abruptly, as soon as the reinforcement starts to detach from the surface of the masonry substrate, and no tensile cracks appear on the pilasters. After the ageing cycles were complete, neither dangerous concentrations of saline efflorescence nor mould were not found in any of the interfaces, and the rust due to the steel fibres remained mostly on the surface of the FRCM system. Furthermore, the ultimate load carrying capacity did not vary significantly between aged and unaged specimens. It was therefore concluded that FRCM reinforced masonry was not affected by wet/dry cycles regarding strength and resistance. Even so, the superficial degradation of the matrices must be avoided through a detailed maintenance programme.

The fourth experimental campaign investigated the durability of a new application of FRCM systems consisting in the reticolatus technique. Four larger masonry panels were assembled and reinforced by means of the reticolatus technique, three of which were repointed with an inorganic mortar provided by Ruredil, MaltaS, and three with a hand mixed cement mortar. Two cement repointed panels were subjected to 50 wet/dry cycles. The wet period lasted for 5 h in a 3% sodium chloride solution, while the dry period was established at 48 h. In this case, given the limited amount of specimens upon which the investigation was based, the scattering of results was quite evident, confirming the need for more extensive testing.

Once again, the comparison of the results of the last three experimental campaigns with the 2012 guidelines is arduous, as the requirements listed in this document state that a total of 1000 h of immersion in saline solutions are necessary for this type of durability testing. The wet/dry campaign on mortar specimens presented cyclic immersion periods which amounted to 25h in the case of specimens subjected to 100 cycles the pilasters in the third campaign were immersed for a total of 112.5 h, while the masonry panels summed up a total of 250h of immersion. The greatest differen-

ces, which exceeded the 15% decrease of resistance allowed in the guidelines for aged specimens, were found in the mortar specimens when tested wet. Otherwise, aged specimens all maintained an 85% of their unaged equivalents.

In sum, this work has investigated the durability of FRCM systems with altogether positive results. The cementitious matrices are not only a more compatible solution for fibre reinforcements in historical masonry buildings, but also appear less affected by environmental conditions than their resin matrix equivalents. Although the experimental campaigns carried out in the present work are to be considered merely a beginning in the much needed research on FRCM durability, the results achieved here provide an encouraging point of departure for future research and regulations.

Appendix I. Preliminary Proposal for Numerical Analysis Applied to Reticolatus

The following segment has been designated as an appendix, due to the nature of the proposed approach illustrated therein, which is numerical in contrast to the experimental focus of the main corpus of the dissertation. Furthermore, it is, as suggested in the title, a preliminary proposal of a possible numerical method, which may be used to determine the resistance of brick masonry structures reinforced through the reticolatus technique, explored both in the state of the art research and in the experimental investigations of the main body of the thesis. Unsurprisingly, as first attempts not tried previously, the results obtained emphasize the need for a more detailed calibration and cannot be confirmed with certainty until larger experimental campaigns have been dedicated to the abovementioned reinforcement typology. Therefore, given the tentative nature of the calculations, this section has not been incorporated into the general body of the present work.

1. A Proposed Technique

The choice of the numerical model in the case of reinforced or consolidated masonry structures with the "Reticolatus" technique is generally delegated to the expert, who may opt for the procedure considered most pertinent, assuming however the hypothesis of a transversal plane section. In fact, a structure reinforced with this technique presents itself as a reinforced masonry (Paradiso et al. 2008), in which the metal mesh ties and bonds the blocks of stone and brick, making the masonry section more compact and monolithic owing to the insertion of transversal elements which clutch the mesh.

For the analysis of masonry panels with the reticolatus technique a non-linear numerical method has been proposed (Paradiso et al., 2013), which implements the non-linearity of the material in an iterative numerical procedure which corrects the elastic-linear solution after having evaluated it, step by step, thus pursuing the final goal of respecting congruence.

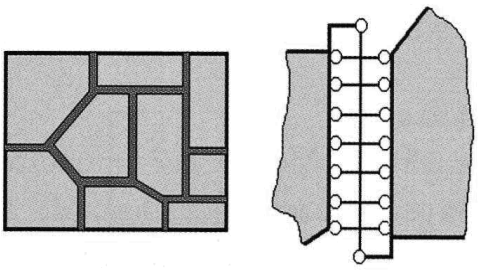

Figure 4.1.1. Modeling of the mortar joint in a discrete form.

The numerical procedure illustrated here is applied to a model of the structure in masonry, constituted by rigid blocks interconnected to each other and to the ground through mortar joints which are elastically deformable. This fact implies that all of the elasticity or deformability of the system is concentrated in its joints.

Every mortar joint is represented in discrete form as a

curtain of trusses positioned perpendicularly to the interface of the block and one truss placed in a tangential direction (Franciosi, 1986; Fig. 4.1.1). The trusses perpendicular to the interface of the blocks are able to transmit only compressive strength and therefore the deformations are comparable to elastic cushions interposed between the masonry blocks. When, instead, tensile strength occurs exceeding a certain predetermined limit, the trusses break, thereby simulating the opening of a crack. For every broken truss it is also possible to measure the width of the crack, whereas the number of broken trusses in a determined interface permits the measurement of its depth. The tangential truss transmits tensile strength, whichever its sign (Galassi et al., 2004).

In this sense and with these hypotheses, the proposed numerical procedure presents itself as a unilateral constraint problem.

The reinforcement is constituted by a mesh made by a steel wire of limited section (c.a 1 mm) in such a way that it can pass through the scraped mortar joints and the clutch in the steel bars inserted in the panel. Since the section of the wire is limited it can sustain only tensile strength. For this reason, the reinforcement is modeled as a sequence of trusses connected to each other and fixed at the ends on the nodes that in reality consist of bars and clutches but in the model are strategic points of the structure positioned at the joints and considered a part of a masonry block, chosen according to the inclination of the sides of the polygon which simulates the wire of the mesh (Tempesta et al., 2011). In brief, if the sides of the polygon which constitutes the wire of the mesh form an acute angle, and therefore converge towards a block of stone or brick, the application point of the two sides, in common with the two, is assumed belonging to the block on which they converge. To wit, if two consecutive reinforcement trusses form an acute angle in correspondence of their point in common, this point is to be assumed as belonging to the block of masonry towards which the angle converges. In Figure 4.1.2 there is an example of this, where the capital letters indicate the nodes and the same letters in lower-case indicate the blocks on which the points are considered to be applied to.

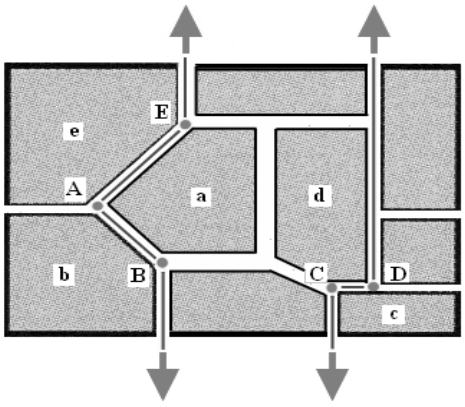

Figure 4.1.2. Model of the wire of the mesh, identification of the nodes at the end and the block to which they belong.

The exact identification of the blocks to which the end nodes of the trusses belong is an essential operation for composing the equilibrium equations of the structure. In fact, the wire-trusses are in-

terpreted by the model as additional internal constraints connected to themselves and to the blocks of the structure relative to which the equilibrium equations are composed.

The numeric procedure, implemented in the code BrickWORK produced by scientific research, can be explicated as follows.

Considering a generic masonry structure built with a certain arrangement of elements composed with or without mortar joints, the system, constituted by n blocks and m interfaces subjected to a certain load condition [F], can be described in static and cinematic term as follows:

$$\begin{cases} AX + F = 0 \\ A^T x + KX = \overline{\delta} \end{cases} \quad \text{sub} \quad \begin{cases} X_n \leq 0 \\ X_r \geq 0 \\ \overline{\delta} \geq 0 \end{cases} \tag{1}$$

In equation (1) the two sub vectors $[X_n]$ and $[X_r]$ contain the unknown $[X]$ of iteration associated respectively with the components in a perpendicular direction to the mortar joint and to the axial forces present in the wire of the mesh, to which the inequalities that are imposed for congruence with the assumed hypothesis for the constitutive model of the joint and the reinforcement correspond; the vector $[x]$ contains the unknown components of the movements of the center of mass of the elements. $[K]$ indicates the matrix of deformability associated with the trusses which represent the elastic mortar joint and the additional reinforcement trusses. The proposed algorithm refers directly to impressed distortions, recalling Colonnetti's theorem, according to which a state of tension can be varied advantageously introducing distortions in a number equal to the degree of static indeterminacy of the system. The distortions vector, expressed as $\overline{\delta} = \overline{\delta}_1 + \overline{\delta}_2$, with the sub vector $[\overline{\delta}_1]$ must obliterate the tensions of a non-compatible sign, i.e. tensile strength in the mortar trusses and compressive strength in the reinforcement trusses, whereas with the sub vector $[\overline{\delta}_2]$ must modify only certain movement components to reinstate the equilibrium of the structure and the congruence of the elastic deformations while respecting the sign conditions on the variables $[X_n]$ and $[X_r]$. The non-null components of the sub vector $[\overline{\delta}_2]$ give the position and the depth of the cracks in the mortar joints.

The solution (X, x) and the vector $[\overline{\delta}]$ of the distortions are determined through an iterative procedure where the first step is the solution, obtained as a standard solution, considering the material as elastic, linear and bilateral:

$$X_0 = K^{-1} A^T (A K^{-1} A^T)^{-1} \cdot F \tag{2}$$

For every compatible system of the type $Ax = b$ the complete system of solutions is given by $x = A^{\otimes}b + (I - A^{\otimes}A)y$, where y is an arbitrary appropriate vector chosen while $A^{\otimes}$ is any inverse matrix that satisfies the equation $AA^{\otimes}A = A$, and the final solution has the general form: $X = X_0 + X_n$. In this case we have:

$$X_N = (I - K^{-1}A^T(AK^{-1}A^T)^{-1}A)\cdot\overline{\delta_1} = C\cdot\overline{\delta_1} \tag{3}$$

The vector $[X_0]$ of the initial solution can result to be compatible with the conditions of sign respecting the inequalities expressed in (1): this case corresponds to that particular case in which the masonry structure, with regard to a fixed condition of external actions, presents all compressed joints and the wire of the mesh subjected to tensile strength or at most null. In the case in which some components of the vector $[X_0]$ do not satisfy the imposed conditions, this vector is modified according to an iterative process in which the choice of the appropriate components of the vector $[\overline{\delta}_1]$ follows the criteria, at every step, of the search of the mortar truss where the maximum tensile strength is present, conserving at every step, in the vectors, the values assumed beforehand. Subsequently the reinforcement trusses are checked and the truss that has the maximum value of compression is rendered null. The trusses are then checked again (Galassi et al., 2008). It is important to remember, as has been observed previously recalling Colonnetti's Theorem that the maximum number of steps is equal to the degree of static indeterminacy of the structure: this fact is sufficient for a criterion of convergence. If convergence has not been reached within the maximum number of steps conceded, it is possible to assert that a state of equilibrium which satisfies the assumed hypothesis for the constitutive materials (masonry, steel) and depending on the external actions does not exist.

To update the components of the distortion vector, the relation $\overline{\delta}_{1i} = -C_i^{-1}X_{0i}$ is used at every step, where X_{0i} $(0 \le i \le g_{iper})$ indicates the vector in which the components correspond the internal reactions of the joints, unacceptable for sign with respect to the conditions in (1).

The final solution of the procedure in terms of equilibrium will provide a solution vector that will be $X_n \le 0$ in the mortar joints and $X_r \ge 0$ in the reinforcement.

The non-null components of the solution vector $[X_n]$ correspond to those parts of the mortar joint which still present mutual contact. Contrarily, the null values identify those sections in which the contact is no longer active. Instead, the non-null components of the vector $[X_r]$ correspond to those parts of the reinforcement wire which are functioning. Furthermore, since the final vector $[X]$ is

generally different from the initial vector $[X_0]$, elastic-cinematic congruence must be restored in the second equation of (2), considering the presence of actual detachments between interfaces. The reconstruction of compatibility is easily obtained by operating on a sub-partition of the matrices associated with the system of elastic-cinematic equations, taking into consideration only the indexes relative to the trusses whose components normal to the interface results acceptable in the iterative process just concluded. In this case, the movement vectors of the centers of mass of the blocks (Penrose, 1955), which corresponds to the effective reactive structure, and the vector $[\bar{\delta}_2]$ capable of reinstating the compatibility of the system are obtained with the following relations:

$$\bar{x} = -(A_c A_c^T)^{-1} A_c K_c X_c \tag{4}$$

$$\overline{\delta_2} = A_i^T \bar{x} \tag{5}$$

Where the non-null components of the vector $[\bar{\delta}_2]$ provide the position and the depth of the cracks.

2. The FEM model

A valid alternative to the numeric procedure described above is provided by the representation of the masonry structure, reinforced or not, through commercial calculus codes which use finite elements method. From the point of view of a structural designer, FEM modeling is a short cut for obtaining valid results for the design of reinforcement systems, but it requires particular attention during the processing phase of the structure. The calculus phase, in effect, must be appropriately guided by the user-expert of the FEM code.

In order to be able to describe the masonry structure under the hypothesis stated above (rigid blocks of masonry and elastically deformable mortar joints represented as unilateral normal trusses and bilateral tangential trusses), what is proposed here is the modeling of masonry blocks (stone and/or brick) representing only the contour using RIGID LINK elements, in a quantity at least equal to the number of sides of every block. Since a block of masonry represented by means of these kinds of finite elements is weightless, the next step is to identify the center of mass where a load may be applied which simulates the total weight of the block. The identification of this point of the blocks occurs with the definition of additional RIGID LINK element inside the blocks, and their intersection provides the coordinates of the node which simulates the centre of mass (Fig. 4.2.1).

After having described the blocks and their loads, the mortar joints must be defined. Once the number k of trusses perpendicular to the interface in which the joint will be divided has been decided, each joint which connects a generic block i with a generic block j must be divided in RIGID LINKS which define the contour of the two blocks corresponding with the joint in (*k-1*) parts (that is, RIGID LINKS) in order to subsequently identify (*k-1*) nodes on block *i* and (*k-1*) nodes on block *j*. These nodes are the end points of the perpendicular trusses of the mortar joints, which can now be defined with BEAM type finite elements that are imposed to work as TRUSS. The additional trusses in tangential direction in the joint are again defined as TRUSS and their end points are obtained by the construction of rigid connections (RIGID LINK elements) in every *k* joint, connecting block *i* with block *j*. Using the same strategy of the rigid connection and considering what has been said about the modeling of the reinforcement with a sequence of trusses positioned in series in the joints and connected to one another and to the blocks of the structure following the criteria of junctures mentioned above, the connection points of the wire of the mesh to the block of the structure can be defined. BEAM elements will be positioned in such a way that simulates the steel wire across these points, which are the characteristic nodes in the FEM model.

At the end of the pre-process phase, the solver is launched in linear static analysis, which will provide the standard solution represented by the vector $[X_0]$ in the program procedure mentioned above. If this solution of the structure results compatible with the mechanical characteristics of the materials constituting the structure (masonry, steel), maintaining that the masonry is all subjected

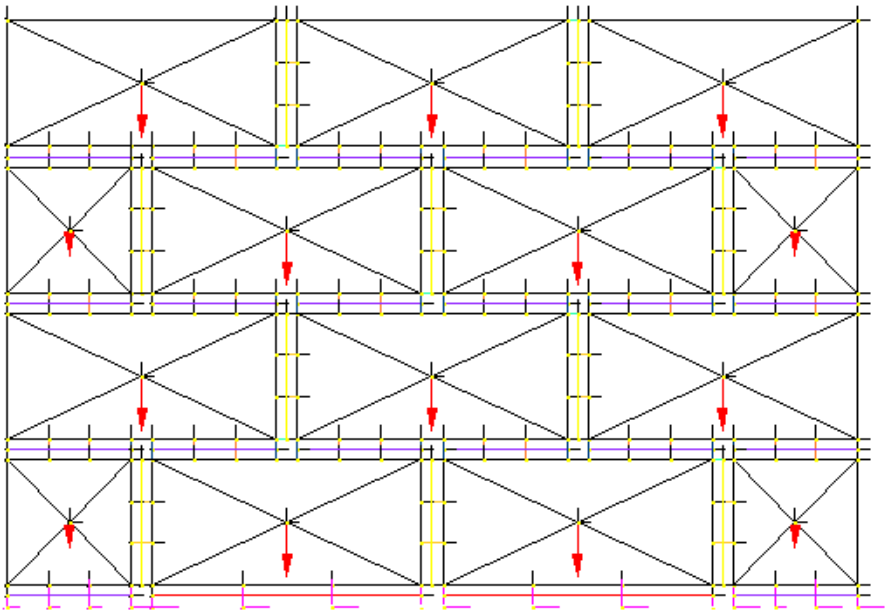

Figure 4.2.1. FEM model of a panel built with rectangular blocks. The intersection of the internal RIGID LINKS provides a node to attribute the specific weight of the blocks.

to compressive strength whereas the reinforcement is subjected only to tensile strength, then it may be accepted as an equilibrated and compatible solution.

If instead the standard solution were to highlight tensile strength in the mortar joints or compression in the wire, the structure must be recalculated eliminating the trusses whose tension is unacceptable. The structure must be calculated various times, until the result is an equilibrated and compatible solution or until the rigidity matrix is unique. In this case, the structure is to be considered unstable since it has lost all of the degrees of static indeterminacy and has been rendered unstable.

In detail, the calculation iteration will be performed various times as follows:

1. If the standard solution shows trusses subjected to tensile strength pass to 2. or 3;
2. Examine all the trusses subjected to tensile strength (from higher to lower values), eliminating these trusses one by one and calculating the structure at every step;
3. If there are Reticolatus trusses subjected to compressive strength pass to 4. or 6;
4. Eliminate the truss subjected to compressive strength and then recalculate.
5. Back to point 1;
6. END.

For clarity, the iterative model is represented in the flow chart illustrated in Figure 4.2.6.

This algorithm derives from considerations on the mechanical behaviour of a masonry panel reinforced with reticolatus. The principle is the containment of masonry elements in “cages” so to activate mechanisms capable of resisting to Morsch. It is a reinforced masonry system in which the compressive strength is absorbed by the masonry and the tensile strength is absorbed by the steel wires of the mesh (Figs. 4.2.2-3.).

Three model panels were calculated with the iteration model proposed above, with random positioning of the reinforcement wire, in order to check the method of the analysis. These models do not suggest how the reinforcement is to be placed on the structure, but represent merely a test run for the numerical method. All model panels were subjected to a diagonal compression impressed only on the upper right corner and then tested. The same panels tested by the program without reinforcement presented maximum resistance at about one third the values tested for the reinforced panels, after which the testing was interrupted. This goes beyond the 100% increment in resistance found in experimental campaigns. In the iterative process, model panel 2 was left with only one reticolatus truss subjected solely to tensile strength while all the other trusses were eliminated

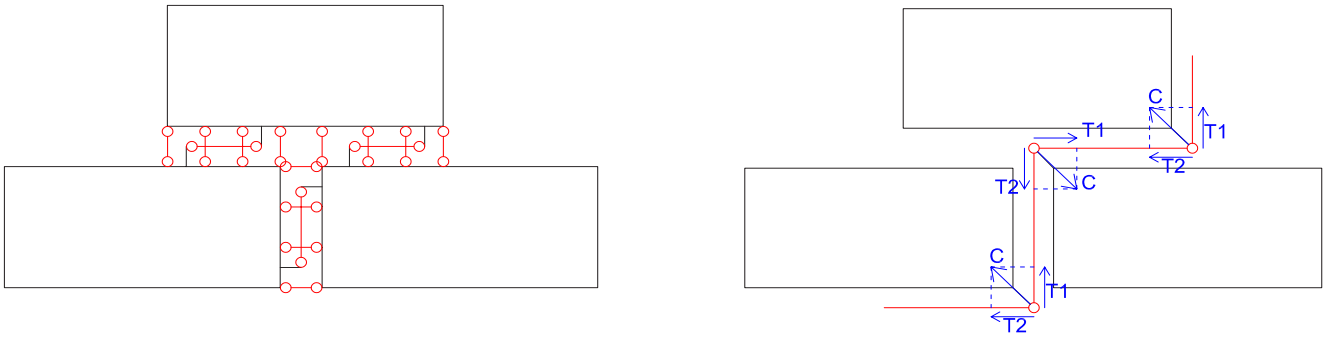

a) b)

Figures 4.2.2-3. Schematic representation of the BEAM elements for a) mortar joints and b) the reticolatus reinforcement.

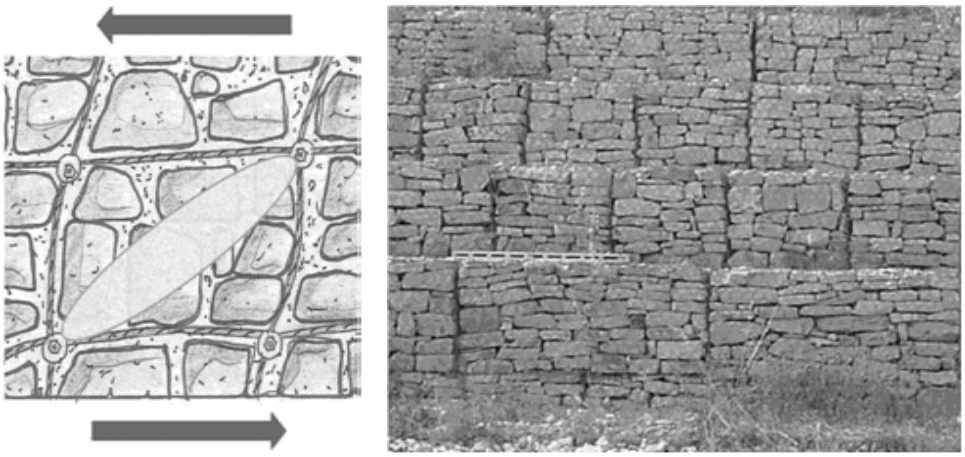

Figures 4.2.4-5. Morsch-type resistant mechanisms and gabions for retaining walls. Images taken from Paradiso et al. (2013).

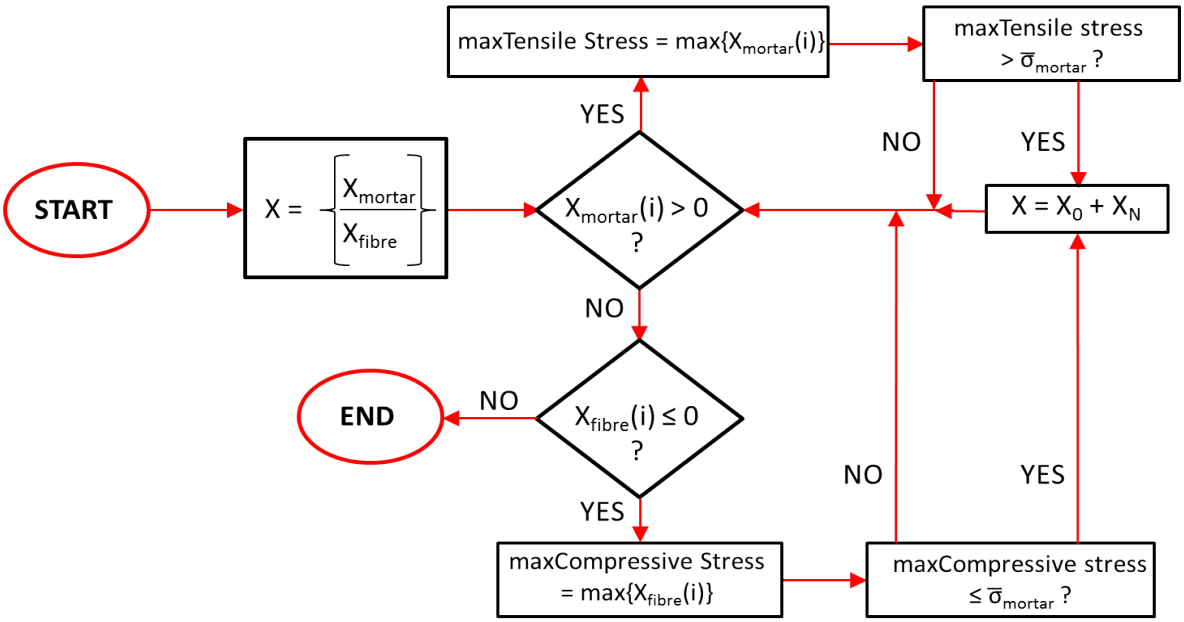

Figure 4.2.6. Flow chart of the iterative model used for the calculation of masonry structures reinforced through the Reticolatus technique.

during calculation and model panel 3 also “lost” a number of trusses due to the fact that they were subjected to compressive strength. Only model panel 1 maintained all of its reinforcement trusses subjected to tensile strength throughout the entire step by step process (Fig. 4.2.7.), thereby proving that all the steel trusses remained subjected to tensile strength.

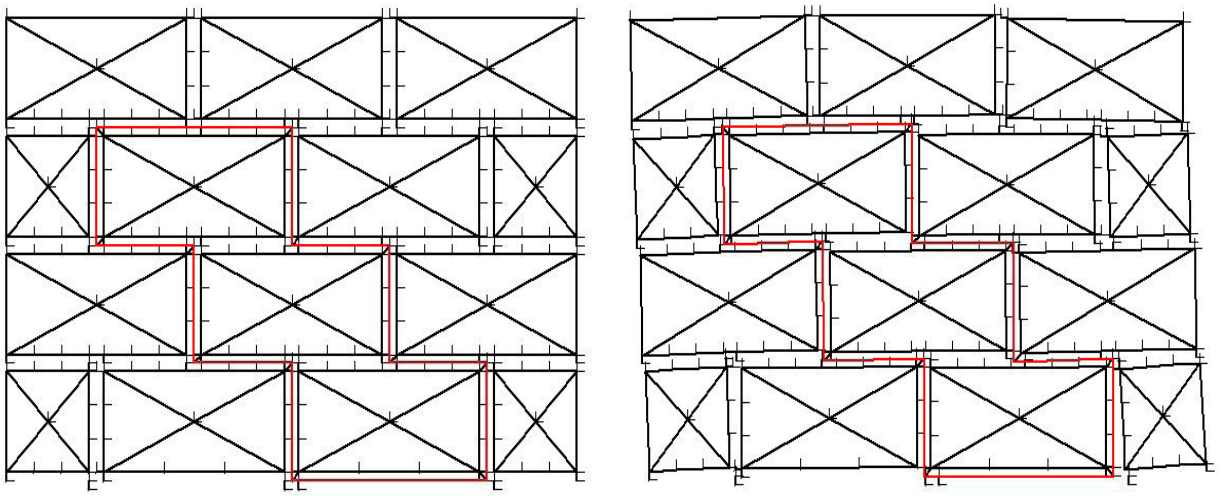

1a and 1b.

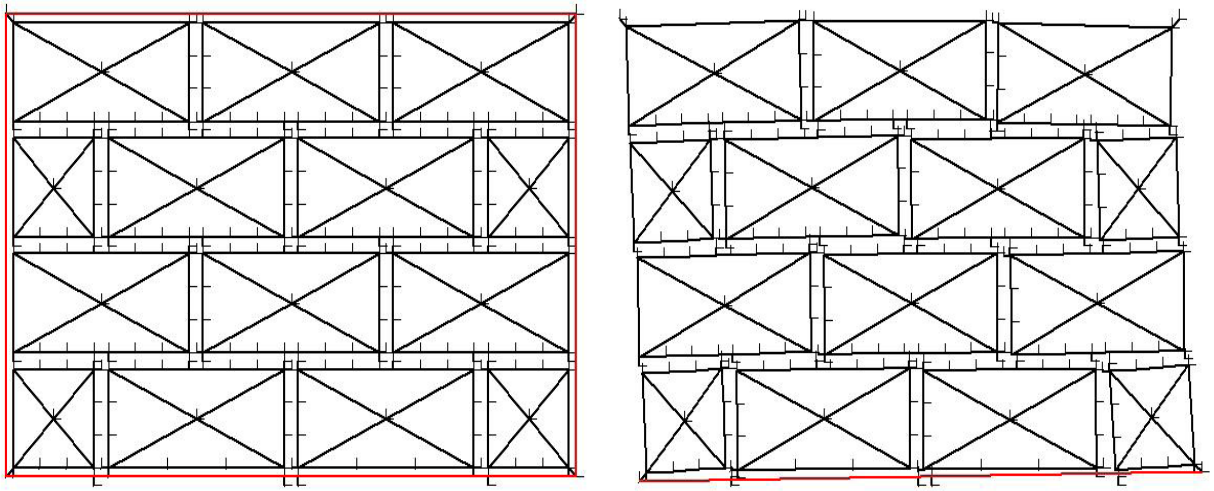

2a and 2b.

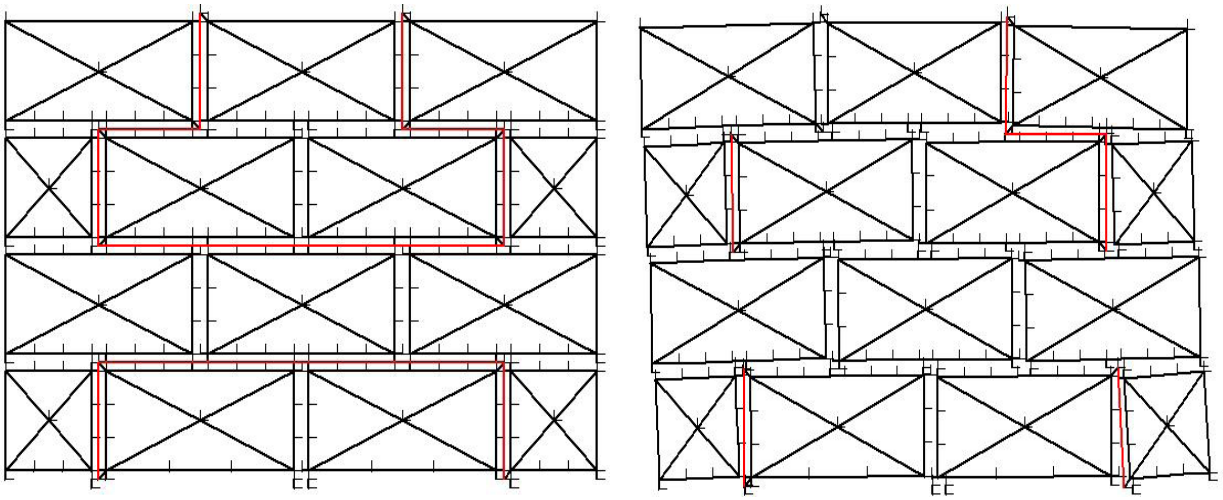

3a and 3b.

Figure 4.2.7. The three model panels with reinforcements before(a) and after FEM processing (b).

Once the test model panels proved the validity of the iteration model, the next step was to compare the results obtained through experimental testing with the calculation method. This is a first step towards understanding how close the processed results converge towards experimental data. Hopefully after a certain number of parallel assessments between experimentation and numerical analysis this method can be useful to the professionals who wish to reinforce or repair their structures with the reticolatus method.

For a first comparison between experimental and numerical analysis, the fourth experimental campaign described above (*Chapter III.4. Wet/Dry Durability on Brick Masonry Panels Reinforced through the Reticolatus Method*) was chosen. A second comparison was carried out on the masonry panels reinforced with Reticolatus and tested by Prof. A. Borri's research team at a Laboratory in Udine, in the Friuli Venezia Giulia region of Italy (see *Chapter I.c. Reticolatus*). Both cases were chosen for their similarity with the test models and accessibility to the test results and data, in addition to the primary factor they presented, which consisted in their being reinforced with the reticolatus technique.

3. Case Study: Reticolatus Reinforced Panels illustrated in Chapter III.4

As described in *Chapter III.4*, the panels used for the experimentation were 51x51 cm in size, with all bricks laid as headers. In the experimental program illustrated above, all four panels were reinforced with the reticolatus technique, two of which were tested in laboratory conditions and two after 50 wet/dry cycles in sodium chloride solution at 3%. In the case study analysed here, the results pertaining to the one panel repointed with cement mortar and tested at laboratory conditions will be used as a comparative value to the values obtained through the iterative model described in the present Chapter.

Given the nature of the testing device used during the experimental campaign, that is diagonal compression, the model input for calculation was one vertical and one horizontal compression force applied to the upper right corner of the masonry panel, representing the decomposition of the experimental compression force, at a 45° angle with respect to the upper right corner of the panel (Fig. 4.3.1.) The first calculations carried out by the iteration process were completed on unreinforced panels. Although there were no experimental values to compare with these calculations, the intent was, ultimately, to verify once again the correct functioning of the method. The

panel was subjected to loading by increments; as unreinforced panels turned out equilibrated with a compatible solution after iterations eliminated all mortar trusses subjected to tensile strength, the load was increased. For example, if calculation on a structure subjected to a vertical and a

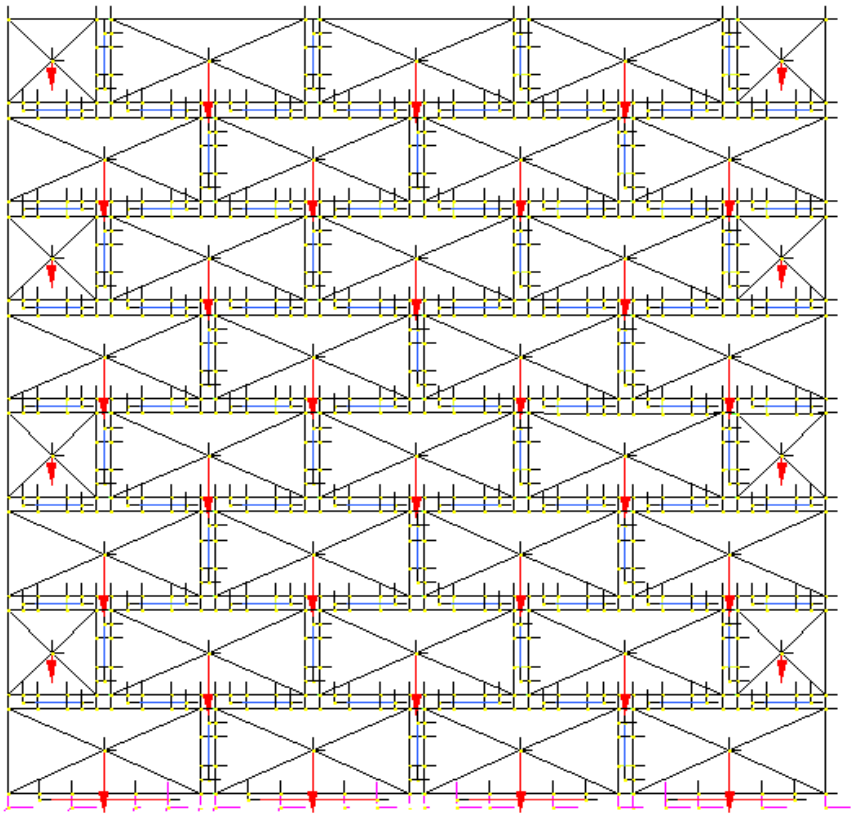

Figure 4.3.1. FEM model of the panel without reticolatus.

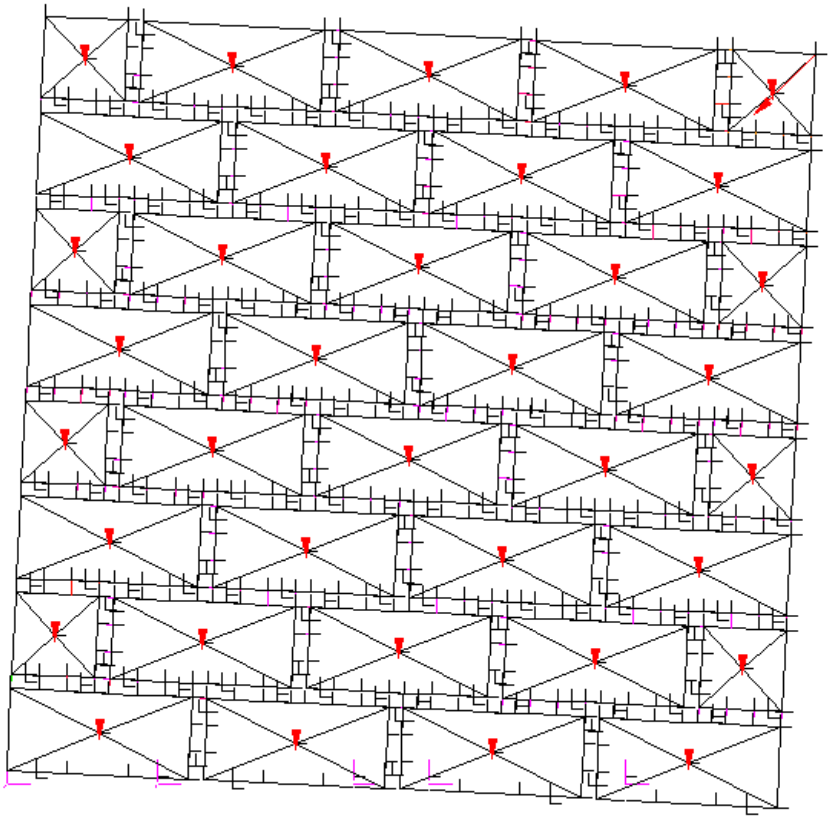

Figure 4.3.2. FEM model of the panel without reticolatus after the iteration process at ultimate strength condition.

Panel Type		Average Experimental Ultimate Strength (N)	FEM Model Ultimate Strength (N)	Increment
51x51cm	Unreinforced panel	---	104280	
	Reinforced panel	122041	122000	17%

Table 4.a. Experimental and numerical ultimate strength values for unreinforced and reinforced panels.

horizontal force of 5000 kg remained in equilibrium after all iterations were complete, the next calculation that was carried out applied a vertical and a horizontal force of 6000 kg. Likewise, when unreinforced panels' rigidity matrix was unique and therefore the structure was unstable, loading was diminished (i.e., from 8000 to 7000 kg). Calculations continued until the very first load condition which gave a unique rigidity matrix was found, indicating the ultimate strength of the unreinforced panel, indicated in Table 4.a. The eliminated mortar trusses simulate the opening of cracks in the mortar layers of the physical panel. Figure 4.3.3 shows a representation of the

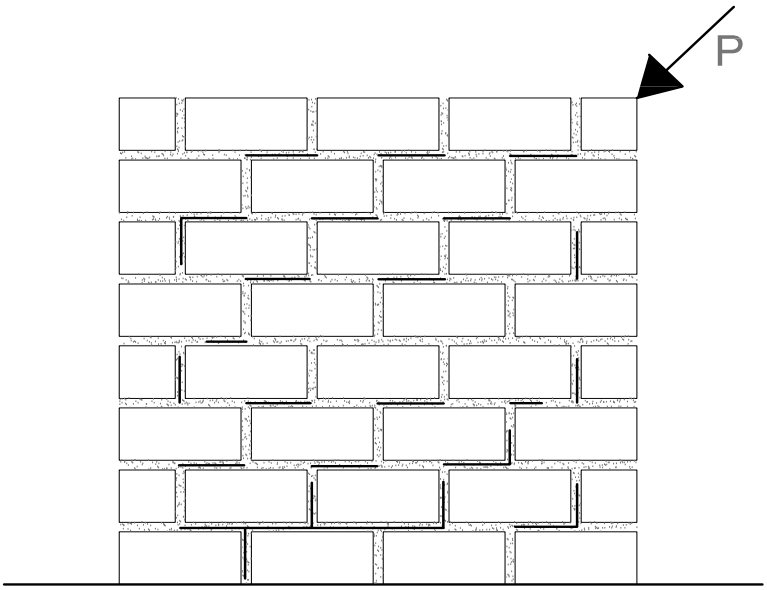

Figure 4.3.3. Representation of the missing mortar trusses at ultimate strength on the unreinforced panel.

cracks, or the eliminated trusses, visible in the last step of the iteration process. The cracks do not exactly follow the usual stepping commonly found in diagonal compression, as many of the vertical cracks do not appear at ultimate load condition but a pattern coherent with cracks which appear in physical structures may be seen.

The same trial and error process was used to find the ultimate strength of the reinforced panels (Figs. 4.3.4-5). The reinforced model panel found its ultimate strength almost at the exact value of the physical panel tested experimentally (Table 4.a). This is not usually the case; numerical values are often more elevated than experimental values since the numerical model is perfect whilst

physical models present imperfections, even if practically undetectable. Numerical procedures are also free from defects, whereas experimental testing presents many variables given by the surrounding conditions. In this specific case, an explanation for why experimental and numerical values are so very similar to each other may be found in the fact that only one masonry panel was

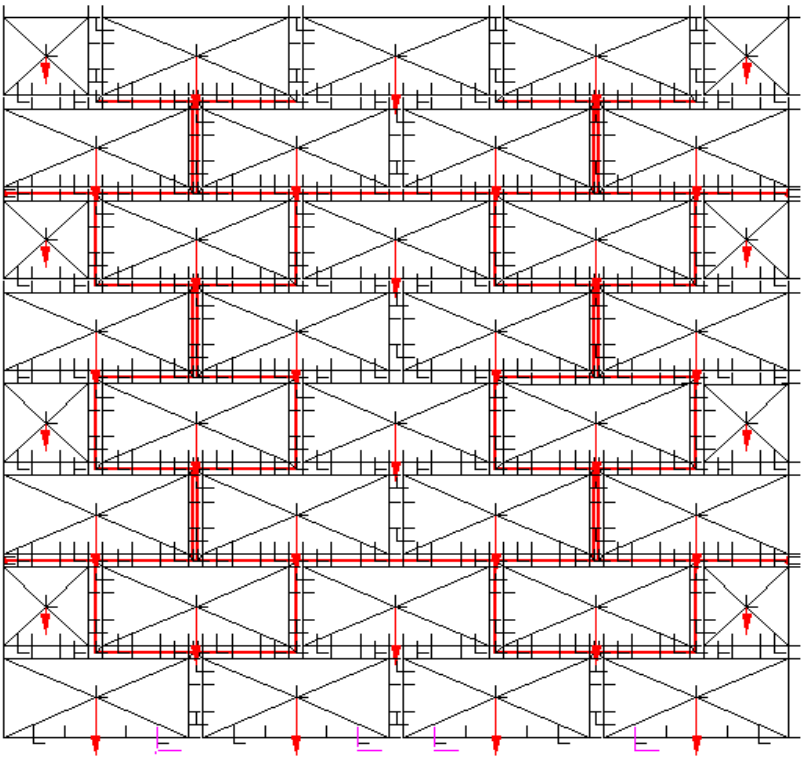

Figure 4.3.4. FEM model of the panel with reticolatus.

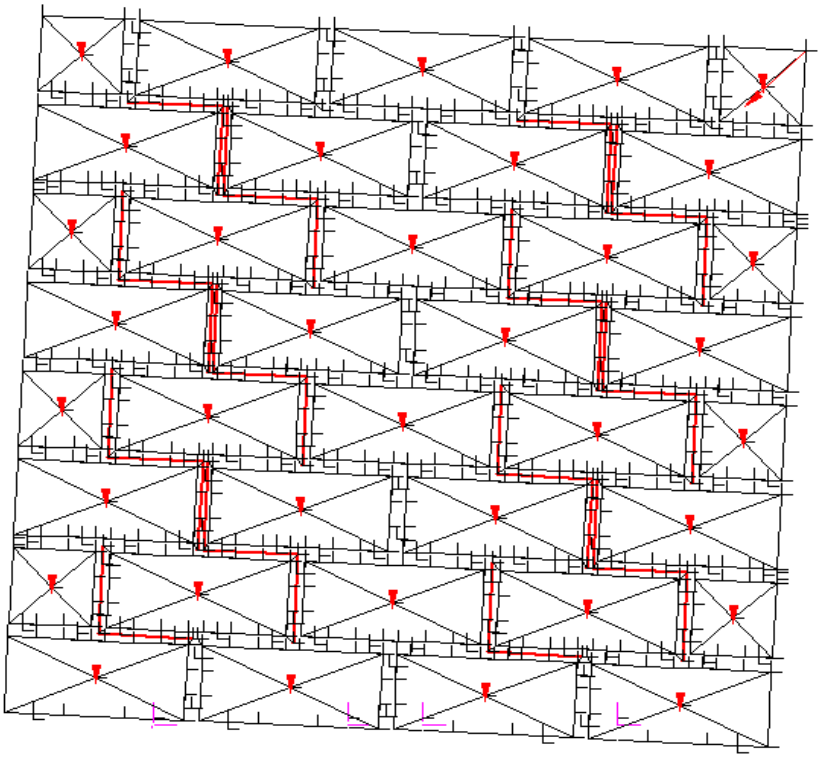

Figure 4.3.5. FEM model of the panel with reticolatus after the iteration process at ultimate strength condition.

tested, therefore there are no other specimens to confront or with which to average its ultimate strength value. The tested panel could have presented particularly high values for various reasons, one of which could be compression values of the hand mixed mortar higher than those inserted in the numerical analysis. Nevertheless, the validity of the numerical method was again confirmed as the ultimate strength of the reinforced panel presented a 17% increment with respect to the unreinforced panel. In Figures 4.3.4-5. the FEM model is shown before and after reaching its break load. In Figure 4.3.6, a representation of the cracks given by the missing mortar trusses in the last step of the iteration process is shown: interestingly, the structure becomes unstable before the iteration process of the elimination of the mortar trusses subjected to tensile strength is complete, leaving the reticolatus trusses intact. The method used in this chapter proceeds according to a specific order by which all the mortar trusses subjected to tensile strength are eliminated before the elimination of the reinforcement trusses subjected to compression. The reason for this choice is base on the assumption that the structure calls upon the aid of the reinforcements once it is subjected to loads it cannot bear on its own. In the steps previous to the ultimate load, the numerical model was in equilibrium after the elimination of all mortar trusses subjected to tensile strength and some reinforcement trusses subjected to compression, namely the two longer cords which run horizontally across the façade of the panel. In the case of the ultimate strength in the numerical model calculated here, it is the mortar that renders the structure unstable.

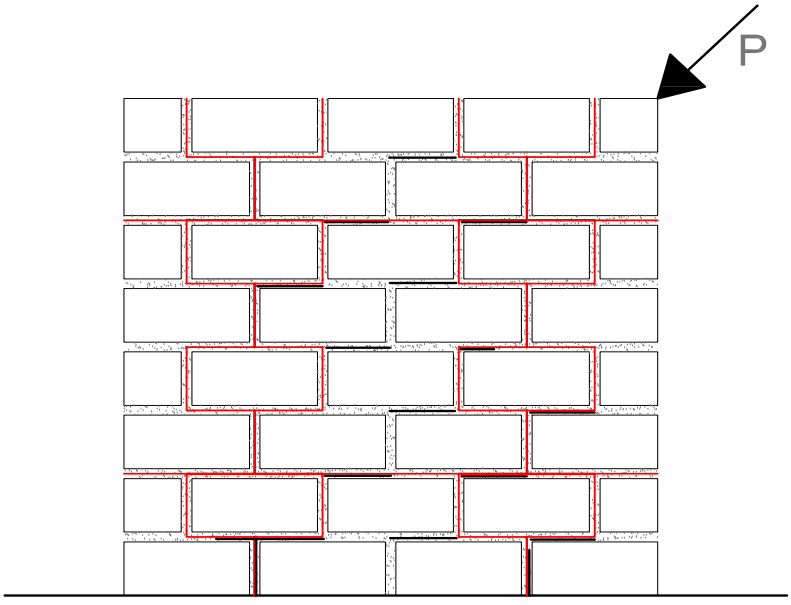

Figure 4.3.6. Representation of the missing mortar trusses at ultimate strength on the reinforced panel.

4. Case Study: Reticolatus Reinforced Panels tested at a Laboratory in Udine, Italy

This second case study that proposed to confirm the validity of the method under consideration was carried out on the masonry panels described in *Chapter 1.c. Reticolatus*. These panels were built to be 120x120 cm (±2 cm) in size, as ASTM standards require for diagonal compression testing (Figs. 1.3.4 and 1.3.6). The panels were tested at a certified testing Laboratory in Udine, Italy, for a total of two unreinforced panels and five reinforced with glass fibre reinforced plaster on one side, and reticolatus on the other (Borri et al., 2013). The average results of the unreinforced and reinforced panels are listed in Table 4.b. As in the case study previously examined, the model for the numerical analysis was constructed with RIGID LINK elements simulating the bricks, and a point force corresponding to the self weight of a standard brick was applied to their geometric centre of mass. The mortar joints were again modeled through beam elements (capable of working as trusses, so as to transfer only axial forces between elements, both normal and shear), and the input for loading was determined by two external forces, in the upper right corner of the masonry panel, one vertical and one horizontal, so that the resultant force was at a 45° angle. The iterative analysis was first conducted on the unreinforced model of the panel. Surprisingly, the model panel seemed to present an infinite load carrying capacity, since after applying almost four times its experimental ultimate strength value collapse, or instability, never occurred. In fact, at 420000 N the panel resulted stable notwithstanding this huge load, and at that point calculations were interrupted given that the value largely exceeded the experimental result and comparison was therefore no longer possible.

The same occurred in the reinforced model panel, subsequently analysed; at 600000 N the panel still resulted stable even though this value is more than triple the experimental average found during testing. At this point, calculations were interrupted. While the iterations completed on both the reinforced and unreinforced models allowed for the elimination of all trusses subjected to tensile strength, the remaining compressed trusses had values that exceeded the compressive strength

Panel Type		Average Experimental Ultimate Strength (N)	FEM Model Ultimate Strength (N)	Increment
120x120 cm	Unreinforced panel	114410	< 424260	< 370 %
	Reinforced panel	166450	< 600000	< 360 %

Table 4.b. Experimental and numerical ultimate strength values for unreinforced and reinforced panels.

of the mortar used for the construction of the panels.

Repeatedly, calibration of the model was attempted, by means of the variation of the elastic modulus of the mortar trusses, but once again instability did not occur for values comparable to experimental results.

The final attempt of calibration of the model was carried out through the elimination of the trusses arranged in the tangential direction (Figs. 4.2.2-3). This procedure was accomplished only when all the corresponding perpendicular mortar trusses had been eliminated due to the fact that they were subjected to tensile strength: when in a given joint, all perpendicular mortar trusses had been eliminated, at that point of the iteration the tangential truss was eliminated as well. The reason for this algorithm modification is that, when a fracture occurs in any given joint, no normal force, and therefore also no tangential one, can be transmitted throughout the interface. However, the model reached instability for load values significantly lower than the experimental results described in Table 4.b. and thus, once again, proved ineffective and futile for our purpose.

As mentioned in the first part of the present section, the experimental panels used as a comparison in this last case study were not reinforced solely with the reticolatus technique; the reinforcement was of a mixed kind, with glass fibre reinforced plaster on one side of the panel, and reticolatus on the other. This would certainly influence the success of the result of the numerical method, since the model is assembled as panels reinforced with reticolatus on both sides, as in the previous case study.

From the unsatisfactory results of this last case study it is clear that the proposed method for the numerical analysis must be thoroughly revisited in a future research project. The lack of experimental data for the comparison of results regarding the reticolatus technique - which, we must recall, has been shown by the state-of-the-art research to be limited to only a few cases on regular brick-masonry panels - and the virtual non-existence of previous attempts at numerical analysis outcomes, show that this effort should become the focus of an independent investigation which exceeds the limits that were defined for this dissertation.

Selected Bibliography

Adamson, M. J. (1980). Thermal expansion and swelling of cured epoxy resin used in graphite/ epoxy composite materials. *Journal of Materials Science 15*, 1736-1745.

Alberti, Leon Battista. (1991) *On the Art of Building in Ten Books.* (J. Rykwert, N. Leach, & R. Tavernor, R., Trans.). Cambridge MA: MIT Press (Original work, *De re aedificatoria*, completed 1450, 1st published 1485.)

Al Far, A., Rostàsy, F., Budelmann, H., Al Hadid, T. (2007, July 16-18). Durability of reinforced concrete members strengthened with CFRP plates and subjected to moisture and salts. In *Proceedings of the 8th International Symposium on Fiber Reinforced Polymer Reinforce ment for Concrete Structures (FRPRCS-8)*,Patras, Greece.

Alecci, V., Fagone, M.,Rotunno, T., De Stefano, M. (2013). Shear strength of brick masonry walls assembled with different types of mortar. *Construction and Building Materials, 40*, 1038–1045.

Allred, R. E. (1981). The Effect of Temperature and Moisture Content on the Flexural Response of Kevlar/Epoxy Laminates: Part I. [0/90] Filament Orientation; Part II. [±45,=/90]. *Journal of Composite Materials, 15*, 100-132.

Anzani, A., Garavaglia, E., Binda, L. (2008). Long-term damage of historic masonry: A probabilistic model. *Construction and Building Materials, 23*, 713-724.

ASTM C666/C666M-03 (2008) Standard Test Method for Resistance of Concrete to Rapid Freezing and Thawing (pp. 365-370). West Conshohocken, Pennsylvania: ASTM Inter national, 2012, www.astm.org

ASTM C1560 - 03 (2009) Standard Test Method for Hot Water Accelerated Aging of Glass-Fiber Reiniforced Cement-Based Composites. West Conshohocken, PA: ASTM International, 2012, www.astm.org

ASTM D1141-98 (2003), Standard Practice for the Preparation of Substitute Ocean Water , (pp. 1-3). West Conshohocken, PA, ASTM International, 2012, www.astm.org

ASTM E519/E519M-10, Standard Test Method for Diagonal Tension (Shear) in Masonry Assemblages (pp. 1428-1432). West Conshohocken, PA: ASTM International, 2012, www.astm.org

ASTM C67-12 Standard Test Methods for Sampling and Testing Brick and Structural Clay Tile (pp. 38-49). West Conshohocken, Pennsylvania: ASTM International, 2012, www.astm.org

Augenti, N., Parisi, F., Prota, A., Manfredi, G. (2011). In-plane lateral response of a full-scale masonry sub-assemblage with and without an inorganic matrix-grid strengthening system. *Journal of Composites for Construction, 15*, 578-590.

Baila, A. et al. (2011a). *Manuale delle Murature Storiche. Vol. I: Analisi e valutazione del comportamento strutturale*. A. Borri, Dir. Scientfico; C. Donà, De Maria, A. (eds.), Rome: DEI S.r.l.

Baila, A. et al. (2011b). *Manuale delle Murature Storiche. Vol. II: Schede operative per gli inter venti di restauro strutturale*. A. Borri, Dir. Scientfico; C. Donà, De Maria, A. (eds.), Rome: DEI S.r.l.

Bakis, C. E., Bank, L.C., Brown,V.L., Cosenza, E., Davalos, J.F., Lesko. J. J., Machida, A., Rizkalla, S.H.,Triantafillou, T.C. (2002). Fiber-Reinforced Polymer Composites for Construction—State-of-the-Art Review. *Journal of Composites for Construction*, 73-87.

Balsamo, A., Nardone, F., Iovinella, I., Ceroni, F., Pecce, M. (2013). Flexural strengthening of concrete beams with EB-FRP, SRP and SRCM: Experimental investigation. *Composites: part B, 46*, 91-101.

Binda, L., Tedeschi, C., Valluzzi, M.R., Garbin, E., Panizza, M. (2011, April 12-15). Salt crystallization tests on brick masonry reinforced by CFRP textiles. In *Proceedings of the XII International Conference on Durability of Building Materials and Components*, Porto, Portugal.

Borri, A., Castori, G. (2011a). Experimental investigations on the durability of composites for use in civil engineering. In *Proceedings of the XIVth National ANIDIS Conference: L'Ingegneria Sismica in Italia*, Bari.

Borri, A., Castori, G., Corradi, M. (2011). Masonry Columns Confined by Steel Fiber Composite Wraps. *Materials, 4*, 311-326.

Borri, A., Castori, G., Corradi, M. (2013a). Utilizzo di Trefoli Metallici per il Rinforzo di Colonne Murarie con Mattoni "Faccia Vista". In *Proceedings of the XV National ANIDIS Conference (Italian National Association of Earthquake Engineering)*, Padua.

Borri, A., Castori, G., Corradi, M. (2013). Shear Resistance of Rubble Stone and Brick-Masonry Panels. In *Proceedings of the XV National ANIDIS Conference (Italian National Association of Earthquake Engineering)*, Padua.

Borri, A., Castori, G., Corradi, M., Sisti, R. (2013b). Tecniche Innovative di Rinforzo di Murature Storiche. In *Proceedings of the XV National ANIDIS Conference (Italian National Association of Earthquake Engineering)*, Padua.

Borri, A., Castori, G., Corradi, M., Speranzini, E. (2011). Shear behavior of unreinforced and reinforced masonry panels subjected to in situ diagonal compression tests. *Construction and Building Materials, 25*, 4403-4414.

Borri, A., Corradi, M., Speranzini, E. (2010). Reinforcement of historic masonry with high strength steel cords. *Masonry International, 23(3)*, 20-36.

Borri, A., Corradi, M., Speranzini, E., Giannantoni, A. (2009, 2-4 December). Reinforcement Of Historic Masonry: The "ReticolatusTechnique". In *Proceedings of the I Convegno di Ingegneria Forense: IV Convegno Su Crolli, Affidabilità Strutturale, Consolidamento (IF CRASC '09)*, Naples.

Borri, A., Corradi, M., Speranzini, E., Giannantoni, A. (2010a, 4-7 JULY). A reinforced repointing grid for strengthening historic stone masonry walls. In *Proceedings of the 8th International Masonry Conference*, Dresden.

Borri, A., Corradi, M., Speranzini, E., Giannantoni, A. (2010b). Reinforcement of historic masonry with high strength steel cords. *Masonry International, 23(3)*, 79-90.

Briccoli Bati, S., Rotunno, T. (2001). Environmental durability of the bond between the CFRP composite materials and masonry structures. *Historical Constructions*, 1039 - 1046.

Cabral-Fonseca, S., Nunes, J.P.,Rodrigues, M.P., Eusébio, M.I. (2009, 27-31 July). Durability of Epoxy Adhesives Used To Bond CFRP Laminates To Concrete Structures. In *Proceedings of the ICCM: 17th International Conference on Composite Materials*, Edinburgh, UK.

Capozucca, R. (2010). Experimental FRP/SRP–historic masonry delamination. *Composite Structures, 92*, 891-903.

Capozucca, R. (2013). Effects of mortar layers in the delamination of GFRP bonded to historic masonry. *Composites: Part B*, 44, 639-649.

Carbon Fibres - The First Five Years. (1971). *Flight International*.

Chajes, M. J., Dennis R., Thomson, T.A. . (1994). Durability of Composite Material Reinforcement. In *Proceedings of the The American Society of Civil Engineers Third Materials Engineering Conference*, San Diego, San Diego, Calilfornia.

CNR - DT200: Consiglio Nazionale delle Ricerche (National Research Council), R. (2004). Guide for the design and construction of externally bonded FRP systems for strengthening existing structures, Rome.

Corradi, M., Tedeschi, C., Binda, L., Borri, A. (2008). Experimental evaluation of shear and compression strength of masonry wall before and after reinforcement: Deep repointing. *Construction and Building Materials, 22*, 463-472.

Consiglio Generale Superiore LL PP (2009). Linee guida per la Progettazione, l'Esecuzione ed il Collaudo di Interventi di Rinforzo di strutture di c.a., c.a.p. e murarie mediante FRP.

De Felice, G., De Santis, S., Garmendia, L., Ghiassi, B., Larrinaga, P., Lourenço, P.B., Oliveira, D.V.,Paolacci, F., Papanicolaou, C.G. (2014). Mortar-based systems for externally bonded strengthening of masonry. *Materials and Structures, 47(12)*, 2021-2037.

De Lorenzis, L., Teng, J.G. (2007). Near-surface mounted FRP reinforcement: An emerging technique for strengthening structures. *Composites: Part B*, 38, 119-143.

De Santis, S., De Felice, G. (2014). Tensile behaviour of mortar-based strengthening systems with glass-aramid textile. *Key Engineering Materials, 624*, 346-353.

Decreto Ministeriale NTC2008: Norme tecniche per le costruzioni. Ministro delle Infrastrutture, Ministro dell'Interno, e Il Capo del Dipartimento della Protezione Civile.

EN 1996-1-1 (2005). Eurocode 6: Design of masonry structures - Part 1-1: General rules for reinforced and unreinforced masonry structures [Authority: The European Union Per Regulation 305/2011, Directive 98/34/EC, Directive 2004/18/EC].

Focacci, F. (2008). *Rinforzo delle Murature con materiali Compositi: Progettazione - Calcolo-Esempi Applicativi*. Palermo.

Franciosi, V. 1986. Su alcune questioni riguardanti la stabilità delle strutture lapidee monodimensionali. In *Atti dell'Accademia Pontaniana*. Napoli: Giannini

Galassi, S., Paradiso, M., Tempesta, G. (2004, November). A Numerical Method for No-Tension Analysis of Masonry Arches. In *Proceedings of the IV International Conference on Arch Bridges: Advances in Assessment, Structural Design and Construction.* Barcelona.

Galassi, S., Paradiso, M., Pieroni, E. & Tempesta, G. . (2011, 12-15 September). Analisi di strutture in muratura soggette a vincoli cedevoli: un algoritmo di calcolo non lineare. In *Proceedings of the XX Congresso Associazione Italiana di Meccanica Teorica e Applicata (AIMETA 2011*), Bologna.

Ghiassi, B., Marcari, G., Oliveira, D.V., Lourenço, P.B. (2013). Water degrading effects on the bond behavior in FRP-strengthened masonry. *Composites: Part B*, 54, 11-19.

Ghiassi, B., Oliveira, D.V. ,Lourenco, P.B. . (2013a) Recent Developments in Durability of FRP-Masonry Systems. In *Proceedings of the International Conference: Rehabilitation and Restoration of Structures, Chennai*, India.

Ghiassi, B., Oliveira, D.V., Lourenço, P.B. (2013b). Experimental Investigation on the Long-term Durability of Bond Between FRP and Masonry Substrates. In *Proceedings of the 11th International symposium on Fiber Reinforced Polymers for reinforced concrete structures (FRPRCS-11).*Guimarães, Portugal.

Ghiassi, B., Oliveira, D.V., Lourenço, P.B., Marcari, G. (2013c). Numerical study of the role of mortar joints in the bond behavior of FRP-strengthened masonry. *Composites: part B*, 46, 21-30.

Ghiassi, B., Silva, M.M.M., Marcari, G., Oliveira, D.V., Lourenço, P.B. (2012, 21 December). Moisture effects on the bond strength of FRP-masonry elements. In *Proceedings of the ISISE - Comunicações a Conferências Internacionais,* Guimarães, Portugal.

Gomez, J. P., Casto, Brian. (1996). Freeze-thaw Durability of Composite Materials. *Virginia Transportation Research Council, 96 - R25*, 1-9.

Grace, N. F. (2004). Concrete Repair with CFRP. Evaluating the durability of externally bonded carbon fiber-reinforced polymer plates and fabric exposed to the environment. *Concrete International*, 45-52.

Hashemi, S., Al-Mahaidi, R. (2008, November 5-7). Cement Based Bonding Material for FRP. In *Proceedings of the 11th International Inorganic Bonded Fiber Composites Conference*, Madrid.

Hollaway, L. C. (2010). A review of the present and future utilisation of FRP composites in the civil infrastructure with reference to their important in-service properties. *Construction and Building Materials, 24*, 2419-2445.

Huang, P.-Y., Zhou, H., Wang, H.-Y., Guo, X.-Y. (2011). Fatigue lives of RC beams strengthened with CFRP at different temperatures under cyclic bending loads. *Fatigue & Fracture of Engineering Materials & Structures, 34*, 708-716.

Huang, X., Birman, V., Nanni, A., Tunis, G. (2005). Properties and Potential for Application of Steel Reinforced Polymer (SRP) and Steel Reinforced Grout (SRG) Composites. *Composites: Part B, 36*, 73-82.

Hulatt, J., Hollaway, L.,Thorne, A. (2002). Preliminary investigations on the environmental effects on new heavyweight fabrics for use in civil engineering. *Composites: Part B*, 33, 407-414.

Jia, J; Boothby. T.E.; Bakis, C.E. ; Brown, T.L., (2005) Durability Evaluation of Glass Fiber: Reinforced-Polymer-Concrete Bonded Interfaces. *Journal of Composites for Construction* © ASCE, 9:348-359.

Jurina, L. (2010, 8-15 May). Tecniche di cerchiatura nel consolidamento di archi e di colonne in muratura. In *Proceedings of the Seminar on "Evoluzione nella sperimentazione per le costruzioni"* , Madrid.

Jurina, L. (2012b, 15-17 November). Tecniche di Consolidamento dei Monumenti: Una Panoramica Attuale. In *Proceedings of the IF CRASC '12: II Convegno di Ingegneria Forense - V Convegno su Crolli, Affidabilità Strutturale, Consolidamento*, Pisa.

Karbhari, V. M., Araceli Abanilla. M. (2007). Design factors, reliability, and durability prediction of wet layup carbon/epoxy used in external trengthening. *Composites: part B, 38*, 10-23.

Karbhari, V. M., Chin, J.W., Hunston, D., Benmokrane, B.,Juska, T., Morgan, R., Lesko, J.J. ; Sorathia, U., Reynaud, D. (2003). Durability Gap Analysis for Fiber-Reinforced Polymer Composites in Civil Infrastructure. *Journal of Composites for Construction*, 238-247.

Lees, J. M., Winistörfer, A. U. (2011). Nonlaminated FRP Strap Elements for Reinforced Concrete, Timber, and Masonry Applications. *Journal of Composites for Construction* © Asce (March/April), 146-155.

Mantegazza, G., Barbieri, A. (2002, 16 October). Composito Fibroso a Matrice Cementizia (FRCM) per il Recupero Strutturale delle Costruzioni. In *Proceedings of the AICO Associazione Italiana Compositi*, Bologna.

Mazzanobile, M. (2005). L'Età Romana. In P. Rocchi (Ed.), *Storia del consolidamento* (Vol. 01). Rome.

Micelli, F., Nanni, A., & (2001, Sept. 9-12, 2001). Issues Related to Durability of FRP Reinforcement for Rc Structures Exposed to Accelerated Ageing. In *Proceedings of the ASC 16th Annual Conference*, Virginia Tech, Blacksburg, VA.

Ministero delle Infrastrutture e dei Trasporti (2012). Linea Guida per la Qualificazione ed il Controllo di accettazione di compositi fibrorinforzatida utilizzarsi per il consolidamento strutturale di costruzioni esistenti.

Modena, C., Valluzzi, M.R., da Porto, F., Casarin, F. (2011). Structural Aspects of the Conservation of Historic Masonry Constructions in Seismic Areas: Remedial Measures and Emergency Actions. *International Journal of Architectural Heritage, 5*, 539–558.

Mu, R., Tian, W., Zhou, M. (2010). Moisture migration in concrete exposed to freeze-thaw cycles. *Journal of Chinese Ceramic Society, 38.9*, 1713-1717.

MS-A.4 RILEM (1998). Determination of the durability of hardened mortar. *Materials and Structures/Matériaux et Constructions,31*, 11-15.

Nanni, A. et al. (1994). State-of-the-Art Report on Application of FRP Composites (pp. i-v, 1-107): Department of Architectural Engineering, Pennsylvania State University.

Papanicolaou, C. G., Triantafillou, T.C., Papathanasiou, M., Karlos, K. (2007). Textile-reinforced mortar (TRM) versus FRP as strengthening material of URM walls: in-plane cyclic loading. *Materials and Structures, 40(10)*, 1081-1097.

Papanicolaou, C. G., Triantafillou, T.C., Papathanasiou, M., Karlos, K. (2008). Textile reinforced mortar (TRM) versus FRP as strengthening material of URM walls: out-of-plane cyclic loading. *Materials for Structures, 41*, 143-157.

Paradiso, M., Borri, A., Sinicropi, D., Galassi, S., Perria, E. (2014, 12-14 November). An Experimental Study on Wet/Dry Effects on FRCM Reinforced Masonry. In *Proceedings*

of the Congreso Internacional Conservar Rehabilitar Innovar: Jornadas Internacionales Conmemorativas del 80° Aniversario del IETcc, Madrid.

Paradiso, M., Galassi, S., Borri, A., Sinicropi, D. . (2013, 24-26 July). "Reticolatus": An Innovative Reinforcement for Irregular Masonry – a Numeric Model. In *Proceedings of the Second International Conference on Structures and Architecture,* Guimaraes, Portugal.

Parisi, F., Iovinella,I., Balsamo, A., Augenti, N., Prota, A. (2013). In-plane behaviour of tuff masonry strengthened with inorganic matrix–grid composites. *Composites: part B, 45*, 1657-1666.

Prota, A., Marcari, G., Fabbrocino, G., Manfredi, G., Aldea, C. . (2006). Experimental in-plane behavior of tuff masonry strengthened with cementitious matrix-grid composites. *Journal of Composites for Construction, 10*, 223-233.

Rahman, A. H., Kingsley, C.Y., Crimi, J. (1996). Durability of a FRP Grid Reinforcement. *Advanced Composite Materials in Bridges and Structures / Materiaux Composites D'Avant Garde Pour Ponts et Charpentes*, 681-690.

RILEM LUMB6; 1994. Diagonal tensile strength tests of small wall specimens. Rilem recommendations for the testing and use of constructions materials.

Sala, G. (2000). Composite degradation due to fluid absorption. *Composites: Part B, 31*, 357-373.

Savoia, M., Ferracuti, B., Mazzotti, C. (2003) Non linear bondslip law for FRP-concrete interface. In *Proceedings of the FRPRCS-6: 6th International Symposium on Fibre-Reinforced Polymer (FRP): Reinforcement for Concrete Structure*s, Singapore.

Schueremans, L., Cizer, Ö., Janssens,E., Serré, G., Van Balen, K. (2011). Characterization of

repair mortars for the assessment of their compatibility in restoration projects: Research and practice.. *Construction and Building Materials, 25*, 4338–4350.

Sciolti, M. S., Aiello, M.A., Frigione, M. (2012). Influence of water on bond behavior between CFRP sheet and natural calcareous stones. *Composites: Part B, 43*, 3239-3250.

Sciolti, M. S., Frigione, M.E., Aiello, M.A. (2010). Wet Lay-Up Manufactured FRPs for Concrete and Masonry Repair: Influence of Water on the Properties of Composites and on their Epoxy Components. *Journal of Composites for Construction* © Asce, 14, 823-833.

Sen, R., Mariscal, D., Shahawy, M. (1993). Durability of fiberglass pretensioned beams. *ACI S tructural Journal, 90(5)*, 525-533.

Serra, E. (2005). Dal Novecento all'epoca moderna. In P. Rocchi (Ed.), *Storia del consolidamento (Vol. 07*). Rome.

Sinicropi D., Perria E., Galassi S., Paradiso M., Borri A. (2014). Artificial Ageing of Mortar Prisms Reinforced through Steel, Glass and Organic Fibres. In A. Di Tommaso, Gentilini, C., Castellazzi, G. (eds.), *Mechanics of Masonry Structure Strengthened with Composite Materials (pp. 542-550)*. Stafa-Zurich: Trans Tech Publications.

Soudki, K., El-Salakawy, E., Craig, B. (2007). CFRP Strengthened Reinforced Concrete Beams in Corrosive Environment, *Journal of Composites for Construction* © Asce, 291-298.

Tempesta, G., Paradiso, M., Galassi, S. (2011). Non Linear Analysis of FRP Reinforced Masonry Arches. In *Proceedings of the ICCS 16: 16th International Conference on Composite Structures,* Porto.

Toutanji, H., Balaguru, P. (1998). Durability Characteristics of Concrete Columns Wrapped with FRP Tow Sheets. *Journal of Materials in Civil Engineering*, 52-57.

Triantafillou, T. C. (1998). Strengthening of Masonry Structures Using Epoxy-Bonded FRP Laminates. *Journal of Composites for Construction*, 96-104.

Triantafillou, T. C., Fardis, M.N. . (1997). Strengthening of historic masonry structures with composite materials. *Materials and Structures/Matériaux et Constructions, 30*, 486-496.

Tuakta, C., Büyüköztürk, O. (2011). Deterioration of FRP/concrete bond system under variable moisture conditions quantified by fracture mechanics. *Composites: part B, 42*, 145-154.

Turco V., S. S., Morbin A., Valluzzi M.R., Modena C. . (2006). Flexural and shear strengthening of un-reinforced masonry with FRP bars. *Composites Science and Technology, 66*, 289-296.

Valluzzi, M. R., Garbin, E., Panizza, M., Binda, L., Tedeschi, C. (2011, April 12-15). Moisture and Temperature Influence on FRP Masonry Bonding In *Proceedings of the XII DBMC: International Conference on Durability of Building Materials and Component*s, Porto.

Vintzileou, E. N., Toumbakari, E.-E.E. (2001). The effect of deep rejointing on the compressive strength of brick masonry. *Historical Constructions*, 995-1002.

Vitruvius. *Ten Books on Architecture*. (2001) I. D. Rowland & T. N. Howe, Eds. Cambridge UK: Cambridge University Press. (Original work, *De Architectura*, 1st Century B.C., rediscovered 1414.)

Yuan, H., Wu, Z., and Yoshizawa, H. (2001). Theoretical solutions on interfacial stress transfer of externally bonded steel/composite laminates. Struct. Eng./Earthquake Eng., 18 (1), 27s–39s.